



# **GEOSCIENCE BC SUMMARY OF ACTIVITIES 2013**

# Documentation and Assessment of Exploration Activities Generated by Geoscience BC Data Publications, QUEST Project, Central British Columbia (NTS 093A, B, G, H, J, K, N, O, 094C, D)

S.A. Reichheld, Consultant, Sooke, BC, sa.reichheld@gmail.com

---

Reichheld, S.A. (2014): Documentation and assessment of exploration activities generated by Geoscience BC data publications, QUEST Project, central British Columbia (NTS 093A, B, G, H, J, K, N, O, 094C, D); in Geoscience BC Summary of Activities 2013, Geoscience BC, Report 2014-1, p. 1–12.

## Introduction

This study focuses on the QUEST (QUesnellia Exploration STRategy) Project, launched by Geoscience BC in 2007. Its goal was to stimulate exploration interest and investment in the underexplored region between Williams Lake and the District Municipality of Mackenzie, in part to help diversify the local forestry-based economies impacted by the mountain pine beetle infestation. Geoscience BC initially funded the re-analysis of 5000 archived regional geochemical samples and the collection of 2200 new geochemical samples, plus two large-scale airborne geophysical surveys (Geotech Limited, 2008; Jackaman, 2008a, b; Sander Geophysics Limited, 2008). The raw data was made available to the public starting in 2008, at which point Geoscience BC also commissioned a number of follow-up, value-added projects that were released in subsequent years (Barnett and Williams, 2009; Fraser and Hodgkinson, 2009; Geotech Limited, 2009; Barlow et al., 2010; Owsiaci and Payie, 2010), providing the industry with announcements and data to continue to attract exploration to the area. As indicated in the preliminary paper for this project (Reichheld, 2013) it is felt that the QUEST Project, with its years of data and development, now has a sufficient track record to produce quantifiable and meaningful results.

This paper details the research completed in order to lay out a framework for reviewing and assessing the impact of this and any public exploration initiative. To ensure the method remains repeatable into the future, only public sources of information are used.

## Method

The study area encompasses the greater QUEST area, including all or parts of NTS map areas 093A, B, G, H, J, K,

N, O and 094 C, D. Exploration data was presented in GIS shapefiles, or in Excel<sup>®</sup> spreadsheets with co-ordinates attached to georeference the datasets. Each dataset used was clipped to the nearest 1:50 000 NTS map area around the QUEST area to maintain equal datasets. ArcGIS 10.2 was used as a platform for working with much of the data. Stock market index and price charts were created using MetaStock Pro software.

The framework for this project includes assimilating relevant data from Mineral Titles Online (MTO), the Assessment Report Indexing System (ARIS), MINFILE and evaluating anecdotal sources including corporate press releases, financial statements, share offerings and stock price data for companies listed on the TSX Venture Exchange.

The period covered is 2007–2010 to ensure that a large portion of the data is publicly available. In 2005, changes in claim staking techniques from on-ground to online methods using MTO and internet staking led to a surge that potentially distorts the true extent of operator participation in the field. As a baseline, only data from 2005 to 2006 are used to offer perspective on developments leading up to the study period.

The MTO claim staking has been used as a general indicator of success within a given region, but while this approach has merit, it must be considered carefully. For QUEST area staking, the presence of large, long-established claims, operating mines and known past anomalies can have a trickle-down effect on the activity statistics because large blocks of surrounding land may be staked as a combination of ground inventorying, pre-emptive staking or claim jumping, but not necessarily for speculative purposes. Determining which staking is genuinely motivated by exploration is a complex task. Rather than break down what could be called ‘defensive staking’, with regards to locking up high-potential lands before they can be worked on by the owner, the merits of mineral titles were used to analyze actual on-the-ground activities. By considering length of tenure, frequency of new claims staked and work submitted on the land through assessment reports, a truer relationship of claim use can be distinguished. ArcGIS was used to exam-

---

**Keywords:** QUEST Project, mineral exploration, grassroots, public funding, SEDAR, assessment reports, MINFILE, investment capital, data release

This publication is also available, free of charge, as colour digital files in Adobe Acrobat<sup>®</sup> PDF format from the Geoscience BC website: <http://www.geosciencebc.com/s/DataReleases.asp>.

ine land tenures to find total land tenure for each year, new land tenure for each year and to determine under what category of tenure assessment reports were submitted (BC Ministry of Energy and Mines, 2013).

The second major source of information, assessment reports for the study period, is just now becoming available to the public (BC Geological Survey, 2013). Assessment reports found in ARIS were examined using ArcGIS to evaluate important variables including expenditures, yearly submissions and exploration location. Given rising demand and commodity prices during this period, a rise in overall exploration spending in the region is at least partly indicative of increased exploration throughout British Columbia. To differentiate this spending from overall totals that may be somewhat misleading, assessment reports were examined using ArcGIS to find the number of assessment reports submitted for each year within the study area, the total reported dollars spent and their locations on newly tenured or previously tenured land. Expenditures could then be broken down into yearly data from which totals and trends within the region could be identified. Questions to ask are: just how successful has the \$5 million investment by Geoscience BC been as a return for the province? Is there a noticeable difference in total activity in general, and in generating new exploration specifically?

Factors often considered peripheral to in-the-field exploration and development, such as the performance of a company's shares in the stock market, can be instrumental to its success. The ability to raise new investment capital each year is an important part of the mine cycle, and investors frequently base their buying decisions on financial performance. How well an enterprise performs in the stock market is often a bellwether to its long-term success in the field. A fundamental question then is: does participation in Geoscience BC projects like QUEST endow companies with superior prospects on public stock exchanges?

Evaluating the financial component includes analysis of the trading record of stock prices and share volumes to ascertain whether individual companies involved in the QUEST Project enjoyed increased market activity, and at an industry level, whether mining stocks in general performed well in the market during the study period. Most firms studied here are micro- and small-cap companies trading on the TSX Venture Exchange. The S&P/TSX Venture Composite Index was tracked as a proxy for observing the industry's performance during the study period. It is described in the exchange's own literature as "...a broad market capitalization-based index which is designed to measure the performance of securities listed on the TSX Venture Exchange, Canada's primary venture equity market" (TSX Inc., 2013).

Next, a 'mini' index, herein named the QUEST venture stock index, comprising eight publicly listed companies with properties in the QUEST Project area, was created for this study using Equis MetaStock Pro and its FIRE add-on (Figure 1). The eight companies range from less than \$1 million in overall exploration projects to tens of millions. The index incorporates the shares of the following companies (using names as they appeared during the period of study): Alpha Gold Corp., Amarc Resources Ltd., Barker Minerals Ltd., Dajin Resources Corp., Fjordland Exploration Inc., Happy Creek Minerals Ltd., Richfield Ventures Corp. and Serengeti Resources Corp.

The S&P/TSX Venture Composite and the mini QUEST venture stock indices were charted in MetaStock Pro (Figure 2).

The research also took an anecdotal look into several larger public companies operating within the QUEST area using ARIS and SEDAR (system for electronic document analysis and retrieval; 2013), the latter of which provides access to public securities documents and information filed by public companies and investment funds. Here, important avenues for research include press releases, corporate financial statements and annual reports. Using SEDAR and ARIS, company press releases and assessment reports were sampled to get an indication of how frequently, or infrequently, Geoscience BC data and the QUEST Project received mention in the media.

Although financial reports and news releases are valuable sources of information, they offer it in a labour-intensive format. Company name changes, mergers and acquisitions, joint ventures and partnerships all tend to muddy the waters of research and hamper understanding of an operator's business. A stock exchange-listed company offers the widest scope for research, but navigating annual reports can be a limiting factor, requiring interpretation in light of accepted accounting principles.

## Results

Mineral tenures were divided into two groups: total ground tenured within each year and newly tenured ground within each year (Figure 3). Both groups peaked in 2007, with total ground staked at 2 916 922 hectares (ha) and newly staked ground at 1 428 387 ha. Evaluating the staking of ground can be difficult due to 'dead staking', which is evident to the eye when examining the large areas of tenure that were allowed to lapse and then return as fresh tenures the following year (Figure 4). With that caveat, land tenured averaged 2 477 037 ha, an increase of more than 35% from its 'pre-QUEST' 2006 value of 1 834 055 ha. Newly staked land averaged 919 823 ha during the same period.

In contrast to the interpretive challenges arising from practices like dead staking and the complexities of claim owner-

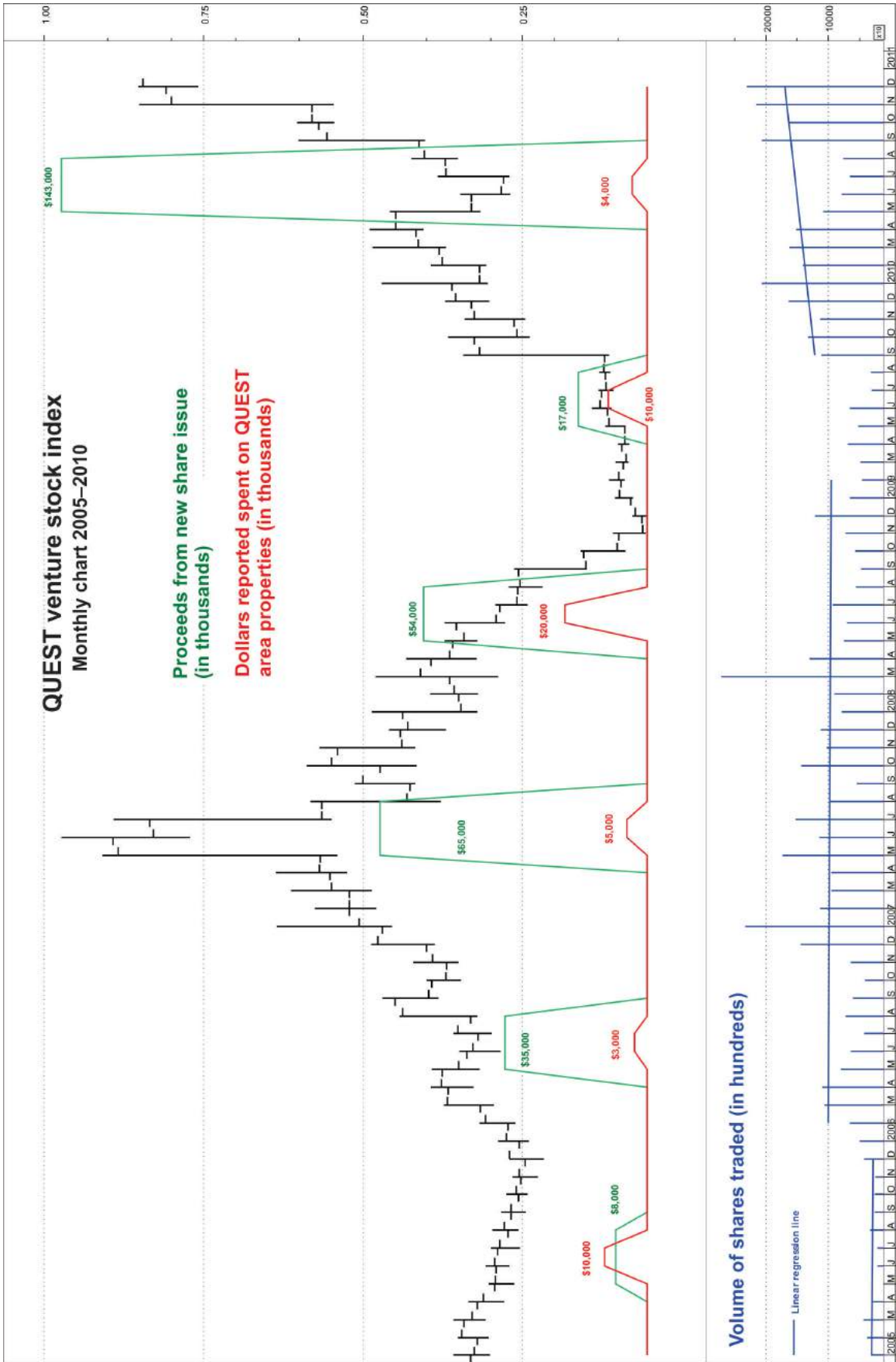


**Figure 1.** Monthly stock price chart of the QUEST venture stock index, representing eight operators within the QUEST (Quesnellia Exploration Strategy) area. The red indicator represents estimated expenditures on QUEST projects as reported in assessment reports. The green indicator represents estimated proceeds arising from new share issues.

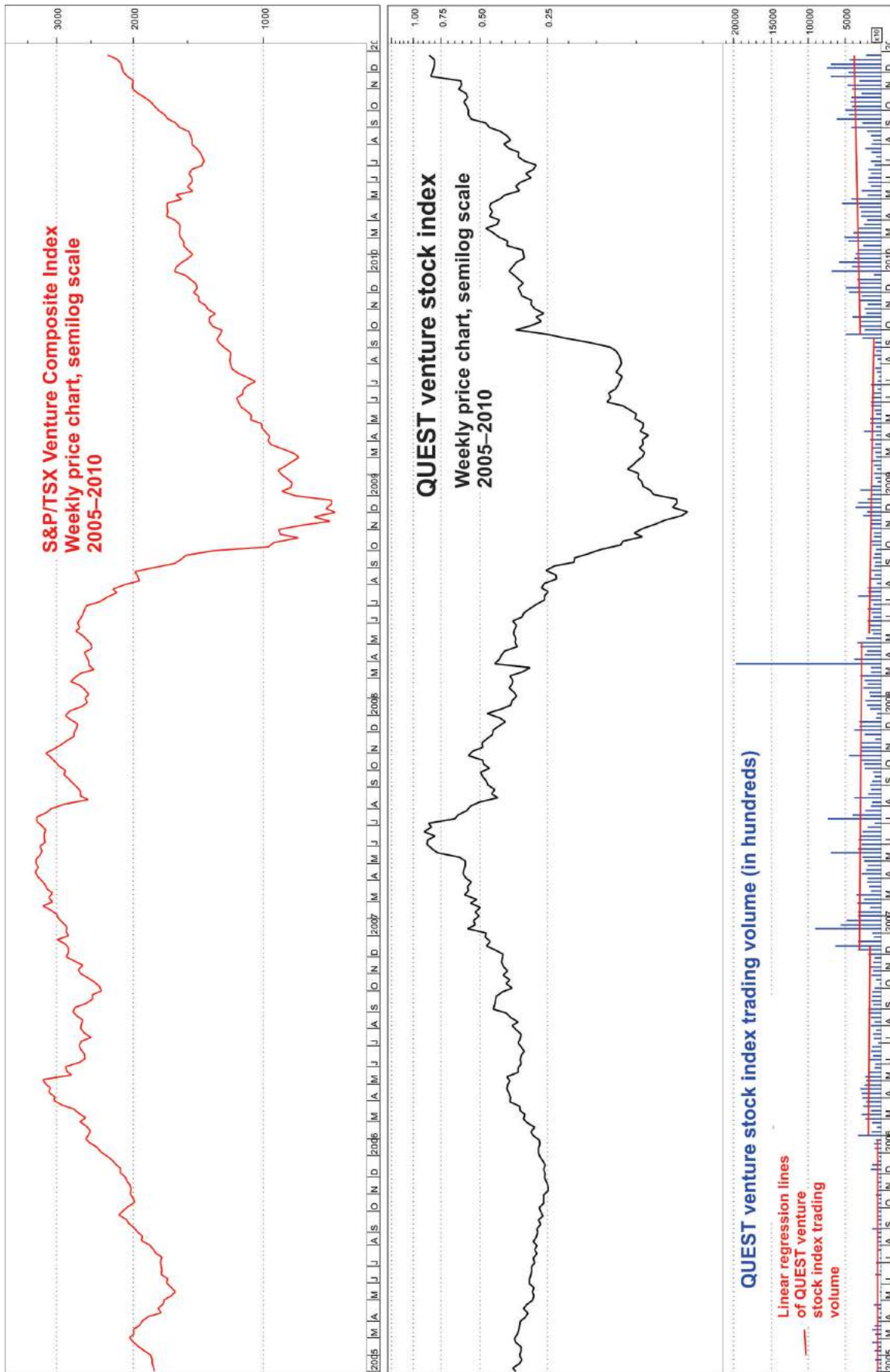


**Figure 2.** Weekly price chart comparing the S&P/TSX Venture Composite Index with the QUEST venture stock index during the 2008 market downturn. The linear regression lines of trading volume for the QUEST venture stock index reveal an upward 'stairstep' pattern of increasing stock market activity leading into the 2008 collapse.

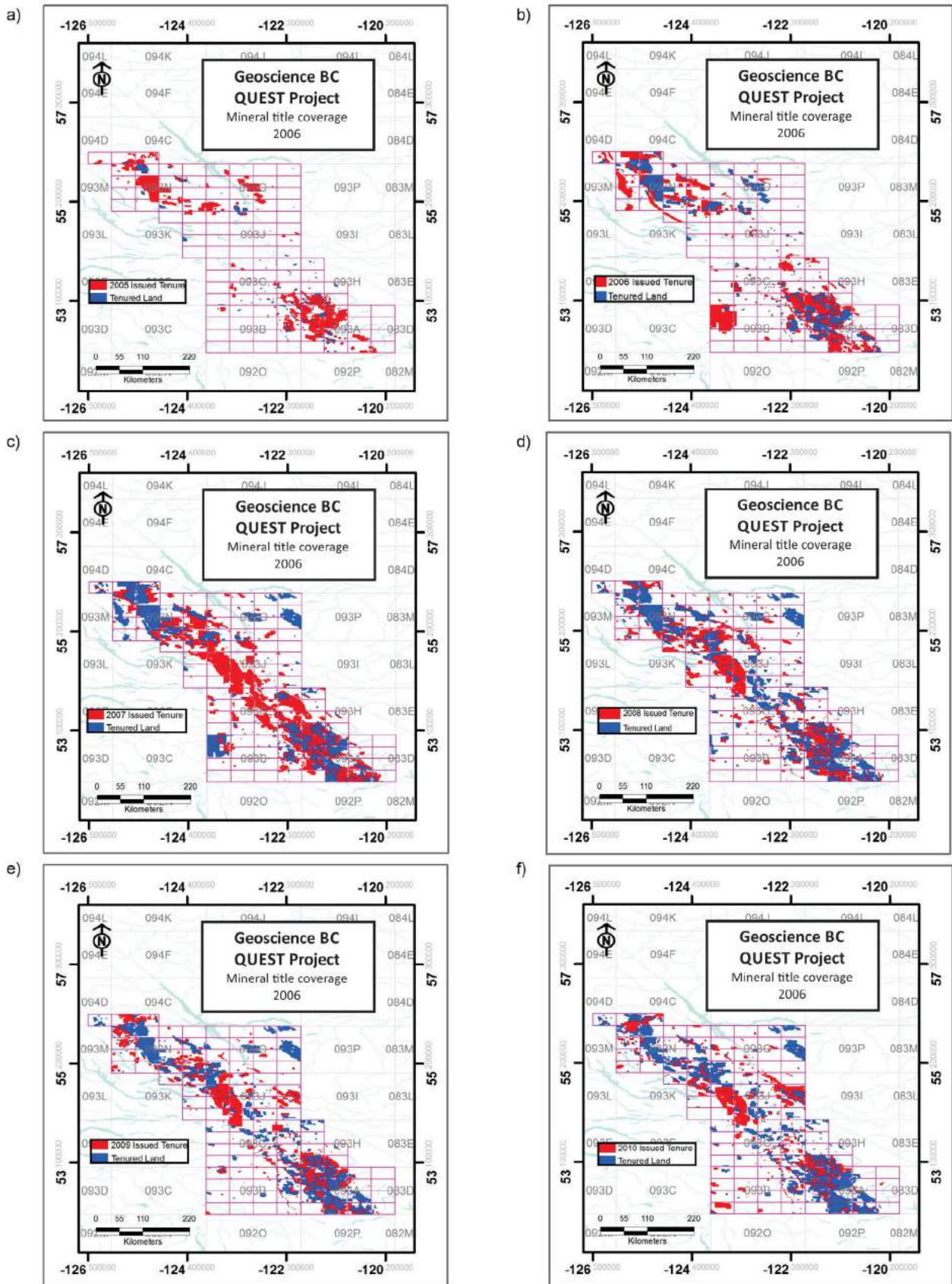


**Figure 3.** Changes in mineral title tenure for the greater QUEST (QUesnellia Exploration STRategy) area: a) 2005; b) 2006; c) 2007; d) 2008; e) 2009; f) 2010.

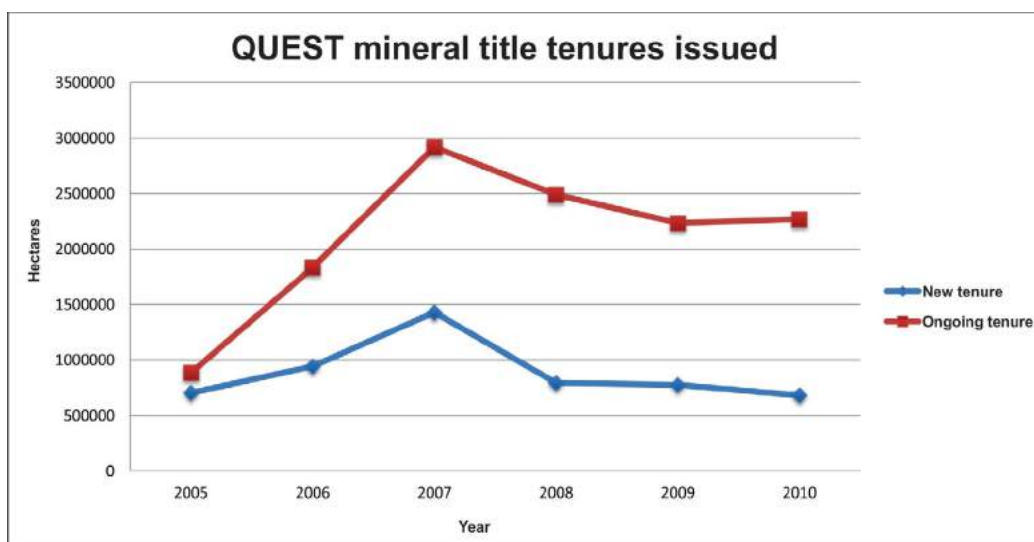


**Figure 4.** QUEST (Quesnellia Exploration Strategy) mineral title tenures issued from 2005 to 2010. The blue line indicates area of new claims issued. The red line shows total tenured land. The increase in tenure is indicative of sustained interest in the area.

ship, assessment reports represent basic, quantifiable results of exploration in terms of monetary expenditure. For the reporting period of 2007–2010, there were 501 assessment reports submitted on the ground within the QUEST Project footprint (Figure 5). In the baseline years 2005 and 2006, there were a total of 153 assessment reports submitted in the same area, indicating an average of 125 per year during the QUEST Project compared to 76 per year before the QUEST Project. Reported expenditures for the study period totalled \$79,106,618.97 (BC Geological Survey, 2013a). The average yearly expenditures for the two years prior to the QUEST Project amounted to \$10,910,220, compared to the four-year QUEST Project average of \$19,776,655—a rise in overall reported spending activity for the area of nearly 100%. Although these numbers clearly reflect a significant increase in exploration within the QUEST area, they do not specifically point to an increase in new exploration development. On land previously untenured before the study period, assessment reports indicate a total of \$15,508,622.51 was spent. Further, as a comparison to work completed on previously tenured land, this data was examined temporally as a proportion of total yearly expenditures. The percentage of exploration work undergone on post-announcement land staked has steadily increased in the QUEST area, to nearly 40% of the total reported exploration expenditures (see Figure 6).

### Anecdotal Results

Anecdotal evidence for the impact of exploration activities generated by Geoscience BC data publications is harder to identify because companies are neither motivated by competition (in staking and developing land before other companies) nor by economics (maintaining claims by registered exploration) to acknowledge government-related organizations within technical documents. A review of 50

assessment reports did not find any explicit mention of Geoscience BC, although a number of times descriptors such as ‘historical BC Geological Survey data,’ or ‘government data’ were used.

As a tool to generate new investor interest and raise capital, however, Geoscience BC could be used as a lightning rod. News releases accessed through SEDAR show several companies crediting Geoscience BC and related work. For example, a Fjordland Exploration Inc. press release from August 1, 2007, announced their ‘QUEST JV’, a joint venture with Serengeti Resources Inc. in anticipation of the Geoscience BC program to be released the following year. They go on to explain what they describe as a ‘mini-staking rush,’ with more than 400 000 ha of new lands registered with MTO. Notably, plans to complete a 3600 line-kilometre airborne geophysics survey were included in the report as an initial start to the program (Schroeter, 2007).

Similarly, Rimfire Minerals Corp. announced adding holdings to its claims in the Quesnel Trough, and the addition of airborne geophysical surveys to work with the coming geophysical and geochemical data from Geoscience BC, in their September 13, 2007 press release (Caulfield, 2007).

Richfield Ventures Corp. (now New Gold Inc.) reported in their February 7, 2008 press release, “the QUEST program covered the entire 250 000 acre land package of Richfield Ventures, and it appears to have yielded encouraging results.” Exploration for the following summer in the QUEST area included preliminary drilling at two properties (Bernier, 2008).

### Stock Market and Share Issuance

Increased activity within the QUEST area during 2005–2010 suggests that the project has stimulated financial ac-

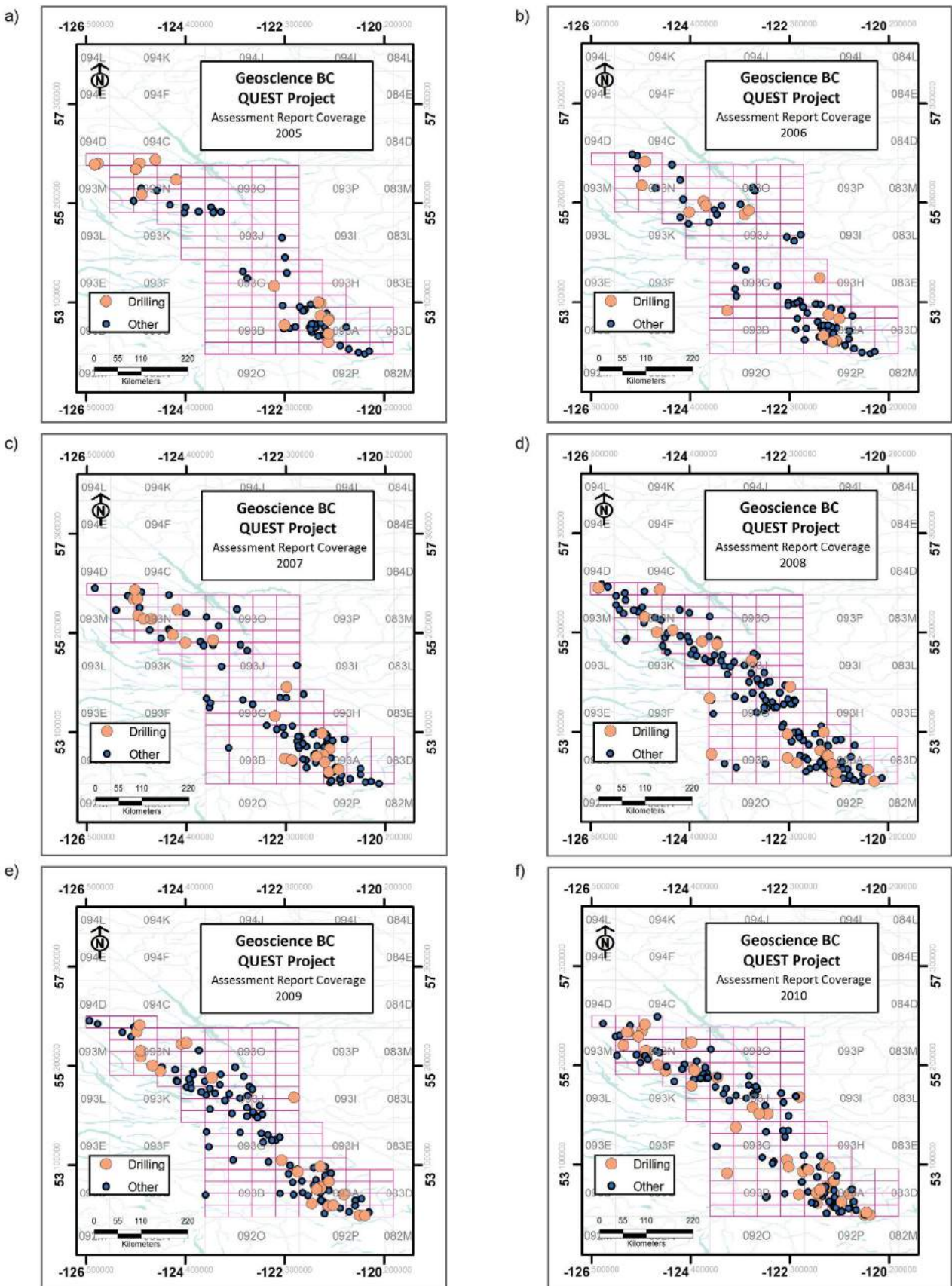


Figure 5. Greater QUEST (QUESnellia Exploration Strategy) area, comparing the increase in exploration activity (via assessment reporting) from prior to the QUEST Project (2005–2006) to during the QUEST Project (2007–2010).

tivity and promoted industry growth, while also mirroring the financial climate of the time. This latter aspect is an interesting artifact of the data.

The two venture indices, the 'mini' QUEST venture stock index of eight companies created for this study and the S&P/TSX Venture Composite Index, chart compellingly similar paths despite being vastly different in size (Figure 2; the S&P/TSX Venture Composite Index includes nearly 400 issues valued at close to \$20 billion), suggesting that financial imperatives prevail irrespective of scale. It is also evident from the price chart of the QUEST venture stock index that average share trading volumes on the Toronto Venture Exchange during the critical years of the QUEST Project tended to be much higher than those immediately preceding the start of the study period (2005), especially late 2006 to late 2008, and then again mid-2009 to 2010, when average trading volumes were triple those prevailing in 2005. Early 2008 witnessed the largest spike of trading volume in the period, coinciding with the public release of geochemical results and airborne electromagnetic survey data by Geoscience BC. While this increase in the publicly traded share volume of the QUEST index (and its constituent companies) cannot be attributed entirely to the heightened profile associated with the QUEST Project, a cursory examination of the chart strongly suggests a relationship.

Similarly, the QUEST venture stock index witnesses a parallel progression of price increase accompanied by increases in proceeds from new share issues and a rising level of expenditures on properties in the QUEST area, a trend that continued until the market downturn of 2008. Notably, the QUEST venture stock index almost immediately began a price recovery from that low and in 2010 saw a large surge in the value of new share issues.

This pattern also scales down to individual companies, as analysis of news releases on private placements of shares and securities archived in SEDAR shows. As one example, Alpha Gold Corp. issued news releases concerning private placements of its shares and securities starting in August 2005 with the closing of a \$600,000 private placement of nearly 1 million units comprising shares, flowthrough shares and stock warrants (Figure 7). In 2006, it announced private placements totalling \$1.4 million, with the bulk of the proceeds used to "... fund the ongoing exploration program at the Company's 100% owned Lustdust Property in central B.C." (Newswire, 2006).

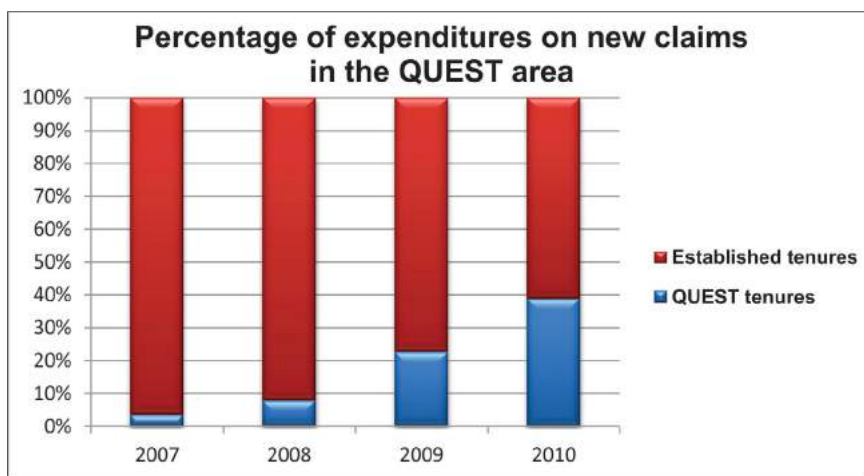


**Figure 6.** Gradual increase in proportional spending on land staked from 2007 to 2010 within the QUEST (Quesnellia Exploration STrategy) area.

Figure 7 shows the amounts raised<sup>1</sup> (in thousands of dollars; in green), amounts spent<sup>2</sup> (in thousands of dollars; in red) and share volumes<sup>3</sup> (in hundreds). Blue lines are linear regression lines reflecting average volumes traded before Geoscience BC started the QUEST Project and then during the critical 2007 and 2008 years. From 2005 to 2006, share volumes traded on the exchange are approximately 160 000 per month; by 2007 this had tripled to 500 000.

In June 2007, it closed private placements totalling \$4 million for use in its exploration programs (Canada Newswire, 2007) and in 2009 announced that its drilling program for the year was estimated at \$1.3 million, with \$3 million in the company's treasury (Canadian Newswire, 2009).

The monthly stock chart of Alpha Gold Corp. (now ALQ Gold Corp.) from 2005 to 2010 shows that according to the company's audited financial reports, it raised \$440,000 and \$470,000 in 2005 and 2006, respectively, from the proceeds of share issues. Beginning midway through 2006 and extending to 2009, a period coinciding first with anticipation in the markets of Geoscience BC's proposed project, its official announcement in 2007 and the public release of large amounts of data from geochemical and airborne geophysics surveys in 2008, share volumes of Alpha Gold Corp. traded on the TSX Venture Exchange tripled from an average of 160 000 shares per month in 2005 and 2006 to

<sup>1</sup>Amounts raised are the proceeds raised from the issuance of company shares, taken from the audited annual financial statements of Alpha Gold Corp. for 2005–2010 (<http://www.sedar.com>; statements of cash flows under Financing activities, Proceeds on issuance of shares, Net of issue costs).

<sup>2</sup>Amounts spent are estimates (similar to amounts raised) derived from the section under Investing Activities, Investment in and expenditures on exploration properties.

<sup>3</sup>Share volumes reflect the trading activity of Alpha Gold Corp.'s shares (trading symbol ALQ) on the TSX Venture Exchange in Toronto.

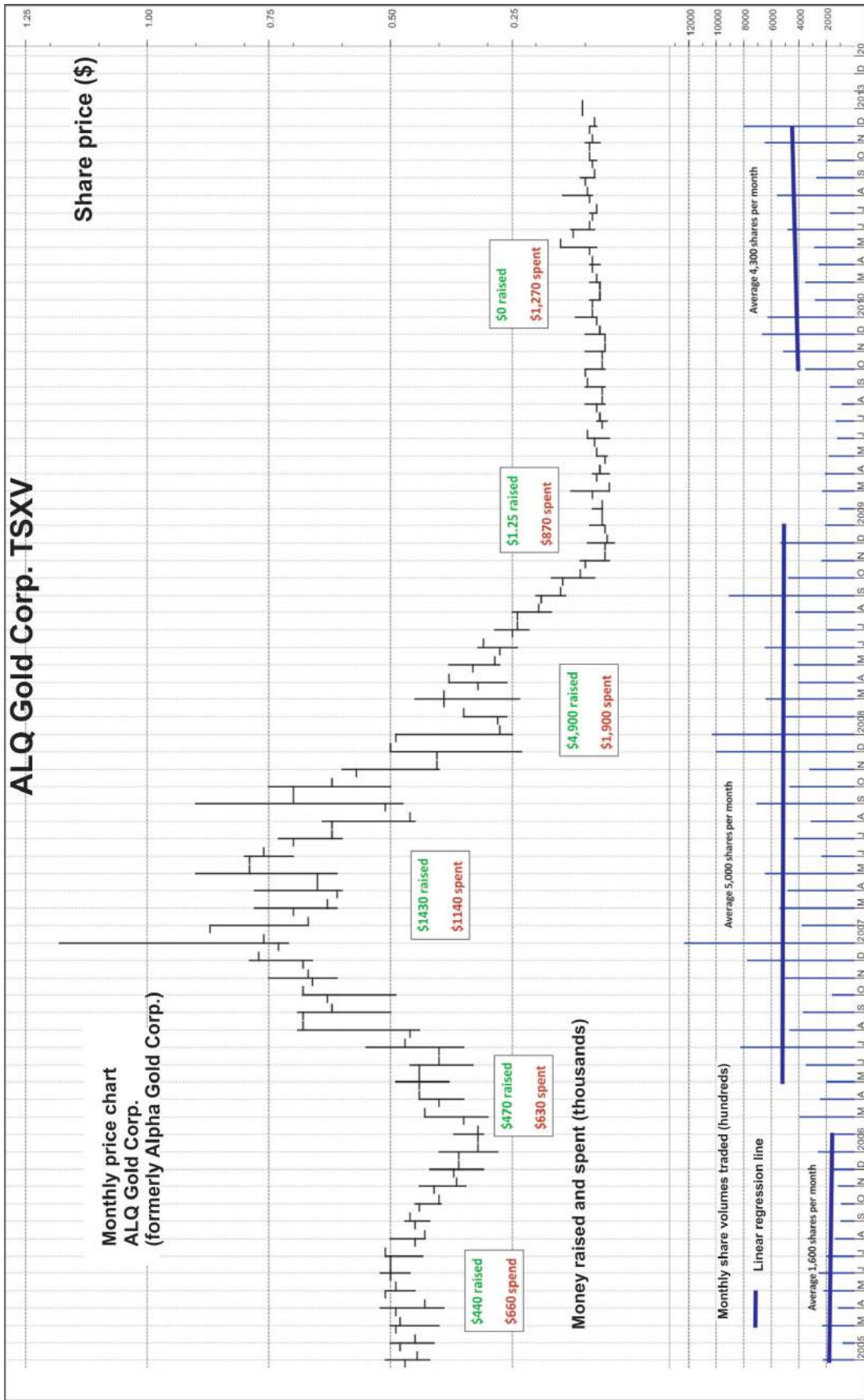


Figure 7. ALQ Gold Corp. (formerly Alpha Gold Corp.) monthly stock price chart 2005–2010.

500 000 shares in 2007 and 2008. During a crucial period of the QUEST Project, Alpha Gold Corp.'s heightened profile, reflected by large trading volumes on the stock exchange, enabled it in 2007 to raise three times as much funding as in previous years (\$1.4 million) and in 2008, more than ten times as much (\$4.9 million) from private placements as in 2006—despite watching its publicly listed share price drop to historic lows in concert with the market downturn of 2008.

## Conclusions

The QUEST initiative has enjoyed success and this is readily revealed in the public sources of information. Marked increases in fundraising and expenditures on new exploration and development by companies working in the QUEST area strongly supports arguments justifying the initial \$5 million that Geoscience BC committed to the project. Operators and mining companies enjoyed a clear boost in visibility in public financial markets and were able to raise much greater levels of funding than would otherwise have been the case in the absence of a 'great story' like the QUEST Project and the tangible contributions of a government-backed incentive program.

The method used here to characterize and measure these successes, based on readily available public sources, makes it repeatable and suggests that similar analytical projects could be undertaken and expanded upon using this preliminary study as a working basis.

## Acknowledgments

The author thanks Geoscience BC for funding this project and the BC Geological Survey, particularly A. Wilcox and P. Desjardins, for their help in acquiring data. A special note is given to W. Jackaman for his insight and knowledge in developing this project and D. Reichheld for assistance and providing editorial comments.

## References

Barlow, N.D., Flower, K.E., Sweeney, S.B., Robinson, G.L. and Barlow, J.R. (2010): QUEST and QUEST-West Property File: analysis and integration of Property File's Industry File documents with British Columbia's MINFILE (NTS 093; 094A, B, C, D; 103I); *in* Geoscience BC Summary of Activities 2009, Geoscience BC, Report 2010-1, p. 175–188, URL <[http://www.geosciencebc.com/i/pdf/SummaryofActivities2009/SoA2009\\_Barlow.pdf](http://www.geosciencebc.com/i/pdf/SummaryofActivities2009/SoA2009_Barlow.pdf)> [October 2013].

Barnett, C.T. and Williams, P.M. (2009): Using geochemistry and neural networks to map geology under glacial cover; Geoscience BC, Report 2009-3, 27 p., URL <[http://www.geosciencebc.com/i/project\\_data/QUESTdata/GBCReport2009-3/GBC\\_Report\\_2009-3.pdf](http://www.geosciencebc.com/i/project_data/QUESTdata/GBCReport2009-3/GBC_Report_2009-3.pdf)> [October 2013].

BC Geological Survey (2013a): ARIS assessment report indexing system; BC Ministry of Energy and Mines, URL <<http://www.empr.gov.bc.ca/Mining/Geoscience/ARIS/Pages/default.aspx>> [October 2013].

BC Ministry of Energy and Mines (2013b): Mineral Titles Online; BC Ministry of Energy and Mines, URL <<http://www.empr.gov.bc.ca/Titles/MineralTitles/mto/Pages/default.aspx>> [October 2013].

Bernier, P. (2008): Under the Rainbow; Richfield Ventures Corporation, press release, February 7<sup>th</sup>, 2008, URL <<http://www.sedar.com/GetFile.do?lang=EN&docClass=8&issuerNo=00026237&fileName=/csfsprod/data86/filings/01214203/00000001/i%3A%5CSEDAR%5CSJC%5CLori%5CRichfieldPRFeb7.pdf>> [October 2013].

Caulfield, D. (2007): Project update; Rimfire Minerals Corporation, press release, September 13, 2007, URL <<http://www.sedar.com/GetFile.do?lang=EN&docClass=8&issuerNo=00011905&fileName=/csfsprod/data84/filings/01158233/00000001/r%3A%5CCorporate%5CElectronicFiling%5CSEDAR%5C2007Filing%5CPR0722.pdf>> [October 2013].

Canadian Newswire (2007): Alpha Gold closes private placement of \$4 million; press release, June 13, 2007, URL <<http://www.newswire.ca/en/story/11449/alpha-gold-closes-private-placement-of-4-million>> [October 2013].

Canadian Newswire (2009): Alpha Gold prepares for 2009 summer drilling; press release, June 3, 2009, URL <<http://www.newswire.ca/en/story/55037/alpha-gold-prepares-for-2009-summer-drilling>> [October 2013].

Fraser, S.J. and Hodgkinson, J.H. (2009): An investigation using SiroSOM for the analysis of QUEST stream-sediment and lake-sediment geochemical data; Geoscience BC, Report 2009-14, 64 p., URL <[http://www.geosciencebc.com/i/project\\_data/GBC\\_Report2009-14/GBC\\_Report\\_2009-14.pdf](http://www.geosciencebc.com/i/project_data/GBC_Report2009-14/GBC_Report_2009-14.pdf)> [October 2013].

Geotech Limited (2008): Report on a helicopter-borne versatile time domain electromagnetic (VTEM) geophysical survey; QUEST Project, central British Columbia (NTS 93A, B, G, H, J, K, N, O & 94C, D); Geoscience BC, Report 2008-4, 35 p., URL <[http://www.geosciencebc.com/i/project\\_data/QUESTdata/report/7042-GeoscienceBC\\_final.pdf](http://www.geosciencebc.com/i/project_data/QUESTdata/report/7042-GeoscienceBC_final.pdf)> [October 2013].

Geotech Limited (2009): Helicopter-borne z-axis tipper electromagnetic (ZTEM) and aeromagnetic survey, Mt. Milligan test block; Geoscience BC, Report 2009-7, 51 p., URL <[http://www.geosciencebc.com/i/project\\_data/GBC\\_Report2009-7/2009-7\\_Report.pdf](http://www.geosciencebc.com/i/project_data/GBC_Report2009-7/2009-7_Report.pdf)> [October 2013].

Jackaman, W. (2008a): Regional lake sediment and water geochemical data, northern Fraser Basin, central British Columbia (parts of NTS 093G, H, J, K, N & O); Geoscience BC, Report 2008-5, 446 p., URL <[http://www.geosciencebc.com/i/project\\_data/QUESTdata/GBCReport2008-5/2008-5\\_Survey\\_Summary.pdf](http://www.geosciencebc.com/i/project_data/QUESTdata/GBCReport2008-5/2008-5_Survey_Summary.pdf)> [October 2013].

Jackaman, W. (2008b): QUEST Project sample reanalysis; Geoscience BC, Report 2008-3, 4 p, URL <[http://www.geosciencebc.com/i/project\\_data/QUESTdata/GBCReport2008-3/2008-3\\_README.pdf](http://www.geosciencebc.com/i/project_data/QUESTdata/GBCReport2008-3/2008-3_README.pdf)> [October 2013].

Newswire (2006): Alpha Gold closes private placement of \$1.4 million, press release, August 1, 2006, URL <<http://www.investorpoint.com/stock/ALQ:CA-ALQ%20Gold%20Corp./news/4170889>> [October 2013].

Owskiacki, G. and Payie, G. (2010): MINFILE update of the QUEST Project area, central British Columbia (parts of NTS 093A, B, G, H, J, K, N, O, 094C, D); *in* Geoscience BC Summary of Activities 2009, Geoscience BC, Report 2010-1, p. 189–202, URL <<http://www.geosciencebc.com/i/pdf>>

- [SummaryofActivities2009/SoA2009\\_Owsiacki.pdf](#)> [October 2013].
- Reichheld, S.A. (2013): Documentation and assessment of exploration activities generated by Geoscience BC data publications; *in* Geoscience BC Summary of Activities 2012, Geoscience BC, Report 2013-1, p. 125–130, URL <[http://www.geosciencebc.com/i/pdf/SummaryofActivities2012/SoA2012\\_Reichheld.pdf](http://www.geosciencebc.com/i/pdf/SummaryofActivities2012/SoA2012_Reichheld.pdf)> [October 2013]
- Sander Geophysics Limited (2008): Airborne gravity survey, Quesnellia Region, British Columbia, 2008; Geoscience BC, Report 2008-8, 121 p., URL <[http://www.geosciencebc.com/i/project\\_data/QUESTdata/GBCReport2008-8/Gravity\\_Technical\\_Report.pdf](http://www.geosciencebc.com/i/project_data/QUESTdata/GBCReport2008-8/Gravity_Technical_Report.pdf)> [October 2013].
- Schroeter, T. (2007): Fjordland and Serengeti partner on QUEST Project; Fjordland Exploration Inc., press release, August 1, 2007, URL <<http://www.sedar.com/GetFile.do?lang=EN&docClass=8&issuerNo=00005747&fileName=/csfsprod/data83/filings/01135462/00000001/C%3A%5CMG%5CFEX%5Cnr%5Cnr07-12.pdf>> [October 2013].
- SEDAR (2013): Public company documents; SEDAR, system for electronic document analysis and retrieval, URL <[http://www.sedar.com/privacy\\_statement\\_en.htm](http://www.sedar.com/privacy_statement_en.htm)> [October 2013].
- TSX Inc. (2013): Overview – S&P/TSX Composite Index; TMX Group Ltd., URL <<http://web.tmxmoney.com/indices.php?section=tsx&index=^TSX#indexInfo>> [October 2013].





© 2014 by Geoscience BC.

All rights reserved. Electronic edition published 2013.

This publication is also available, free of charge, as colour digital files in Adobe Acrobat® PDF format from the Geoscience BC website: <http://www.geosciencebc.com/s/DataReleases.asp>.

Every reasonable effort is made to ensure the accuracy of the information contained in this report, but Geoscience BC does not assume any liability for errors that may occur. Source references are included in the report and the user should verify critical information.

When using information from this publication in other publications or presentations, due acknowledgment should be given to Geoscience BC. The recommended reference is included on the title page of each paper. The complete volume should be referenced as follows:

Geoscience BC (2014): Geoscience BC Summary of Activities 2013; Geoscience BC, Report 2014-1, 138 p.

ISSN 1916-2960 Summary of Activities (Geoscience BC)

**Cover photo:** Glacially carved U-shaped valley in the Itcha and Ilgachuz mountain ranges, TREK project area, British Columbia

**Photo credit:** David Sacco



## Acknowledgments

I would like to thank the government of British Columbia for its ongoing support in making it possible for Geoscience BC to fund quality geoscience research and data collection. I would also like to express appreciation for the leaders in British Columbia's mineral exploration, mining, and oil and gas sectors who support our organization through their guidance, use and recognition of the information that we collect and distribute.

Robin Archdekin  
President & CEO  
Geoscience BC  
[www.geosciencebc.com](http://www.geosciencebc.com)



## Foreword

Geoscience BC is pleased to present results from several of our ongoing geoscience projects and surveys in this, our seventh edition of the *Geoscience BC Summary of Activities*. The volume is divided into two sections, 'Minerals' and 'Oil and Gas', and contains a total of 14 papers.

The 'Minerals' section contains 11 papers from Geoscience BC minerals projects throughout the province. In the first paper, Geoscience BC's QUEST (QUesnellia Exploration STRategy) Project, a minerals research project launched in 2007, is used as a case study to measure investment in the province based on Geoscience BC-funded research. Reichheld addresses the success of Geoscience BC's investments as a return for the province from 2007 to 2010, using readily available public sources to ensure repeatability for similar analytical projects in the future.

The next three papers describe activities of Geoscience BC's newest major project, TREK (Targeting Resources through Exploration and Knowledge). Clifford and Hart provide an overview of 2013 activities, focusing on the TREK airborne magnetic survey and the purchase of proprietary industry airborne magnetic data. Sacco et al. describe the regional geochemistry program and basal-till potential mapping methods, and Lett and Jackaman detail the geothermal sampling program undertaken around the Nazko cone.

The papers following the TREK Project papers present interim results from three smaller Geoscience BC partnership projects in the same region of the province. Bordet et al. present a three-dimensional thickness model for the Chilcotin and Nechako plateaus; Celis et al. describe continued work on porphyry indicator minerals from alkalic porphyry Cu-Au deposits, including Mount Polley, Mount Milligan and Copper Mountain; and del Real et al. present new work on the paragenesis, alteration and mineralization at two of the porphyry deposits on the Woodjam property.

Moving to southern BC, the paper by Mortensen presents U-Pb ages, geochemistry and Pb-isotopic compositions of intrusions and associated mineralization in the southern Quesnel terrane. Webster and Pattison build on their project on the southern Kootenay Arc with new U-Pb ages to help constrain the area's geological evolution and associated mineralizing events. Clifford provides an update on Geoscience BC's SEEK (Stimulating Exploration in the East Kootenays) Project and summarizes two projects undertaken during 2013: an updated East Kootenay Gravity Database plus newly acquired gravity data in the St. Mary River area (released November 2013); and a paleomagnetic study that involved the collection of samples this past field season, with final results expected by summer 2014.

The last paper in this section describes research into a resource new to Geoscience BC's project portfolio. Derry et al. detail the creation of a database and heat favourability maps to quantify the resource potential for BC's geothermal power.

In the 'Oil and Gas' section of this year's volume, we present three papers. Salas and Walker provide an update on the regional seismograph network in northeastern BC. Following this is a description of a new subsurface aquifer study, recently undertaken by Hayes and Costanzo in the Liard Basin of northeastern BC to support unconventional oil and gas development. In the last paper of this section, Salas et al. give an update on the three-year surface-water monitoring program in the Horn River Basin, now entering its final year.

Readers are encouraged to visit our website for additional information on all Geoscience BC-funded projects, including project descriptions, posters and presentations, previous *Summary of Activities* or *Geological Fieldwork* papers, and final datasets and reports. The website also contains information on many of Geoscience BC's other activities, including workshops and student scholarships. All papers in this and past volumes are available for download through Geoscience BC's website ([www.geosciencebc.com](http://www.geosciencebc.com)). Limited print copies of past volumes are also available from the Geoscience BC office.

### Geoscience BC Publications 2013

In addition to this *Summary of Activities* volume, Geoscience BC releases interim and final products from our projects as Geoscience BC reports. All Geoscience BC data and reports can be accessed through our website at [www.geosciencebc.com/s/DataReleases.asp](http://www.geosciencebc.com/s/DataReleases.asp). Geoscience BC datasets and reports released in 2013 are:

- 14 technical papers in the *Geoscience BC Summary of Activities 2012* volume
- **Heliborne High Resolution Aeromagnetic Survey: Northern Vancouver Island, BC**, by Geo Data Solutions (Geoscience BC Report 2013-02)

- **Heliborne High Resolution Aeromagnetic Survey: QUEST-Northwest Project Area, BC, Block 3**, by Geo Data Solutions (Geoscience BC Report 2013-03)
- **Lardeau (NTS 082K) Sample Reanalysis (ICP-MS)**, by W. Jackaman (Geoscience BC Report 2013-04)
- **Iskut River Area Geology, Northwest BC (104B/08, 09, 10 & part of 104B/01, 07/11)**, by P.D. Lewis (Geoscience BC Report 2013-05)
- **McLeod Lake (NTS 093J) Sample Reanalysis (INAA)**, by W. Jackaman (Geoscience BC Report 2013-06)
- **Burrell Creek Map**, by T. Hoy and W. Jackaman (Geoscience BC Report 2013-07)
- **Ice Flow Patterns in NTS 093G, H (west half) & J, and Detailed Ice Flow History for NTS 093J/05, 06, /11, /12, /13 & /14**, by D.A. Sacco, B.C. Ward and D.E. Maynard (Geoscience BC Report 2013-08)
- **Nelson (NTS 082F) Sample Reanalysis (ICP-MS)**, by W. Jackaman (Geoscience BC Report 2013-09)
- **New Terrain Maps in the McLeod Lake Map Area (NTS 093J), British Columbia**, by D.A. Sacco, B.C. Ward, M. Geertsema and D.E. Maynard (Geoscience BC Report 2013-10)
- **Regional Stream Sediment and Water Geochemical Data, Northern Vancouver Island, British Columbia**, by W. Jackaman (Geoscience BC Report 2013-11)
- **Northern Vancouver Island Till Sample Reanalysis (ICP-MS)**, by W. Jackaman (Geoscience BC Report 2013-12)
- **Leveraging Earth Science Standards to Enhance Mineral Exploration Success in British Columbia: Seeking the Efficiencies of Order**, by C. Smyth (Geoscience BC Report 2013-13)
- **Linking Porphyry Deposit Geology to Geophysics via Physical Properties: Adding Value to Geoscience BC Geophysical Data**, by D.E. Mitchinson, R.J. Enkin and C.J.R. Hart (Geoscience BC Report 2013-14)
- **Drift Prospecting for Porphyry Copper-Gold, Volcanogenic Massive Sulphide Mineralization and Precious and Base Metal Veins within the QUEST Project Area, Central British Columbia (NTS 093J)**, by B.C. Ward, M.I. Leybourne, D.A. Sacco, R.E. Lett and L.C. Struik (Geoscience BC Report 2013-15)
- **Geochemical Techniques for Detection of Blind Porphyry Copper-Gold Mineralization under Basalt Cover, Woodjam Property, South-Central British Columbia (NTS 093A/03, 06)**, by T. Bissig, D.R. Heberlein and C.E. Dunn (Geoscience BC Report 2013-17)
- **Examining Present and Future Water Resources for the Kiskatinaw River Watershed, British Columbia**, by University of Northern British Columbia (Geoscience BC Report 2013-19)
- **Use of Organic Media in the Geochemical Detection of Blind Porphyry Copper-Gold Mineralization in the Woodjam Property Area, South-Central BC (NTS 093A/03, /06)**, by D.R. Heberlein, C.E. Dunn and B. MacFarlane (Geoscience BC Report 2013-20)
- **Geology of the Mount Polley Intrusive Complex (Draft Version)**, by C. Rees, G. Gillstrom, L. Ferreira, L. Bjornson and C. Taylor (Geoscience BC Report 2013-21)
- **A Geo-Exploration Atlas of the Endako Porphyry Molybdenum District (Draft Version)**, by F. Devine, M. Pond, D.R. Heberlein, P. Kowalczyk, W. Kilby and F. Ma (Geoscience BC Report 2013-22)
- **Stimulating Exploration in the East Kootenays (SEEK Project): The Updated East Kootenay Gravity Database (EKGDB) and the 2013 St. Mary Gravity Survey**, by T. Sanders (Geoscience BC Report 2013-23)

All releases of Geoscience BC reports and data are announced through our website and e-mail list. If you are interested in receiving e-mail regarding these reports and other Geoscience BC news, please contact [info@geosciencebc.com](mailto:info@geosciencebc.com).

Andrea Clifford  
Project Co-ordinator & Communications Manager  
Geoscience BC  
[www.geosciencebc.com](http://www.geosciencebc.com)

## Contents

### Minerals Projects

<b>S.A. Reichheld:</b> Documentation and assessment of exploration activities generated by Geoscience BC data publications, QUEST Project, central British Columbia . . . . .	1	Deerhorn porphyry deposits, Woodjam property, central British Columbia . . . . .	63
<b>A.L. Clifford and C.J.R. Hart:</b> Targeting Resources through Exploration and Knowledge (TREK): Geoscience BC's newest minerals project, Interior Plateau region, British Columbia . . . . .	13	<b>J.K. Mortensen:</b> U-Pb ages, geochemistry and Pb-isotopic compositions of Jurassic intrusions, and associated Au(-Cu) skarn mineralization, in the southern Quesnel terrane, southern British Columbia . . . . .	83
<b>D.A. Sacco, W. Jackaman and T. Ferbey:</b> Targeted geochemical and mineralogical surveys in the TREK Project area, central British Columbia . . . . .	19	<b>E.R. Webster and D.R.M. Pattison:</b> U-Pb dates for the Nelson and Bayonne magmatic suites in the Salmo-Creston area, southeastern British Columbia: tectonic implications for the southern Kootenay Arc . . . . .	99
<b>R.E. Lett and W. Jackaman:</b> Geochemical expression in soil and water of carbon dioxide seepages near the Nazko volcanic cone, central British Columbia . . . . .	35	<b>A.L. Clifford:</b> SEEK project update: Stimulating Exploration in the East Kootenays, southeastern British Columbia . . . . .	115
<b>E. Bordet, M.G. Mihalynuk, C.J.R. Hart and M. Sanchez:</b> Three-dimensional thickness model for the Eocene volcanic sequence, Chilcotin and Nechako plateaus, south-central British Columbia . . . . .	43		
<b>M.A. Celis, F. Bouzari, T. Bissig, C.J.R. Hart and T. Ferbey:</b> Petrographic characteristics of porphyry indicator minerals from alkalic porphyry copper-gold deposits in south-central British Columbia . . . . .	53		
<b>I. del Real, C.J.R. Hart, F. Bouzari, J.L. Blackwell, A. Rainbow and R. Sherlock:</b> Relationships between calcalkalic and alkalic mineralization styles at the copper-molybdenum Southeast Zone and copper-gold			

### Oil and Gas Projects

<b>A.A. Derry, A. Thompson, L. Deibert, D. Yang, A. Pollock:</b> British Columbia geothermal power and heat favourability maps and database . . . . .	119
<b>C.J. Salas and D. Walker:</b> Update on regional seismograph network in northeastern British Columbia. . . . .	123
<b>B.J.R. Hayes and S. Costanzo:</b> Subsurface aquifer study to support unconventional gas and oil development, Liard Basin, northeastern British Columbia . . . . .	127
<b>C.J. Salas, D. Murray and C. Davey:</b> Horn River Basin Water Project update, northeastern British Columbia .	135



# Documentation and Assessment of Exploration Activities Generated by Geoscience BC Data Publications, QUEST Project, Central British Columbia (NTS 093A, B, G, H, J, K, N, O, 094C, D)

S.A. Reichheld, Consultant, Sooke, BC, sa.reichheld@gmail.com

---

Reichheld, S.A. (2014): Documentation and assessment of exploration activities generated by Geoscience BC data publications, QUEST Project, central British Columbia (NTS 093A, B, G, H, J, K, N, O, 094C, D); in Geoscience BC Summary of Activities 2013, Geoscience BC, Report 2014-1, p. 1–12.

## Introduction

This study focuses on the QUEST (QUesnellia Exploration STRategy) Project, launched by Geoscience BC in 2007. Its goal was to stimulate exploration interest and investment in the underexplored region between Williams Lake and the District Municipality of Mackenzie, in part to help diversify the local forestry-based economies impacted by the mountain pine beetle infestation. Geoscience BC initially funded the re-analysis of 5000 archived regional geochemical samples and the collection of 2200 new geochemical samples, plus two large-scale airborne geophysical surveys (Geotech Limited, 2008; Jackaman, 2008a, b; Sander Geophysics Limited, 2008). The raw data was made available to the public starting in 2008, at which point Geoscience BC also commissioned a number of follow-up, value-added projects that were released in subsequent years (Barnett and Williams, 2009; Fraser and Hodgkinson, 2009; Geotech Limited, 2009; Barlow et al., 2010; Owsiaci and Payie, 2010), providing the industry with announcements and data to continue to attract exploration to the area. As indicated in the preliminary paper for this project (Reichheld, 2013) it is felt that the QUEST Project, with its years of data and development, now has a sufficient track record to produce quantifiable and meaningful results.

This paper details the research completed in order to lay out a framework for reviewing and assessing the impact of this and any public exploration initiative. To ensure the method remains repeatable into the future, only public sources of information are used.

## Method

The study area encompasses the greater QUEST area, including all or parts of NTS map areas 093A, B, G, H, J, K,

N, O and 094 C, D. Exploration data was presented in GIS shapefiles, or in Excel<sup>®</sup> spreadsheets with co-ordinates attached to georeference the datasets. Each dataset used was clipped to the nearest 1:50 000 NTS map area around the QUEST area to maintain equal datasets. ArcGIS 10.2 was used as a platform for working with much of the data. Stock market index and price charts were created using MetaStock Pro software.

The framework for this project includes assimilating relevant data from Mineral Titles Online (MTO), the Assessment Report Indexing System (ARIS), MINFILE and evaluating anecdotal sources including corporate press releases, financial statements, share offerings and stock price data for companies listed on the TSX Venture Exchange.

The period covered is 2007–2010 to ensure that a large portion of the data is publicly available. In 2005, changes in claim staking techniques from on-ground to online methods using MTO and internet staking led to a surge that potentially distorts the true extent of operator participation in the field. As a baseline, only data from 2005 to 2006 are used to offer perspective on developments leading up to the study period.

The MTO claim staking has been used as a general indicator of success within a given region, but while this approach has merit, it must be considered carefully. For QUEST area staking, the presence of large, long-established claims, operating mines and known past anomalies can have a trickle-down effect on the activity statistics because large blocks of surrounding land may be staked as a combination of ground inventorying, pre-emptive staking or claim jumping, but not necessarily for speculative purposes. Determining which staking is genuinely motivated by exploration is a complex task. Rather than break down what could be called ‘defensive staking’, with regards to locking up high-potential lands before they can be worked on by the owner, the merits of mineral titles were used to analyze actual on-the-ground activities. By considering length of tenure, frequency of new claims staked and work submitted on the land through assessment reports, a truer relationship of claim use can be distinguished. ArcGIS was used to exam-

---

**Keywords:** QUEST Project, mineral exploration, grassroots, public funding, SEDAR, assessment reports, MINFILE, investment capital, data release

This publication is also available, free of charge, as colour digital files in Adobe Acrobat<sup>®</sup> PDF format from the Geoscience BC website: <http://www.geosciencebc.com/s/DataReleases.asp>.

ine land tenures to find total land tenure for each year, new land tenure for each year and to determine under what category of tenure assessment reports were submitted (BC Ministry of Energy and Mines, 2013).

The second major source of information, assessment reports for the study period, is just now becoming available to the public (BC Geological Survey, 2013). Assessment reports found in ARIS were examined using ArcGIS to evaluate important variables including expenditures, yearly submissions and exploration location. Given rising demand and commodity prices during this period, a rise in overall exploration spending in the region is at least partly indicative of increased exploration throughout British Columbia. To differentiate this spending from overall totals that may be somewhat misleading, assessment reports were examined using ArcGIS to find the number of assessment reports submitted for each year within the study area, the total reported dollars spent and their locations on newly tenured or previously tenured land. Expenditures could then be broken down into yearly data from which totals and trends within the region could be identified. Questions to ask are: just how successful has the \$5 million investment by Geoscience BC been as a return for the province? Is there a noticeable difference in total activity in general, and in generating new exploration specifically?

Factors often considered peripheral to in-the-field exploration and development, such as the performance of a company's shares in the stock market, can be instrumental to its success. The ability to raise new investment capital each year is an important part of the mine cycle, and investors frequently base their buying decisions on financial performance. How well an enterprise performs in the stock market is often a bellwether to its long-term success in the field. A fundamental question then is: does participation in Geoscience BC projects like QUEST endow companies with superior prospects on public stock exchanges?

Evaluating the financial component includes analysis of the trading record of stock prices and share volumes to ascertain whether individual companies involved in the QUEST Project enjoyed increased market activity, and at an industry level, whether mining stocks in general performed well in the market during the study period. Most firms studied here are micro- and small-cap companies trading on the TSX Venture Exchange. The S&P/TSX Venture Composite Index was tracked as a proxy for observing the industry's performance during the study period. It is described in the exchange's own literature as "...a broad market capitalization-based index which is designed to measure the performance of securities listed on the TSX Venture Exchange, Canada's primary venture equity market" (TSX Inc., 2013).

Next, a 'mini' index, herein named the QUEST venture stock index, comprising eight publicly listed companies with properties in the QUEST Project area, was created for this study using Equis MetaStock Pro and its FIRE add-on (Figure 1). The eight companies range from less than \$1 million in overall exploration projects to tens of millions. The index incorporates the shares of the following companies (using names as they appeared during the period of study): Alpha Gold Corp., Amarc Resources Ltd., Barker Minerals Ltd., Dajin Resources Corp., Fjordland Exploration Inc., Happy Creek Minerals Ltd., Richfield Ventures Corp. and Serengeti Resources Corp.

The S&P/TSX Venture Composite and the mini QUEST venture stock indices were charted in MetaStock Pro (Figure 2).

The research also took an anecdotal look into several larger public companies operating within the QUEST area using ARIS and SEDAR (system for electronic document analysis and retrieval; 2013), the latter of which provides access to public securities documents and information filed by public companies and investment funds. Here, important avenues for research include press releases, corporate financial statements and annual reports. Using SEDAR and ARIS, company press releases and assessment reports were sampled to get an indication of how frequently, or infrequently, Geoscience BC data and the QUEST Project received mention in the media.

Although financial reports and news releases are valuable sources of information, they offer it in a labour-intensive format. Company name changes, mergers and acquisitions, joint ventures and partnerships all tend to muddy the waters of research and hamper understanding of an operator's business. A stock exchange-listed company offers the widest scope for research, but navigating annual reports can be a limiting factor, requiring interpretation in light of accepted accounting principles.

## Results

Mineral tenures were divided into two groups: total ground tenured within each year and newly tenured ground within each year (Figure 3). Both groups peaked in 2007, with total ground staked at 2 916 922 hectares (ha) and newly staked ground at 1 428 387 ha. Evaluating the staking of ground can be difficult due to 'dead staking', which is evident to the eye when examining the large areas of tenure that were allowed to lapse and then return as fresh tenures the following year (Figure 4). With that caveat, land tenured averaged 2 477 037 ha, an increase of more than 35% from its 'pre-QUEST' 2006 value of 1 834 055 ha. Newly staked land averaged 919 823 ha during the same period.

In contrast to the interpretive challenges arising from practices like dead staking and the complexities of claim owner-

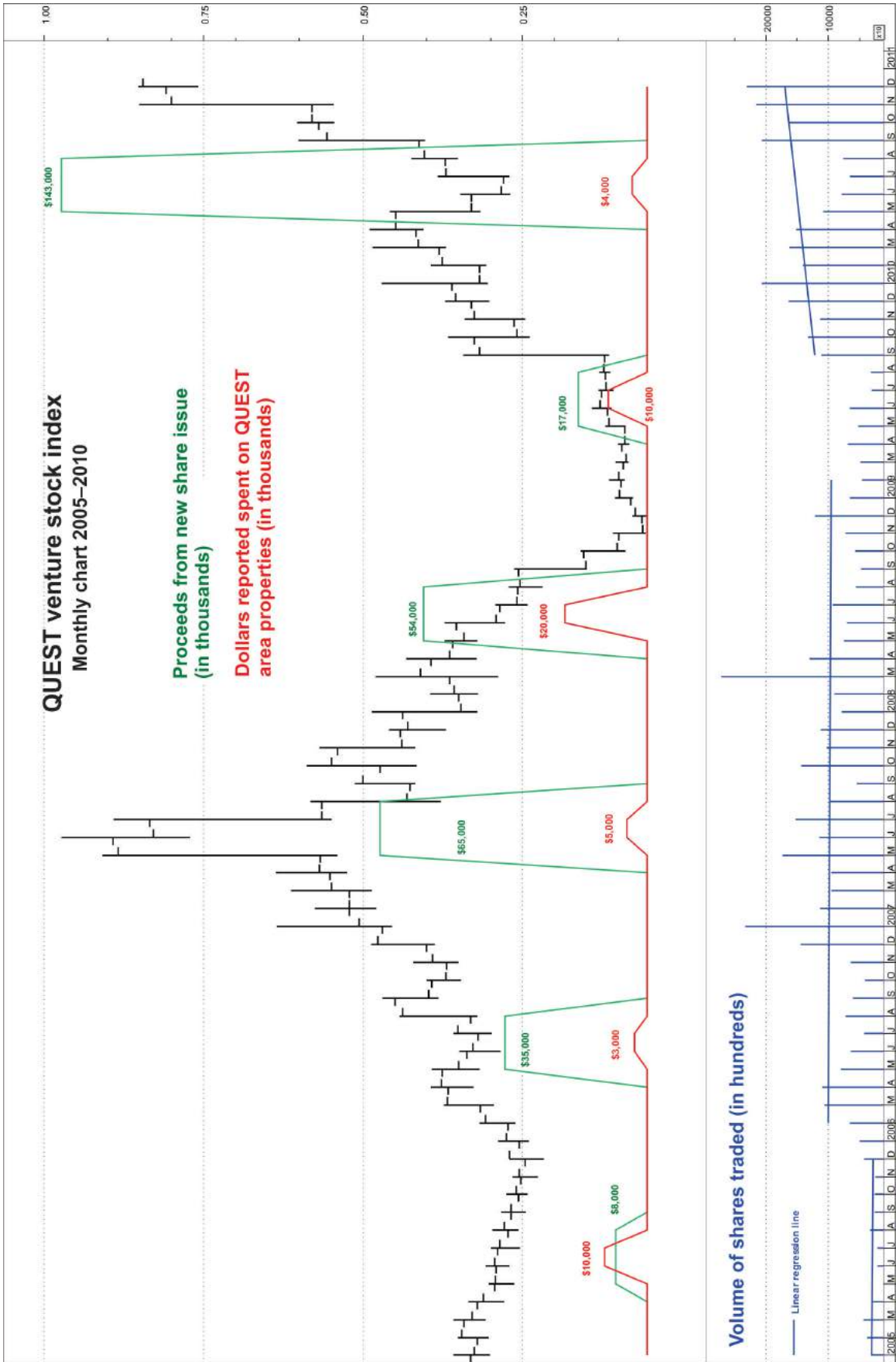


**Figure 1.** Monthly stock price chart of the QUEST venture stock index, representing eight operators within the QUEST (Quesnellia Exploration Strategy) area. The red indicator represents estimated expenditures on QUEST projects as reported in assessment reports. The green indicator represents estimated proceeds arising from new share issues.

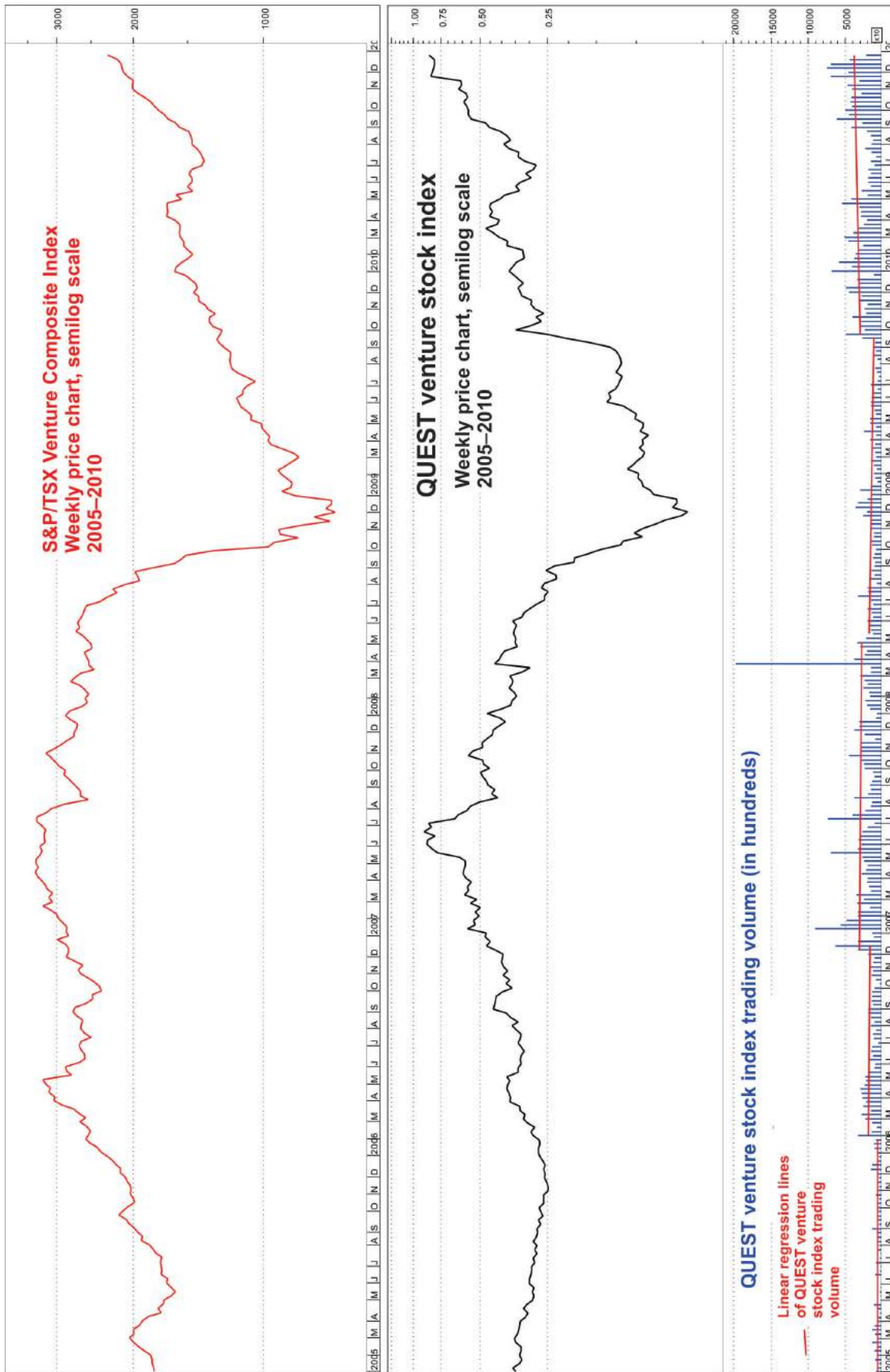


**Figure 2.** Weekly price chart comparing the S&P/TSX Venture Composite Index with the QUEST venture stock index during the 2008 market downturn. The linear regression lines of trading volume for the QUEST venture stock index reveal an upward 'stairstep' pattern of increasing stock market activity leading into the 2008 collapse.

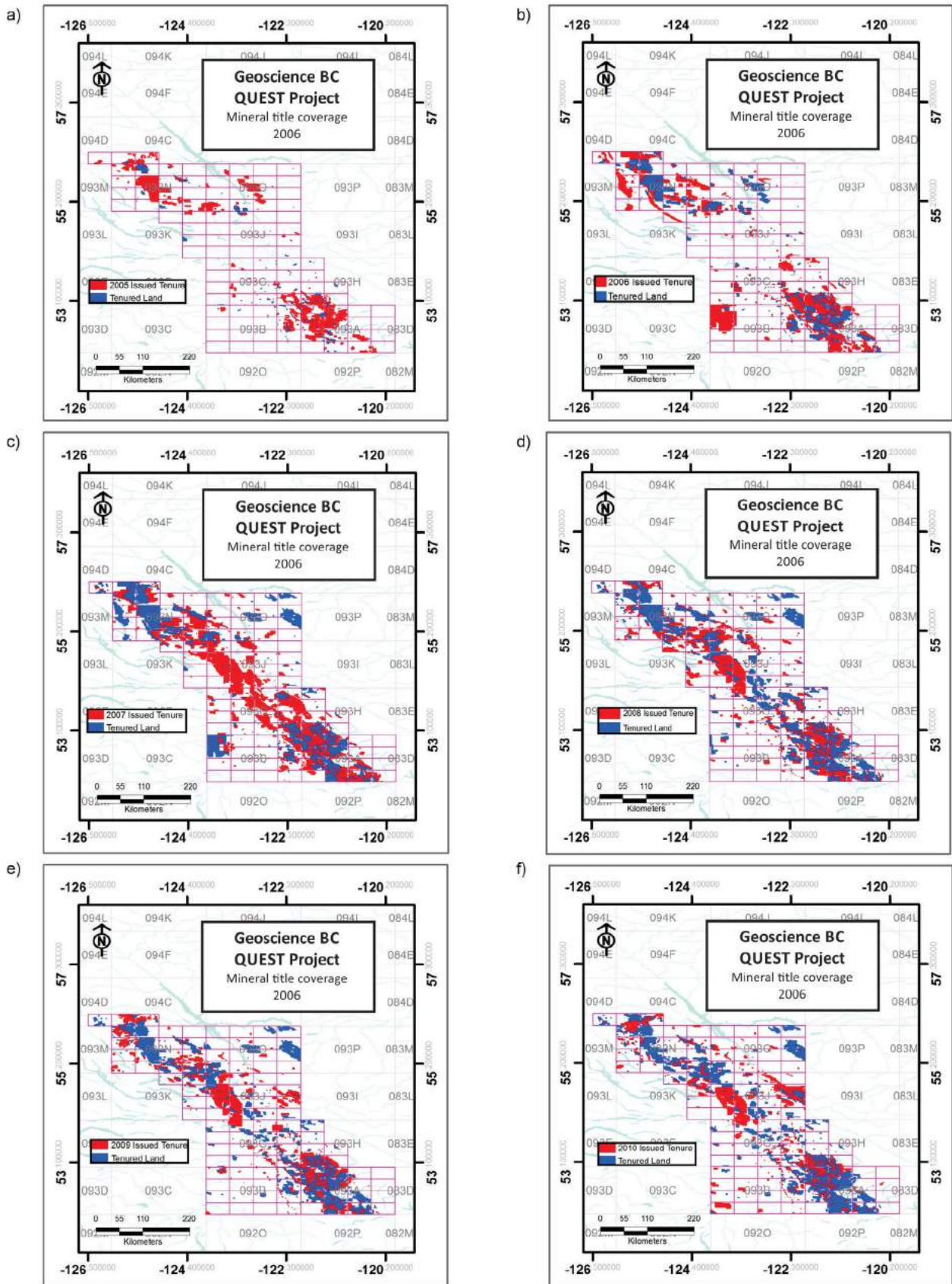


**Figure 3.** Changes in mineral title tenure for the greater QUEST (QUesnellia Exploration STRategy) area: a) 2005; b) 2006; c) 2007; d) 2008; e) 2009; f) 2010.

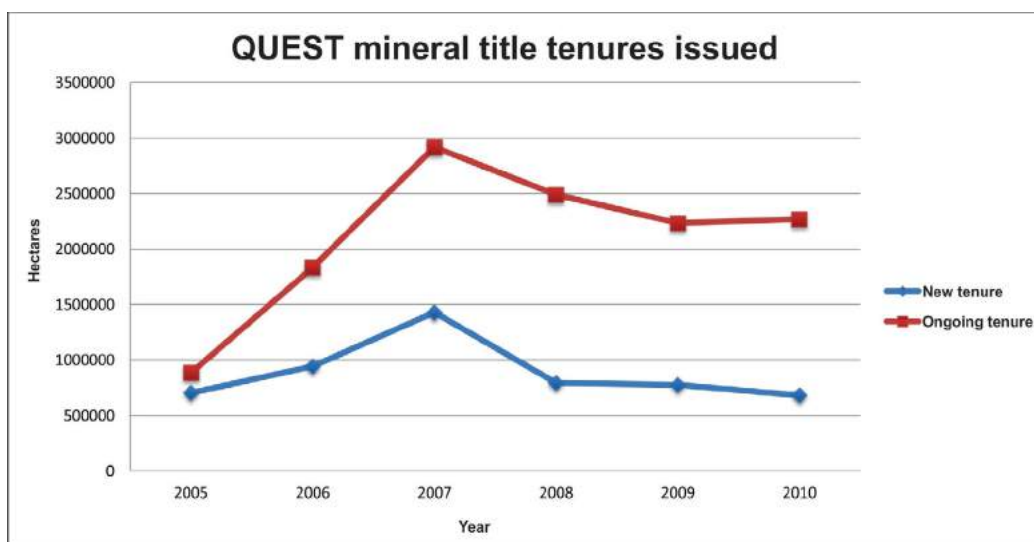


**Figure 4.** QUEST (Quesnellia Exploration Strategy) mineral title tenures issued from 2005 to 2010. The blue line indicates area of new claims issued. The red line shows total tenured land. The increase in tenure is indicative of sustained interest in the area.

ship, assessment reports represent basic, quantifiable results of exploration in terms of monetary expenditure. For the reporting period of 2007–2010, there were 501 assessment reports submitted on the ground within the QUEST Project footprint (Figure 5). In the baseline years 2005 and 2006, there were a total of 153 assessment reports submitted in the same area, indicating an average of 125 per year during the QUEST Project compared to 76 per year before the QUEST Project. Reported expenditures for the study period totalled \$79,106,618.97 (BC Geological Survey, 2013a). The average yearly expenditures for the two years prior to the QUEST Project amounted to \$10,910,220, compared to the four-year QUEST Project average of \$19,776,655—a rise in overall reported spending activity for the area of nearly 100%. Although these numbers clearly reflect a significant increase in exploration within the QUEST area, they do not specifically point to an increase in new exploration development. On land previously untenured before the study period, assessment reports indicate a total of \$15,508,622.51 was spent. Further, as a comparison to work completed on previously tenured land, this data was examined temporally as a proportion of total yearly expenditures. The percentage of exploration work undergone on post-announcement land staked has steadily increased in the QUEST area, to nearly 40% of the total reported exploration expenditures (see Figure 6).

### Anecdotal Results

Anecdotal evidence for the impact of exploration activities generated by Geoscience BC data publications is harder to identify because companies are neither motivated by competition (in staking and developing land before other companies) nor by economics (maintaining claims by registered exploration) to acknowledge government-related organizations within technical documents. A review of 50

assessment reports did not find any explicit mention of Geoscience BC, although a number of times descriptors such as ‘historical BC Geological Survey data,’ or ‘government data’ were used.

As a tool to generate new investor interest and raise capital, however, Geoscience BC could be used as a lightning rod. News releases accessed through SEDAR show several companies crediting Geoscience BC and related work. For example, a Fjordland Exploration Inc. press release from August 1, 2007, announced their ‘QUEST JV’, a joint venture with Serengeti Resources Inc. in anticipation of the Geoscience BC program to be released the following year. They go on to explain what they describe as a ‘mini-staking rush,’ with more than 400 000 ha of new lands registered with MTO. Notably, plans to complete a 3600 line-kilometre airborne geophysics survey were included in the report as an initial start to the program (Schroeter, 2007).

Similarly, Rimfire Minerals Corp. announced adding holdings to its claims in the Quesnel Trough, and the addition of airborne geophysical surveys to work with the coming geophysical and geochemical data from Geoscience BC, in their September 13, 2007 press release (Caulfield, 2007).

Richfield Ventures Corp. (now New Gold Inc.) reported in their February 7, 2008 press release, “the QUEST program covered the entire 250 000 acre land package of Richfield Ventures, and it appears to have yielded encouraging results.” Exploration for the following summer in the QUEST area included preliminary drilling at two properties (Bernier, 2008).

### Stock Market and Share Issuance

Increased activity within the QUEST area during 2005–2010 suggests that the project has stimulated financial ac-

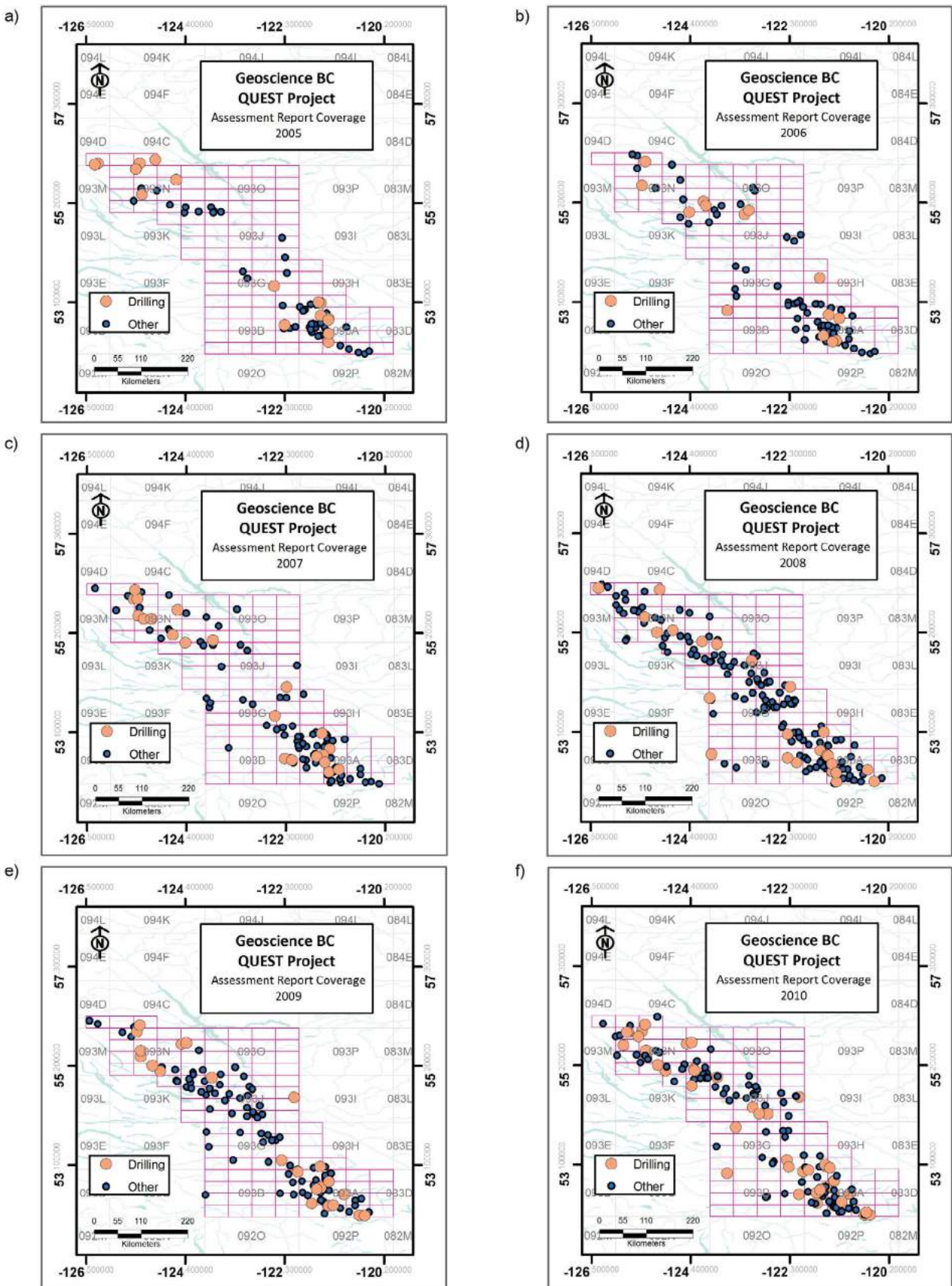


Figure 5. Greater QUEST (QUESnellia Exploration Strategy) area, comparing the increase in exploration activity (via assessment reporting) from prior to the QUEST Project (2005–2006) to during the QUEST Project (2007–2010).

tivity and promoted industry growth, while also mirroring the financial climate of the time. This latter aspect is an interesting artifact of the data.

The two venture indices, the 'mini' QUEST venture stock index of eight companies created for this study and the S&P/TSX Venture Composite Index, chart compellingly similar paths despite being vastly different in size (Figure 2; the S&P/TSX Venture Composite Index includes nearly 400 issues valued at close to \$20 billion), suggesting that financial imperatives prevail irrespective of scale. It is also evident from the price chart of the QUEST venture stock index that average share trading volumes on the Toronto Venture Exchange during the critical years of the QUEST Project tended to be much higher than those immediately preceding the start of the study period (2005), especially late 2006 to late 2008, and then again mid-2009 to 2010, when average trading volumes were triple those prevailing in 2005. Early 2008 witnessed the largest spike of trading volume in the period, coinciding with the public release of geochemical results and airborne electromagnetic survey data by Geoscience BC. While this increase in the publicly traded share volume of the QUEST index (and its constituent companies) cannot be attributed entirely to the heightened profile associated with the QUEST Project, a cursory examination of the chart strongly suggests a relationship.

Similarly, the QUEST venture stock index witnesses a parallel progression of price increase accompanied by increases in proceeds from new share issues and a rising level of expenditures on properties in the QUEST area, a trend that continued until the market downturn of 2008. Notably, the QUEST venture stock index almost immediately began a price recovery from that low and in 2010 saw a large surge in the value of new share issues.

This pattern also scales down to individual companies, as analysis of news releases on private placements of shares and securities archived in SEDAR shows. As one example, Alpha Gold Corp. issued news releases concerning private placements of its shares and securities starting in August 2005 with the closing of a \$600,000 private placement of nearly 1 million units comprising shares, flowthrough shares and stock warrants (Figure 7). In 2006, it announced private placements totalling \$1.4 million, with the bulk of the proceeds used to "... fund the ongoing exploration program at the Company's 100% owned Lustdust Property in central B.C." (Newswire, 2006).

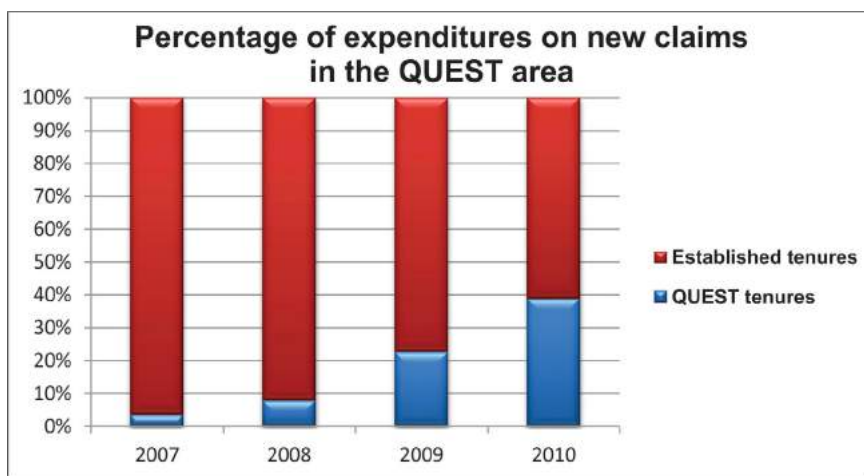


**Figure 6.** Gradual increase in proportional spending on land staked from 2007 to 2010 within the QUEST (Quesnellia Exploration SStrategy) area.

Figure 7 shows the amounts raised<sup>1</sup> (in thousands of dollars; in green), amounts spent<sup>2</sup> (in thousands of dollars; in red) and share volumes<sup>3</sup> (in hundreds). Blue lines are linear regression lines reflecting average volumes traded before Geoscience BC started the QUEST Project and then during the critical 2007 and 2008 years. From 2005 to 2006, share volumes traded on the exchange are approximately 160 000 per month; by 2007 this had tripled to 500 000.

In June 2007, it closed private placements totalling \$4 million for use in its exploration programs (Canada Newswire, 2007) and in 2009 announced that its drilling program for the year was estimated at \$1.3 million, with \$3 million in the company's treasury (Canadian Newswire, 2009).

The monthly stock chart of Alpha Gold Corp. (now ALQ Gold Corp.) from 2005 to 2010 shows that according to the company's audited financial reports, it raised \$440,000 and \$470,000 in 2005 and 2006, respectively, from the proceeds of share issues. Beginning midway through 2006 and extending to 2009, a period coinciding first with anticipation in the markets of Geoscience BC's proposed project, its official announcement in 2007 and the public release of large amounts of data from geochemical and airborne geophysics surveys in 2008, share volumes of Alpha Gold Corp. traded on the TSX Venture Exchange tripled from an average of 160 000 shares per month in 2005 and 2006 to

<sup>1</sup>Amounts raised are the proceeds raised from the issuance of company shares, taken from the audited annual financial statements of Alpha Gold Corp. for 2005–2010 (<http://www.sedar.com>; statements of cash flows under Financing activities, Proceeds on issuance of shares, Net of issue costs).

<sup>2</sup>Amounts spent are estimates (similar to amounts raised) derived from the section under Investing Activities, Investment in and expenditures on exploration properties.

<sup>3</sup>Share volumes reflect the trading activity of Alpha Gold Corp.'s shares (trading symbol ALQ) on the TSX Venture Exchange in Toronto.

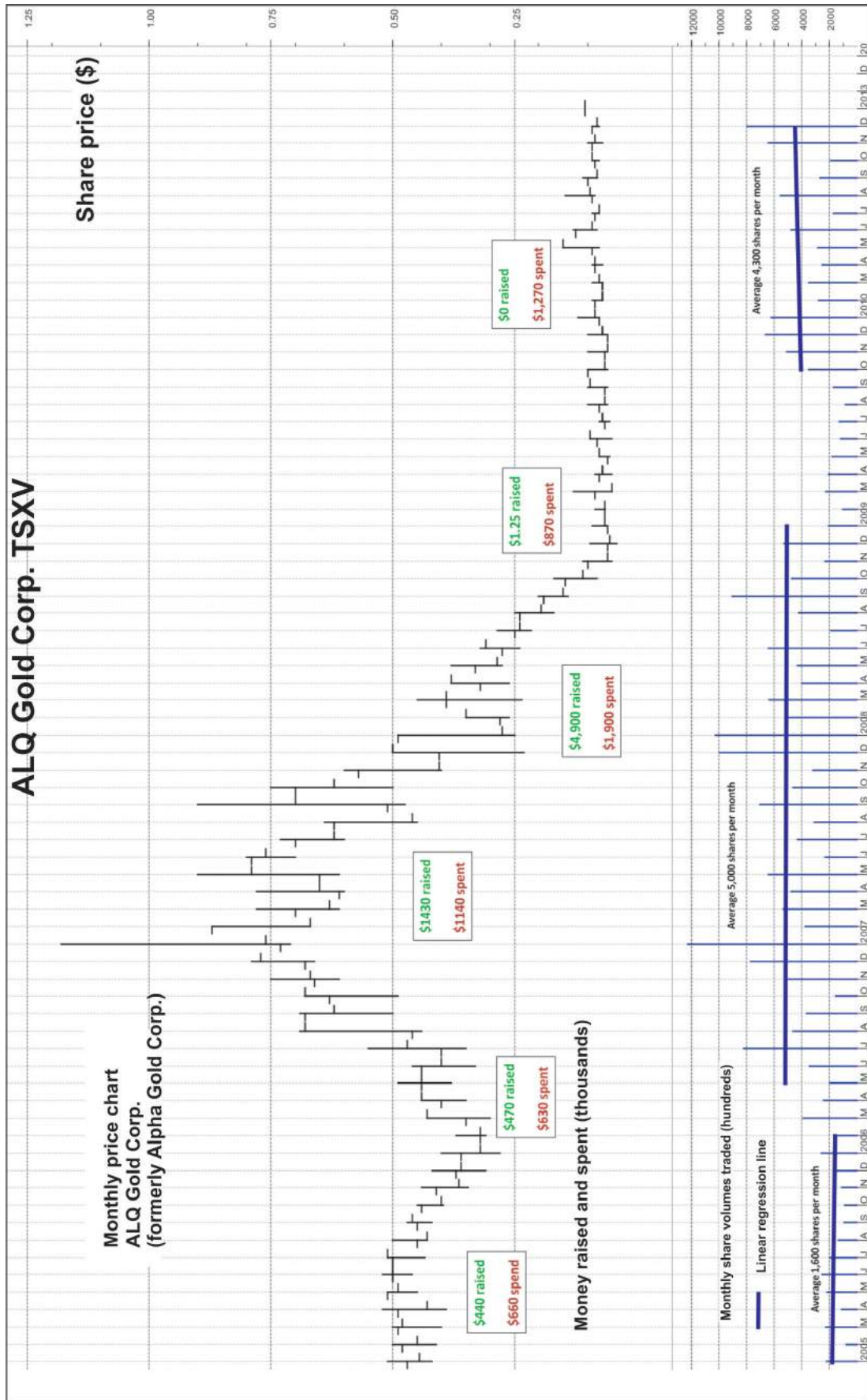


Figure 7. ALQ Gold Corp. (formerly Alpha Gold Corp.) monthly stock price chart 2005–2010.

500 000 shares in 2007 and 2008. During a crucial period of the QUEST Project, Alpha Gold Corp.'s heightened profile, reflected by large trading volumes on the stock exchange, enabled it in 2007 to raise three times as much funding as in previous years (\$1.4 million) and in 2008, more than ten times as much (\$4.9 million) from private placements as in 2006—despite watching its publicly listed share price drop to historic lows in concert with the market downturn of 2008.

## Conclusions

The QUEST initiative has enjoyed success and this is readily revealed in the public sources of information. Marked increases in fundraising and expenditures on new exploration and development by companies working in the QUEST area strongly supports arguments justifying the initial \$5 million that Geoscience BC committed to the project. Operators and mining companies enjoyed a clear boost in visibility in public financial markets and were able to raise much greater levels of funding than would otherwise have been the case in the absence of a 'great story' like the QUEST Project and the tangible contributions of a government-backed incentive program.

The method used here to characterize and measure these successes, based on readily available public sources, makes it repeatable and suggests that similar analytical projects could be undertaken and expanded upon using this preliminary study as a working basis.

## Acknowledgments

The author thanks Geoscience BC for funding this project and the BC Geological Survey, particularly A. Wilcox and P. Desjardins, for their help in acquiring data. A special note is given to W. Jackaman for his insight and knowledge in developing this project and D. Reichheld for assistance and providing editorial comments.

## References

Barlow, N.D., Flower, K.E., Sweeney, S.B., Robinson, G.L. and Barlow, J.R. (2010): QUEST and QUEST-West Property File: analysis and integration of Property File's Industry File documents with British Columbia's MINFILE (NTS 093; 094A, B, C, D; 103I); *in* Geoscience BC Summary of Activities 2009, Geoscience BC, Report 2010-1, p. 175–188, URL <[http://www.geosciencebc.com/i/pdf/SummaryofActivities2009/SoA2009\\_Barlow.pdf](http://www.geosciencebc.com/i/pdf/SummaryofActivities2009/SoA2009_Barlow.pdf)> [October 2013].

Barnett, C.T. and Williams, P.M. (2009): Using geochemistry and neural networks to map geology under glacial cover; Geoscience BC, Report 2009-3, 27 p., URL <[http://www.geosciencebc.com/i/project\\_data/QUESTdata/GBCReport2009-3/GBC\\_Report\\_2009-3.pdf](http://www.geosciencebc.com/i/project_data/QUESTdata/GBCReport2009-3/GBC_Report_2009-3.pdf)> [October 2013].

BC Geological Survey (2013a): ARIS assessment report indexing system; BC Ministry of Energy and Mines, URL <<http://www.empr.gov.bc.ca/Mining/Geoscience/ARIS/Pages/default.aspx>> [October 2013].

BC Ministry of Energy and Mines (2013b): Mineral Titles Online; BC Ministry of Energy and Mines, URL <<http://www.empr.gov.bc.ca/Titles/MineralTitles/mto/Pages/default.aspx>> [October 2013].

Bernier, P. (2008): Under the Rainbow; Richfield Ventures Corporation, press release, February 7<sup>th</sup>, 2008, URL <<http://www.sedar.com/GetFile.do?lang=EN&docClass=8&issuerNo=00026237&fileName=/csfsprod/data86/filings/01214203/00000001/i%3A%5CSEDAR%5CSJC%5CLori%5CRichfieldPRFeb7.pdf>> [October 2013].

Caulfield, D. (2007): Project update; Rimfire Minerals Corporation, press release, September 13, 2007, URL <<http://www.sedar.com/GetFile.do?lang=EN&docClass=8&issuerNo=00011905&fileName=/csfsprod/data84/filings/01158233/00000001/r%3A%5CCorporate%5CElectronicFiling%5CSEDAR%5C2007Filing%5CPR0722.pdf>> [October 2013].

Canadian Newswire (2007): Alpha Gold closes private placement of \$4 million; press release, June 13, 2007, URL <<http://www.newswire.ca/en/story/11449/alpha-gold-closes-private-placement-of-4-million>> [October 2013].

Canadian Newswire (2009): Alpha Gold prepares for 2009 summer drilling; press release, June 3, 2009, URL <<http://www.newswire.ca/en/story/55037/alpha-gold-prepares-for-2009-summer-drilling>> [October 2013].

Fraser, S.J. and Hodgkinson, J.H. (2009): An investigation using SiroSOM for the analysis of QUEST stream-sediment and lake-sediment geochemical data; Geoscience BC, Report 2009-14, 64 p., URL <[http://www.geosciencebc.com/i/project\\_data/GBC\\_Report2009-14/GBC\\_Report\\_2009-14.pdf](http://www.geosciencebc.com/i/project_data/GBC_Report2009-14/GBC_Report_2009-14.pdf)> [October 2013].

Geotech Limited (2008): Report on a helicopter-borne versatile time domain electromagnetic (VTEM) geophysical survey; QUEST Project, central British Columbia (NTS 93A, B, G, H, J, K, N, O & 94C, D); Geoscience BC, Report 2008-4, 35 p., URL <[http://www.geosciencebc.com/i/project\\_data/QUESTdata/report/7042-GeoscienceBC\\_final.pdf](http://www.geosciencebc.com/i/project_data/QUESTdata/report/7042-GeoscienceBC_final.pdf)> [October 2013].

Geotech Limited (2009): Helicopter-borne z-axis tipper electromagnetic (ZTEM) and aeromagnetic survey, Mt. Milligan test block; Geoscience BC, Report 2009-7, 51 p., URL <[http://www.geosciencebc.com/i/project\\_data/GBC\\_Report2009-7/2009-7\\_Report.pdf](http://www.geosciencebc.com/i/project_data/GBC_Report2009-7/2009-7_Report.pdf)> [October 2013].

Jackaman, W. (2008a): Regional lake sediment and water geochemical data, northern Fraser Basin, central British Columbia (parts of NTS 093G, H, J, K, N & O); Geoscience BC, Report 2008-5, 446 p., URL <[http://www.geosciencebc.com/i/project\\_data/QUESTdata/GBCReport2008-5/2008-5\\_Survey\\_Summary.pdf](http://www.geosciencebc.com/i/project_data/QUESTdata/GBCReport2008-5/2008-5_Survey_Summary.pdf)> [October 2013].

Jackaman, W. (2008b): QUEST Project sample reanalysis; Geoscience BC, Report 2008-3, 4 p, URL <[http://www.geosciencebc.com/i/project\\_data/QUESTdata/GBCReport2008-3/2008-3\\_README.pdf](http://www.geosciencebc.com/i/project_data/QUESTdata/GBCReport2008-3/2008-3_README.pdf)> [October 2013].

Newswire (2006): Alpha Gold closes private placement of \$1.4 million, press release, August 1, 2006, URL <<http://www.investorpoint.com/stock/ALQ:CA-ALQ%20Gold%20Corp./news/4170889>> [October 2013].

Owskiacki, G. and Payie, G. (2010): MINFILE update of the QUEST Project area, central British Columbia (parts of NTS 093A, B, G, H, J, K, N, O, 094C, D); *in* Geoscience BC Summary of Activities 2009, Geoscience BC, Report 2010-1, p. 189–202, URL <<http://www.geosciencebc.com/i/pdf/>>

- [SummaryofActivities2009/SoA2009\\_Owsiacki.pdf](#)> [October 2013].
- Reichheld, S.A. (2013): Documentation and assessment of exploration activities generated by Geoscience BC data publications; *in* Geoscience BC Summary of Activities 2012, Geoscience BC, Report 2013-1, p. 125–130, URL <[http://www.geosciencebc.com/i/pdf/SummaryofActivities2012/SoA2012\\_Reichheld.pdf](http://www.geosciencebc.com/i/pdf/SummaryofActivities2012/SoA2012_Reichheld.pdf)> [October 2013]
- Sander Geophysics Limited (2008): Airborne gravity survey, Quesnellia Region, British Columbia, 2008; Geoscience BC, Report 2008-8, 121 p., URL <[http://www.geosciencebc.com/i/project\\_data/QUESTdata/GBCReport2008-8/Gravity\\_Technical\\_Report.pdf](http://www.geosciencebc.com/i/project_data/QUESTdata/GBCReport2008-8/Gravity_Technical_Report.pdf)> [October 2013].
- Schroeter, T. (2007): Fjordland and Serengeti partner on QUEST Project; Fjordland Exploration Inc., press release, August 1, 2007, URL <<http://www.sedar.com/GetFile.do?lang=EN&docClass=8&issuerNo=00005747&fileName=/csfsprod/data83/filings/01135462/00000001/C%3A%5CMG%5CFEX%5Cnr%5Cnr07-12.pdf>> [October 2013].
- SEDAR (2013): Public company documents; SEDAR, system for electronic document analysis and retrieval, URL <[http://www.sedar.com/privacy\\_statement\\_en.htm](http://www.sedar.com/privacy_statement_en.htm)> [October 2013].
- TSX Inc. (2013): Overview – S&P/TSX Composite Index; TMX Group Ltd., URL <<http://web.tmxmoney.com/indices.php?section=tsx&index=^TSX#indexInfo>> [October 2013].



## Targeting Resources through Exploration and Knowledge (TREK): Geoscience BC's Newest Minerals Project, Interior Plateau Region, South-Central British Columbia (NTS 093B, C, F, G)

A.L. Clifford, Geoscience BC, Vancouver, BC, [clifford@geosciencebc.com](mailto:clifford@geosciencebc.com)

C.J.R. Hart, Mineral Deposit Research Unit, University of British Columbia, Vancouver, BC

---

Clifford, A. and Hart, C.J.R. (2014): Targeting Resources through Exploration and Knowledge (TREK): Geoscience BC's newest minerals project, Interior Plateau Region, central British Columbia (NTS 093B, C, F, G); *in* Geoscience BC Summary of Activities 2013, Geoscience BC, Report 2014-1, p. 13–18.

### Introduction

Geoscience BC's newest multiyear regional minerals project is called the TREK Project, which stands for **T**argeting **R**esources through **E**xploration and **K**nowledge. The TREK Project is focused on British Columbia's northern Interior Plateau region and covers more than 25 000 km<sup>2</sup>, extending south from Fraser Lake and Vanderhoof to Anahim Lake, and west from Quesnel to the eastern edges of Entiako and Tweedsmuir South provincial parks (Figure 1). The project area includes the active Blackwater gold district and is considered highly prospective for mineral resources. It is characterized by thick overburden and is presently considered to be underexplored due to the difficulties caused by its complicated and poorly understood bedrock geology.

The \$3.9 million in funding for the TREK Project was announced by Geoscience BC in March 2013. First-year TREK activities, undertaken in summer 2013, included an airborne geophysical survey, a regional geochemical survey (stream, lake, soil and till sampling) and local biogeochemical and geothermal sampling programs (Geoscience BC, 2013). Details of the geochemical program are outlined in Sacco et al. (2014). The results of the new geochemical sampling programs will be released in late spring 2014. Details of the geothermal program are presented in Lett and Jackaman (2014).

### Geophysical Program

The 2013 TREK geophysical program consisted of a regional aeromagnetic survey and acquisition of proprietary industry data. In May 2013, Geoscience BC issued a public request for proposals for a high-resolution, regional airborne magnetic survey, which was subsequently awarded

to Aeroquest Airborne Ltd. In addition to the acquisition of new regional aeromagnetic data, Geoscience BC purchased high-resolution, proprietary, industry airborne magnetic data from three exploration companies operating within the TREK Project area: Amarc Resources Ltd. (Amarc), Deveron Resources Ltd. (Deveron) and RJK Explorations Ltd. (RJK).

### Airborne Magnetic Survey

The regional survey was flown by two Cessna Grand Caravan C208B short take-off and landing (STOL) aircraft (Figure 2). Approximately 104 000 line-km of aeromagnetic data were acquired over a 24 000 km<sup>2</sup> area from August to November 2013. Flight lines were flown east-west with a 250 m line spacing. North-south tie lines were flown with an average spacing of 2 500 m. A minimum terrain clearance of 100 m was maintained using a preplanned drape surface. The aircraft had three magnetometers and measured both total magnetic intensity and horizontal gradients.

The aeromagnetic system used provides bidirectional horizontal-gradient information using wing-tip magnetometers in addition to a tail-mounted stinger magnetometer. The lateral-gradient measurement reduces the effective line spacing and assists with mapping of small magnetic sources, locating the termination of magnetic sources between lines and identifying small structure-induced offsets in linear magnetic sources. The three magnetic sensors measure total magnetic intensity as well as lateral and longitudinal gradients, allowing a greater understanding of the magnetic structure in the survey area (Aeroquest Airborne Ltd., pers. comm., 2013). This gradiometer system provided resolution of magnetic anomalies equivalent to that of a single-sensor system flown at a line spacing of less than 200 m.

The data acquisition on a preplanned drape surface with STOL aircraft allows the economical collection of high-quality data in steep terrain while maintaining a safe ground clearance and minimizing the effect of differing aircraft flight altitudes going uphill and downhill on adjacent flight lines. Data acquisition on a smooth drape surface also facil-

---

**Keywords:** *airborne magnetics, aeromagnetic data, TREK Project, northern Interior Plateau region*

*This publication is also available, free of charge, as colour digital files in Adobe Acrobat® PDF format from the Geoscience BC website: <http://www.geosciencebc.com/s/DataReleases.asp>.*

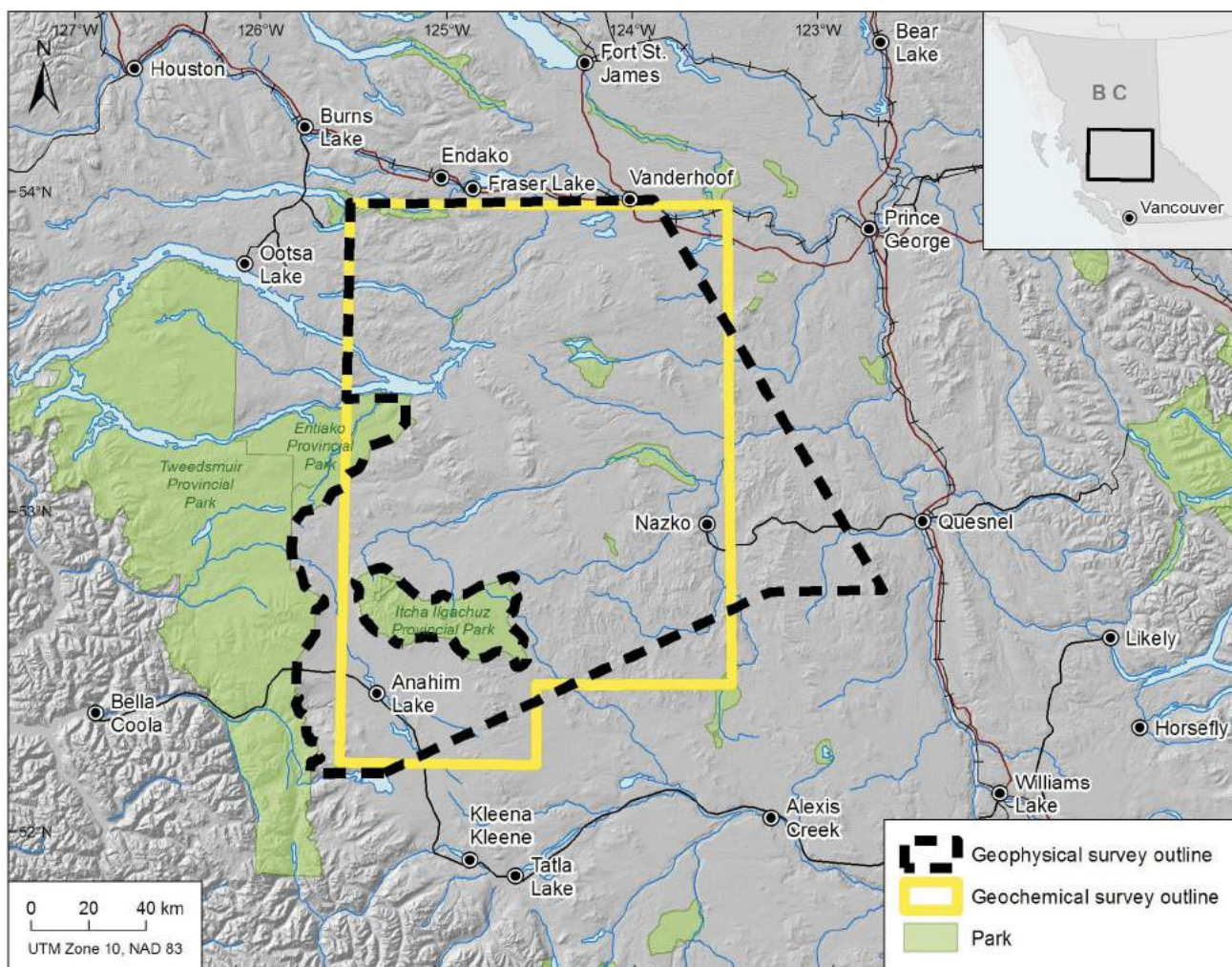


**Figure 1.** Geoscience BC's TREK Project area in the Interior Plateau region of central British Columbia, with regional project activities outlined. Data from GeoBase® (2004), Natural Resources Canada (2007) and DataBC (2008).

itates spatial filtering and the calculation of derivative products from the magnetic dataset.

### Purchase of Proprietary Industry Data

Simpson et al. (2013) described Geoscience BC's implementation of a program to purchase proprietary, industry geophysical data, which was modelled after the Ontario Geological Survey's 'Request for Data – Purchase of Proprietary Airborne Geophysical Data'. In December 2012, Geoscience BC issued a Request for Expressions of Interest for the sale of proprietary industry airborne magnetic datasets, with the intention of integrating and compiling the data for public release. The request specified that only digital data meeting the following criteria would be considered:

- collected within the Interior Plateau region of BC
- helicopter or fixed-wing airborne magnetics
- collected at a line spacing of 250 m or less
- survey area greater than 200 km<sup>2</sup> (smaller areas considered under special circumstances)

- survey well documented and supported by logistics reports, flight logs, data-archive descriptions and calibration files



**Figure 2.** Aeroquest Airborne Ltd. Cessna Caravan C208B used to fly the TREK survey over the Interior Plateau region of south-central British Columbia. Photo courtesy of Aeroquest Airborne Ltd.

- digital data not publicly available, although maps and images already within public domain that had been derived from the data would be considered acceptable

Data Sale Agreements were successfully executed with three exploration companies, all of which have properties within the TREK Project area (Figure 3). Helicopter airborne magnetic data were purchased from each of the three companies. All survey data underwent a thorough technical assessment, after which they were valued based on the following factors: survey method (a higher factor was assigned to helicopter versus fixed-wing acquisition), number of line-kilometres, age (newer survey data are more valuable than older data), and quality and assessment credit (surveys that had never been submitted for assessment were assigned a higher factor).

Airborne magnetic data purchased from Amarc Resources Ltd. were from their Galileo and Hubble properties. The combined area of these two properties was 1340 km<sup>2</sup>, and the acquisition of these data facilitated an increase in the area of the originally planned regional TREK aeromagnetic

survey. The survey purchased from Amarc was flown using a line spacing of 200 m. The Amarc data, collected during electromagnetic (EM) survey work, had a typical sensor height of 49 m, whereas surveys flown using a helicopter-stinger system have a typical sensor height of 103 m.

The aeromagnetic data purchased from both RJK Explorations Ltd. and Deveron Resources Ltd. covered significantly smaller areas than the Amarc surveys. RJK's Blackwater East and West claim blocks together totalled 138 km<sup>2</sup>, and Deveron's Nechako property 137 km<sup>2</sup>. Although the survey areas did not meet all outlined criteria for purchase (i.e., >200 km<sup>2</sup>), both were close to New Gold's Blackwater Davidson deposit (i.e., an area of high interest) and, for this reason, the data merited procurement. The survey data from both the RJK and Deveron are of high quality, both surveys having been flown at a flight-line spacing of 100 m.

The aeromagnetic data purchased from Amarc, Deveron and RJK will be merged with the regional fixed-wing TREK survey data collected by Aeroquest. Public release of all data is anticipated in early 2014.

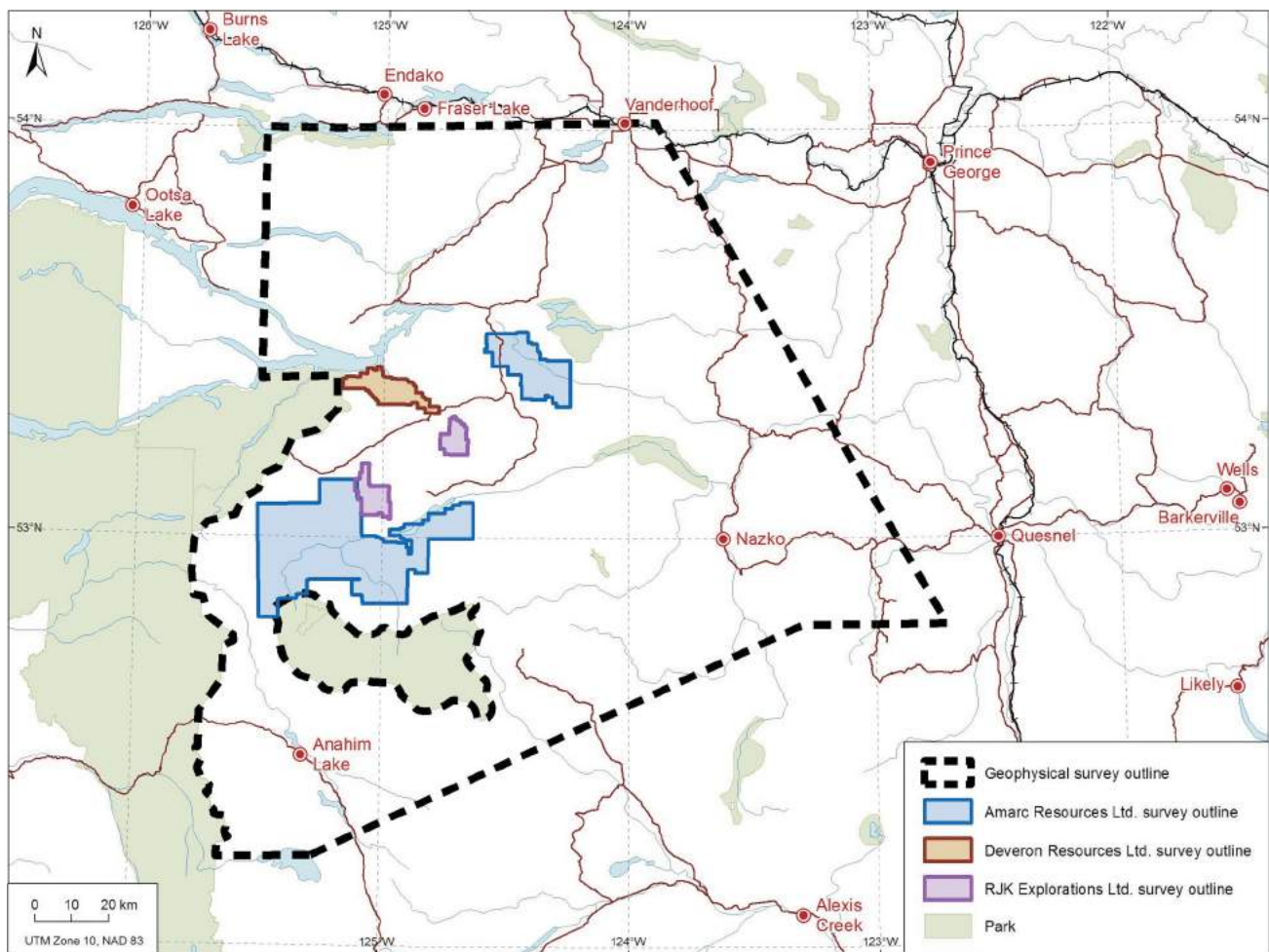


**Figure 3.** Geoscience BC's TREK airborne geophysical survey area in the Interior Plateau region of central British Columbia, showing the outlines of airborne geophysical survey data purchased from industry. Data from Massey et al. (2005) and DataBC (2008).

## Geochemical Program

The first year of the TREK geochemical program was completed during summer 2013 and involved the collection of 684 till samples that will be analyzed for major, minor and trace elements (Sacco et al., 2014). The TREK geochemical sampling program is focused on regions that have not previously been sampled, using basal-till potential maps created in advance of the summer field program. The collection of new samples is expected to take two to three years to complete. The geochemical work is being done by Noble Exploration Services Ltd. in partnership with the BC Geological Survey (BC Ministry of Energy and Mines). In addition to new sampling, Geoscience BC, in co-operation with the BC Geological Survey and the Geological Survey of Canada, has recovered from archive storage approximately 1800 till samples for reanalysis to the same standard as that of the new surveys. Full details of the 2013 geochemical program are outlined in Sacco et al. (2014). Release of the new sampling results is expected in spring 2014.

## Geothermal Program

In support of local First Nations' interest in potential geothermal resources, Geoscience BC included a geothermal component as part of the TREK Project. Gas seepages from the soil, travertine deposits and carbon-enriched surface water all occur near the Nazko volcanic cone, together suggesting a magmatic and possibly geothermal source for the phenomena. Lett et al. (2014) describe the geothermal sampling program undertaken during summer 2013. Groundwater, surface water and soil in the Nazko bog and surrounding area were sampled to study the geochemical signature associated with the carbon-dioxide gas seepages.

## Geology and Integration Program

The TREK geology and integration program phases will commence after a review of the first year activities. The geochemical and airborne geophysical data will be used to inform the planning of new geological mapping and mineral deposit studies to be conducted by the Mineral Deposit Research Unit at the University of British Columbia.

The geology component of TREK is intended to improve geological understanding of the Interior Plateau region. A series of enhanced geological map products will be produced using new and existing lithological, lithochemical, structural, gravity and age data, and products from Geoscience BC's Nechako Seismic Project (<http://www.geosciencebc.com/s/NechakoSeismic.asp>). The results are expected to generate new geological and thematic maps that will be field tested and updated throughout the life of the TREK Project.

The integration component of TREK will include new TREK data. An updated geological framework for the area

will incorporate the new geophysical and geochemical layers and their integration and subsequent interpretation with available geological information. These products will add value to the regional aeromagnetic and geochemical surveys. A new geology map and various related geological map products, including structural maps, metallogenic maps, geochronological maps, digital databases and GIS layers, are expected products of this program.

## Summary

The TREK Project is a multidisciplinary, integrated project located in a region with high potential for new mineral discoveries. The first-year TREK Project activities included the acquisition of new airborne magnetic survey data, completion of the first year of a new two- to three-year geochemical survey, plus geothermal and biogeochemical sampling. Geoscience BC purchased proprietary industry airborne magnetic data within the TREK airborne magnetic survey, adding areas of especially high-resolution information to the project area. These new data, in combination with compilation of past geological mapping efforts, will be used to guide geological studies that will commence in 2014. TREK Project data will be made available on Geoscience BC's website (<http://www.geosciencebc.com/s/TREK.asp>) beginning in early 2014. Results from the project will provide relevant geoscience information to assist mineral exploration efforts in the region.

## Acknowledgments

Aeroquest Ltd. is thanked for providing survey specification details and for providing an image for the manuscript. The manuscript benefited from review by P. Kowalczyk. F. Ma is thanked for creating the figures. The digital elevation model in Figure 1 was prepared by K. Shimamura.

## References

- DataBC (2008): TANTALIS—parks, ecological reserves, and protected areas; BC Ministry of Citizens' Services and Open Government, URL <<https://apps.gov.bc.ca/pub/geometadata/metadataDetail.do?recordUID=54259&recordSet=ISO19115>> [November 2013].
- GeoBase® (2004): Canadian digital elevation data; Canadian Council on Geomatics, URL <<http://www.geobase.ca/geobase/en/data/cded/description.html>> [November 2013].
- Geoscience BC (2013): Geoscience BC launches new TREK Project; Geoscience BC press release, March 26, 2013, URL <[http://www.geosciencebc.com/s/NewsReleases.asp?ReportID=577925&\\_Type=News&\\_Title=Geoscience-BC-Launches-New-TREK-Project](http://www.geosciencebc.com/s/NewsReleases.asp?ReportID=577925&_Type=News&_Title=Geoscience-BC-Launches-New-TREK-Project)> [November 2013].
- Lett, R.E. and Jackaman, W. (2014): Geochemical expression in soil and water of carbon dioxide seepages near the Nazko cone, central British Columbia (NTS 093B/13); *in* Geoscience BC Summary of Activities 2013, Geoscience BC, Report 2014-1, p. 35–42.

- Massey, N.W.D, MacIntyre, D.G., Desjardins, P.J. and Cooney, R.T. (2005): Digital geology map of British Columbia: whole province; BC Ministry of Energy and Mines, GeoFile 2005-1, URL <<http://www.empr.gov.bc.ca/Mining/Geoscience/PublicationsCatalogue/GeoFiles/Pages/2005-1.aspx>> [November 2013].
- Natural Resources Canada (2007): Atlas of Canada base maps; Natural Resources Canada, Earth Science Sector, URL <<http://geogratis.gc.ca/geogratis/search?lang=en>> [November 2013].
- Sacco, D., Jackaman, W. and Ferbey, T. (2014): Targeted geochemical and mineralogical surveys in the TREK Project area, central British Columbia (parts of NTS 093B, C, F, G); *in* Geoscience BC Summary of Activities 2013, Geoscience BC, Report 2014-1, p. 19–34.
- Simpson, K.A., Kowalczyk, P.L. and Kirkham, G.D. (2013): Update on Geoscience BC's 2012 geophysical programs; *in* Geoscience BC Summary of Activities 2013, Geoscience BC, Report 2013-1, p. 1–4, URL <<http://www.geosciencebc.com/i/pdf/SummaryofActivities2012/SoA2012-Simpson.pdf>> [November 2013].



## Targeted Geochemical and Mineralogical Surveys in the TREK Project Area, Central British Columbia (Parts of NTS 093B, C, F, G)

D.A. Sacco, Consulting Quaternary Geologist, New Westminster, BC, [saccoda@gmail.com](mailto:saccoda@gmail.com)

W. Jackaman, Noble Exploration Services Ltd., Sooke, BC

T. Ferbey, British Columbia Geological Survey, Victoria, BC

---

Sacco, D.A., Jackaman, W. and Ferbey, T. (2014): Targeted geochemical and mineralogical surveys in the TREK Project area, central British Columbia (parts of NTS 093B, C, F, G); in Geoscience BC Summary of Activities 2013, Geoscience BC, Report 2014-1, p. 19–34.

### Introduction

The Targeting Resources for Exploration and Knowledge (TREK) Project is focused on providing a new geological understanding of the central part of British Columbia's Interior Plateau through the integration of surficial geochemistry, airborne geophysics and geology data (Figure 1). The project is focused on an area of Stikine terrane that has the potential to host a variety of mineral deposit types, including porphyry Cu, porphyry Mo and epithermal Au deposits (e.g., Prosperity, Endako, Blackdome). In addition, the recent discovery of the Blackwater-Davidson Au deposit in the TREK Project area has identified another deposit type with significant economic potential. Exploration in this region has been hindered by Neogene Chilcotin Group basalt flows and extensive glacial drift, which obscures underlying and prospective bedrock units.

As a part of the TREK Project, a surficial geochemistry program is currently underway that aims to provide comprehensive geochemical dataset for the project area. Presented here are the program details and results from the first year of the two- to three-year program.

The TREK geochemistry program consists of three components:

- compilation of historical data from previous geochemical surveys;
- collection of new geochemical and mineralogical data; and
- reanalysis of archived till samples.

A combination of lake and stream sediment and till geochemical and biogeochemical data exist for various parts of the project area, with no one dataset covering the entire region. Typically, geochemical data from these media types are not comparable due to different methods of transport

and accumulation. Lake sediment and till geochemical data, however, have been shown to be correlative (Cook et al., 1995; Rencz et al., 2002). The survey discussed here targets basal till, a common material throughout the region, which is well suited to assessing the mineral potential of areas covered by glacial drift (McClenaghan et al., 2000; Levson, 2001, 2002; Lett et al., 2006). Basal till potential maps (BTPMs) were produced and used to assist in the planning and execution of this ambitious survey. Where basal till could not be sampled, higher order bedrock derivatives, such as lake or stream sediments that are comparable to the historic geochemical data, were collected. Till geochemical data from previous surveys will be integrated with new data from this survey. Different analytical methods were used to produce these older data and so available archived till samples will be reanalyzed using modern laboratory techniques to produce a directly comparable master till geochemical dataset for the project area.

### Project Area

The project area is located in the relatively low relief area of the Interior Plateau (Mathews, 1986), south of Vanderhoof and approximately 60 km west of Quesnel. It occupies parts of NTS 093B, C, F and G and covers more than twenty-eight 1:50 000 scale NTS map areas, a total of approximately 25 000 km<sup>2</sup> (Figure 1). Access is through a network of forest service roads in the Vanderhoof, Quesnel, Chilcotin and Central Cariboo forest districts.

The project area includes parts of the Nechako Plateau, Fraser Plateau and the Fraser Basin physiographic regions (Holland, 1976; Figure 1). The Nechako Plateau has low to moderate relief between 900 and 1200 m above sea level (asl) and includes the Nechako and Fawnie mountain ranges, which have peaks over 1600 and 2000 m asl, respectively. The Fraser Plateau has moderate to low relief between 1000 and 1500 m and includes the Ilgachuz and Itcha mountain ranges, which have peaks over 2200 m asl. Thick surficial deposits composed dominantly of till obscure most bedrock exposures on plateau surfaces. The Fraser Basin is characterized by low relief between 675 and 1000 m asl. Thick glaciolacustrine units occur over large

---

**Keywords:** TREK, till geochemistry, regional geochemistry, basal till potential mapping, Quaternary geology

This publication is also available, free of charge, as colour digital files in Adobe Acrobat® PDF format from the Geoscience BC website: <http://www.geosciencebc.com/s/DataReleases.asp>.

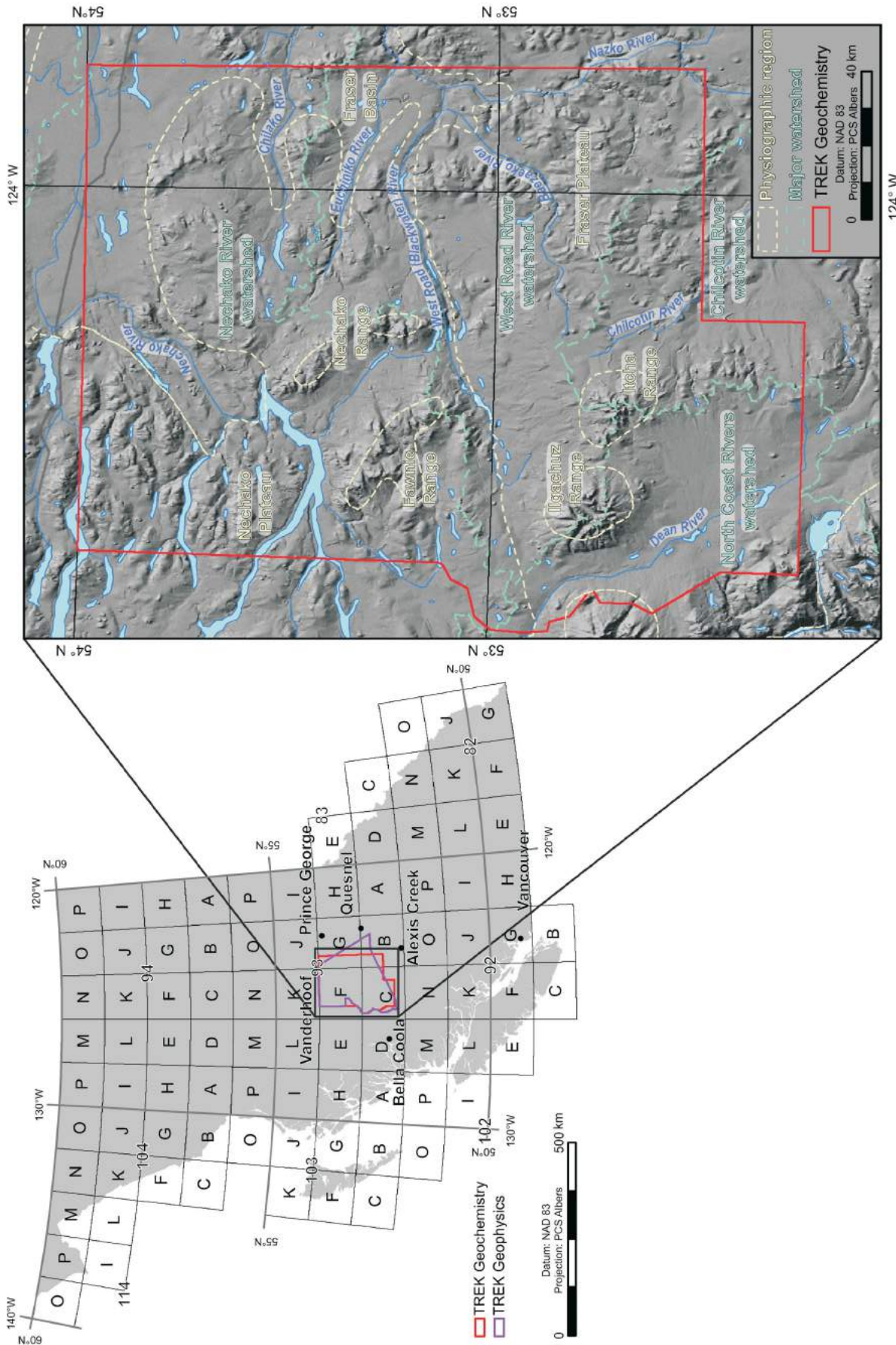


**Figure 1.** TREK Project geochemistry and airborne geophysics boundaries in central British Columbia. Inset map illustrates physiographic regions (Holland, 1976) and major drainages of the geochemical survey area. Digital elevation model from Canadian digital elevation data (GeoBase®, 2007).

areas of the Fraser Basin. The project area is dissected by several major rivers including the West Road (Blackwater), Baezaeko, Clisbako, Chilcotin and Clusko. Most large rivers have incised the plateau surface, exposing combinations of till, glaciofluvial and glaciolacustrine sediments, or bedrock. Major watersheds are the Nechako and West Road rivers systems that drain into the Strait of Georgia via the Fraser River, and the north coast rivers system that drains the southwest corner of the TREK Project area into the Pacific Ocean (Figure 1).

## Bedrock and Economic Geology

The regional geological framework was initially established by Tipper (1969), and then compiled by Massey et al. (2005) and recompiled with regional revisions by Riddell (2006) that focused on oil and gas exploration. Bedrock mapping at 1:50 000 scale has been completed for parts of NTS 093F (Diakow and Webster, 1994; Diakow et al., 1997), NTS 093B (Metcalf et al., 1998) and NTS 093C (Mihalynuk et al., 2008, 2009). Provided here is a geological summary of the project area from these sources (Figure 2). Basement rocks include the Devonian to Jurassic arc complex of the Stikine terrane, and in the northeast corner, the Mississippian to Early Jurassic accretionary complex of the Cache Creek terrane (Monger et al., 1991). The oldest rocks in the project area belong to the Permian to Jurassic Cache Creek Complex and the Vanderhoof metamorphic complex. The intrusive Triassic to Jurassic Brooks diorite complex is found in the north-central part of the project area. Jurassic rocks are dominant in the northeastern quadrant of the project area. These include volcanic rocks of the Entiako, Naglico and Nechako formations of the Hazelton Group; Fawnie volcanics and Ashman Formation of the Bowser Lake Group; intrusive rocks of the Stag Lake plutonic and Francois Lake suites of the Endako batholith; and the Laidman batholith. The Eocene Frank Lake pluton occurs in the northeast. Units from the Cretaceous include the Kasalka Group volcanic rocks in the northwest, the Capoose pluton in the west-central region, and unnamed andesitic volcanic rocks in the southwest. The north and southwest are composed largely of Eocene to Oligocene volcanic rocks of the Nechako Plateau Group including the Endako and Ootsa Lake formations. The majority of the project area is overlain by Miocene to Pleistocene Chilcotin Group volcanic rocks. The Ilgachuz and Itcha ranges in the southwestern part of the project area are composed of the Miocene to Pleistocene Anahim volcanics.

There are five developed prospects, seven prospects and 39 mineral showings in the TREK Project area (Figure 2). Four of the five developed prospects contain Au, Ag, Zn, Pb and Cu mineralization and include the Blackwater-Davidson intermediate sulphidation epithermal Au-Ag deposit (NTS 093F/02; MINFILE 093F 037; BC Geological Survey, 2013), the Capoose subvolcanic Cu-Ag-Au (As-

Sb) and porphyry-related Au deposit (NTS 093F/06; MINFILE 093F 040), and the 3Ts polymetallic Ag-Pb-Zn±Au veins (NTS 093F/03; MINFILE 093F 068) and low-sulphide epithermal Au-Ag-Cu deposit (NTS 093F/03; MINFILE 093F 055). The fifth developed prospect, the CHU deposit, hosts porphyry Mo (low F-type) mineralization (NTS 093F/07; MINFILE 093F 001).

The Baez (NTS 093C/16; MINFILE 093C 015), Clisbako (NTS 093C/09; MINFILE 093C 016), Trout (NTS 093F/10; MINFILE 093F 044) and Wolf (NTS 093F/03; MINFILE 093F 045) prospects all host low sulphidation epithermal Au-Ag mineralization. In contrast, the April Au-Ag-Zn prospect has been classified as high sulphidation epithermal Au-Ag-Cu mineralization (NTS 093F/07; MINFILE 093F 060). At the Laidman prospect (NTS 093F/03; MINFILE 093F 067), Au, Ag, Pb and Zn occur within Au-quartz veins whereas at the Bob prospect Au, Ag, As, Sb and Hg occur within carbonate-hosted and disseminated Au-Ag mineralization (NTS 093B/13; MINFILE 093B 054).

## Quaternary Geology

The Quaternary geology of the project area was first described by Tipper (1971a, b) during reconnaissance glacial and geomorphological mapping in the Interior Plateau. Soils and terrain mapping at a 1:50 000 scale was conducted from the 1970s to the 1990s by the BC Ministry of Environment; these references are too numerous to list here, but can be accessed through their website ([http://www.env.gov.bc.ca/tei/access\\_terrain.html](http://www.env.gov.bc.ca/tei/access_terrain.html)). Quaternary stratigraphic framework, glacial history and surficial geology mapping for the Nechako Plateau map area (NTS 093F) can be found in Giles and Levson (1994, 1997), Levson and Giles (1994), Levson et al. (1994), Weary et al. (1997) and Plouffe et al. (2001). Levson and Giles (1997) discuss the Quaternary geology for the Nechako and Fraser plateaus. Giles and Kerr (1993) and Proudfoot (1993) discuss the Quaternary geology for parts of NTS 093C, and Ferbey (2009), Ferbey et al. (2009) and Vickers and Ferbey (2009) discuss the Quaternary geology south of the project area in NTS 093B.

Through the Quaternary, BC has repeatedly been covered by a mass of interconnected glaciers collectively known as the Cordilleran Ice Sheet (CIS; Armstrong et al., 1965; Flint, 1971; Clague, 1989). Sediments of the most recent glaciation, the Fraser Glaciation, are ubiquitous within the project area; sediments deposited prior to this are rare (e.g., Giles and Kerr, 1993; Plouffe and Levson, 2001). During the Fraser Glaciation, thick units of till were deposited beneath the CIS that flowed from the Coast Mountains across the project area. Ice-flow indicators compiled for BC by Ferbey et al. (2013) indicate that flow directions were dominantly to the northeast in the northern part of the project

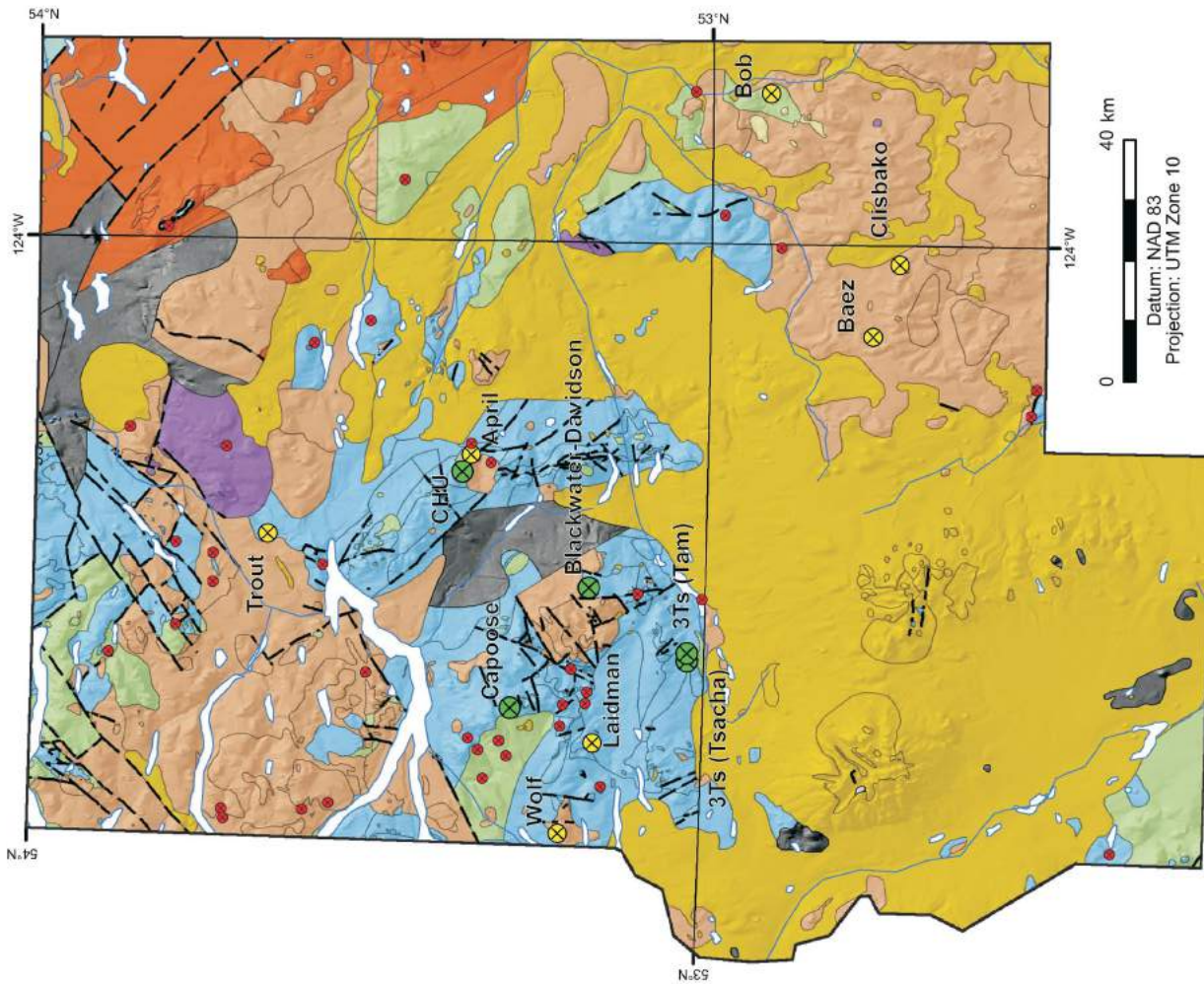


**Figure 2.** Generalized bedrock geology (after Massey et al., 2005) and mineral occurrences (MINFILE; BC Geological Survey, 2013) of the TREK geochemistry project area. Digital elevation model from Canadian digital elevation data (GeoBase®, 2007).

**Mineral occurrences (MINFILE)**

- Showing
- ⊗ Prospect
- ⊗ Developed prospect
- Mapped faults



area, toward the north in the southeastern region, and toward the southeast in the south (Figure 3). Sparse southeast- and northeast-directed ice-flow indicators in the southwest could be the products of a late-glacial readvance through the Anahim Lake region from the Coast Mountains to the west (Tipper, 1971b). Ice-flow features from the glacial maximum may have been destroyed during this readvance, or covered by ablation and melt-out tills as the ice stagnated.

Deglaciation was likely a combination of frontal retreat in the northern and eastern regions of the project area (cf. Fulton, 1991) with widespread stagnation in the southwest (Giles and Kerr, 1993). During this time, large glacial lakes

formed in major drainages that were impeded by ice (e.g., Clague, 1989; Plouffe, 1997), and locally in tributary valleys. Subglacial meltwater channels and eskers developed under the ice and glaciofluvial sand and gravel were deposited in channels and outwash plains in front of the ice.

### Surficial Geology

Till is the dominant surficial material in the project area and occurs mostly as basal and ablation till facies. A strict definition for basal till is used here: an unsorted diamicton deposited by lodgment or melt-out processes at the base of a glacier with little or no reworking by water (Dreimanis, 1989; Benn and Evans, 2010). Basal till is typically a dense,

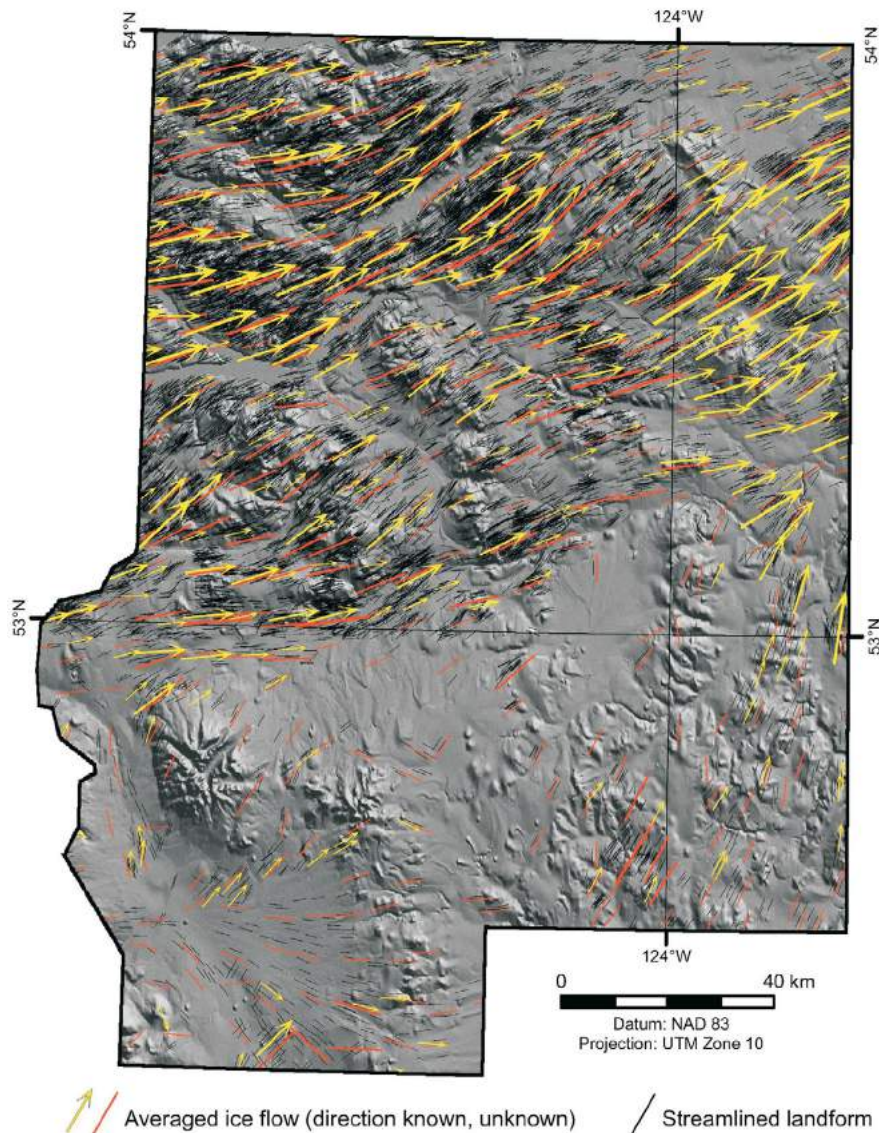


**Figure 3.** Ice-flow directions indicated by streamlined landforms (black symbols; compiled by Ferbey et al., 2013) for the project area in central British Columbia; generalized ice-flow arrows were produced by averaging azimuth values of streamlined landforms within an 8 km grid cell based on unidirectional (yellow symbol) and bidirectional (red symbol) features. The sizes of the generalized arrows are a function of the density of original streamlined landform data. Digital elevation model from Canadian digital elevation data (GeoBase®, 2007).

overconsolidated, matrix-supported diamicton. It generally conforms to the underlying topography with thicknesses varying from less than one metre at high elevations and in areas of high relief to tens of metres in areas of low relief. In the northern portion of the TREK Project area, it forms drumlinized and fluted terrain, indicating ice flow toward the northeast.

Ablation till is deposited during deglaciation and consists dominantly of far-travelled supraglacial and englacial material (Benn and Evans, 2010). Ablation till is found in areally small deposits in depressions or basins throughout the project area, and is widespread to the north and west of the Ilgachuz and Itcha mountain ranges. Ablation till is differentiated from basal till by its lack of density and high sand content in the matrix. It is generally matrix supported, shows some stratification, and contains sand or gravel lenses, but can also be clast supported or massive. Ablation till typically exhibits a hummocky or undulating surface expression, but in the project area it was observed conforming to the underlying topography near deposit margins.

Other glacial sediments occur within the project area. Well-sorted glaciofluvial sand and/or gravel units are found within meltwater channels and on the upper terraces of major rivers. Less sorted glaciofluvial deposits are commonly spatially associated with ablation till. Areally extensive glaciolacustrine deposits occur within the Fraser Basin in the northeastern part of the project area and in the north coast rivers watershed in the southwest. Less extensive deposits occur within tributary valleys adjacent to ablation till and ice-contact glaciofluvial deposits. Glaciolacustrine sediments in the project area vary from laminated silt and sand to unsorted diamicton. Glaciolacustrine diamicton is particularly common near the limits of glacial Lake Fraser (generally confined by the Fraser Basin; Figure 1) in the northeastern part of the project area and are interpreted as undermelt diamicton (cf. Gravenor et al., 1984). These deposits can be difficult to distinguish from basal till as they commonly part along horizontal planes. In contrast to basal tills, however, they typically lack density and have a matrix composed almost entirely of silt. Aeolian deposits are common around larger glaciolacustrine and glaciofluvial deposits. They occur as veneers (<1 m thick) and extensive dune fields, such as in the southeast corner of NTS 093G/05.

### Historic Geochemical Data

Previously published biogeochemical, lake and stream sediment, and till

geochemical data are summarized in Table 1 and depicted in Figure 4. Pine tree bark was targeted for biogeochemical sampling. The bark was reduced to ash and analyzed for multiple elements by instrumental neutron activation analysis (INAA), and inductively coupled plasma–emission spectrometry (ICP-ES) following an aqua-regia digestion (Dunn and Hastings, 1998, 1999, 2000). Many archived lake and stream sediment samples were recently reanalyzed by Jackaman (2006, 2008a, b, 2009a, b). Reanalysis of lake sediments was by INAA (25 elements) and inductively coupled plasma–mass spectrometry (ICP-MS; 35 elements) following an aqua-regia digestion. Lake sediments were also analyzed for fluoride by specific ion electrode (SIE) analysis, and organic content by loss-on-ignition. Archived till samples were originally analyzed by INAA for total gold determinations plus 34 elements.

### Till Geochemical and Mineralogical Survey

Basal till is well suited to assessing mineral potential of an area because it is a first derivative of bedrock (Shilts, 1993) and therefore has a similar geochemical signature. It was eroded, transported and deposited under ice, thus its transport history is relatively simple and can be determined by reconstructing ice-flow histories. Furthermore, it produces a geochemical signature that is areally more extensive than the bedrock source and potentially easier to locate (Levson, 2001). Basal till in the project area is a massive, dense, dark brown, matrix-supported diamicton. In most exposures, it exhibits subhorizontal fissility and vertical jointing resulting in a blocky appearance (Figure 5). The matrix composition in the project area varies; generally, in the north it is silt to sandy silt and in the south it has a higher sand content. The matrix proportion varies from 70 to 85% with a modal clast size of small pebble and ranges up to boulder.

**Table 1.** Previous geochemical sampling conducted in the project area, central British Columbia.

Survey year	NTS map area	Type	Sample sites <sup>1</sup>	Reference
1996	093F/09, /10, /15, /16	Tree bark	224	Dunn and Hastings, 2000
1997	093F/13, /14, /12	Tree bark	100	Dunn and Hastings, 1998
1998	093K/02, /03	Tree bark	2	Dunn and Hastings, 1999
1980, 1985 <sup>2</sup>	093A, B, G, H, J, K, N, O	Stream	470	Jackaman, 2008a
2005	093C, F	Stream	66	Jackaman, 2006
2008	093E, F, G, J, K, L, M, N, O	Stream	32	Jackaman, 2009b
1993	093F	Lake	380	Jackaman, 2009a
2005	093C, F	Lake	1324	Jackaman, 2006
2007	093G, H, J, K, N, O	Lake	89	Jackaman, 2008b
1992	093C/09, /16	Till	176	Lett et al., 2006
1993	093F/03	Till	171	Levson et al., 1994; Plouffe et al., 2001
1994	093F/07	Till	143	Weary et al., 1997; Plouffe et al., 2001
1994, 1998	093F	Till	292	Plouffe et al., 2001
1996, 1997	093F	Till	314	Plouffe and Williams, 1998; Plouffe et al., 2001

<sup>1</sup>Only sample sites within the study area are listed

<sup>2</sup>Samples reanalyzed in 2007.

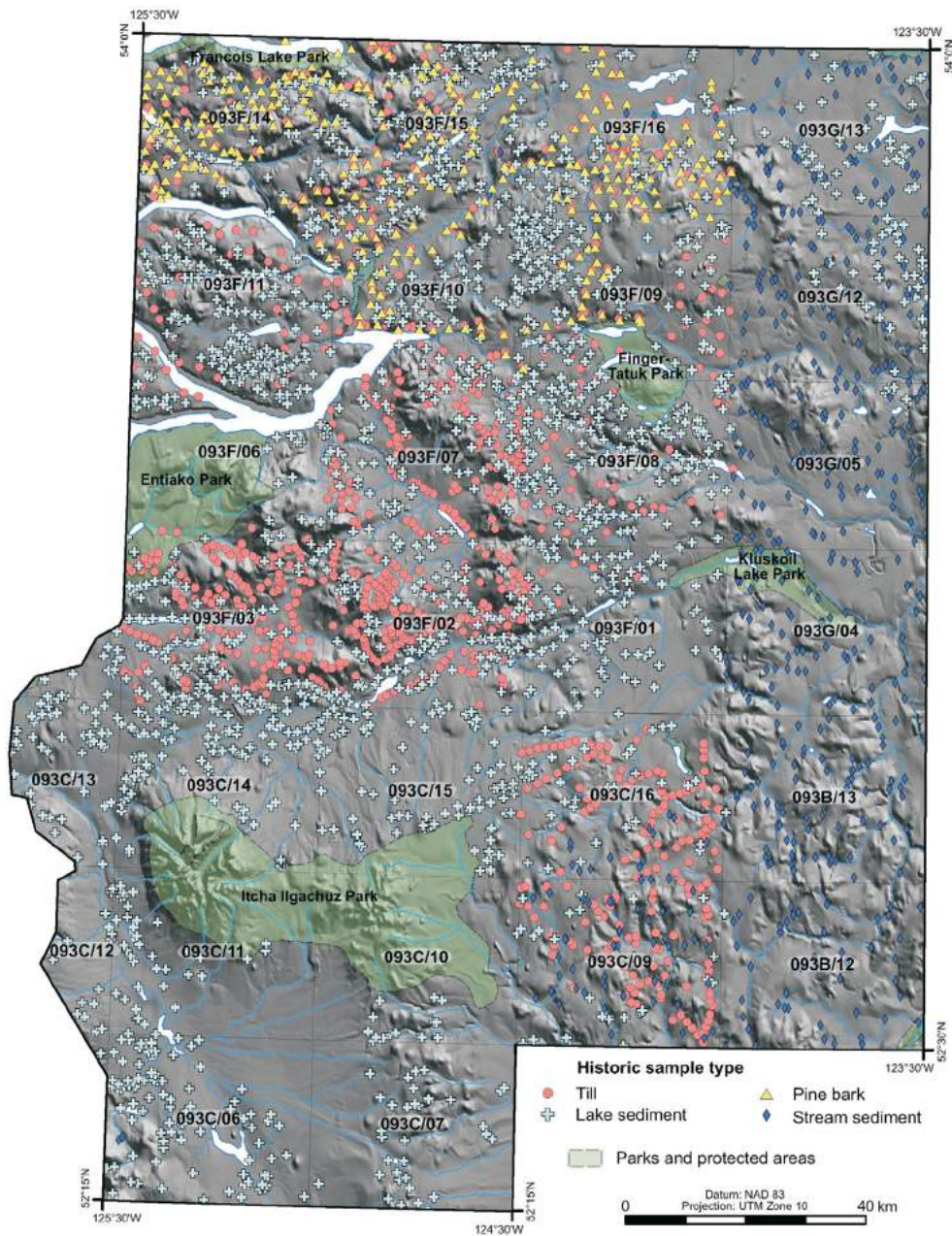


**Figure 4.** Distribution of archive till (red circle), lake (light blue cross) and stream (dark blue diamond) sediment geochemical data and biogeochemical (pine bark) data (yellow triangle), central British Columbia. See text for references. Digital elevation model from Canadian digital elevation data (GeoBase®, 2007).

### Basal Till Potential Mapping

Basal till potential maps delineate areas where basal till is likely to occur and identify the most likely locations for basal till sample collection (Figure 6). Conversely, BTPMs highlight regions where it may be necessary to implement different geochemical sampling protocols or consider alternative sample media due to a lack of basal till.

Drift exploration potential and applicability maps have been produced in the past to assist with geochemical survey design in drift-covered terrain (e.g., Meldrum and Bobrowsky, 1994a, b; Huntley and Bobrowsky, 1995; Proud-

foot et al., 1995). These derivative maps rely on existing surficial geology mapping and can be limited by the detail and scope of the original mapping. A classification scheme is applied to the existing surficial mapping and the classified polygons are symbolized on the map (i.e., original surficial geology polygons labels are not included). In contrast to this, BTPMs incorporate existing surficial geology mapping and also include a significant component of new mapping. This new mapping is focused in areas where mapping detail can be improved upon or where insights into till facies or genesis can be gained using, for example, newer, higher resolution, digital imagery.

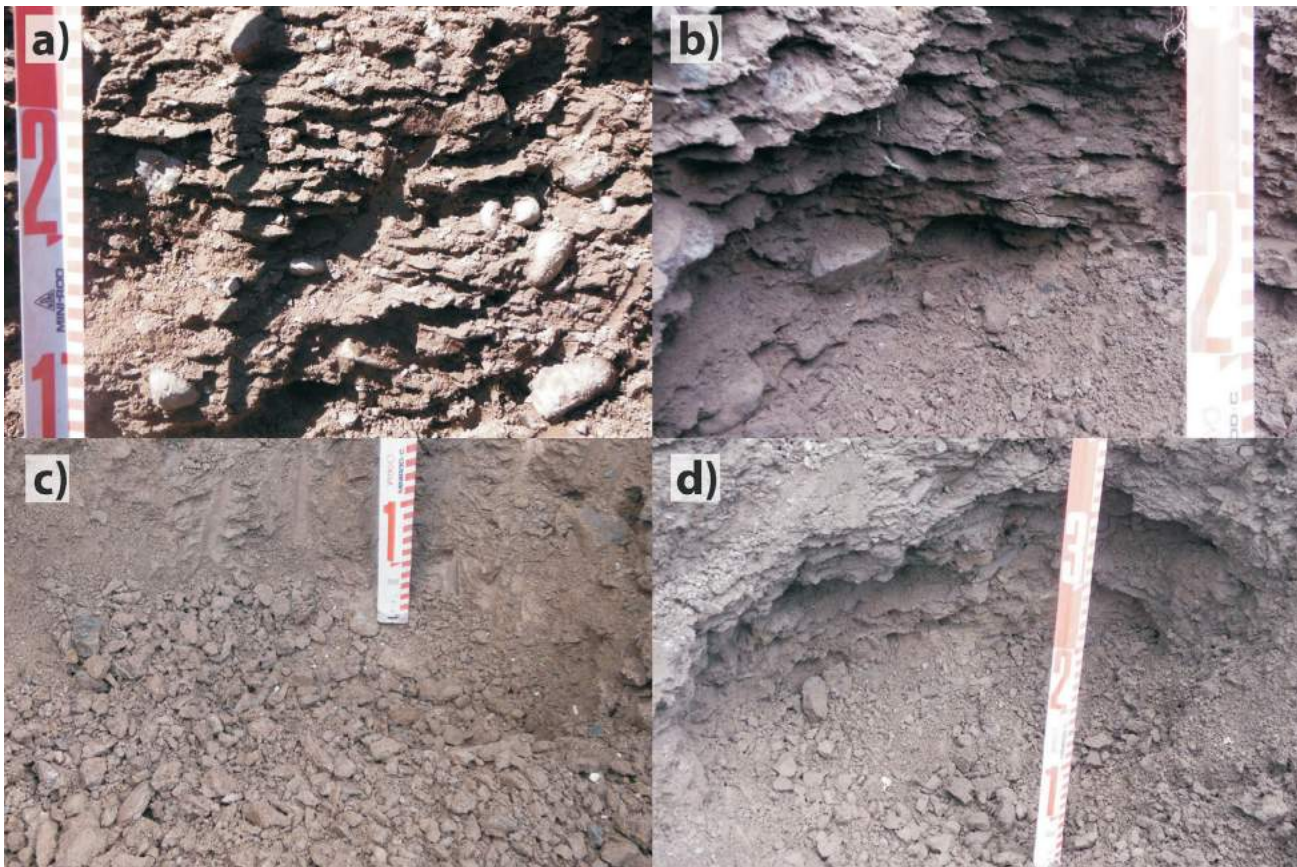


**Figure 5.** Exposures of basal till from different regions of the project area, central British Columbia. Note characteristic horizontal fissility in **a)** and **b)** and resulting blocky appearance in **c)** and **d)**. Till colour and composition vary with the local bedrock units.

The BTPMs used for the TREK Project were created using DAT/EM's Summit Evolution photogrammetry software (DAT/EM Systems International, 2012) and Esri's ArcGIS (Esri, 2012). On a PC workstation, digital airphotos are viewed in stereo in Summit Evolution. By interfacing with ArcGIS, shapefiles of existing surficial geology contacts can be superimposed on the digital airphoto stereopairs and be edited. New surficial geology linework can be added to existing or newly created shapefiles. Polygon labels are based on the terrain classification system for British Columbia (Howes and Kenk, 1997). During the production of BTPMs, emphasis was placed on differentiating basal till from ablation till, the latter of which is not suitable for geochemical sampling. Areas with limited indication of basal till are left unmapped.

Similar to drift exploration potential and applicability maps, a classification scheme is applied to the mapping to highlight areas (using colours) where basal till is likely to occur and therefore identify the most likely locations for basal till sample collection. A polygon's potential is largely determined by the areal extent of basal till within the polygon and its association with other surficial materials and their depositional environments (Figure 6). For example, a polygon containing only basal till would be assigned high

potential as a sampler would have a good chance of collecting a basal till sample anywhere within that polygon. Conversely, a polygon containing ablation till and glaciofluvial deposits would be assigned low potential, in part because basal till has not been mapped (although it is under the ablation till), but also because these surficial materials can be associated with ice-stagnation (conducive to deposition of sand and/or gravel units) and not active ice. Unlike drift exploration potential and applicability maps, BTPMs include the original surficial geology polygon label (surficial material and surface expression). This allows the user to better understand how the classification was applied and to gain some insight into the spatial and genetic associations between different surficial material types and surface expressions. Ice-flow indicators from Ferbey et al. (2013) are also included on the maps to illustrate dominant transport directions in basal till.

This process of 'soft-copy digitizing' significantly increases the speed and efficiency of map production by eliminating the need for transferring linework from hard-copy aerial photographs to the digital environment and the inevitable corrections associated with the digitization process. Soft-copy digitizing produces files that can be immediately transferred to any GIS for planning or use in the field. Basal

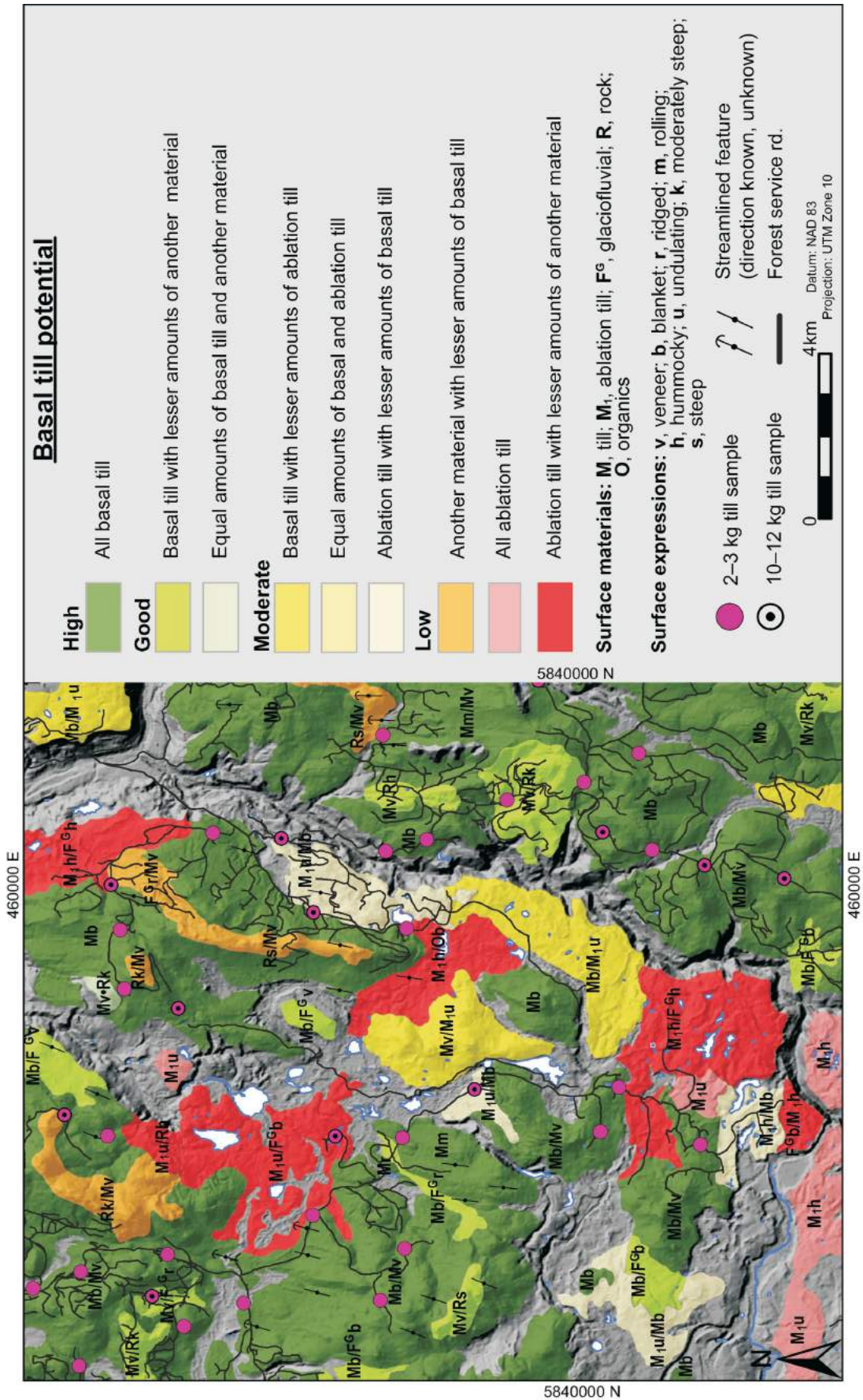


**Figure 6.** Example of basal till potential mapping from the southeast corner of NTS 093B/13. High potential is represented in green and low potential in red. Polygon labels are based on the terrain classification system for British Columbia (Howes and Kenk, 1997) and describe surface materials (upper-case letters) and their surface expression (lower-case letters). Emphasis is placed on differentiating basal till (M) and ablation till (M<sub>1</sub>). Ice-flow indicators compiled by Ferby et al. (2013). Digital elevation model from Canadian digital elevation data (GeoBase®, 2007).

till potential maps were completed for sixteen 1:50 000 scale map areas during a four month period. Extensive ground-truthing was conducted during sampling traverses throughout the 2013 field season.

## Field Methods

The 2013 field season focused on regions that have not previously been sampled. Six hundred and eighty-four till samples (2–3 kg) were collected for major-, minor-, and trace-element geochemical analyses (Figure 7). At each sample site, 50 stones, of large pebble to small cobble size, were collected for lithological studies. At approximately every other site, a 10–12 kg sample was collected for mineral separation and gold grain counts (336 samples in total). Where archive sample density was low, infill sampling was conducted. Because most archived samples do not have mineralogical data, 10–12 kg samples were collected at nearly every infill site in an effort to produce an equivalent till dataset for the entire project area.

Sampling locations are based on a 2 km, staggered grid, aligned with ice flow (see Levson, 2001). These locations, however, are restricted in some areas due to lack of access or exposure. For example, large regions in NTS 093C/10, /11, /14, /15 and 093F/01 have no road access. Natural or anthropogenic exposures (>1 m) were typically required to obtain in situ basal till; till which had not been altered by soil-forming processes or biological activity. These exposures occurred dominantly as roadcuts and, in some cases, borrow pits or river and lake cuts. Soil pits were dug in some situations, although usually avoided because of time constraints.

The largest hindrance to sample collection was the lack of basal till. In large drainage networks, basal till has mostly been eroded by (glacio) fluvial processes. Some valleys, however, do have exposed stratigraphic sections from which till can be sampled. In the northeast, thick glacio-lacustrine units were deposited up to an elevation of 875 m asl (Figure 8). Basal till is only found at surface where the relief is higher than the lake limit. Extensive units of ablation till were deposited by stagnating ice in the southwest, whereas areally smaller deposits of ablation till occur locally throughout the project area.

A backhoe was used to test if basal till could be accessed in areas mantled by a thin layer of ablation till. Four test sites were chosen based on the local surface expression. The first two sites were located in a clearcut that exposed a complex of hummocky ablation till and glaciofluvial deposits. Hummocks here have a maximum relief of 4 m. A 5 m wide melt-water channel incised the deposit. The first pit was excavated in a hollow between large hummocks. Bedrock was reached at 1 m below surface through a sandy diamict. The second pit was 2.5 m in depth and adjacent to the channel in an area of 1–2 m high hummocks. Exposed from the top

down were interbedded sand and gravel, silt and sand laminations, and massive silt and sand. Basal till was not reached at this location. The third and fourth sites were spaced about 1.5 km apart and were situated near the contact between basal till and ablation till deposits. The surface expression was undulating, with relief of  $\leq 1$  m. Two pits were excavated to a depth of 2.5 m exposing 2 m of ablation till over at least 0.5 m of basal till. In both pits, the contact was gradational over about 10 cm and was highlighted by a brown to grey colour change and a significant increase in density and silt and clay content in the matrix of the basal till (Figure 9). These test pit results demonstrate that it may be possible to reach basal till at a reasonable depth near the contact with ablation till deposits, and that mechanized sample collection methods can be effective in certain situations.

Helicopter-supported lake sediment and lakewater geochemical sampling was conducted on the east side of the project area, where basal till exposures were limited and lake sediment samples were not previously collected. Survey protocols were based on established guidelines in Cook (1997). A total of 280 samples were collected from 264 lakes (Figure 7). Lake sites were accessed using a float-equipped Bell 206 helicopter. Sediment samples were collected from the deepest part of the lake using a torpedo-style Hornbrook sampler. Lake sediment samples generally represent a 35 cm section of material obtained from below the water-sediment interface. Samples typically consisted of organic gels with varying amounts of inorganic sediment and organic matter. Water samples were collected from the surface in 250 ml bottles.

## Sample Analysis

Till and lake samples collected for geochemistry were sent to Acme Analytical Laboratories Ltd. (Vancouver, BC) for preparation. Tills were dried, an archive of the original till sample was generated, and the remaining material was sieved to produce splits of the silt plus clay-sized (<0.063 mm) fraction. Lake sediments were dried and milled with a ceramic ball to <0.0177 mm. Organic content was determined by loss-on-ignition (LOI). The 10–12 kg till samples were sent to Overburden Drilling Management Limited (Nepean, ON) where mineral concentrates (0.25–2.0 mm) and gold grain (<2.0 mm) concentrates were produced using a combination of gravity tables and heavy liquids.

New till samples were analyzed for minor and trace elements by ICP-MS following aqua-regia digestion (53 elements), major and minor elements by ICP-ES following a lithium borate fusion and dilute acid digestion (11 major oxides and 8 elements), and total gold determinations plus 34 elements by INAA. Reanalysis of the archived till samples was done by ICP-MS and for selected samples,

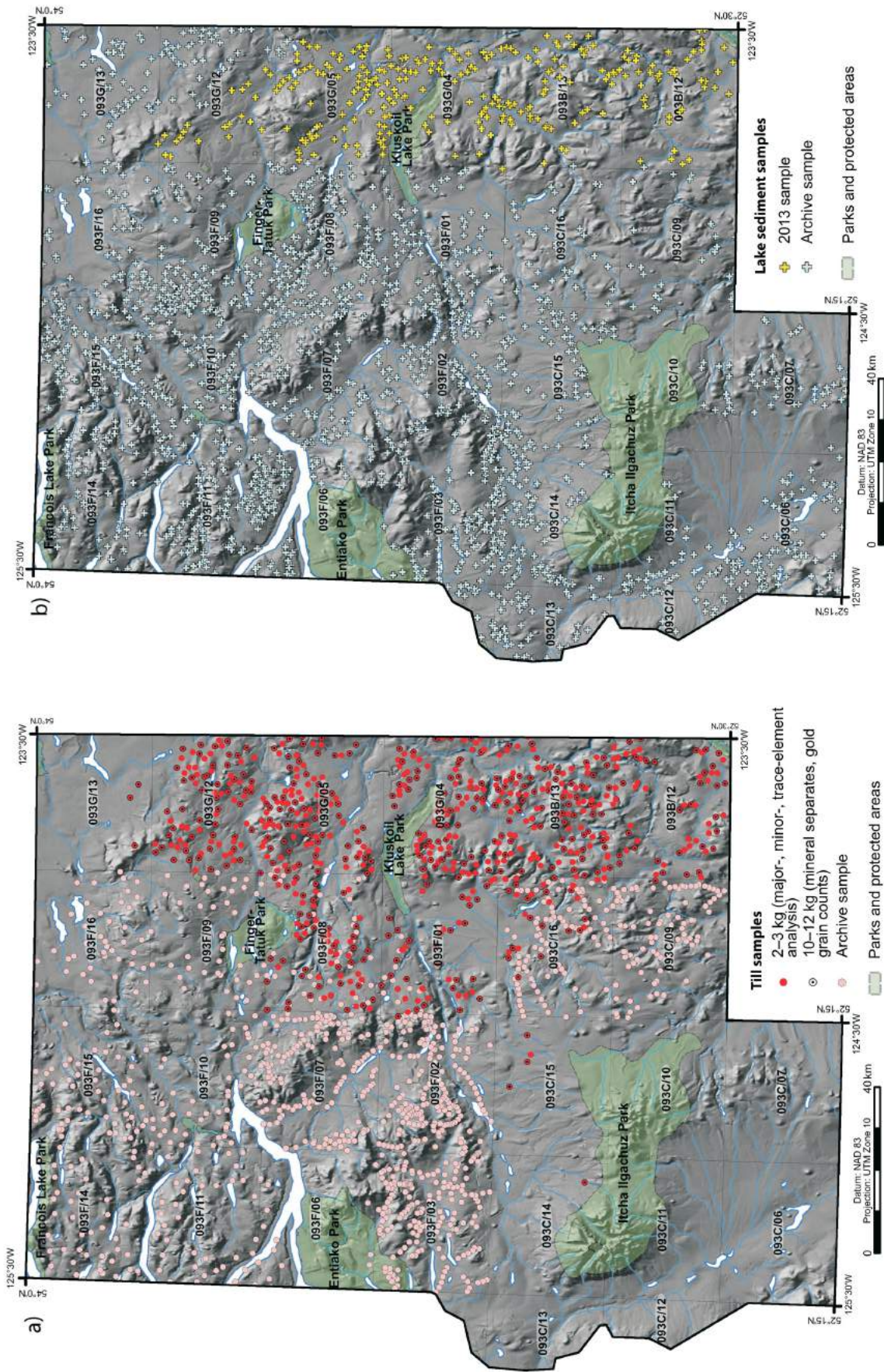


**Figure 7.** Distribution of previous and new sample locations in the project area, central British Columbia: **a)** till and **b)** lake sediment. Digital elevation model from Canadian digital elevation data (GeoBase®, 2007).

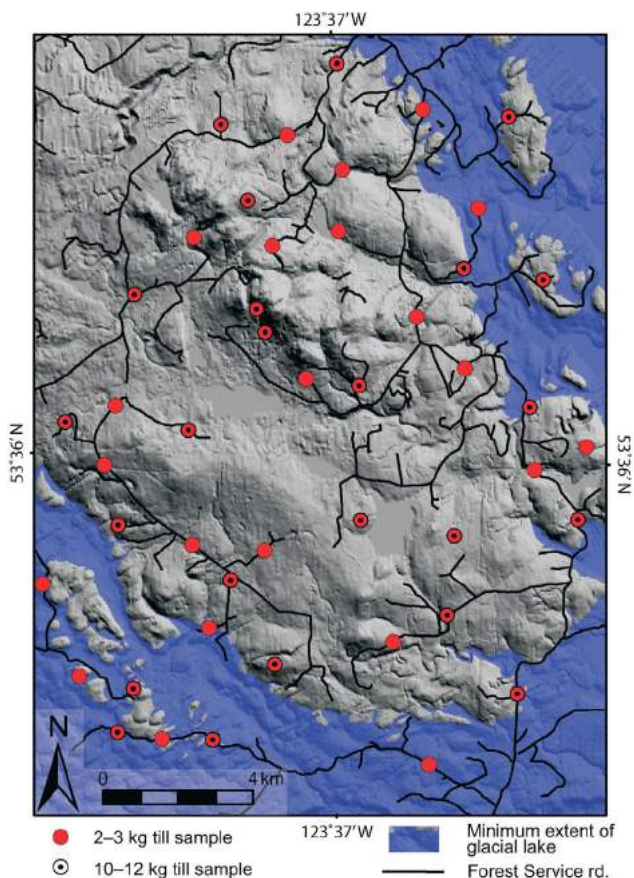


**Figure 8.** Digital elevation model (from Canadian digital elevation data [GeoBase®, 2007]) of the northeast corner of NTS 093G/12. The maximum level of glaciolacustrine sediments (875 m above sea level) delineates the minimum extent of one large, or several smaller glacial lakes. Within the extent of the lake, till samples were collected from islands above 875 m elevation and in natural or anthropogenic exposures, which provided access to basal till that was under the glaciolacustrine sediments.

ICP-ES. Lake sediments were analyzed for minor and trace elements by ICP-MS following aqua-regia digestion (53 elements), fluoride by SIE analysis, and total gold determinations plus 34 elements by INAA. Conductivity and pH were determined for lakewater samples. All geochemical analyses were completed at Acme Analytical Laboratories Ltd. (Vancouver, BC), except INAA, which was conducted at Becquerel Laboratories Inc. (Mississauga, ON). See Table 2 for analytical methods used for each sample type.

**Table 2.** Sample media and analytical methods used for this program. Abbreviations: ICP-ES, inductively coupled plasma–emission spectrometry; ICP-MS, inductively coupled plasma–mass spectrometry; INAA, instrumental neutron activation analysis; SIE, specific ion electrode.

Sample type	ICP-MS (53 elements)	ICP-ES (11 oxides, 8 elements)	INAA (35 elements)	SIE (fluoride)	pH	Conductivity
Till	•	•	•			
Archived till	•	• <sup>1</sup>	•			
Lake sediment	•		•	•		
Lakewater					•	•

<sup>1</sup>Select samples

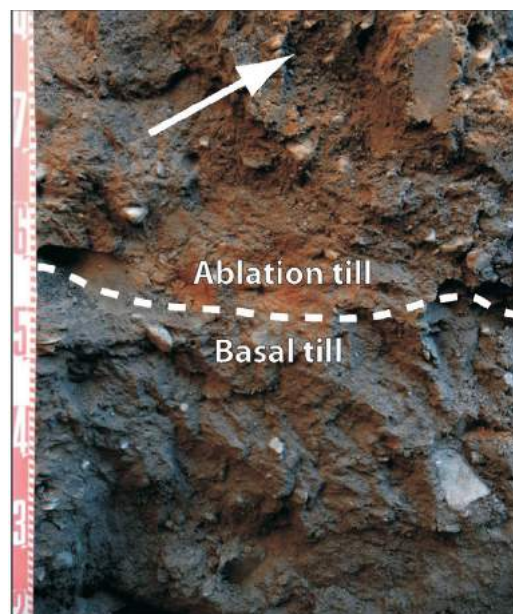


**Figure 9.** Gradational contact between basal till and overlying ablation till exposed in a 2.5 m deep pit. Ablation till is less dense and slightly oxidized with concentrations of sand and gravel (white arrow). Scale in centimetres.

### Quality Control

Quality control for analytical determinations includes the use of field duplicates, analytical duplicates, reference standards and blanks and is based on established protocols (Spirito et al., 2011). For each block of 20 samples, one field duplicate (taken at a randomly selected sample site), one analytical duplicate (a sample split during the preparation process), and one reference standard was included in geochemical analyses. Reference standards are CANMET till 1 and 4, TREK till standards A and B, and NVI standards 1, 2, 3 and 4. TREK and NVI standards were produced by homogenizing and sieving till with a known range of element values and elevated key metal values (e.g., Cu, Au, Mo). Duplicate samples determine sampling and analytical variability and reference standards measure the accuracy and precision of the analytical methods. Blanks are introduced throughout the sample stream to determine if there is any cross-contamination between samples.

## Future Work

As a multiyear program, future TREK Project geochemical activities will include the assembly of recently acquired survey data plus the further development of geoscience information required for additional field surveys planned for the second year. The project action plan includes the following:

- evaluate and compile analytical results and field data for new basal till and pebble samples;
- evaluate and compile new lake sediment and lakewater analytical results and field data;
- evaluate and compile analytical data determined from the reanalysis of archived samples;
- update existing BTPMs based on field survey ground-truthing exercises; and
- assess alternate geochemical data collection techniques, such as treetop biogeochemical surveys and mechanically assisted methods that can be used to cover areas with challenging access or limited availability of other target media types.

Generating a comprehensive collection of high quality geochemical analytical data and field information is a primary objective of the geochemical component of the TREK Project. This is being accomplished through the collection of new samples, the reanalysis of samples collected during previous surveys and the development of BTPMs, which supports both field survey work and follow-up exercises. When packaged and released to the public, this dataset will become an important tool that will be used in the exploration for and discovery of new mineral occurrences.

## Acknowledgments

This program was funded by Geoscience BC. Contributions by A. Plouffe, A. Grenier and A. Therriault (Geological Survey of Canada), A. Hickin (BC Ministry of Energy and Mines), T. Høe, and the BC Ministry of Forests, Lands and Natural Resource Operations have assisted with the development and application of these activities. A special thanks to the field crew: E. Jackaman, J. Dimock, B. Elder, J. Constable, B. Edgington and J. Balfour, whose hard work, determination and unflinching sediment discriminations provided a high quality dataset. Thanks to M. King (White Saddle Air Services) and J. Faulkner (Sky Helicopters Inc.) for air transport. H. Paul and T. Clement from the Nazko First Nation are also thanked for their participation in year one of the TREK geochemistry program.

## References

Armstrong, J.E., Crandell, D.R., Easterbrook, D.J. and Noble, J.B. (1965): Late Pleistocene stratigraphy and chronology in southwestern British Columbia and northwestern Washington; *Geological Society of America Bulletin*, v. 76, p. 321–330.

BC Geological Survey (2013): MINFILE BC mineral deposits database; BC Ministry of Energy and Mines, BC Geological Survey, URL <<http://minfile.ca/>> [October 2013].

Benn, D.I. and Evans, D.J.A. (2010): *Glaciers & Glaciation* 2<sup>nd</sup> ed.; Oxford University Press Inc., New York, 816 p.

Clague, J.J. (1989): Quaternary geology of the Canadian Cordillera; Chapter 1 *in* Quaternary Geology of Canada and Greenland, R.J. Fulton (ed.), Geological Survey of Canada, Geology of Canada Series no. 1, p. 15–96.

Cook, S.J. (1997): Regional and property-scale application of lake sediment geochemistry in the search for buried mineral deposits in the southern Nechako Plateau area, British Columbia (093C, E, F, K, L); *in* Interior Plateau Geoscience Project: Summary of Geological, Geochemical and Geophysical Studies, L.J. Diakow, P. Metcalfe and J.M. Newell (ed.), BC Ministry of Energy and Mines, Paper 1997-2, p. 175–203.

Cook, S.J., Levson, V.M., Giles, T.R. and Jackaman, W. (1995): A comparison of regional lake sediment and till geochemistry surveys: a case study from the Fawnie Creek area, central British Columbia; *Exploration Mining Geology*, v. 4, p. 93–101.

DAT/EM Systems International (2012): Summit Evolution Lite software suite; software, DAT/EM Systems International, Anchorage, Alaska.

Diakow, L.J. and Webster, I.C.L. (1994): Geology of the Fawnie Creek map area (NTS 93F/3); *in* Geological Fieldwork 1993, BC Ministry of Energy and Mines, BC Geological Survey, Paper 1994-1, p. 15–26, URL <<http://www.empr.gov.bc.ca/Mining/Geoscience/Publications/Catalogue/Fieldwork/Documents/1993/015-026-diakow.pdf>> [October 2013].

Diakow, L.J., Webster, I.C.L., Richards, T.A. and Tipper, H.W. (1997): Geology of the Fawnie and Nechako ranges, southern Nechako Plateau, central British Columbia (93F/2, 3, 6, 7); *in* Interior Plateau Geoscience Project: Summary of Geological, Geochemical and Geophysical Studies, L.J. Diakow, P. Metcalfe and J. Newell (ed.), BC Ministry of Energy and Mines, Paper 1997-2, p. 7–30, URL <[http://www.empr.gov.bc.ca/Mining/Geoscience/Publications/Catalogue/Papers/Documents/P1997-02\\_02.pdf](http://www.empr.gov.bc.ca/Mining/Geoscience/Publications/Catalogue/Papers/Documents/P1997-02_02.pdf)> [October 2013].

Dreimanis, A. (1989): Tills: their genetic terminology and classification; *in* Genetic Classification of Glacigenic Deposits, R.P. Goldthwait and C.L. Matsch (ed.), A.A. Balkema, Rotterdam, The Netherlands, p. 17–83.

Dunn, C.E. and Hastings, N.L. (1998): Biogeochemical survey of the Ootsa-Francois lakes using outer bark of lodgepole pine (NTS 93F13/14 and parts of 12 – north-central British Columbia): digital listings and summary notes; Geological Survey of Canada, Open File 3587d, 1 diskette, URL <<http://geoscan.nrcan.gc.ca/starweb/geoscan/servlet.starweb?path=geoscan/download.web&search1=R=209916>> [October 2013].

Dunn, C.E. and Hastings, N.L. (1999): Biogeochemical survey of the Fraser Lake area using outer bark of lodgepole pine (NTS93K/2 and parts of 93K/3 – north-central British Columbia): digital data listings and summary notes; Geological Survey of Canada, Open File 3696d, 1 diskette, URL <<http://geoscan.nrcan.gc.ca/starweb/geoscan/servlet.starweb?path=geoscan/download.web&search1=R=210377>> [October 2013].

- Dunn, C.E. and Hastings, N.L. (2000): Biogeochemical survey of the Nechako River area using outer bark of lodgepole pine (NTS 93 F/9, 93 F/10, 93 F/15, 93 F/16 and parts of 93 F/11, 93 F/14, 93 K/1 and 93 K/2), central British Columbia: digital data release for Open files 3594a-c; Geological Survey of Canada, Open File 3594d, 1 diskette, URL <<http://geoscan.nrcan.gc.ca/starweb/geoscan/servlet.starweb?path=geoscan/download.web&search1=R=211478>> [October 2013].
- Esri (2012): ArcGIS Desktop, release 10; software, Esri, Redlands, California.
- Ferbey, T. (2009): Till geochemical exploration targets, Redstone and Loomis Lake maps areas (NTS 93B/04 and 05), central British Columbia; BC Ministry of Energy and Mines, BC Geological Survey, Open File 2009-09, 48 p., URL <<http://www.empr.gov.bc.ca/Mining/Geoscience/PublicationsCatalogue/OpenFiles/2009/Documents/2009-09/OF2009-9.pdf>> [October 2013].
- Ferbey, T., Arnold, H. and Hickin, A.S. (2013): Ice-flow indicator compilation, British Columbia; BC Ministry of Energy and Mines, BC Geological Survey, Open File 2013-06, scale 1:1 650 000, URL <[http://www.empr.gov.bc.ca/Mining/Geoscience/PublicationsCatalogue/OpenFiles/2013/Pages/OF2013-06\\_iceflow.aspx](http://www.empr.gov.bc.ca/Mining/Geoscience/PublicationsCatalogue/OpenFiles/2013/Pages/OF2013-06_iceflow.aspx)> [October 2013].
- Ferbey, T., Vickers, K.J., Hietava, T.J.O. and Nicholson, S.C. (2009): Quaternary geology and till geochemistry of the Redstone and Loomis Lake map areas, central British Columbia (NTS 093B/04, 05); *in* Geological Fieldwork 2008, BC Ministry of Energy and Mines, BC Geological Survey, Paper 2009-1, p. 117–126, URL <[http://www.empr.gov.bc.ca/Mining/Geoscience/PublicationsCatalogue/Fieldwork/Documents/2008/11\\_Ferbey.pdf](http://www.empr.gov.bc.ca/Mining/Geoscience/PublicationsCatalogue/Fieldwork/Documents/2008/11_Ferbey.pdf)> [October 2013].
- Flint, R.F. (1971): *Glacial and Quaternary Geology*; Wiley, New York, 906 p.
- Fulton, R.J. (1991): A conceptual model for growth and decay of the Cordilleran Ice Sheet; *Géographie physique et Quaternaire*, v. 45, p. 333–339.
- GeoBase<sup>®</sup> (2007): Canadian digital elevation data, edition 3.0; Canadian Council on Geomatics, URL <<http://www.geobase.ca/geobase/en/find.do?produit=cded>> [October 2013].
- Giles, T.R. and Kerr, D.E. (1993): Surficial geology in the Chilanko Forks and Chezacut areas (93C/1,8); *in* Geological Fieldwork 1992, BC Ministry of Energy and Mines, BC Geological Survey, Paper 1993-1, p. 483–490, URL <<http://www.empr.gov.bc.ca/Mining/Geoscience/PublicationsCatalogue/Fieldwork/Documents/1992/483-490-giles.pdf>> [October 2013].
- Giles, T.R. and Levson, V.M. (1994): Surficial geology and drift exploration studies in the Fawnie Creek region (93/F3); *in* Geological Fieldwork 1993, BC Ministry of Energy and Mines, BC Geological Survey, Paper 1994-1, p. 27–38, URL <<http://www.empr.gov.bc.ca/Mining/Geoscience/PublicationsCatalogue/Fieldwork/Documents/1993/027-038-giles.pdf>> [October 2013].
- Giles, T.R. and Levson, V.M. (1995): Surficial geology and Quaternary stratigraphy of the Tsacha Lake area (NTS 093/F2); BC Ministry of Energy and Mines, BC Geological Survey, Open File 1995-10, scale 1:50 000, URL <<http://www.empr.gov.bc.ca/Mining/Geoscience/PublicationsCatalogue/OpenFiles/1995/Pages/1995-10.aspx>> [October 2013].
- Gravenor, C.P., von Brunn, V. and Dreimanis, A. (1984): Nature and classification of waterlain glaciogenic sediments, exemplified by Pleistocene, Late Palaeozoic and Late Precambrian deposits; *Earth Science Reviews*, v. 20, p. 105–166.
- Holland, S.S. (1976): Landforms of British Columbia: a physiographic outline; BC Ministry of Mines and Energy, Bulletin 48, 138 p.
- Howes, D.E. and Kenk, E. (1997): Terrain classification system for British Columbia (version 2); BC Ministry of Environment, URL <<http://archive.ilmb.gov.bc.ca/risc/pubs/teecolo/terclass/index.html>> [October 2013].
- Huntley, D.H. and Bobrowsky, P.T. (1995): Drift exploration applicability of the Mahatta Creek area (NTS 92L/5); BC Ministry of Energy and Mines, BC Geological Survey, Open File 1995-18, scale 1:50 000, URL <<http://www.empr.gov.bc.ca/Mining/Geoscience/PublicationsCatalogue/OpenFiles/1995/Documents/OF1995-18.pdf>> [October 2013].
- Jackaman, W. (2006): Regional drainage sediment and water geochemical data Anahim Lake – Nechako River, central British Columbia (NTS 93C and 93F); Geoscience BC, Report 2006-4 and BC Ministry of Energy and Mines, BC Geological Survey, GeoFile 2006-11, 463 p., URL <<http://www.geosciencebc.com/s/2006-04.asp>> [October 2013].
- Jackaman, W. (2008a): QUEST Project sample reanalysis; Geoscience BC, Report 2008-3, 4 p., URL <<http://www.geosciencebc.com/s/2008-03.asp>> [October 2013].
- Jackaman, W. (2008b): Regional lake sediment and water geochemical data, northern Fraser Basin, central British Columbia (parts of NTS 093G, H, J, K, N & O); Geoscience BC, Report 2008-5, 446 p., URL <<http://www.geosciencebc.com/s/2008-05.asp>> [October 2013].
- Jackaman, W. (2009a): QUEST-West project sample reanalysis; Geoscience BC, Report 2009-5, 4 p., URL <<http://www.geosciencebc.com/s/2009-05.asp>> [October 2013].
- Jackaman, W. (2009b): Regional drainage sediment and water geochemical data, central British Columbia (parts of NTS 93E, F, G, J, K, L, M, N & O); Geoscience BC, Report 2009-11, 347 p., URL <<http://www.geosciencebc.com/s/2009-11.asp>> [October 2013].
- Lett, R.E., Cook, S.J. and Levson, V.M. (2006): Till geochemistry of the Chilanko Forks, Chezacut, Clusko River and Toil Mountain area, British Columbia (NTS 93C/1, 8, 9, and 16); BC Ministry of Energy and Mines, BC Geological Survey, GeoFile 2006-1, 272 p., URL <<http://www.empr.gov.bc.ca/Mining/Geoscience/PublicationsCatalogue/GeoFiles/Pages/2006-1.aspx>> [October 2013].
- Levson, V.M. (2001): Regional till geochemical surveys in the Canadian Cordillera: sample media, methods, and anomaly evaluation; *in* Drift Exploration in Glaciated Terrain, M.B. McClenaghan, P.T. Bobrowsky, G.E.M. Hall and S.J. Cook (ed.), Geological Society, Special Publication, no. 185, p. 45–68.
- Levson, V.M. (2002): Quaternary geology and till geochemistry of the Babine porphyry copper belt, British Columbia (NTS 93 L/9, 16, M/1, 2, 7, 8); BC Ministry of Energy and Mines, BC Geological Survey, Bulletin 110, 278 p., URL <<http://www.empr.gov.bc.ca/Mining/Geoscience/PublicationsCatalogue/BulletinInformation/BulletinsAfter1940/Pages/Bulletin110.aspx>> [October 2013].
- Levson, V.M. and Giles, T.R. (1994): Surficial geology and Quaternary stratigraphy of the Fawnie Creek area; BC Ministry of Energy and Mines, BC Geological Survey, Open File 1994-9, scale 1:50 000, URL <<http://www.empr.gov.bc.ca/>>

- Mining/Geoscience/PublicationsCatalogue/OpenFiles/1994/Documents/OF1994-09.pdf> [October 2013].
- Levson, V.M. and Giles, T.R. (1997): Quaternary geology and till geochemistry studies in the Nechako and Fraser plateaus, central British Columbia (NTS 93C/1, 8, 9, 10; F/2, 3, 7; L/16; M/1); *in* Interior Plateau Geoscience Project: Summary of Geological, Geochemical and Geophysical Studies, L.J. Diakow, P. Metcalfe and J.M. Newell (ed.), BC Ministry of Energy and Mines, BC Geological Survey, Paper 1997-2, p. 121–145, URL <<http://www.empr.gov.bc.ca/Mining/Geoscience/PublicationsCatalogue/Papers/Pages/1997-2.aspx>> [October 2013].
- Levson, V.M., Giles, T.R., Cook, S.J. and Jackaman, W. (1994): Till geochemistry of the Fawnie Creek area (93F/03); BC Ministry of Energy and Mines, BC Geological Survey, Open File 1994-18, 40 p., URL <<http://www.empr.gov.bc.ca/Mining/Geoscience/PublicationsCatalogue/OpenFiles/1994/Pages/1994-18.aspx>> [October 2013].
- Massey, N.W.D., MacIntyre, D.G., Desjardins, P.J. and Cooney, R.T. (2005): Digital geology map of British Columbia: whole province; BC Ministry of Energy and Mines, BC Geological Survey, GeoFile 2005-1, scale 1:250 000, URL <<http://www.empr.gov.bc.ca/Mining/Geoscience/PublicationsCatalogue/GeoFiles/Pages/2005-1.aspx>> [October 2013].
- Mathews, W.H. (1986): Physiographic map of the Canadian Cordillera; Geological Survey of Canada, “A” Series Map 1710A, scale 1:5 000 000, URL <<http://geoscan.nrcan.gc.ca/starweb/geoscan/servlet.starweb?path=geoscan/download.web&search1=R=122821>> [October 2013].
- McClenaghan, M.B., Bobrowsky, P.T., Hall, G.E.M. and Cook, S.J., editors (2000): Drift exploration in glaciated terrain; Geological Society, Special Publication no. 185, 360 p.
- Meldrum, D.G. and Bobrowsky, P.T. (1994a): Drift exploration potential of the Alice Lake area (92L/6); BC Ministry of Energy and Mines, BC Geological Survey, Open File 1994-12, scale 1:50 000, URL <<http://www.empr.gov.bc.ca/Mining/Geoscience/PublicationsCatalogue/OpenFiles/1994/Documents/OF1994-12.pdf>> [October 2013].
- Meldrum, D.G. and Bobrowsky, P.T. (1994b): Drift exploration potential of the Port McNeill area (92L/11); BC Ministry of Energy and Mines, BC Geological Survey, Open File 1994-11, scale 1:50 000, URL <<http://www.empr.gov.bc.ca/Mining/Geoscience/PublicationsCatalogue/OpenFiles/1994/Documents/OF1994-11.pdf>> [October 2013].
- Metcalfe, P., Richards, T.A., Villeneuve, M.E., White, J.M. and Hickson, C.J. (1998): Physical and chemical volcanology of the Eocene Mount Clisbako volcano, central British Columbia; *in* Interior Plateau Geoscience Project: Summary of Geological, Geochemical and Geophysical Studies, L.J. Diakow, P. Metcalfe and J.M. Newell (ed.), BC Ministry of Energy and Mines, BC Geological Survey, Paper 1997-2, p. 31–61, URL <[http://www.empr.gov.bc.ca/Mining/Geoscience/PublicationsCatalogue/Papers/Documents/P1997-02\\_03.pdf](http://www.empr.gov.bc.ca/Mining/Geoscience/PublicationsCatalogue/Papers/Documents/P1997-02_03.pdf)> [October 2013].
- Mihalynuk, M.G., Orovan, E.A., Larocque, J.P., Freidman, R.M. and Bachiu, T. (2009): Geology, geochronology and mineralization of the Chilanko Forks to southern Clusko River area, west-central British Columbia (NTS 093C/01, 08, 09S); *in* Geological Fieldwork 2008, BC Ministry of Energy and Mines, BC Geological Survey, Paper 2009-1, p. 81–100, URL <[http://www.empr.gov.bc.ca/Mining/Geoscience/PublicationsCatalogue/Fieldwork/Documents/2008/08\\_Mihalynuk.pdf](http://www.empr.gov.bc.ca/Mining/Geoscience/PublicationsCatalogue/Fieldwork/Documents/2008/08_Mihalynuk.pdf)> [October 2013].
- Mihalynuk, M.G., Peat, C.R., Terhune, K. and Orovan, E.A. (2008): Regional geology and resource potential of the Chezacut map area, central British Columbia (NTS093C/08); *in* Geological Fieldwork 2007, BC Ministry of Energy and Mines, BC Geological Survey, Paper 2008-1, p. 117–134, URL <<http://www.empr.gov.bc.ca/Mining/Geoscience/PublicationsCatalogue/Fieldwork/Documents/2007/13-Mihalynuk-Chezacut34526.pdf>> [October 2013].
- Monger, J.W.H., Wheeler, J.O., Tipper, H.W., Gabrielse, H., Harms, T., Struik, L.C., Campbell, R.B., Dodds, C.J., Gehrels, G.E. and O’Brien, J. (1991): Cordilleran terranes (Chapter 8: Upper Devonian to Middle Jurassic assemblages); *in* Geology of the Cordilleran Orogen in Canada, H. Gabrielse and C.J. Yorath (ed.), Geological Survey of Canada, Geology of Canada Series no. 4, p. 281–327.
- Plouffe, A. (1997): Ice-flow and late-glacial lakes of the Fraser Glaciation, central British Columbia; *in* Current Research 1997-A/B, Geological Survey of Canada, p. 1333–1343.
- Plouffe, A. and Levson, V.M. (2001): Late quaternary glacial and interglacial environments of the Nechako River–Cheslatta Lake area, central British Columbia; *Canadian Journal of Earth Sciences*, v. 38, p. 719–731.
- Plouffe, A. and Willams, S.P. (1998): Regional till geochemistry, gold and pathfinder elements, northern Nechako River, British Columbia; Geological Survey of Canada, Open File 3687, 3 p., scale 1:400 000, URL <<http://geoscan.nrcan.gc.ca/starweb/geoscan/servlet.starweb?path=geoscan/download.web&search1=R=210023>> [October 2013].
- Plouffe, A., Levson, V.M. and Mate, D.J. (2001): Till geochemistry of the Nechako River map area (NTS 93F), central British Columbia; Geological Survey of Canada, Open File 4166, 66 p., 1 CD-ROM, URL <<http://geoscan.nrcan.gc.ca/starweb/geoscan/servlet.starweb?path=geoscan/download.web&search1=R=212986>> [October 2013].
- Proudfoot, D.N. (1993): Drift exploration and surficial geology of the Clusko River and Toil Mountain map sheets (93C/9, 16); *in* Geological Fieldwork 1992, BC Ministry of Energy and Mines, BC Geological Survey, Paper 1993-1, p. 491–498, URL <<http://www.empr.gov.bc.ca/Mining/Geoscience/PublicationsCatalogue/Fieldwork/Documents/1992/491-498-proudfoot.pdf>> [October 2013].
- Proudfoot, D.N., Bobrowsky, P.T. and Meldrum, D.G. (1995): Drift exploration potential maps derived from terrain geology maps; *in* Drift Exploration in the Canadian Cordillera, P.T. Bobrowsky, S.J.N. Sibbick, J.M. Newell and P.F. Matysek (ed.), BC Ministry of Energy and Mines, BC Geological Survey, Paper 1995-2, p. 22–31, URL <<http://www.empr.gov.bc.ca/Mining/Geoscience/PublicationsCatalogue/Papers/Pages/1995-2.aspx>> [October 2013].
- Rencz, A.N., Klassen, R.A. and Moore, A. (2002): Comparison of geochemical data derived from till and lake sediment samples, Labrador, Canada; *Geochemistry, Exploration, Environment, Analysis*, v. 2, p. 27–35.
- Riddell, J.M. (2006): Geology of the southern Nechako Basin (NTS 92N, 92O, 93C, 93F, 93G), sheet 3 of 3 — geology with contoured gravity underlay; BC Ministry of Energy and Mines, Petroleum Geology Map 2006-1, scale 1:400 000, URL <<http://www.empr.gov.bc.ca/Mining/Geoscience/PublicationsCatalogue/PetroleumGeology/Maps/2006-1-3.pdf>> [October 2013].

[Geoscience/PublicationsCatalogue/OilGas/OpenFiles/Pages/PGOF2006-3.aspx](#) [October 2013].

- Shilts, W. (1993): Geological Survey of Canada's contributions to understanding the composition of glacial sediments; Canadian Journal of Earth Sciences, v. 30, p. 333–353.
- Spirito, W.A., McClenaghan, M.B., Plouffe, A., McMartin, I., Campbell, J.E., Paulen, R.C., Garrett, R.G. and Hall, G.E.M. (2011): Till sampling and analytical protocols for GEM projects: from field to archive; Geological Survey of Canada, Open File 6850, 83 p.
- Tipper, H.W. (1969): Anahim Lake, British Columbia; Geological Survey of Canada, Map 1202A, scale 1:250 000.
- Tipper, H.W. (1971a): Glacial geomorphology and Pleistocene history of central British Columbia; Geological Survey of Canada, Bulletin 196, 89 p.
- Tipper, H.W. (1971b): Multiple glaciations in central British Columbia; Canadian Journal of Earth Sciences, v. 8, p. 743–752.
- Vickers, K.J. and Ferbey, T. (2009): Surficial geology of the Redstone area (NTS 093B/04); BC Ministry of Energy and Mines, BC Geological Survey, Open File 2009-05, scale 1:50 000, URL <<http://www.empr.gov.bc.ca/Mining/Geoscience/PublicationsCatalogue/OpenFiles/2009/Documents/2009-05/OF2009-5.pdf>> [October 2013].
- Weary, G.F., Levson, V.M. and Broster, B.E. (1997): Till geochemistry of the Chedakuz Creek map area (93F/7); BC Ministry of Energy and Mines, BC Geological Survey, Open File 1997-11, 97 p., URL <<http://www.empr.gov.bc.ca/Mining/Geoscience/PublicationsCatalogue/OpenFiles/1997/Pages/1997-11.aspx>> [October 2013].

# Geochemical Expression in Soil and Water of Carbon Dioxide Seepages Near the Nazko Cone, Central British Columbia (NTS 093B/13)

R.E. Lett, Consultant, Victoria, BC, raylett@shaw.ca

W. Jackaman, Noble Exploration Services Ltd., Sooke, BC

Lett, R.E. and Jackaman, W. (2014): Geochemical expression in soil and water of carbon dioxide seepages near the Nazko cone, central British Columbia (NTS 093B/13); in Geoscience BC Summary of Activities 2013, Geoscience BC, Report 2014-1, p. 35–42.

## Introduction

Travertine deposits, soil gas seepages, organic soil mixed with calcium carbonate mud and pools of stagnant or slow-flowing water are among surface features observed in two wetlands, informally called the North and South bogs, near the Nazko cone (unofficial place name), British Columbia (Figure 1). During preliminary geothermal exploration conducted at these wetlands in 2012, Alterra Power Corp. detected carbon dioxide with traces of methane and helium in the seepage gas (C. Hickson, pers. comm., 2013; N. Vigouroux, pers. comm., 2013). The isotopic composition ( $\delta^{13}\text{C}$  between  $-6.2$  and  $-6.9$  per mil Pee Dee Belemnite [PDB]) of the gases suggests that they are magmatic in origin (G. Williams-Jones, pers. comm., 2013).

Analysis of the carbonate mud in the bogs reveals a dominance of aragonite (66%), with equal parts remaining of calcite and dolomite, precipitated from the carbon-enriched surface water. Although the surface water temperature is typically below  $12^\circ\text{C}$ , the carbon dioxide seepages, travertine deposits and the nearby Nazko cone together suggest a magmatic, possibly geothermal, source for the gas, similar to the setting described by Fouke et al. (2000) at Mammoth hot springs, Wyoming (Yellowstone) and at the Mt. Etna volcano, Italy (D'Alessandro et al., 2007). Magmatic carbon dioxide discharging into the near-surface environment forms 'thermogenic' travertine that is predominantly cal-

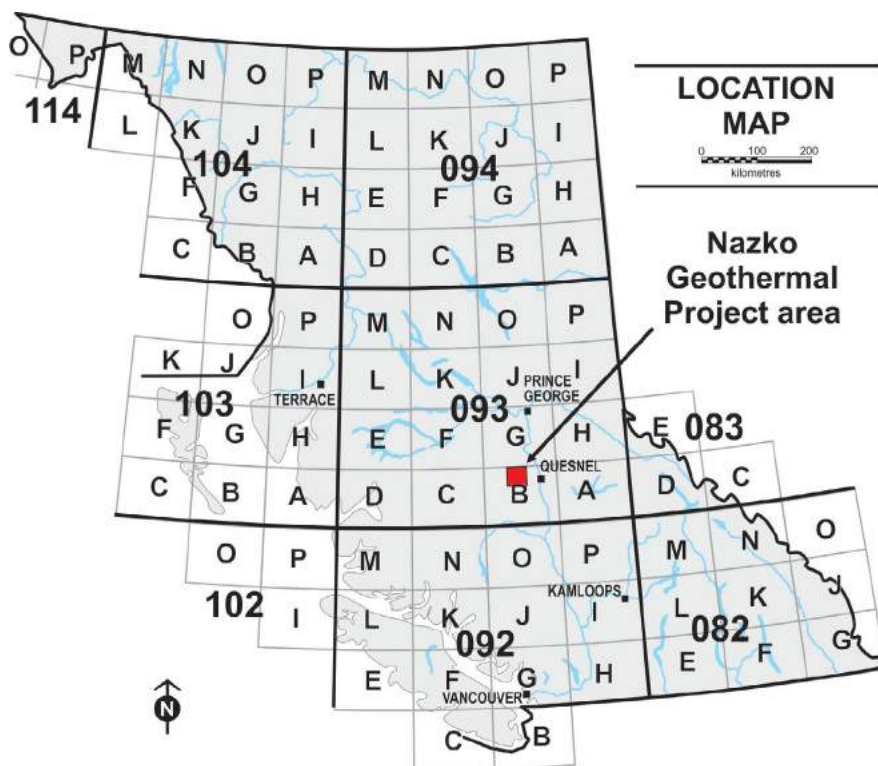


Figure 1. Location of the Nazko Geothermal Project area, near the Nazko cone, central British Columbia.

cite and aragonite enriched in  $^{13}\text{C}$  and  $^{18}\text{O}$  (Pentecost, 1995; Ford and Pedley, 1996).

Even though the cool surface waters do not suggest an active near-surface geothermal source beneath the Nazko wetlands, springwater temperatures in other areas of Canada where there are travertine deposits can be as low as  $20^\circ\text{C}$ , such as at the Rabbitkettle spring, Northwest Territories (Fouke et al., 2000). The springwater chemistry in these areas typically shows elevated Ca, dissolved  $\text{CO}_2$ , Li and B. At the Starlite mineral occurrence (MINFILE 082KSW074; BC Geological Survey, 2013) near the village of Hills, BC, travertine deposits on Arthur Creek are associated with warm springs.

This paper includes a description of groundwater, surface water and soil sampling in the Nazko bogs and the sur-

**Keywords:** geochemistry, soil, water, geothermal, carbon dioxide

This publication is also available, free of charge, as colour digital files in Adobe Acrobat® PDF format from the Geoscience BC website: <http://www.geosciencebc.com/s/DataReleases.asp>.

rounding area to study the geochemical signature associated with carbon dioxide gas seepages. This study is being supported by Geoscience BC as part of the 2013 TREK Project and was designed to complement earlier investigations on the potential for geothermal occurrences in the region (G. Williams-Jones, pers. comm., 2013) and support local community interest in geothermal resources.

## Geology and Surface Environment

The North and South bogs lie within the Anahim volcanic belt, an east-trending belt of Pleistocene–Holocene volcanoes that include the Nazko cone (Cassidy et al., 2011; Riddell, 2011). Eocene Ootsa Lake Group, Miocene Endako Group and Pleistocene–Holocene volcanic and sedimentary rocks underlie the area. Souther et al. (1987) tentatively estimated that the Nazko volcanism began during the Fraser glaciation, forming a pyroclastic mound beneath the Cordilleran Ice Sheet. A subaerial, flow-layered, non-vesicular basalt buried by more recent tephra and till is the earliest eruptive rock. This unit is partially covered by a later, blocky, highly vesicular basalt and tuff breccia forming the western part of the cone. Postglacial deposition of red pyroclastic ash, lapilli and volcanic bombs ejected from vents in the cone created the present-day edifice. During this eruption event, two olivine basalt lava streams flowed for several hundred metres from the volcano to the south and west. In 2007, an earthquake swarm occurred a few kilometres to the west of the Nazko cone (Hickson et al., 2009).

Glacial deposits in the area include till and glaciofluvial sediments (as eskers) that extend from the base of the cone into the wetlands. Souther et al. (1987) described sampling a 6 m vertical profile in the ‘volcano bog’ (probably the North bog) northwest from the Nazko cone. Sediments sampled here were a mix of gravel and mud overlain by gyttja and more than 5 m of peat interbedded with a tephra layer. This ash layer was interpreted by Souther et al. (1987) to have been deposited by an eruption from the cone at an estimated 7200 years BP.

Parts of the North and South bogs are covered by sedge and scattered wetland shrubs; calcium carbonate-rich mud; stagnant pools or slow-moving streams; small, isolated outcrops of travertine; forest-dominated bogs and meandering streams flowing through the wetlands. In the carbonate-mud-dominated parts of the bog, carbon dioxide can be observed as bubbles seeping through the bottom sediment of stagnant ponds and a calcium-carbonate (possibly aragonite) precipitate often occurs on the water surface (Figure 2). Two streams draining uplands to the east and south flow west through the bogs into Fishpot Lake (Figure 3). Luvisolic and brunisolic soils exist on the better drained hillslopes above the wetlands, whereas gleysolic soils have formed along the bog margin where the water table is close

to the land surface. Peat mixed with calcium-carbonate mud is the most common organic bog soil.

Travertine is typically a rusty to white coloured rubble forming small, isolated and elevated areas in the bogs. Near the northern edge of the North bog, there is a small, 35 cm high inverted cone-shaped travertine deposit concealed by undergrowth. This cone encloses a partially submerged vent from which there is a steady flow of carbon dioxide. There is a less active carbon dioxide seep from another vent on a rusty travertine mound close to the east edge of the South bog. Figure 4 shows the wetland surface features including the location of the two carbon dioxide discharging vents.

## Fieldwork

In July and August 2013, fieldwork in the North and South bogs and surrounding area completed the following:

- Bog surface features, such as gas discharge vents and travertine deposits, were mapped.
- Groundwater was sampled from shallow dug pits, springs and gas vents. Water pH, temperature, salinity and conductivity were measured on-site with an Oakton PCSTestr 35 multimeter. Details of the site such as water flow rates, water table depth and presence of discharging carbon dioxide were recorded.
- Surface water was sampled in bog pools, streams flowing into and out of the wetland and from Fishpot Lake. Water pH, temperature, salinity and conductivity were measured and site details such as water flow rates, channel width and depth were recorded. Channel sediment was also collected at several stream sites.
- Bog and well-drained soil and travertine deposits were sampled.

## Sample Preparation and Analysis

Three water samples were collected in high-density polyethylene (HDPE) bottles at each site. The samples underwent the following analyses:

- Within 12 hours of collection, one sample was analyzed for Na with a HANNA model pHep<sup>®</sup> pocket meter and total alkalinity and dissolved carbon dioxide were measured with Hach<sup>®</sup> field test kits.
- A second sample was filtered through a Phenex<sup>™</sup> polyethersulfone (PES) 0.45 µm membrane, and stored at 4°C for later analysis by ALS Global (Vancouver) for hardness, total alkalinity, bicarbonate alkalinity and hydroxyl alkalinity by titration and for Br<sup>-</sup>, Cl<sup>-</sup>, F<sup>-</sup>, NO<sub>3</sub><sup>-</sup>, NO<sub>2</sub><sup>-</sup> and SO<sub>4</sub><sup>2-</sup> by ion chromatography.
- A third sample was filtered through a Phenex<sup>™</sup> polyethersulfone (PES) 0.45 µm membrane, acidified with ultrapure nitric acid to pH 1 and later analyzed by ALS



Figure 2. Photograph of the North and South bogs and Fishpot Lake to the west.

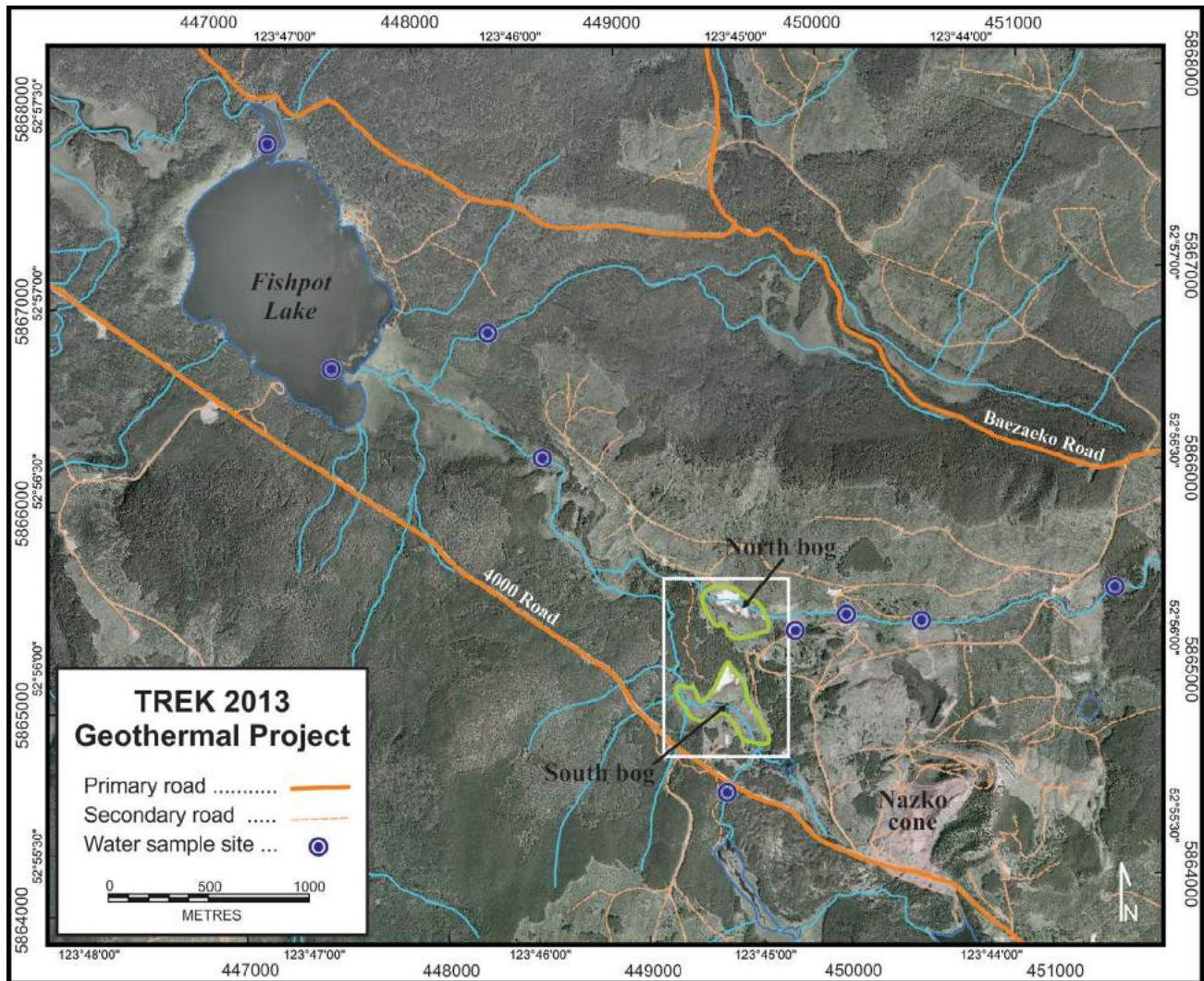


Figure 3. Streams draining from the Nazko cone area through the North and South bogs into Fishpot Lake.

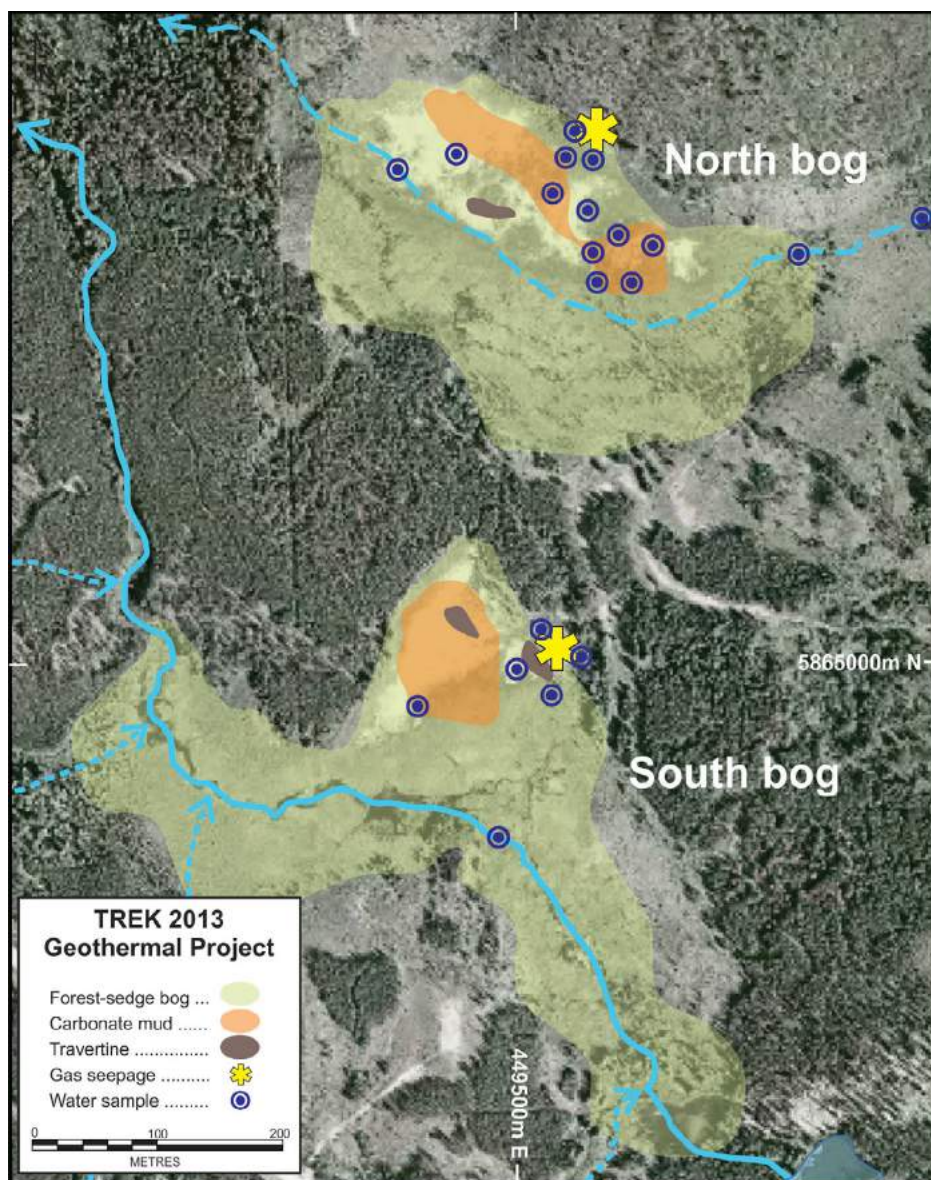


Figure 4. North and South bog surface features and distribution of water samples.

Global for Ag, Al, As, B, Ba, Be, Bi, Ca, Cd, Co, Cr, Cs, Cu, Fe, Ga, K, Li, Mn, Mo, Na, Ni, P, Pb, Rb, Re, Sb, Se, Si, Sn, Sr, Te, Th, Ti, Tl, U, V, Y, Zn and Zr by high-resolution mass spectrometry. Three distilled, deionized water sample blanks and two samples of the National Research Council Canada (NRCC) river water standard, SLRS 3, were analyzed with the field samples to monitor data accuracy and precision.

Sediment samples were dried at below 60°C, sieved to -80 mesh (<0.177 mm) and the -80 fraction was analyzed at Acme Laboratories Ltd. (Vancouver) for trace and minor elements including Ag, Al, As, B, Ba, Be, Bi, Ca, Cd, Co, Cr, Cs, Cu, Fe, Ga, Hg, K, Li, Mn, Mo, Na, Ni, P, Pb, Rb, Re, Sb, Se, Si, Sn, Sr, Te, Th, Ti, Tl, U, V, Y, Zn and Zr by aqua regia digestion and inductively coupled plasma-mass spectrometry (ICP-MS);

major oxides by lithium borate fusion-ICP-MS; C and S by Leco analysis; loss on ignition (LOI) by sintering at 1000°C; and B by sodium peroxide sinter-ICP-MS.

### Water Geochemistry: Preliminary Results

Table 1 lists element detection limits, the mean measured value for water standard SLRS 3, the percent relative standard deviation (%RSD) calculated from two SLRS 3 analyses and an element value for the SLRS 3 standard where reported by NRCC. Analyses of filtered water blanks reveals that only Li, Sr and Ca are detected in concentrations that are less than twice the detection limit. Only Be and Li in the water standard SLRS 3 have %RSD values that are more than 10%. Where the NRCC reports a value for an element in SLRS 3, the detected concentration is within 10% of the recommended value.

**Table 1.** Analytical detection limits and results of National Research Council Canada river water standard SLRS 3 duplicate analysis. Abbreviations: NRCC, National Research Council Canada; RSD, relative standard deviation; SLRS 3, river water standard.

Analyte	Detection limit	Mean SLRS 3	%RSD	NRCC SLRS 3
Br (ppm)	0.05			
Cl (ppm)	0.5			
F (ppm)	0.02			
NO <sub>3</sub> (ppm)	0.005	392	0.4	
NO <sub>2</sub> (ppm)	0.001	-0.05	0	
SO <sub>4</sub> (ppm)	0.5	-25	0	
Al (ppb)	1	33	0.6	31
Sb (ppb)	0.01	0.17	0.8	0.12
As (ppb)	0.05	0.84	1.9	0.72
Ba (ppb)	0.1	14.1	1.5	13.4
Be (ppb)	0.005	0.0096	28.0	0.005
Bi (ppb)	0.05	-0.05	0.00	
B (ppb)	5.00	9.70	10.2	
Cd (ppb)	0.005	0.0148	6.2	0.013
Ca (ppm)	0.076	5.505	4.2	6
Cs (ppb)	0.005	0.0064	0.0	
Cr (ppb)	0.5	-0.5	0.0	0.3
Co (ppm)	0.05	-0.05	0.0	0.027
Cu (ppb)	0.2	1.52	2.3	1.35
Ga (ppb)	0.05	-0.05	0.0	
Fe (ppb)	30.0	100.0	7.1	100
Pb (ppb)	0.05	0.072	1.0	0.068
Li (ppb)	0.2	0.5	25.1	
Mg (ppm)	0.1	1.6	7.6	1.6
Mn (ppb)	0.2	4.10	0.9	3.9
Mo (ppb)	0.05	0.224	0.3	0.19
Ni (ppb)	0.2	0.84	1.7	0.83
P (ppm)	0.3	-0.3	0.0	
K (ppm)	2	-2	0	0.7
Re (ppb)	0.005	-0.005	0.0	
Rb (ppb)	0.02	1.70	3.0	
Se (ppb)	0.2	-0.2	0.0	
Si (ppm)	0.05	1.66	3.0	
Ag (ppb)	0.005	-0.005	0.0	
Na (ppm)	2	2.5	5.7	2.3
Sr (ppm)	0.001	0.0319	2.9	0.028
Te (ppb)	0.010	-0.01	0.0	
Tl (ppb)	0.002	0.007	1.0	
Th (ppb)	0.005	0.014	1.5	
Sn (ppb)	0.2	-0.20	0.0	
Ti (ppb)	0.2	0.70	8.1	
W (ppb)	0.01	-0.01	0.00	
U (ppb)	0.002	0.041	0.69	0.045
V (ppb)	0.05	0.320	2.0	0.3
Y (ppb)	0.005	0.128	3.3	
Zn (ppb)	1.00	1.60	0.00	1.04
Zr (ppb)	0.05	0.08	8.7	

Comparison of surface- and groundwater geochemistry statistics listed in Table 2 reveals the following:

- Surface water has a higher pH than groundwater. Streams flowing into the wetlands have a pH above 8. Vesicular basalt outcrops along the bank of one stream has abundant calcite in the vesicles and dissolution of this calcite may explain the alkaline streamwater. The highest pH value detected (9.26) is from a water sample from Fishpot Lake.
- Groundwater has a higher mean dissolved carbon dioxide value than surface water, reflecting the active flow of carbon dioxide from seeps into the groundwater and precipitation of calcium carbonate mud.
- Mean groundwater temperature is slightly lower than surface water. The lowest water temperature (5.6°C) was measured in water from the active gas flow from the travertine cone vent in the North bog.
- Mean element concentrations are higher in groundwater compared to surface water. Water that has accumulated in the travertine cone vent in the North bog has the highest detected levels of dissolved As, Cd, Fe and Ni.

## Future Work

Completion of this project will involve

- preparation and geochemical analysis of the soil and rock samples for major oxides, loss on ignition, minor and trace elements;
- statistical analysis and interpretation of water, soil and sediment data; and
- final reporting, which is scheduled to be published in spring 2014.

## Summary

Geology, surface features, carbon dioxide seepages and anecdotal evidence of a thermal anomaly beneath the Nazko bogs and surrounding area (such as snow-free wetland areas in winter), combined with the preliminary results from this and other recent studies, support the existence of a geothermal source. Clear evidence for geothermal activity, such as the presence of thermal springs, may be absent, however, because of masking by the wetland geochemistry and sediments and possibly because of the amount of recharge/groundwater flow in the area. It is also possible that any thermal anomaly, such as hot water, is lost to deeper aquifers, which would explain the presence of cold, noncondensable gases only at the surface. Additional field studies intended to better detect evidence for concealed geothermal activity could include resampling groundwater in the bogs where high levels of carbon dioxide have been recently detected in soil gas, <sup>16</sup>O/<sup>18</sup>O isotope analysis of the groundwater near seeps and <sup>13</sup>C/<sup>12</sup>C isotope analysis of the seepage gas. Further soil sampling and soil gas flux moni-

**Table 2.** Mean, median, 3<sup>rd</sup> quartile (quart.) and maximum statistics calculated from data for 11 groundwater and 20 surface water samples; Ag, Bi, Cl<sup>-</sup>, Ga, P, Re, Sn, Tl, and were not included because most values are below the detection limit. Hardness and alkalinity are reported in parts per million CaCO<sub>3</sub>. Abbreviations: bicarb, bicarbonate; Cond, conductivity; GW, groundwater; SW, springwater; TDS, total dissolved solids; Temp, temperature.

Analyte	Mean GW	Median GW	3rd quart. GW	Max. GW	Mean SW	Median SW	3rd quart. SW	Max. SW
pH (Field)	6.61	6.59	6.745	7.03	7.6	7.73	8.15	9.26
Temp (field)	12.2	13.5	14.4	14.8	13.7	14	15.6	23
Cond (µS; field)	2907	3390	3635	4380	1000	333	1670	4450
Na (ppm; field)	208	160	235	450	127	70	138	900
Salinity (ppm; field)	1606	1740	1900	2460	488	155	735	2250
TDS (ppm; field)	2355	2520	2740	3380	552	206	499	3080
Alkalinity (ppm; field)	2364	2400	2800	3000	763	160	1850	3000
CO <sub>2</sub> (ppm; field)	414	400	525	750	149	38	194	850
Hardness (ppm)	1617	1570	1745	2570	548	148	874	2500
Alkalinity, Bicarb (ppm)	2218	2410	2490	3260	708	165	1275	3230
Total Alkalinity (ppm)	2218	2410	2490	3260	708	165	1275	3230
F (ppm)	0.47	0.47	0.505	0.54	0.241	0.1715	0.4	0.59
NO <sub>3</sub> (ppm)	0.1	0.1	0.1	0.11	0.1	0.02	0.1	0.44
NO <sub>2</sub> (ppm)	0.02	0.02	0.02	0.02	0.01	0.001	0.02	0.089
SO <sub>4</sub> (ppm)	15	16	18	29	6.6	2.8	10.125	32
Al (ppb)	1.79	2	2.05	3.8	10.59	3.05	16.15	49.3
Sb (ppb)	0.029	0.02	0.0365	0.066	0.093	0.043	0.0508	0.618
As (ppb)	0.6	0.1	0.66	2.56	0.5	0.53	0.7	0.85
Ba (ppb)	175	182	202	234	62	53	67.3	204
Be (ppb)	0.016	0.005	0.025	0.059	0.0133	0.005	0.016	0.045
B (ppb)	376	380	446	637	89	11.4	207	430
Cd (ppb)	0.0245	0.0171	0.0238	0.0916	0.026	0.005	0.0061	0.203
Ca (ppm)	221	220	235	383	74	29	68	358
Cs (ppb)	2.047	2.08	2.625	3.18	0.535	0.0139	0.745	3.93
Cr (ppb)	0.64	0.5	0.75	1	0.5	0.5	0.5	0.5
Co (ppm)	1.1	0.114	1.221	6.73	0.132	0.077	0.206	0.44
Cu (ppb)	0.31	0.21	0.4	0.64	0.71	0.405	0.7	3.05
Fe (ppb)	566.4	147	430.5	3920	282.9	68.5	352	1290
Pb (ppb)	0.07	0.05	0.1	0.137	0.05	0.05	0.05	0.057
Li (ppb)	335	341	379.5	475	105.4	5.06	231.5	547
Mg (ppm)	259	247	307	393	88	18	170	390
Mn (ppb)	225	193	203.5	657	83	35.6	125	278
Mo (ppb)	0.221	0.13	0.341	0.574	0.725	0.655	1.1975	1.64
Ni (ppb)	12.96	2.42	22.57	44	2.28	1.015	2.035	13.4
K (ppm)	30.6	31.5	35.5	41.4	10.64	3.95	17.1	41.1
Rb (ppb)	39.1	40.1	45.55	52.4	12.86	3.415	24.1	56.1
Se (ppb)	0.3	0.2	0.3	0.4	0.7	0.2	0.4575	3.26
Si (ppm)	12.2	12.3	15.3	16.8	13.7	13.65	15.13	18.7
Na (ppm)	267	281	302.5	412	69	9.25	157.5	311
Sr (ppm)	8.6	7.68	8.725	15	2.479	0.249	2.58	15.9
Tl (ppb)	0.106	0.004	0.1895	0.429	0.045	0.002	0.006	0.487
Th (ppb)	0.006	0.005	0.0075	0.01	0.0072	0.005	0.008	0.018
Ti (ppb)	0.36	0.35	0.4	0.64	1.06	0.36	1.34	4.28
W (ppb)	0.013	0.01	0.015	0.02	0.014	0.01	0.01	0.042
U (ppb)	0.14	0.061	0.1165	0.687	0.081	0.079	0.108	0.242
V (ppb)	0.513	0.157	0.66	2.36	1.387	1.22	1.68	5.73
Y (ppb)	0.1404	0.0464	0.1717	0.64	0.238	0.081	0.458	0.927
Zn (ppb)	5.5	3.6	9.85	12.6	2.4	1	1.575	10.3
Zr (ppb)	1.303	0.55	2.08	4.67	0.727	0.51	0.96	4.79

toring could map the carbon dioxide seeps. Over a wider area around the Nazko cone, additional work could find evidence for thermal water in other springs and seepages. For example, a self-potential geophysical survey may be useful for detecting structures capable of transporting thermal water into the bogs.

### Acknowledgments

In the field, assistance from J. Constable, H. Paul, T. Clement and D. Sacco with sample collection, sample analysis and data collection was very much appreciated. G. Williams-Jones and B. Ward, from Simon Fraser University, C. Hickson, from Alterra Power Corp., and N. Vigouroux from Douglas College, generously provided information about the Nazko wetlands and loaned sampling equipment. A. Rukhlov, from the BC Ministry of Energy and Mines, is thanked for allowing the use of water testing equipment from the BC Geological Survey laboratory. Critical reviews of this paper by T. Ferbey, from the BC Geological Survey, by N. Vigouroux, from Douglas College, and G. Williams-Jones, from Simon Fraser University, are very much appreciated. Funding is being provided by Geoscience BC as part of the 2013 TREK Project.

### References

- BC Geological Survey (2013): MINFILE BC mineral deposits database; BC Ministry of Energy and Mines, BC Geological Survey, URL <<http://minfile.ca/>> [November 2013].
- D'Alessandro, W., Giammanco, S., Bellomo, S. and Parello, F. (2007): Geochemistry and mineralogy of travertine deposits of the SW flank of Mt. Etna (Italy): relationship with past volcanoes and degassing activity; *Journal of Volcanology and Geothermal Research*, v. 165, p. 64–70.
- Cassidy, J.F., Balfour, N., Hickson, C., Kao, H., White, R., Caplan-Auerbach, J., Mazzotti, S., Rogers, G.C., Al-Khoubbi, I., Bird, A.L., Esteban, L., Kelman, M., Hutchinson, J. and McCormack, D. (2011): The 2007 Nazko, British Columbia, earthquake sequence: injection of magma deep in the crust beneath the Anahim volcanic belt; *Bulletin of the Seismological Society of America*, v. 101, no. 4, p. 1734–1741.
- Ford, T.D. and Pedley, H.M. (1996): A review of tufa and travertine deposits the world; *Earth Science Reviews*, v. 41, p. 117–175.
- Fouke, B.W., Farmer, J.D., Des Marais, D.J., Pratt, L., Sturchio, N.C., Burns, P.C. and Discipulo, M. (2000): Depositional facies and aqueous-solid geochemistry of the travertine-depositing hot springs (Angel Terrace, Mammoth hot springs, Yellowstone National Park, U.S.A.); *Journal of Sedimentary Research*, v. 70, p. 565–585.
- Hickson, C.J., Kelman, M., Chow, W., Shimamura, K., Servranckx, R., Bensimon, D., Cassidy, J., Trudel, S. and Williams-Jones, G. (2009): Nazko region volcanic hazard map; Geological Survey of Canada, Open File 5978.
- Pentecost, A. (1995): Geochemistry of carbon dioxide in six travertine-depositing springs of Italy; *Journal of Hydrology*, v. 167, p. 263–278.
- Riddell, J. (2011): Lithostratigraphic and tectonic framework of Jurassic and Cretaceous intermountain sedimentary basins of south-central British Columbia; *Canadian Journal of Earth Sciences*, v. 48, p. 870–896.
- Souther, J.G., Clague, J.J. and Mathews, R.W. (1987): Nazko cone: a Quaternary volcano in eastern Anahim belt; *Canadian Journal of Earth Sciences*, v. 24, p. 2477–2485.



# Three-Dimensional Thickness Model for the Eocene Volcanic Sequence, Chilcotin and Nechako Plateaus, Central British Columbia (NTS 092O, P, 093A, B, C, E, F, G, K, L)

**E. Bordet**, Mineral Deposit Research Unit, University of British Columbia, Vancouver, BC, [ebordet@eos.ubc.ca](mailto:ebordet@eos.ubc.ca)

**M.G. Mihalynuk**, Geological Survey and Resource Development Branch, BC Ministry of Energy and Mines, Victoria, BC

**C.J.R. Hart**, Mineral Deposit Research Unit, University of British Columbia, Vancouver, BC

**M. Sanchez**, Mineral Deposit Research Unit, University of British Columbia, Vancouver, BC

---

Bordet, E., Mihalynuk, M.G., Hart, C.J.R. and Sanchez, M. (2014): Three-dimensional thickness model for the Eocene volcanic sequence, Chilcotin and Nechako plateaus, central British Columbia (NTS 092O, P, 093A, B, C, E, F, G, K, L); *in* Geoscience BC Summary of Activities 2013, Geoscience BC, Report 2014-1, p. 43–52.

## Introduction

Eocene volcanic rocks in the Chilcotin and Nechako plateaus of central British Columbia are mapped over ~26 400 km<sup>2</sup> (Figure 1; Massey et al., 2005). The original extent of these volcanic rocks, deposited during a short-lived episode of continental magmatism (~55–46 Ma; Bordet et al., *in press*), is presumed to have been much greater. Regionally included in the Ootsa Lake Group (OLG; Figure 2), these widespread, dominantly felsic sequences display significant lateral thickness variations. In particular, Eocene volcanic successions >3000 m thick are preserved in extensional basins, characterized by north-trending half-grabens in southern BC (Church, 1973, 1985; Ewing, 1981; Thorkelson, 1988; Souther, 1991), with similarly thick sections inferred in central BC (Hayward and Calvert, 2011; Bordet et al., 2013, work in progress).

Eocene OLG strata host low-sulphidation epithermal Au-Ag occurrences (Figure 2; BC Geological Survey, 2013) and also overlie Mesozoic volcanic and sedimentary successions containing mineral and hydrocarbon resources. For example, Late Cretaceous magmatic rocks host the Blackwater Au-Ag epithermal deposit (8.6 million oz. Au; Portmann, 2013; Figure 2a), and a belt of Early Cretaceous Skeena Group sedimentary rocks has hydrocarbon-reservoir potential (Figure 2b; Ferri and Riddell, 2006; Riddell, 2011). Mesozoic hydrocarbon and mineral resources capped by Eocene volcanic sequences may be further obscured by overlying discontinuous Neogene Chilcotin

Group flood basalt (CGB; Figure 2; Dohaney et al., 2010) and by a thick and continuous cover of glacial till (Fulton, 1995).

In order to better define the distribution of Eocene volcanic rocks in this region, a three-dimensional (3-D) thickness model for the OLG in the Chilcotin and Nechako plateaus (Figure 1) is developed and presented in this paper. This model is generated from geological constraints, including field maps, cross-sections and stratigraphic columns, and interpreted geophysical-survey data (Figure 2, Table 1). Objectives of this model are to 1) image regional thickness variations of the OLG where it has been mapped previously; 2) identify areas of eroded or covered Eocene volcanic rocks; 3) investigate the spatial and temporal correlation between Eocene volcanic rock accumulations and fault-bounded basins; 4) generate new surface and volume estimates for the Eocene volcanic event; and 5) correlate and extend OLG intervals containing known mineralization into regions covered by CGB and glacial till, with implications for mineral exploration.

## Regional Geology

Three main lithostratigraphic packages are represented in the Chilcotin and Nechako plateaus of central BC, a high-standing (~800–1600 m) region with subdued topography (Figures 1, 2a; Holland, 1976). They are Stikine and Cache Creek terrane basement rocks, Ootsa Lake Group (OLG) volcanic rocks, and younger cover rocks that include the Neogene Chilcotin Group basalt (CGB).

**Basement rocks** include accreted terrane successions of the Stikine (volcanic arc) and Cache Creek terranes (subduction-related accretionary complex; Figure 1; Coney et al., 1980), as well as postaccretion Jurassic to Cretaceous rock packages. In particular, Lower to Middle Jurassic

---

**Keywords:** *Nechako Plateau, Chilcotin Plateau, thickness model, Eocene, Ootsa Lake Group, mineral exploration, hydrocarbon exploration*

*This publication is also available, free of charge, as colour digital files in Adobe Acrobat® PDF format from the Geoscience BC website: <http://www.geosciencebc.com/s/DataReleases.asp>.*

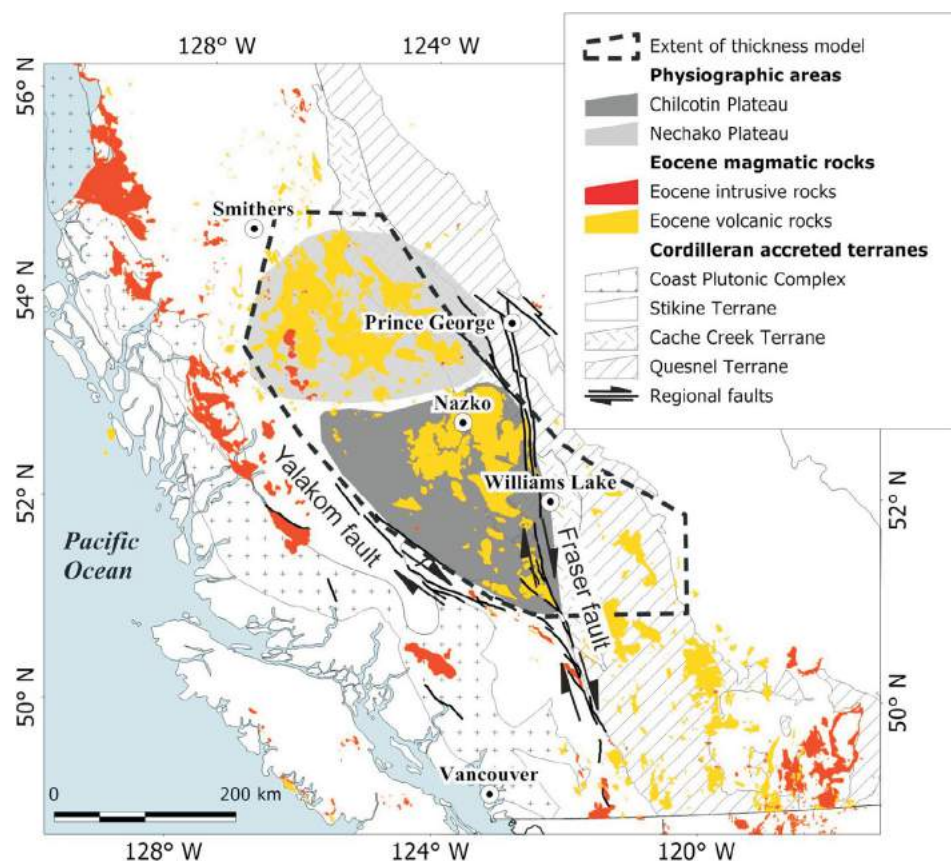


**Figure 1.** Distribution of Eocene volcanic and intrusive rocks in the Chilcotin and Nechako plateaus of central British Columbia with respect to Cordilleran accreted terranes and major faults. The thickness model covers the Chilcotin and Nechako plateaus, as well as the Williams Lake area east of the Fraser fault. Geology polygons, faults and terranes are after Massey et al. (2005). Map projection UTM Zone 10, NAD 83.

strata of the Hazelton Group (Stikine terrane) occur in the Chilcotin Plateau west of Nazko (Figure 2b; Tipper, 1959), whereas thick beds of Cretaceous chert-pebble conglomerate and sandstone of the Aptian to Albian Skeena Group are exposed for ~150 km along the Nazko River (Figure 2b; Riddell, 2011).

**Eocene volcanic rocks** of the OLG (Figure 2; Duffell, 1959) comprise mainly rhyolite and dacite lavas, and minor pyroclastic and reworked volcanoclastic deposits, locally capped by andesitic lavas (Bordet et al., work in progress). New isotopic dates indicate a range of 55–46 Ma (Bordet et al., in press). A Paleocene volcanoclastic sequence that was identified in a hydrocarbon-exploration well (B-16-J; Figure 2b) is inferred to overlie Cretaceous basement rocks (Riddell, 2011) and is combined with the OLG for the purpose of this study.

**Cover rocks** of the Neogene CGB (Figure 2; Bevier, 1983; Mathews, 1989) unconformably overlie the OLG and are of variable thickness but mostly less than 25 m (Mihalynuk, 2007; Andrews et al., 2011). Holocene volcanoes of the Ana-

him belt (Souther, 1986) occur to the west of the study area (Figure 2).

## Eocene Structure

The Cretaceous to Early Cenozoic structural architecture of the study area is characterized by a series of north-trending horsts and grabens that occupy a region between two regional-scale northwest- and north-trending dextral strike-slip faults, the Yalakom and Fraser faults, respectively (Figures 1, 3). The thickest OLG sections are preserved mainly within Eocene grabens, while Mesozoic rocks are exposed along exhumed horst blocks, as established from stratigraphic investigations (Bordet et al., work in progress), hydrocarbon-exploration drilling (Riddell, 2011) and geophysical surveys (e.g., Hayward and Calvert, 2011; Talinga and Calvert, work in progress).

Province-wide transtensional deformation in the Eocene was concentrated along north- and northwest-trending dextral strike-slip fault systems, in some cases reactivating crustal-scale faults such as the Fraser and Yalakom faults (Figure 3; Souther, 1970; Ewing, 1980; Struik, 1993),

along which several tens to hundreds of kilometres of displacement are inferred (Eisebacher, 1977; Ewing, 1980; Umhoefer and Schiarizza, 1996). Early Eocene, steeply dipping northwest-trending faults (e.g., Yalakom fault) accommodated dextral transtension. This fault motion was kinematically linked to secondary, northeast-trending, synvolcanic extensional faults (Figure 3, inset map; Struik, 1993) that formed pull-apart basins in which OLG strata accumulated and were preserved. Late Eocene to Early Oligocene, north-trending, en échelon dextral faults (e.g., Fraser fault) are inferred to be coeval with northwest-directed extension (Struik, 1993). The exhumation of metamorphic core complexes (Figure 3, inset map) in central and southern BC occurred coevally with regional extensional deformation and Eocene volcanism (e.g., Struik, 1993).

## Methods and Model Constraints

### Thickness Model

An Eocene thickness model was computed for the region of Eocene OLG distribution in the Chilcotin and Nechako plateaus (Figures 1, 2) using Manifold™ GIS software. Methodologies used here are adapted from Mihalynuk (2007) and detailed in Bordet et al. (2011). The modelling workflow includes the following steps:

- 1) **Generate input points from surface, section and point datasets** (Table 1): Eocene and Neogene cover thickness and elevation information attributed to each point is either obtained from direct measurements or calculated.
- 2) **Organize input data points into two datasets:** a) post-Eocene cover sequence (Chilcotin Group basalts and

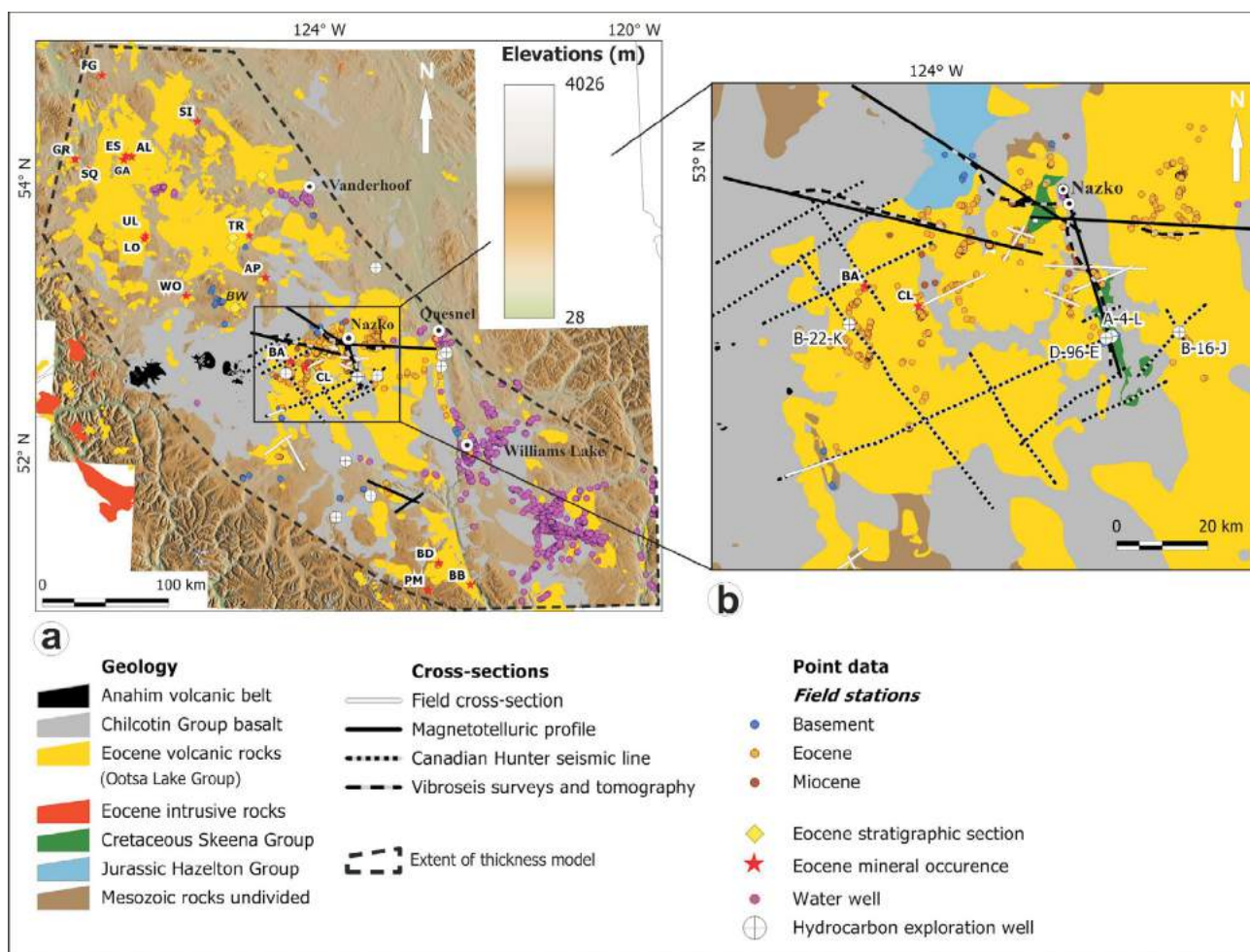


**Table 1.** Datasets and sources used for building the thickness model of the Eocene volcanic sequence, Chilcotin and Nechako plateaus.

	Input data	Sources
Polygons	Eocene geology polygons	Massey et al. (2005) Mihalynuk et al. (2008, 2009)
	CGB polygons	Interactive Chilcotin Database (Dohaney et al., 2010)
	Digital Elevation Model	Centre for Topographic Information (1997)
Sections	Geological cross-sections	Mihalynuk et al. (2008, 2009), field sections (this study)
	Magnetotelluric profiles A, B, C, D, G, H	Spratt and Craven (2011), Spratt et al. (2012)
	Tomography models lines 5, 10, 15 and 6	Smithyman (2013), Smithyman et al. (2014) Talinga and Calvert (2014)
	Canadian Hunter seismic lines	Interpreted lines by Hayward and Calvert (2011) after reprocessing by Arcis Corporation
	Geoscience BC vibroseis	Reprocessed lines by WesternGeco MDIC (2010)
	Oil and gas wells	Compiled thicknesses from Bordet et al. (2011), after Riddell (2011) and previous drilling reports
Points	Water wells	Interactive Chilcotin Database (Dohaney et al., 2010)
	Stratigraphic sections	Bordet et al. (in press)
	Mineral occurrences	Mineral exploration drill hole logs as recorded in ARIS (BC Ministry of Energy and Mines, 2013) and linked to MINFILE (BC Geological Survey, 2013). Drilling depths at Eocene prospects rarely exceed 150 m and represent minimum thicknesses. Maximum drilled thicknesses of Eocene are reported for Blackdome (400 m; Faulkner, 1986) and Equity Silver (460 m; Cyr et al., 1984).
	Field stations	Field mapping (this study)

Holocene volcanoes); and b) Eocene sequence (generally anything between the basement and cover).

- 3) Generate a **base elevation model for the cover sequence and for the Eocene + cover sequence**. All elevation surfaces are generated using 1 by 1 km cell size, 10 neighbours and the Kriging interpolation method.
- 4) Generate a **thickness model for the cover sequence and for the Eocene + cover sequence** by subtracting the corresponding base elevation models from a digital elevation model (DEM).
- 5) Generate an **Eocene thickness model** by subtracting the thickness model of the cover sequence from the thickness model of the Eocene + cover sequence.

The resulting model was tested by comparison with a surface directly generated from thicknesses assigned to individual points, and by interpolating these thicknesses over the model area. Results obtained from the two methods are similar, with only minor differences occurring in areas with fewer constraints, such as the Nechako Plateau.

### Structural Interpretations

Structures and lineaments for the Chilcotin and Nechako plateaus were interpreted (Bordet et al., 2013) from processed aeromagnetic data (Geological Survey of Canada, 1994) and digital topographic data (Centre for Topographic

Information, 1997; Figure 3, inset map). These interpretations were refined (Figure 4) using seismic-reflection data (WesternGeco MDIC, 2010; Hayward and Calvert, 2011), tomographic models (Smithyman, 2013; Smithyman et al., work in progress; Talinga and Calvert, work in progress) and magnetotelluric inversion models (e.g., Spratt and Craven, 2011; Spratt et al., 2012), which utilize contrasting electromagnetic properties at depth to illustrate the lateral continuity of lithological packages.

### Results

A model of OLG thickness in central BC is presented in Figure 3 (regional model) and Figure 4 (focused model). The OLG volcanic successions are generally 100–500 m thick within the previously mapped boundaries of Eocene rocks. The thickest accumulations of OLG rocks range from  $\geq 1000$  to  $\geq 2000$  m and are imaged in the Chilcotin Plateau southwest of Nazko (Figure 3), where numerous geophysical, field and well data are available to constrain and validate the model (Figure 2b). To the north, in the Nechako Plateau, thickness variations are only constrained by the previously mapped Eocene boundaries, by a few stratigraphic sections and by shallow-drilling information from mineral prospects distributed within these boundaries (Figure 2a, Table 1). Notably, the model extrapolates OLG thicknesses below the expected base of the CGB (Figure 3).

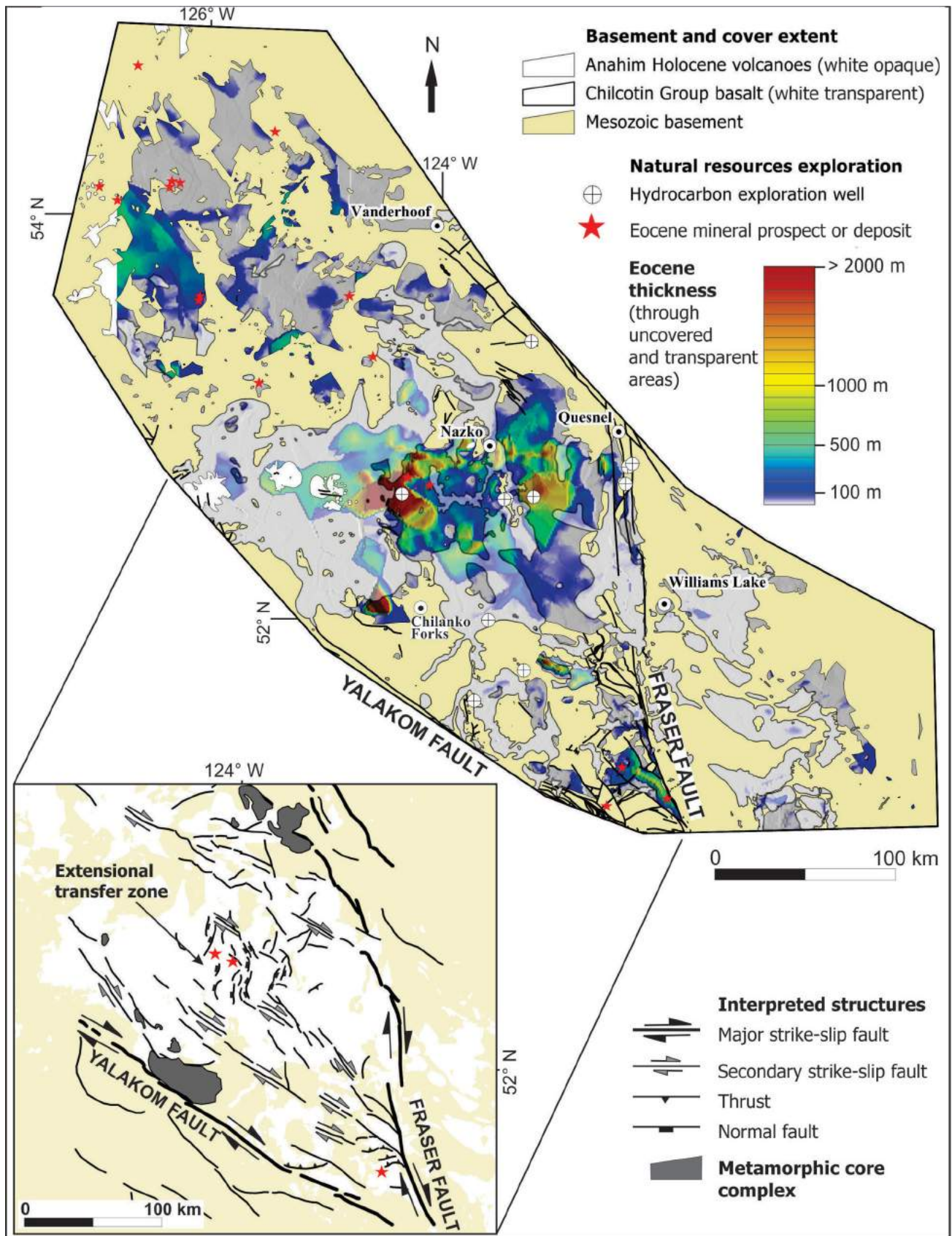


**Figure 3.** Thickness model of the Eocene volcanic sequence for the Chilcotin and Nechako plateaus, and interpreted structural lineaments in a selected area of the Chilcotin Plateau (inset map; after Bordet et al., 2013). Map projection UTM Zone 10, NAD 83.

The focused model area (Figure 4a) displays rectangular domains with OLG thicknesses of greater than ~1000 m separated by areas of 100–500 m thickness. Areas of thinner OLG are typically proximal to, and include, mapped basement exposures (e.g., Cretaceous conglomerate of the Nazko River valley and Jurassic exposures west of Nazko; Figure 2b), or occur where field constraints or geophysical sections were not available (e.g., ~20 km south of Nazko; Figure 2b). The OLG can attain thicknesses of >3000 m in the better constrained areas, such as at hydrocarbon-exploration well sites B-22-K and B-16-J (Figure 4a), along magnetotelluric and tomographic sections, and along seismic lines reprocessed from the 1980s Canadian Hunter data (Hayward and Calvert, 2011) and 2008 Geoscience BC vibroseis surveys (WesternGeco MDIC, 2010).

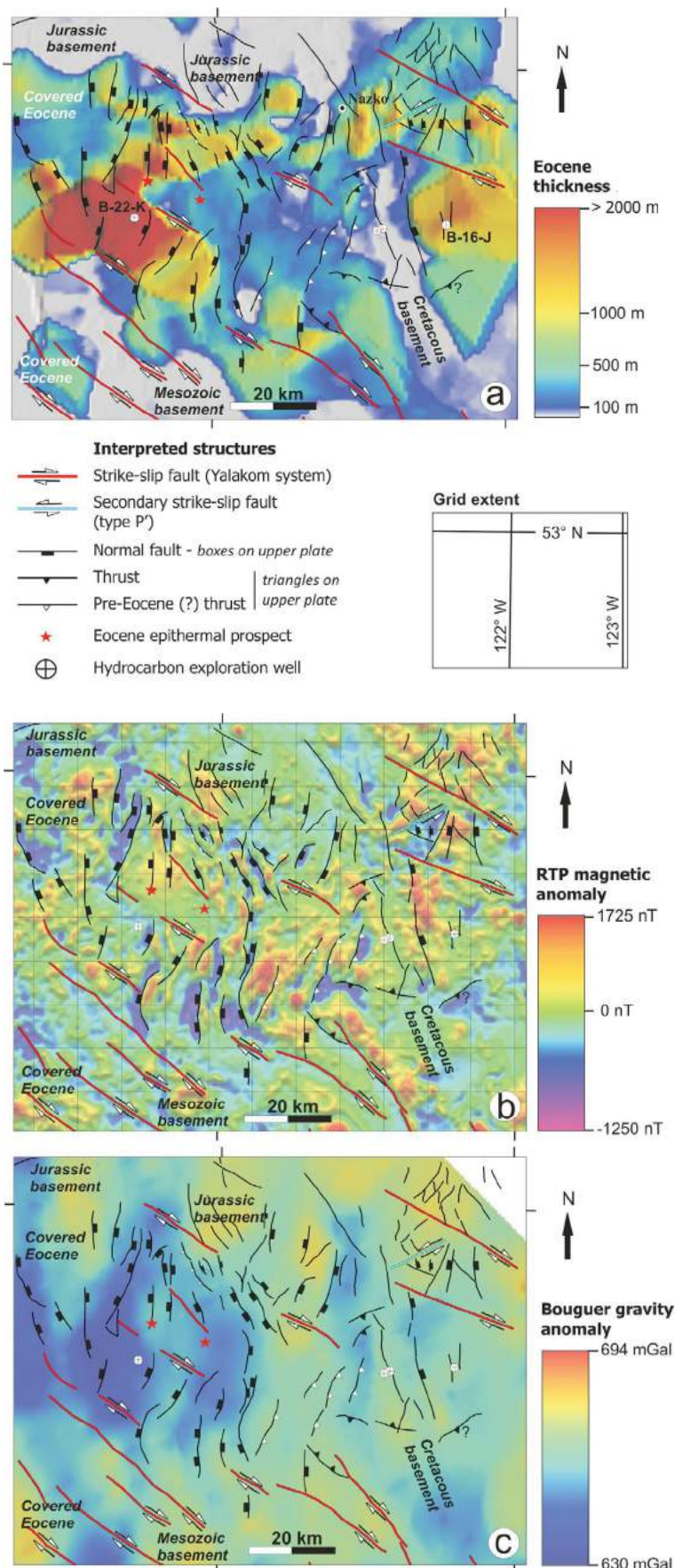
## Discussion

### Limitations of the Model

Data sources at variable scales of observation were integrated to evaluate the thickness and structural patterns for the Eocene volcanic rocks in the Chilcotin and Nechako plateaus. Considering the heterogeneity in the distribution of the available datasets and variable confidence levels of thickness estimates made from these disparate data, the following limitations of the resultant thickness model should be considered:

- The basal contact of Eocene rocks is exposed only at a few locations. Therefore, for most areas, the basal contact depth is inferred from interpretation of geophysical data.
- Ambiguities exist in the age determinations made on cuttings from hydrocarbon well B-22-K (Bordet et al., in press, work in progress). These potentially large errors are amplified when propagated to interpreted seismic and tomographic sections, which rely on thickness constraints from the well.

**Figure 4.** Interpreted structural lineaments in the focused model area draped over **a)** Eocene thickness model, **b)** reduced-to-the-pole (RTP) magnetic anomaly (Geological Survey of Canada, 1994), and **c)** gravity anomaly (Ferri and Riddell, 2006). Interpretations are developed from integration of magnetic and topographic lineaments (from the RTP and DEM), seismic reflectors (after Hayward and Calvert, 2011) and tomographic models (Smithyman, 2013; Smithyman et al., work in progress). Two Eocene epithermal prospects are within the transfer zone located on Figure 3. Map projection UTM Zone 10, NAD 83.



- The distribution of water wells used to constrain the thickness of Chilcotin Group basalt is of sufficient density only in the southeast corner of the study area (NTS 092P, 093A, B; Figure 1). Basalt layers are confirmed to cap sections in two other areas where intersected by oil and gas wells, but isotopic dates to confirm correlation with Neogene Chilcotin Group are lacking. Such uncertainties are compounded during Eocene thickness calculation, because the calculation involves subtraction of post-Eocene unit thicknesses from the depth to the base of the Eocene.
- The sharp gradients of modelled Eocene accumulations (Figure 4a) may be a visual bias of the model due to the uneven distribution of input constraints that produce artifacts in the Kriging method employed. However, some of these boundaries may be real and are interpreted as faults (see below).

### Distribution and Volume of the Eocene Volcanic Sequence

Eocene igneous rock units are currently interpreted to extend over ~26 400 km<sup>2</sup> within the area modelled and over 60 700 km<sup>2</sup> in total in BC (33 400 km<sup>2</sup> of volcanic rocks, 27 300 km<sup>2</sup> of intrusive rocks; Table 2; Massey et al., 2005). However, these are erosional relicts of originally more areally extensive deposits, and any volume calculations are conservative on this basis.

Isolated Eocene erosional remnants occur locally in areas dominated by Mesozoic basement (Figure 3), and are emphasized by the distribution of mineralized prospects, such as in the Nechako Plateau. Using a buffer of 10 km around these Eocene remnants (corresponding to half the average distance between isolated polygons) and generating a new surface corresponding to merged buffered polygons, an ‘eroded Eocene surface’ of ~26 500 km<sup>2</sup> is generated (Table 2).

A partly transparent fill is applied to the extensive CGB cover to reveal significant thickness of Eocene under cover, such as to the west of well B-22-K and northwest of Chilanko Forks (Figure 3). This ‘covered Eocene surface’ is estimated at ~5 200 km<sup>2</sup> (Table 2).

Mapped, eroded and covered extents of Eocene volcanic rocks for the modelled area total ~58 000 km<sup>2</sup> (Table 2). This is more than double the original estimate, and increases the total Eocene volcanic extent for BC to 65 100 km<sup>2</sup>. The corresponding volume of Eocene volcanic rocks for the modelled area is calculated at ~12 000 km<sup>3</sup>, an estimate that does not consider vertical erosion of the original volume.

### Structural Controls on Regional Variations in Thickness

The focused OLG thickness model (Figure 4a) highlights the spatial correlation between areas of significant Eocene

**Table 2.** Surface-area calculations for the Eocene volcanic sequence, for British Columbia and the thickness model area. Calculations are based on summation of polygon areas using Manifold™.

Area	Name	Surface area estimate (km <sup>2</sup> )	Polygon source
British Columbia	Eocene - volcanic	33 412	
	Eocene - intrusive	27 316	Massey et al. (2005)
	Eocene - volcanic + intrusive	60 728	
Modelled area (total surface 100 000 km <sup>2</sup> )	Existing Eocene - volcanic	26 355	Massey et al. (2005)
	Eroded + existing Eocene - volcanic	52 822	Massey et al. (2005). Buffer around Eocene polygons that display surface area less than or equal to 200 km <sup>2</sup> within the basement surface extent. Union of buffer polygons defines surface of eroded Eocene
	Eroded Eocene - volcanic	26 467	Calculated
	Covered Eocene - Volcanic	5 237	Thickness model. 100 m thickness contour defines polygon of Eocene extent. Covered Eocene corresponds to intersection of this polygon with the Chilcotin Group basalt
	Combined existing + eroded + covered Eocene - volcanic	58 059	Calculated
British Columbia	Combined existing + new estimate for Eocene volcanic rocks only	65 116	Calculated

accumulation and large structures interpreted from magnetic anomalies (Figure 4b). The orientation and kinematics of the interpreted structures are in agreement with a transtensional regime (Struik, 1993). In this context, north-west-trending thickness discontinuities are interpreted as dextral strike-slip faults, and north-trending lineaments are cospatial with normal faults interpreted from seismic-reflection data and from tomographic and seismic-velocity models (Figure 4). Within this strain system, east-trending lineaments may correspond to thrusts (Figure 4). West of a north-trending ridge of Cretaceous basement in the central part of the detailed study area, a series of north- to north-east-trending lineaments correlates with shallow-angle reflectors that are interpreted as thrust faults on the seismic reflection profiles (Figure 4). These structures are interpreted to result from pre-Eocene tectonic shortening and were possibly reactivated as extension faults during the Eocene.

The thickest Eocene accumulation in the vicinity of well B-22-K is inferred to have developed in an extensional transfer zone, where the deformation is accommodated mainly by extensional displacements between large dextral faults. This transfer zone also correlates with areas of low gravity that replicate the shape and orientation of north-trending extensional basins (Figure 4c). Interestingly, this area also hosts two of the known Eocene epithermal prospects within the region investigated here (Figure 4).

These structural interpretations are consistent with coeval eruption of Eocene volcanic rocks during extensional deformation and with the preservation of remnant Eocene sequences within extensional basins.

### Implications for Exploration

Eocene mineral prospects and deposits occur within areas of known rock exposure (e.g., Wolf, Free Gold; Figures 2a, 3, Table 1). This OLG thickness model provides a new perspective on areas where Eocene rocks may be present beneath cover. Stratigraphic investigations by Bordet et al. (2013, work in progress) suggest that Eocene mineralization is hosted in rhyolite lavas and breccias that form the lowest OLG stratigraphic levels. The identified structural domains seem to strategically control the distribution of known mineralization. The spatial correlation of a fault transfer zone, which links the Yalakom and Fraser faults, and the occurrence of epithermal-style Au mineralization at the Blackdome mine (Figure 3) suggest a local structural control on Eocene mineralization. Similarly, the Baez and Clisbako epithermal Au prospects (Figure 2b) are located in a domain interpreted as an extensional transfer zone between large dextral faults (Figures 3, 4). Finally, the new Eocene thickness and structural framework provides insights into areas where hydrocarbon-rich Cretaceous

basins may have been deformed or thermally affected by a thick Eocene volcanic cover.

### Acknowledgments

This project is partly funded by a Geoscience BC grant. Additional support was provided through a Natural Sciences and Engineering Research Council of Canada Industrial Postgraduate Scholarship, in partnership with Golder Associates Ltd. The senior author also thanks Endeavour Silver Corp. for granting a graduate scholarship, and D. Mitchinson for her constructive review of the paper.

British Columbia Geological Survey contribution 2013-2.

### References

- Andrews, G.D.M., Plouffe, A., Ferbey, T., Russell, J.K., Brown, S.R. and Anderson, R.G. (2011): The thickness of Neogene and Quaternary cover across the central Interior Plateau, British Columbia: analysis of water-well drill records and implications for mineral exploration potential; *Canadian Journal of Earth Sciences*, v. 48, p. 973–986.
- BC Geological Survey (2013): MINFILE BC mineral deposits database; BC Ministry of Energy and Mines, URL <<http://minfile.ca/>> [November 2013].
- BC Ministry of Energy, and Mines (2013): ARIS assessment report indexing system; BC Ministry of Energy and Mines, BC Geological Survey, URL <<http://aris.empr.gov.bc.ca>> [November 2013].
- Bevier, M.L. (1983): Regional stratigraphy and age of Chilcotin Group basalts, south-central British Columbia; *Canadian Journal of Earth Sciences*, v. 20, p. 515–524.
- Bordet, E., Hart, C.J.R. and Mihalynuk, M.G. (2013): A stratigraphic framework for Late Cretaceous and Eocene Au-Ag mineralization in central British Columbia; SEG 2013 Meeting, Whistler, BC, September 2011, poster presentation.
- Bordet, E., Hart, C.J.R. and Mitchinson, D. (2011): Preliminary lithological and structural framework of Eocene volcanic rocks in the Nechako region, central British Columbia; Geoscience BC, Report 2011-13, 80 p.
- Bordet, E., Mihalynuk, M.G., Hart, C.J.R., Mortensen, J.K., Friedman, R.M. and Gabites, J. (in press): Chronostratigraphy of Eocene volcanism, central British Columbia; *Canadian Journal of Earth Sciences*.
- Centre for Topographic Information (1997): Digital elevation model for NTS areas 093B, 093C, 093G, 093F, 092N, 092O, North American Datum of 1983; Natural Resources Canada, Centre for Topographic Information, Canadian Digital Elevation Data, Level 1 (CDED1).
- Church, B.N. (1973): Geology of the White Lake Basin; BC Ministry of Energy and Mines, Bulletin 61, 141 p.
- Church, B.N. (1985): Volcanology and structure of Tertiary outliers in south-central British Columbia, Trip 5; *in* Field Guides to Geology and Mineral Deposits in the Southern Canadian Cordillera, D.J. Tempelman-Kluit (ed.), GSA Cordilleran Section meeting, Vancouver, BC, p. 5-1–5-46.
- Coney, P.J., Jones, D.L. and Monger, J.W.H. (1980): Cordilleran suspect terranes; *Nature (London)*, v. 288, p. 329–333.

- Cyr, J.B., Pease, R.B. and Schroeter, T.G. (1984): Geology and mineralization at Equity silver mine; *Economic Geology*, v. 79, p. 947–968.
- Dohaney, J., Andrews, G.D.M., Russell, J.K., and Anderson, R.G. (2010): Distribution of the Chilcotin Group, Taseko Lakes and Bonaparte Lake map areas, British Columbia; Geological Survey of Canada, Open File 6344 and Geoscience BC Map 2010-2-1, 1 sheet, scale 1:250 000.
- Duffell, S. (1959): Whitesail Lake map-area, British Columbia; Geological Survey of Canada, Memoir 299, 119 p.
- Eisbacher, G.H. (1977): Mesozoic-Tertiary basin models for the Canadian Cordillera and their geological constraints; *Canadian Journal of Earth Sciences*, v. 14, p. 2414–2421.
- Ewing, T.E. (1980): Paleogene tectonic evolution of the Pacific Northwest; *Journal of Geology*, v. 88, no. 6, p. 619–638.
- Ewing, T.E. (1981): Regional stratigraphy and structural setting of the Kamloops Group, south-central British Columbia; *Canadian Journal of Earth Sciences*, v. 18, p. 1464–1477.
- Faulkner, E.L. (1986): Blackdome deposit; *in* Geological Fieldwork 1985, BC Ministry of Energy and Mines, Paper 1986-1, p. 107–111.
- Ferri, F. and Riddell, J. (2006): The Nechako Basin project: new insights from the southern Nechako Basin; *in* Summary of Activities 2006, BC Ministry of Energy and Mines, p. 89–124.
- Fulton, R.J. (1995): Surficial materials of Canada; Geological Survey of Canada, Map 1880A, scale 1:5 000 000.
- Geological Survey of Canada (1994): Magnetic residual total field, Interior Plateau of British Columbia; Geological Survey of Canada, Open File 2785.
- Hayward, N. and Calvert, A.J. (2011): Interpretation of structures in the southeastern Nechako Basin, British Columbia, from seismic reflection, well log and potential field data; *Canadian Journal of Earth Sciences*, v. 48, p. 1000–1020.
- Holland, S.S. (1976): Landforms of British Columbia: a physiographic outline; BC Ministry of Energy and Mines, Bulletin 48, 138 p.
- Massey, N.W.D., MacIntyre, D.G., Desjardins, P.J. and Cooney, R.T. (2005): Digital geology map of British Columbia: whole province; BC Ministry of Energy and Mines, GeoFile 2005-1.
- Mathews, W.H. (1989): Neogene Chilcotin basalts in south-central British Columbia: geology, ages, and geomorphic history; *Canadian Journal of Earth Sciences*, v. 18, p. 1478–1491.
- Mihalynuk, M.G. (2007): Neogene and Quaternary Chilcotin Group cover rocks in the Interior Plateau, south-central British Columbia: a preliminary 3D thickness model; *in* Geological Fieldwork 2006, BC Ministry of Energy and Mines, Paper 2007-1, p. 143–148.
- Mihalynuk, M.G., Orovan, E.A., Larocque, J.P., Bachiu, T. and Wardle, J. (2009): Geology of the Chilanko Forks and southern Clusko River map areas (NTS 093C/01 and 09 south); BC Ministry of Energy and Mines, Open File 2009-6, scale 1:50 000.
- Mihalynuk, M.G., Peat, C.R., Orovan, E.A., Terhune, K., Ferby, T. and McKeown, M.A. (2008): Chezacut area geology (NTS 093C/08); BC Ministry of Energy and Mines, Open File 2008-2, scale 1:50 000.
- Portmann, H. (2013): New Gold announces increased gold resources at Blackwater project; New Gold Inc., press release, April 4, 2013, URL <[http://www.newgold.com/files/documents\\_news/Blackwater%20Resource%20update%20vFinal.pdf](http://www.newgold.com/files/documents_news/Blackwater%20Resource%20update%20vFinal.pdf)> [October 2013].
- Riddell, J.M. (2011): Lithostratigraphic and tectonic framework of Jurassic and Cretaceous intermontane sedimentary basins of south-central British Columbia; *Canadian Journal of Earth Sciences*, v. 48, p. 870–896.
- Smithyman, B.R. (2013): Developments in waveform tomography of land seismic data with applications in south-central British Columbia; Ph.D. thesis, University of British Columbia.
- Souther, J.G. (1970): Volcanism and its relationships to recent crustal movements in the Canadian Cordillera; *Canadian Journal of Earth Sciences*, v. 7, no. 2, p. 553–568.
- Souther, J.G. (1986): The western Anahim Belt: root zone of a peralkaline magma system; *Canadian Journal of Earth Sciences*, v. 23, p. 895–908.
- Souther, J.G. (1991): Volcanic regimes; Chapter 14 *in* Geology of the Cordilleran Orogen in Canada, J. Gabrielse and C.J. Yorath (ed.), Geological Survey of Canada, Geology of Canada, no. 4 (also Geological Society of America, Geology of North America, v. G-2), p. 457–490.
- Spratt, J.E. and Craven, J.A. (2011): Near surface and crustal-scale images of the Nechako Basin, British Columbia, Canada, from magnetotelluric investigations; *Canadian Journal of Earth Sciences*, v. 48, p. 987–999.
- Spratt, J.E., Welford, J.K., Farquharson, C. and Craven, J.A. (2012): Modelling and investigation of airborne electromagnetic data, and reprocessing of vibroseis data, from Nechako Basin, BC, guided by magnetotelluric results; Geoscience BC, Report 2012-14, 93 p.
- Struik, L.C. (1993): Intersecting intracontinental Tertiary transform fault systems in the North American Cordillera; *Canadian Journal of Earth Sciences*, v. 30, p. 1262–1274.
- Thorkelson, D.J. (1988): Eocene sedimentation and volcanism in the Fig Lake graben, southwestern British Columbia; *Canadian Journal of Earth Sciences*, v. 26, p. 1368–1373.
- Tipper, H.W. (1959): Geology, Quesnel, Cariboo district, British Columbia; Geological Survey of Canada, Map 12-1959, scale 1:253 440.
- Umhoefer, P.J. and Schiarizza, P. (1996): Latest Cretaceous to early Tertiary dextral strike-slip faulting on the southeastern Yakom fault-system, southeastern Coast Belt, British Columbia; *Geological Society of America Bulletin*, v. 108, p. 768–785.
- WesternGeco MDIC (2010): 2-D land joint inversion of seismic, magnetotelluric and gravity for prestack depth migration imaging; Nechako Basin, British Columbia, lines 05, 10 and 15; Geoscience BC, Report 2010-16, 49 p.



# Petrographic Characteristics of Porphyry Indicator Minerals from Alkalic Porphyry Copper-Gold Deposits in South-Central British Columbia (NTS 092, 093)

M.A. Celis, Mineral Deposit Research Unit, University of British Columbia, Vancouver, BC, mcelis@eos.ubc.ca

F. Bouzari, Mineral Deposit Research Unit, University of British Columbia, Vancouver, BC

T. Bissig, Mineral Deposit Research Unit, University of British Columbia, Vancouver, BC

C.J.R. Hart, Mineral Deposit Research Unit, University of British Columbia, Vancouver, BC

T. Ferbey, British Columbia Geological Survey, Victoria, BC

---

Celis, M.A., Bouzari, F., Bissig, T., Hart, C.J.R. and Ferbey, T. (2014): Petrographic characteristics of porphyry indicator minerals from alkalic porphyry copper-gold deposits in south-central British Columbia (NTS 092, 093); in Geoscience BC Summary of Activities 2013, Geoscience BC, Report 2014-1, p. 53–62.

## Introduction

The occurrence of resistate minerals such as apatite, titanite, garnet and rutile in the surficial environment proximal to mineralized and altered portions of British Columbia's alkalic porphyry copper deposits suggests that these minerals can be utilized as exploration tools, especially in terrains covered by glacial till (Bouzari et al., 2011). Before such minerals can be utilized for exploration, the physical and chemical properties of these porphyry indicator minerals (PIMs) must first be established. This paper will characterize the occurrence, type, relative amount and composition of selected PIMs at the Copper Mountain, Mount Polley and Mount Milligan porphyry deposits (Figure 1), in order to elucidate important PIM signatures and then evaluate these signatures in proximal tills, stream sediments and heavy mineral concentrates. This paper presents the results of a project that evaluates PIMs that are directly associated with alkalic porphyry deposits, and builds upon information previously presented (Celis et al., 2013).

A detailed petrographic study of 60 samples representing various hostrocks, and alteration and mineralization assemblages from the Copper Mountain, Mount Polley and Mount Milligan deposits, was undertaken using transmitted and reflected light microscopy, as well as scanning electron microscopy (SEM). In addition, heavy mineral separates derived from bedrock (16 samples) and from till sediments (14 samples), covering the Mount Polley and Mount Milligan deposits, were collected and are currently under investigation. This paper summarizes the results of

the petrographic study, characterizing PIMs occurring within the porphyry deposit.

## Resistate Minerals in Alkalic Porphyry Deposits

Resistate minerals occur as rock-forming minerals in alkalic intrusions and are modified or precipitated during the hydrothermal processes that result in the formation of porphyry copper deposits. The occurrence and some key characteristics of resistate minerals such as apatite, magnetite, garnet, rutile and zircon have been previously described for porphyry deposits (e.g., Bouzari et al., 2011). Primary magmatic apatite in hostrock and in early potassic alteration can record a history of dissolution and precipitation during subsequent hydrothermal alteration. Magnetite can form a resistate phase when aggregated with rutile, titanite and quartz. Magnetite with a uniform pinkish-grey colour in reflected light (RL) indicates a high Ti content and probable magmatic origin. Rims of hematite and titanite around magnetite indicate an increase in the oxidation state of the latest crystallizing melt. Garnet can occur at the peripheries of porphyry deposits and can display mineral zoning, dissolution and changes in chemical composition in response to hydrothermal evolution. In potassically altered rocks, rutile occurs as relicts of altered biotite, ilmenite, titanomagnetite and amphibole. Titanite is commonly magmatic, occurring within the host intrusion, and displays a characteristic blonde colour in transmitted light (TL; Bouzari et al., 2011).

Magnetite and titanomagnetite are common oxide phases in alkalic plutonic rocks. During the magmatic processes, the occurrence and composition of the Fe-Ti oxides is determined by the composition of the melt from which they crystallized and also by re-equilibrium reactions between the oxides and the silicates in the hostrock.

---

**Keywords:** *alkalic porphyry deposits, indicator minerals, petrographic characteristics*

*This publication is also available, free of charge, as colour digital files in Adobe Acrobat® PDF format from the Geoscience BC website: <http://www.geosciencebc.com/s/DataReleases.asp>.*

Hydrothermal fluids may partially or totally modify the original physical properties of these resistate minerals, which can ultimately result in the precipitation of a new hydrothermal mineral phase. For example, small (<100 μm), euhedral, colourless and uniform-textured magmatic apatite crystals are commonly regrown and modified to show subhedral to anhedral habits, and display a distinctive cloudy, highly porous texture. Some of the processes and reactions responsible for the generation of resistate minerals by magmatic and hydrothermal reactions are listed below (Table 1).

## Analytical Methods

### Petrography and SEM

Petrographic analysis of 60 thin sections from Mount Polley, Mount Milligan and Copper Mountain was performed using TL and RL microscopy, as well as scanning electron microscopy (SEM). Mineralogical and textural characteristics of different alteration assemblages were documented first. This was followed by the characterization of resistate minerals occurring within the fresh hostrock, as well as within representative samples of each

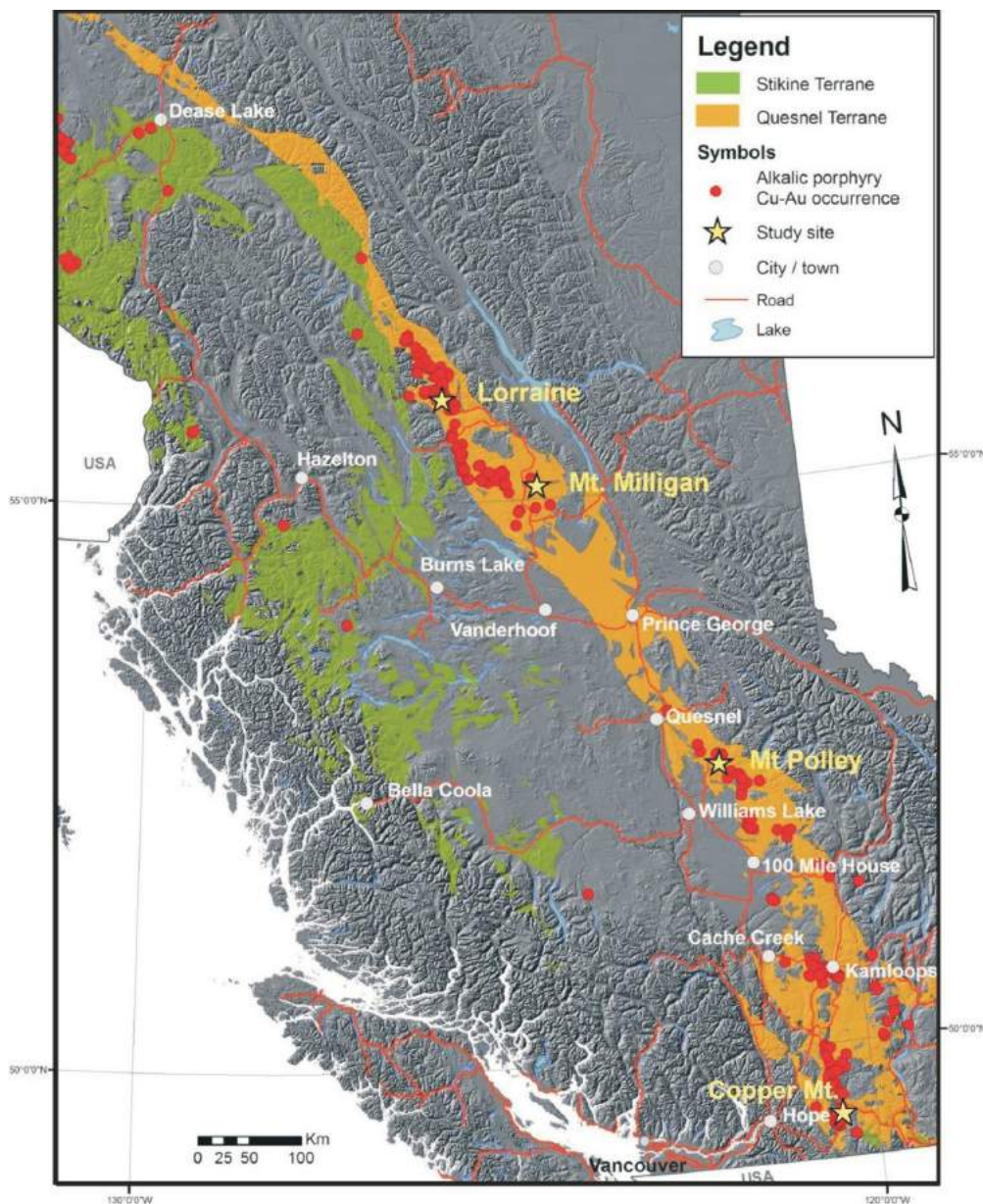


**Figure 1.** Digital elevation map showing Triassic and Early Jurassic Quesnel and Stikine terranes of south-central British Columbia and location of selected deposits (modified from Tosdal et al., 2008). Figure compiled using digital elevation data from GeoBase® (2004) with postprocessing by K. Shimamura (Geological Survey of Canada); MINFILE database (porphyry occurrences; BC Geological Survey, 2013); and the tectonic assemblage map of the Vancouver area (Journeay et al., 2000).

**Table 1.** Summary of magmatic and hydrothermal reactions that generate resistate minerals.

<p><b>An increase in the oxidation state of the magma during cooling results in the formation of ilmenite and magnetite as exsolution lamellae after titanomagnetite (Lindsley 1991).</b></p> $6\text{Fe}_2\text{TiO}_4 + \text{O}_2 = 6\text{FeTiO}_3 + 2\text{Fe}_3\text{O}_4$ <p>(titanomagnetite = ilmenite + magnetite)</p>
<p><b>During K-feldspar alteration, interaction between titanomagnetite/ilmenite and sulphur-rich fluids form rutile and sulphide phases (Lindsley 1991).</b></p> $2(\text{H}_2\text{S}, \text{Cu}^{2+}) + 2\text{FeTiO}_3/\text{Fe}_2\text{TiO}_4 = \text{FeS}_2/\text{CuFeS}_2 + \text{TiO}_2$ <p>(fluid + ilmenite/titanomagnetite = pyrite/chalcopyrite + rutile)</p>
<p><b>Hydrothermal fluids interacting with Ti-bearing mafic phenocrysts form rutile and sulphides (Lindsley 1991).</b></p> $2(\text{H}_2\text{S}, \text{Cu}^{2+}) + 2\text{K}(\text{Fe}, \text{Ti})_3\text{AlSi}_3\text{O}_{10}(\text{OH})_2 = \text{CuFeS}_2 + (\text{Fe}, \text{Al})_3(\text{Si}, \text{Al})_4\text{O}_{10}(\text{OH})_2 + \text{K}(\text{Al}, \text{Fe})_2(\text{SiAl})_4\text{O}_{10}(\text{OH})_2n\text{H}_2\text{O} + \text{TiO}_2$ <p>(fluid + Ti-biotite = chalcopyrite + chlorite + sennite + rutile)</p>
<p><b>Titanite is a common Ti-bearing resistate mineral in alkalic hostrocks. During early magmatic processes, titanite can form after augite and ilmenite (Xirouchakis and Lindsley 1998).</b></p> $3\text{CaFeSi}_2\text{O}_6 + 3\text{FeTiO}_3 = 3\text{CaTiSiO}_5 + \text{Fe}_3\text{O}_4 + 9\text{SiO}_2$ <p>(augite + ilmenite = titanite + magnetite + quartz)</p>
<p><b>A similar reaction accompanying K-feldspar alteration forms titanite and sulphide phases (Lindsley, 1991).</b></p> $3\text{CaFeSi}_2\text{O}_6 + 3\text{FeTiO}_3 + (\text{H}_2\text{S}, \text{Cu}) = 3\text{CaTiSiO}_5 + 6\text{FeS}_2/\text{CuFeS}_2 + 9\text{SiO}_2$ <p>(augite + ilmenite + fluid = titanite + pyrite/chalcopyrite + quartz)</p>
<p><b>Hydrothermal fluids interacting with carbonate mineral phases result in the formation of mineral phases such as andraditic garnet (Dasgupta and Supratim, 2005).</b></p> $3\text{SiO}_2 + 3\text{CaCO}_3 + \text{Ca}_2\text{Al}_2(\text{Fe}_3+\text{Al})(\text{SiO}_4)(\text{Si}_2\text{O}_7)\text{O}(\text{OH}) = \text{Ca}_3\text{Fe}_2+2(\text{SiO}_4)_3 + 3\text{CO}_2$ <p>(quartz + calcite + epidote = andradite)</p>

alteration assemblage. The PIMs were then characterized within each alteration according to their paragenesis and physical properties such as colour, habit, texture and grain size.

## Geology and Alteration

### Copper Mountain

The Copper Mountain deposit is centred on two Late Triassic intrusions, composed predominantly of pyroxene diorite to monzonite and syenite, and hosted within the Triassic Nicola volcanic sequence (Stanley et al., 1992). Alteration assemblages comprise an early stage of hornfels alteration, overprinted by sodic and potassic alteration.

Potassic alteration is characterized by pink K-feldspar replacing plagioclase, locally crosscuts zones of pre-existing sodic-calcic alteration, and is widely distributed throughout the deposit (Stanley et al., 1992). Magnetite-chalcopyrite and titanite-chalcopyrite assemblages are common within the potassic alteration zone. Magnetite occurs as coarse subhedral to anhedral grains up to 500 µm. Titanite grains display characteristic wedge-shaped crystal habit and show a distinctive brownish colour in TL.

Sodic alteration is characterized by abundant albite that is confined to the central portion of the deposit and typically expressed as bleached, pale greyish-green or mottled white alteration of the hostrock (Stanley et al., 1992). Augite and titanite are common within sodic alteration. Rhombohedral titanite grains up to 300 µm display characteristic colourless to pale brown colour. Partial replacement of mafic phenocrysts and titanite grains by small anhedral rutile grains is also common.

A dark to light green chlorite+actinolite+epidote±pyrite±calcite alteration assemblage typically occurs at the periphery of the deposit, but also may occur in the central part along with potassic alteration (Stanley et al., 1992). Magnetite and titanite grains within this alteration zone are less abundant and smaller in size. A magnetite-titanite assemblage replacing mafic phenocrysts is typical within this alteration.

Apatite is ubiquitously distributed and occurs as coarse (500 µm) subhedral to anhedral colourless grains with a cloudy appearance and highly porous texture. Small (<10 µm) monazite inclusions may occur.

## Mount Polley

The Mount Polley deposit is centred within and around several diorite to monzonite intrusions of Upper Triassic to Lower Jurassic age hosted in the Triassic Nicola volcanic sequence (Fraser et al., 1995). Alteration at Mount Polley consists of three concentrically zoned alteration assemblages (Fraser et al., 1995): a potassic core surrounded by a constrained garnet-epidote zone and an outer propylitic zone. The potassic core has been further divided into three distinct zones: biotite (100 m wide), actinolite (250 m wide), and K-feldspar–albite zone (1 km wide; Hodgson et al., 1976; Bailey and Hodgson, 1979). Magnetite is the dominant Fe-oxide mineral in the potassic alteration zone and commonly occurs as vein material and disseminated grains. Rhombohedral- to wedge-shaped titanite grains are commonly associated with chalcopyrite, whereas less abundant small (<50 µm) anhedral rutile replaces biotite phenocrysts. Garnet occurs as very coarse (>1000 µm) pale yellow grains in the garnet-epidote zone. The outer ‘green alteration’ propylitic zone includes a mineral assemblage of albite, epidote, chlorite with calcite veins and variable amounts of disseminated pyrite. Replacement of mafic phenocrysts by epidote±titanite is common. Titanite typically occurs as rhombohedral- to wedge-shaped grains with a distinctive pale brownish colour in TL. Apatite is ubiquitously distributed and occurs as coarse (500 µm) subhedral to anhedral colourless grains with a cloudy highly porous texture.

## Mount Milligan

Mount Milligan consists of three main monzonite stocks of Middle Jurassic age (MBX, South Star, Rainbow dike) hosted within the Late Triassic Takla Group volcanic sequence (Sketchley et al., 1995; Jago and Tosdal, 2009). Two principal alteration patterns are recognized, the first of which is a zone of intense potassic alteration consisting of biotite+K-feldspar±magnetite that lies between the MBX stock and the Rainbow dike. The second is a lower temperature ‘green alteration’, consisting of chlorite+epidote+calcite that typically occurs below the footwall of the monzonitic Rainbow dike where it overprints potassic alteration in volcanic hostrocks (Jago et al., 2009).

In potassic alteration, magnetite typically occurs as coarse (200–400 µm) subhedral grains with homogeneous to lamellar texture. Mafic phenocrysts replaced by magnetite-pyrite are common. Generally, magnetite is less common in Mount Milligan relative to Mt. Polley and Copper Mountain.

Small (<50 µm) anhedral to acicular rutile crystals commonly occur within magnetite, titanite and mafic phenocrysts. Titanite at Mount Milligan is rare and in TL displays

a characteristic pale brown colour and anhedral to wedge-shaped habits.

Apatite is ubiquitously distributed and occurs as coarse (500 µm) subhedral to anhedral colourless grains with cloudy highly porous texture.

## Characterization of Selected PIMs

Mineral paragenesis and their physical properties such as habit, colour, texture and size are the key parameters used to characterize PIMs in alkalic porphyry systems. PIMs are divisible into four types: 1) those that crystallized from magma (magmatic); 2) those magmatic minerals that have been physically or chemically modified by hydrothermal fluids (altered); 3) those that exsolved from previously crystallized minerals (exsolved); and, 4) those that precipitated directly from a hydrothermal fluid (hydrothermal). Some examples of magmatic PIMs are rock-forming minerals such as olivine, pyroxenes, amphiboles, K-feldspar, plagioclase and opaque minerals such as magnetite and titanite. Altered PIMs are most typically magmatic minerals that have undergone compositional change because of hydrothermal fluid interactions. Variation in the chemistry of apatite or the conversion of magnetite to hematite represent two examples of hydrothermally altered PIMs. Exsolved PIMs are those forming as lamellae and in exsolution textures such as in many Fe-Ti oxides. Hydrothermal PIMs are those grains newly precipitated either as flooding, disseminations or veins, and include secondary K-feldspar, secondary biotite, chlorite, actinolite and magnetite.

## Magnetite

Magmatic magnetite typically displays euhedral cubic grains, from 100 to 300 µm in size with abundant ilmenite lamellar textures at all three studied deposits (Figure 2a, b). In potassically altered rocks at Mount Polley and Copper Mountain, hydrothermal magnetite grains are commonly coarse (>500 µm), show subhedral to anhedral habit with uniform texture and are distributed within the K-feldspar groundmass. Magnetite occurrences can be massive to vein type with common magnetite-chalcopyrite assemblages (Figure 2c, d). In the propylitic zone at all three deposits magnetite is less abundant and tends to preserve its subhedral to anhedral habit and homogeneous texture, but its size tends to decrease (<200 µm), and massive to vein-type occurrences are absent. Magnetite-pyrite replacing mafic phenocrysts (Figure 2e) is common within propylitic-altered rocks of Mount Milligan. Some diagnostic characteristics of magnetite are: euhedral to subhedral cubic habit, light grey colour in RL with lamellar texture in least-altered hostrocks (magmatic magnetite), and subhedral to vein habit, pinkish-grey colour in RL and uniform texture in potassically altered rocks (altered magnetite).

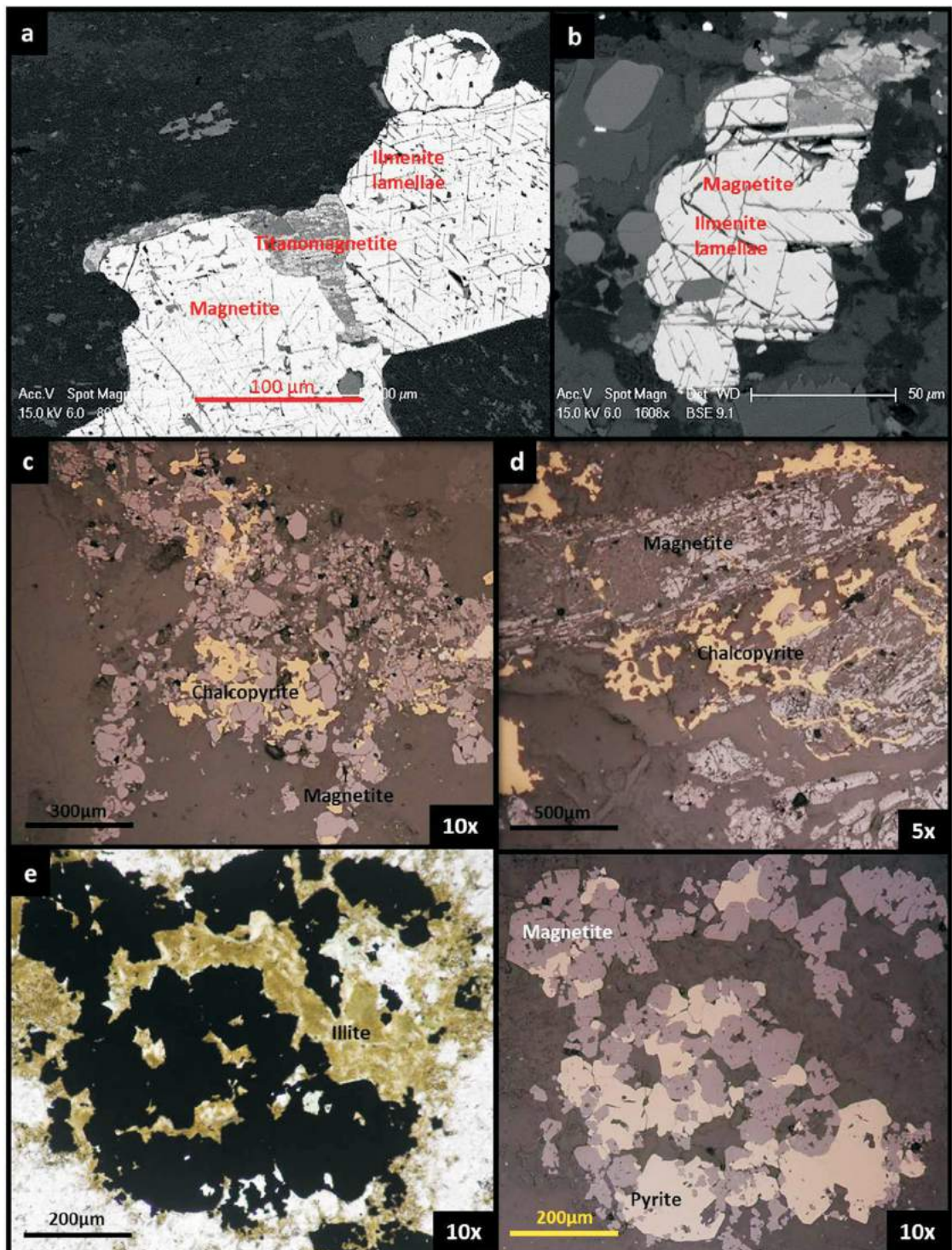


**Figure 2.** Photomicrographs of magnetite, south-central British Columbia: **a)** scanning electron microscope (SEM) backscattered image of euhedral magnetite, 400 µm grain size, with abundant ilmenite lamellae and exsolution texture of least-altered rocks, Copper Mountain, sample from south access to mine road (UTM 681500N, 5468302E, NAD 83, Zone 19; CMT-13); **b)** SEM backscattered image of magnetite, subhedral habit, 100 µm size, with abundant ilmenite lamellae and exsolution texture, in least-altered rocks, Mount Polley, sample from road to the tailings (UTM 5822071N, 592687E; P-10); **c)** magnetite with homogeneous texture, subhedral habit, 100–200 µm size, containing chalcopyrite bodies in K-feldspar alteration, Mount Polley, sample from Springer pit (P-1); **d)** magnetite with homogeneous texture, subhedral to anhedral habit, 100 µm size, intergrown by chalcopyrite in K-feldspar alteration, Copper Mountain, sample from Alabama pit (CM12AB12\_65.5m); **e)** magnetite with homogeneous to lamellar texture, subhedral habit, 200 µm size, intergrown with pyrite replacing a mafic phenocryst in propylitic altered rocks containing green clay illite, Mount Milligan, sample from 66 zone (07992\_81.5m).

## Titanite

Titanite is the most abundant titanium-bearing mineral in the studied deposits. Copper Mountain and Mount Polley contain up to 3% titanite, and Mount Milligan contains less than 1%.

Magmatic titanite grains have typical rhombohedral habit, uniform texture and are colourless to pale brownish colour in TL with sizes ranging from 100 to 300  $\mu\text{m}$ . Typical augite-titanite assemblages can be found within sodic alteration at Copper Mountain (Figure 3a). Hydrothermal titanite typically occurs within the potassic-altered rocks at all three deposits. These grains are rhombohedral, wedge shaped to anhedral in habit, with serrated edges and display a more brownish colour in TL than magmatic titanite. Typical occurrences of hydrothermal titanite at Copper Mountain are titanite-chalcopyrite clusters (Figure 3b) and rutile replacements (Figure 3c)

Titanite within propylitic-altered rocks tends to have smaller grain size (100  $\mu\text{m}$ ) and lower modal abundance (1%). Titanite with a wedge-shaped crystal habit, together with chlorite and epidote is common. In addition, a titanite-magnetite assemblage (Figure 3d) replacing mafic phenocrysts occurs locally.

Diagnostic characteristics of magmatic titanite include rhombohedral- to wedge-shaped habit, colourless to pale brownish colour and high relief in TL, dark grey colour in RL and uniform texture.

## Apatite

Apatite is a rock-forming accessory mineral that crystallizes late from residual magma, occupying interstitial spaces within the groundmass of intrusive hostrocks or adjacent to mafic phenocrysts. Its diagnostic characteristics include euhedral prismatic colourless crystals of small size (<100  $\mu\text{m}$ ) and uniform texture (Figure 4a). Hydrothermal apatite is typically coarse (300–1000  $\mu\text{m}$ ), colourless, subhedral to anhedral habit, and displays a characteristic cloudy, highly porous texture (Figure 4b, c). Hydrothermal apatite is ubiquitously distributed in all studied deposits and its relative abundance is significantly higher (2%) than magmatic apatite (<1%).

## Garnet

Garnet occurs exclusively within a transitional garnet-epidote alteration zone between the potassic core and the outer propylitic zone at the Mount Polley deposit. Garnet typically occurs as very coarse (>1000  $\mu\text{m}$ ) subhedral to anhedral grains of yellow colour in TL (Figure 4c). Massive garnet veins (Figure 4e) and epidote±garnet assemblages suggest a hydrothermal origin. The diagnostic features of garnet are its brown to honey-brown colour and high relief

in TL, isotropy under cross-polarized light (XPL), subhedral cubic to vein habits and fractured texture.

Table 2 summarizes characteristics of the selected porphyry indicator minerals. Classification is on the basis of their origin and characteristic physical properties within least-altered and altered rocks from alkalic porphyry deposits.

## Discussion

Detailed petrographic characterization of apatite, garnet, magnetite and titanite from the Copper Mountain, Mount Polley and Mount Milligan deposits, confirmed high abundances of magnetite (10%) and titanite (>4%) in potassically altered alkalic plutonic rocks. Also, exsolution lamellae and replacement textures are consistently found in euhedral to subhedral magmatic magnetite grains. These mineralogical features represent a late magmatic stage of a porphyry-type intrusion as Fe-Ti oxides re-equilibrated during cooling.

Subsequently, rhombohedral titanite is the dominant titanium-bearing mineral in the studied deposits and mainly originates from the augite-titanomagnetite (oxide-silicate) equilibrium during cooling.

As hydrothermal fluid-rock interaction developed within the studied alkalic porphyry systems, a new precipitation of magnetite and titanite took place. Hydrothermal magnetite typically occurs as disseminated medium to coarse grains and local veins. Magnetite together with chalcopyrite±bornite is a common assemblage in potassically altered rocks, whereas magnetite±pyrite replacement of augite and other mafic minerals is characteristic in propylitic alteration. Generally, magnetite distribution and grain size tend to decrease from the centre (1000  $\mu\text{m}$ ) to the periphery (<100  $\mu\text{m}$ ) of each deposit.

Hydrothermal titanite precipitated together with chalcopyrite±bornite and displays subhedral to anhedral habit with serrated edges and a characteristic brown colour in TL. Also, titanite interacting with CO<sub>2</sub>-rich fluids may have resulted in precipitation of very small (<50  $\mu\text{m}$ ) subhedral to acicular rutile grains. The very small size of rutile makes it an impractical PIM due to its low preservation and recovery potential in porphyry-derived sediments. Generally, titanite and rutile abundance tends to be higher in the potassic centre of a deposit and gradually decreases outward to the propylitic zone.

Garnet occurs exclusively in a transitional garnet+epidote alteration zone between the potassic and propylitic alteration zones at the Mount Polley deposit as very coarse (>1000  $\mu\text{m}$ ) anhedral grains to veins. Its coarse-grained to massive occurrence, honey-brown colour, high relief in

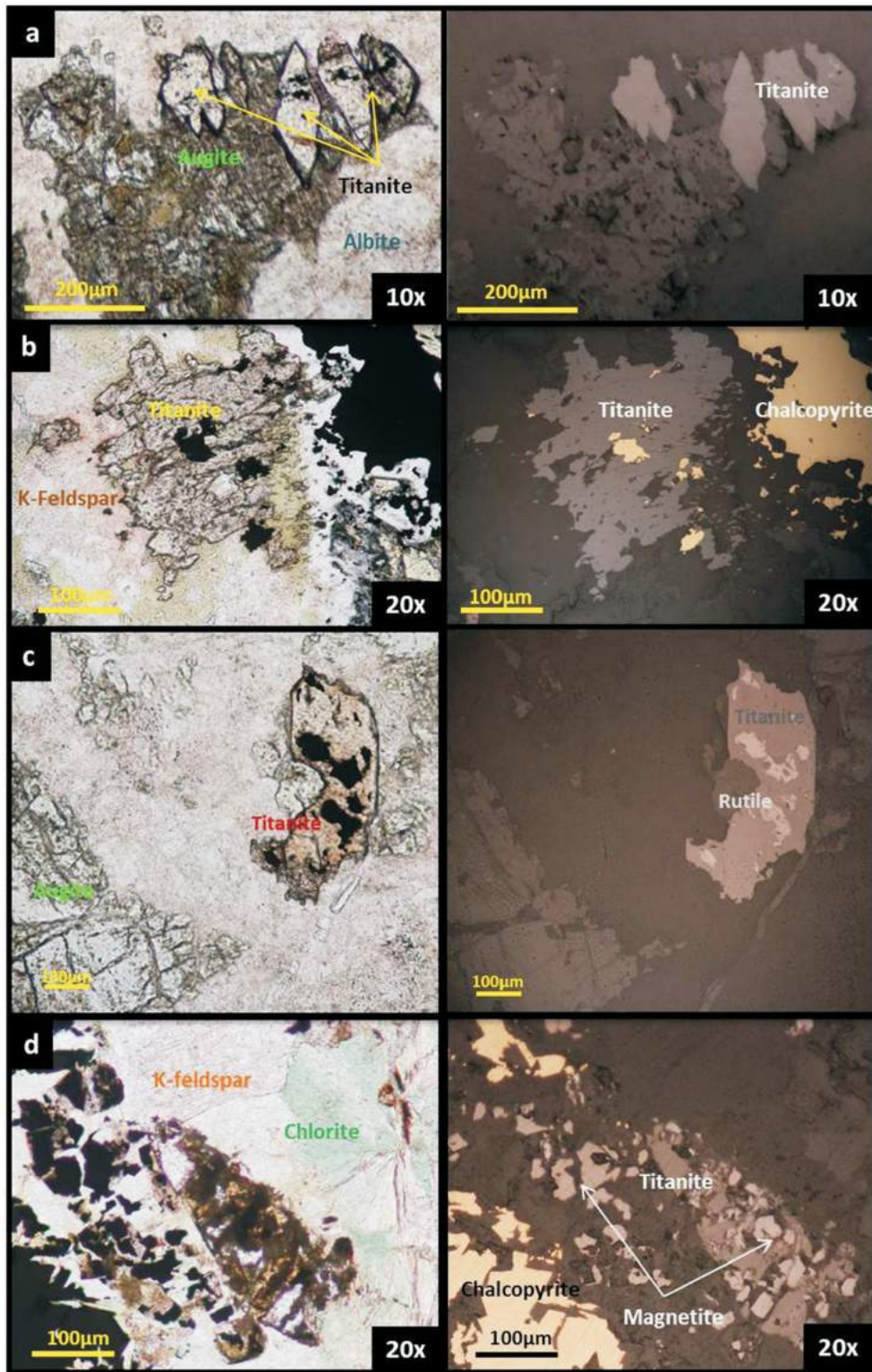


**Figure 3.** Photomicrographs of titanite taken using both transmitted light (left) and reflected light (right): **a)** titanite, rhombohedral habit, colourless to pale brown, 200 µm size grains in association with larger augite phenocryst in sodic alteration zone, Copper Mountain, sample from Pit 2 (CM12AB19\_181.5m); **b)** titanite, anhedral habit, colourless to pale brown, 100–200 µm size grains with chalcopyrite inclusion in K-feldspar alteration zone, Copper Mountain, sample from Pit 2 (CM12P221\_241m); **c)** titanite, subhedral to anhedral habit, pale brownish, 300 µm size grains with rutile exsolution texture in K-feldspar alteration, Copper Mountain, sample from Pit 2 (CM12P221\_144.5m); and **d)** titanite, subhedral habit, brownish, 100 µm size grains in association with small subhedral magnetite grains in propylitic alteration zone, Copper Mountain, sample from Virginia pit (CMT-1).

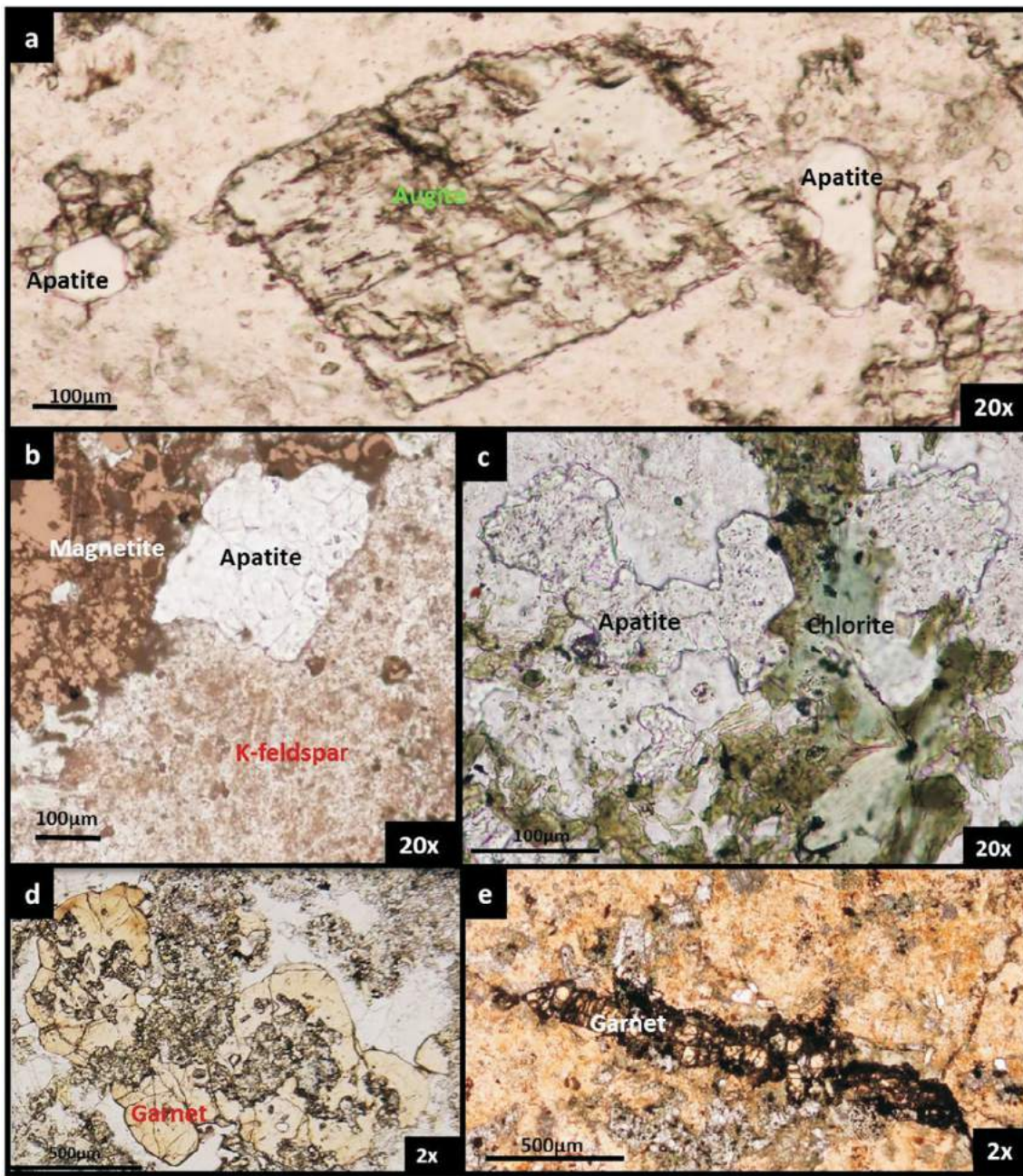


**Figure 4.** Photomicrographs of apatite and garnet, south-central British Columbia: **a)** apatite, colourless, uniform texture, euhedral prismatic habit, 100  $\mu\text{m}$  size crystals intergrown with large augite phenocrysts in sodic alteration zone, Copper Mountain, sample from Pit 2 (CMT-6); **b)** apatite, colourless, cloudy, highly porous texture, anhedral habit, 400  $\mu\text{m}$  size crystal adjacent to anhedral magnetite grains in K-feldspar alteration, Mount Polley, sample from Springer pit (Polley-1); **c)** apatite, colourless, cloudy, highly porous texture, subhedral habit, 200  $\mu\text{m}$  size crystals adjacent to chlorite after biotite phenocrysts in propylitic alteration, Mount Milligan, sample from 66 zone (07992\_81.5m); **d)** garnet, pale yellow, subhedral to anhedral habit, very coarse grain size (1500  $\mu\text{m}$ ), intergrown with epidote in garnet-epidote alteration zone, Mount Polley, sample from Springer pit (Polley-4); and **e)** garnet, pale yellow, very coarse grain size (1500  $\mu\text{m}$ ) within a vein in the garnet-epidote alteration zone, Mount Polley, sample from Whight pit (Polley-9).

TL, and its isotropic property under XPL, are diagnostic characteristics of garnet.

Apatite is ubiquitously distributed throughout all three studied deposits. Its common, very coarse (500–1000  $\mu\text{m}$ ), anhedral grains with a characteristically cloudy appearance

and highly porous texture, demonstrate magmatic origin that has been modified by hydrothermal alteration. Magmatic apatite is less common and occurs as small (100  $\mu\text{m}$ ) euhedral prismatic grains that occupy interstitial spaces of the silicate matrix, as well as spaces adjacent to mafic phenocrysts.

**Table 2.** Classification and characterization of porphyry indicator minerals (PIMs) within alkalic porphyry deposits, south-central British Columbia.

PIM	Origin	Physical properties			Common paragenesis		
		Shape	Colour in TL	Colour in RL		Texture	Size
Apatite	Magmatic	Euhedral prismatic	Colourless		Clean	<100 µm	Interstitial spaces, adjacent to mafic minerals
	Hydrothermal	Subhedral to anhedral, prismatic	Colourless		Cloudy, high porosity	>300 µm	Adjacent to mafic minerals, magnetite and sulphides
Garnet	Hydrothermal	Anhedral to vein shaped	Pale yellow		Cloudy; fractured	>1000 µm	Epidote-garnet assemblages
Magnetite	Magmatic	Euhedral cubic		Grey	Ilmenite lamellae ± titanomagnetite exsolution	100–300 µm	Adjacent to mafic minerals
	Altered	Subhedral cubic		Grey	Homogeneous ± ilmenite lamellae; rims of titanite/hematite	100–500 µm	Intergrain exchange with chalcopyrite ± pyrite
	Hydrothermal	Anhedral to vein shaped		Grey	Homogeneous	>300 µm	Intergrain exchange with chalcopyrite ± pyrite ± rutile
Titanite	Magmatic	Rhombohedral	Colourless to pale brown	Dark grey	Homogeneous	100–300 µm	Interstitial spaces, titanite-augite assemblage
	Hydrothermal	Rhombohedral to wedge shaped, anhedral with serrated edges	Pale brown to brown	Dark grey	Homogeneous to rutile exsolution	100–300 µm	Intergrain exchange with chalcopyrite

Abbreviations: RL, reflected light; TL, transmitted light

To summarize, hydrothermal magnetite and titanite phases interacting with chalcopyrite±bornite in potassic-altered rocks from all three deposits suggest an important link to Cu-Au mineralization. Further detailed characterization of hydrothermally formed magnetite and titanite is necessary to determine selected PIMs that can be effectively used as prospecting tools for alkalic Cu-Au porphyry deposits.

### Future Work

Further work will include a detailed classification and characterization of PIMs from mineral separates obtained from rock samples by electric pulse selective fragmentation (SELFRAG) method. A correlation between petrographic observations and mineral separates made from rock samples is required in order to confirm the PIMs physical parameters that help diagnose hydrothermal activity in alkalic porphyry systems. This will be followed by chemical characterization using a mineral liberation analyzer (MLA) and laser ablation–inductively coupled plasma–mass spectrometry (LA-ICP-MS). Finally, a detailed comparison between physical properties and chemical composition of selected mineral separates and till mineral separates will be explored to determine the feasibility of PIMs as a potential exploration tool for alkalic porphyry deposits in covered regions.

### Acknowledgments

The authors would like to thank Copper Mountain Mining Corporation, Imperial Metals Corporation and Thompson Creek Metals Company Inc. for allowing access and sampling at their Copper Mountain, Mount Polley and Mount Milligan deposits, respectively. Geoscience BC is thanked for its generous financial contribution in support of this project. Also thanked is M. Allan, Mineral Deposit Research Unit, for review and comments on this paper.

### References

Bailey, D.G. and Hodgson, C.J. (1979): Transported altered wallrock in laharic breccias at Cariboo-Bell Cu-Au porphyry deposit, British Columbia; *Economic Geology*, v. 74, p. 125–128.

BC Geological Survey (2013): MINFILE BC mineral deposits database; BC Ministry of Energy and Mines, BC Geological Survey, URL <<http://minfile.ca/>> [December 2013].

Bouzari, F., Hart, C.J.R., Barker, S. and Bissig, T. (2011): Porphyry indicator minerals (PIMs): a new exploration tool for concealed deposits in south-central British Columbia; *Geoscience BC Report 2011-17*, 31 p., URL <<http://www.geosciencebc.com/s/Report2011-17.asp>> [November 2013].

Celis, M.A., Hart, C.J.R., Bouzari, F., Bissig, T. and Ferbey, T. (2013): Porphyry indicator minerals (PIMs) from alkalic

porphyry copper-gold deposits in south-central British Columbia (NTS 092, 093); *in* *Geoscience BC Summary of Activities 2012*, Geoscience BC, Report 2013-1, p. 37–46.

Dasgupta S. and Supratim P. (2005): Origin of grandite garnet in calc-silicate granulites: mineral-fluid equilibria and petrogenetic grids; *Journal of Petrology* v. 46, no. 5, p. 1045–1076.

Fraser, T.M., Stanley, C.R., Nikic, Z.T., Pesalj, R. and Gorc, D. (1995): The Mount Polley copper-gold alkaline porphyry deposit, south-central British Columbia; *in* *Porphyry Deposits of the Northwestern Cordillera of North America*, T.G. Schroeter (ed.), Canadian Institute of Mining, Metallurgy and Petroleum, Special Volume 46, p. 609–622.

GeoBase® (2004): Canadian digital elevation data, edition 2; Canadian Council on Geomatics, URL <<http://www.geobase.ca/geobase/en/data/cded/description.html>> [December 2013].

Hodgson, C.J., Bailes, R.J. and Verzosa, R.S. (1976): Cariboo-Bell; *in* *Porphyry Deposits of the Canadian Cordillera*, A. Sutherland Brown (ed.), Canadian Institute of Mining and Metallurgy, Special Volume 15, p. 388–396.

Jago, C.J. and Tosdal, R.M. (2009): Distribution of alteration in an alkaline porphyry copper-gold deposit at Mount Milligan, central British Columbia (NTS 094N/01); *in* *Geoscience BC Summary of Activities 2008*, Geoscience BC, Report 2009-1, p. 33–48.

Journeay, J.M., Williams, S.P. and Wheeler, J.O. (2000): Tectonic assemblage map, Vancouver, British Columbia–U.S.A.; Geological Survey of Canada, Open File 2948a, scale 1:1 000 000, URL <<http://geogratias.gc.ca/?id=211051>> [December 2013].

Lindsley, D.H., ed. (1991): Oxide minerals: petrologic and magnetic significance; *Mineralogical Society of America, Reviews in Mineralogy Series*, v. 25, 509 p.

Sketchley, D.A., Rebagliati, C.M. and DeLong, C. (1995): Geology, alteration and zoning patterns of the Mt. Milligan copper-gold deposits; *in* *Porphyry Deposits of the Northwestern Cordillera of North America*, T.G. Schroeter (ed.), Canadian Institute of Mining and Metallurgy and Petroleum, Special Volume 46, p. 650–665.

Stanley, C.R., Holbek, P.M., Huyck, H.L.O., Lang, J.R., Preto, V.A.G., Blower, S.J. and Bottaro, J.C. (1995): Geology of the Copper Mountain alkaline Cu-Au porphyry deposit, Princeton, British Columbia; *in* *Porphyry Deposits of the Northwestern Cordillera of North America*, T.G. Schroeter (ed.), Canadian Institute of Mining and Metallurgy and Petroleum, Special Volume 46, p. 552–562.

Tosdal, R.M., Jackson, M., Pass, H.E., Rees, C., Simpson, K.A., Cooke, D.R., Chamberlain, C.M. and Ferreira, L. (2008): Hydrothermal breccia in the Mount Polley alkalic porphyry copper-gold deposit, British Columbia; *in* *Geoscience BC Summary of Activities 2007*, Geoscience BC, Report 2008-1, p. 105–114.

Xirouchakis, D. and Lindsley, D.H. (1998): Equilibria among titanite, hedenbergite, fayalite, quartz, ilmenite, and magnetite: experiments and internally consistent thermodynamic data for titanite; *American Mineralogist*, v. 83, p. 712–725.

# Relationships Between Calcalkalic and Alkalic Mineralization Styles at the Copper-Molybdenum Southeast Zone and Copper-Gold Deerhorn Porphyry Deposits, Woodjam Property, Central British Columbia (NTS 093A)

I. del Real, Mineral Deposit Research Unit, University of British Columbia, Vancouver, BC, [idelreal@eos.ubc.ca](mailto:idelreal@eos.ubc.ca)

C.J.R. Hart, Mineral Deposit Research Unit, University of British Columbia, Vancouver, BC

F. Bouzari, Mineral Deposit Research Unit, University of British Columbia, Vancouver, BC

J.L. Blackwell, Gold Fields Canada Exploration, Vancouver, BC

A. Rainbow, Gold Fields Canada Exploration, Vancouver, BC

R. Sherlock, Gold Fields Canada Exploration, Vancouver, BC

---

del Real, I., Hart, C.J.R., Bouzari, F., Blackwell, J.L., Rainbow, A. and Sherlock, R. (2014): Relationships between calcalkalic and alkalic mineralization styles at the copper-molybdenum Southeast Zone and copper-gold Deerhorn porphyry deposit, Woodjam property, central British Columbia; *in* Geoscience BC Summary of Activities 2013, Geoscience BC, Report 2014-1, p. 63–82.

## Introduction

Porphyry deposits of Late Triassic to Middle Jurassic age (216 to 183 Ma) occur in the Quesnel and Stikine terranes in British Columbia (McMillan et al., 1995). They are subdivided into calcalkalic and alkalic types on the basis of their hostrock chemistry and styles of alteration and mineralization (Lang et al., 1995; McMillan et al., 1995). Alkalic porphyry deposits such as Mount Milligan, Mount Polley and Lorraine, and calcalkalic porphyry deposits such as Brenda, Highland Valley and Gibraltar, among others, are examples of these two classes. These porphyry deposits commonly occur as clusters of several porphyry centres. The metal ratios, alteration assemblages and hostrock intrusive textures of each porphyry deposit can vary within each cluster (e.g., Casselman et al., 1995; Fraser et al., 1995). Such differences are commonly attributed to emplacement at different crustal depths of the now spatially related porphyry stocks (e.g., Panteleyev et al., 1996; Chamberlain et al., 2007). Recently, porphyry clusters such as Red Chris (Norris, 2011) and Woodjam (Figure 1) displaying both alkalic and calcalkalic features have been recognized. However, the genetic and spatial links between the various deposits in each camp, especially with contrasting assemblages (i.e., calcalkalic and alkalic) are not well understood.

The Woodjam property hosts several discrete porphyry deposits, including the Megabuck (Cu-Au), Deerhorn (Cu-Au), Takom (Cu-Au), Southeast Zone (Cu-Mo) and Three Firs (Cu-Au; Figure 2). These deposits display various

styles and assemblages of alteration and mineralization. Whereas the Southeast Zone Cu-Mo deposit is hosted in quartz monzonite intrusive units and displays alteration and mineralization comparable to calcalkalic porphyry deposits, the nearby Deerhorn Cu-Au deposit is associated with narrow (<100 m) monzonite intrusive bodies and hosts mineralization similar to alkalic porphyry deposits. These differences have resulted in the separation of the Southeast Zone (SEZ) from the Megabuck and Deerhorn deposits as a different mineralization event (Logan et al., 2011). However, similar ages of the host intrusive rocks ( $197.48 \pm 0.44$  Ma for SEZ and  $196.35 \pm 0.19$  Ma for Deerhorn; Rainbow et al., 2013) and characteristics of alteration and mineralization suggest that deposits within the Woodjam property may be genetically related.

Recent exploration at the Deerhorn Cu-Au deposit has shown two contrasting alteration assemblages of K-feldspar+magnetite, typical of alkalic systems, and illite ( $\pm$ tourmaline) and Mo mineralization typical of calcalkalic systems. The SEZ, located less than 4 km from the Deerhorn deposit, displays some features not typical of calcalkalic deposits, such as infrequent quartz veining. These observations suggest that temporal and paragenetic relationships between the two deposits may exist, thus providing a unique opportunity to study the relationship between alkalic and calcalkalic deposits in BC.

Thus, a research project was jointly initiated in 2012 by the Mineral Deposit Research Unit at the University of British Columbia, Gold Fields Canada Exploration and Geoscience BC. The focus of this project is to increase the understanding of the paragenesis and alteration of the variable calcalkalic and alkalic deposits and the magmatic evolution in the Woodjam property. Results of this investigation will have important implications for the understanding of the

---

**Keywords:** *alkalic porphyry, calcalkalic porphyry, Woodjam property*

*This publication is also available, free of charge, as colour digital files in Adobe Acrobat® PDF format from the Geoscience BC website: <http://www.geosciencebc.com/s/DataReleases.asp>.*

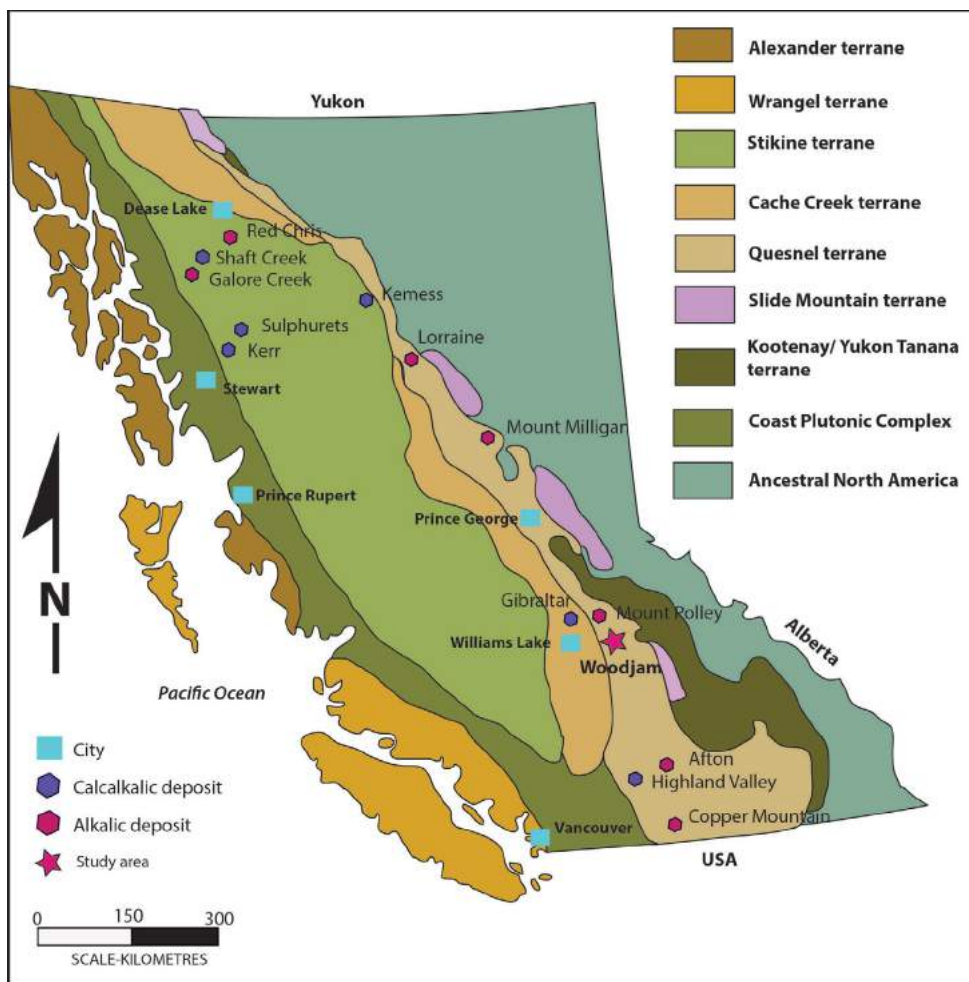


**Figure 1.** Major tectonic terranes and associated Mesozoic porphyry deposits of the Canadian Cordillera in British Columbia (from McMillan et al., 1995).

formation of porphyry clusters and the exploration of new targets in known mineralized districts in BC and similar regions worldwide.

Fieldwork focused on the SEZ and Deerhorn deposits and was carried out in summer 2012 and June 2013. A total of seven drillholes for the SEZ and ten for the Deerhorn deposit were graphically relogged (Figures 2, 3) and sampled. Hostrock texture, alteration assemblages and intensity, vein types and crosscutting relationships, sulphide ratios and shortwave infrared spectroscopy (SWIR) sampling were recorded and form the basis for ongoing detailed petrographic and chemical analyses. Paragenesis and alteration relationships were previously discussed on the basis of 2012 field observations (del Real et al., 2013). In this paper, results of the 2013 fieldwork, detailed geology and alteration cross-sections, petrography of the hostrocks and alteration assemblages, SWIR analysis and preliminary geochemical analyses are presented.

The Woodjam property is located in the Cariboo Mining Division, central British Columbia, approximately 50 km east-northeast of Williams Lake (Figure 1). The property is owned by Gold Fields Horsefly Exploration (51%) and Consolidated Woodjam Copper Corporation (49%). The Southeast Zone is the only deposit with a public pit-constrained resource estimated to be 146.5 Mt at 0.33% Cu (Sherlock et al., 2012).

### Tectonic Setting

Much of BC comprises tectonic blocks that were accreted onto the western margin of ancient North America during the Mesozoic. Three of these accreted terranes, the Quesnel, Stikine and Cache Creek terranes, form most of the Intermontane Belt that occupies much of central BC (Figure 1; Monger and Price, 2002). The Stikine and Quesnel volcanic arc terranes have similar compositions and stratigraphy, and are interpreted to have originally been part of the same arc that was folded oroclinally, enclosing the Cache Creek terrane (Mihalynuk et al., 1994). Within the Quesnel

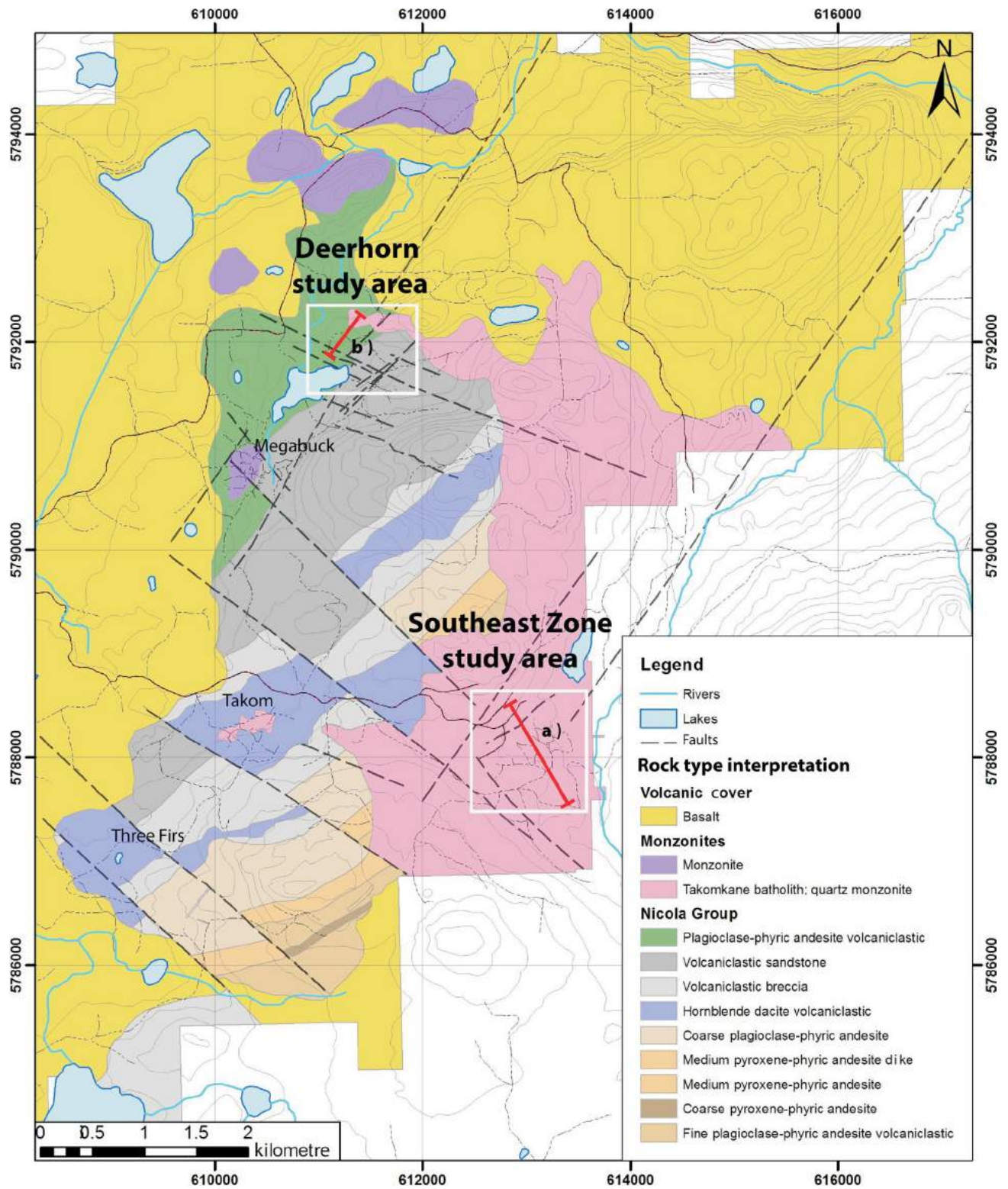


**Figure 2.** Geology of the Woodjam property. Cross-section lines of drillholes relogged in this study are shown (red line) for the **a)** Southeast Zone and **b)** Deerhorn deposits (from Gold Fields Canada Exploration, pers. comm., 2012).

and Stikine terranes, the emplacement of pre- to synaccretion of both alkalic and calcalkalic Cu±Mo±Au deposits, occurred between 216 and 187 Ma (McMillan et al., 1995). The Woodjam porphyry cluster is hosted in the Late Triassic to Early Jurassic arc in the central portion of the Quesnel terrane.

## Regional Geology

The Quesnel terrane consists of upper Paleozoic and lower Mesozoic volcanic, sedimentary and plutonic rocks. The Paleozoic components are unconformably overlain by the Late Triassic and Early Jurassic island arc volcanic and sed-

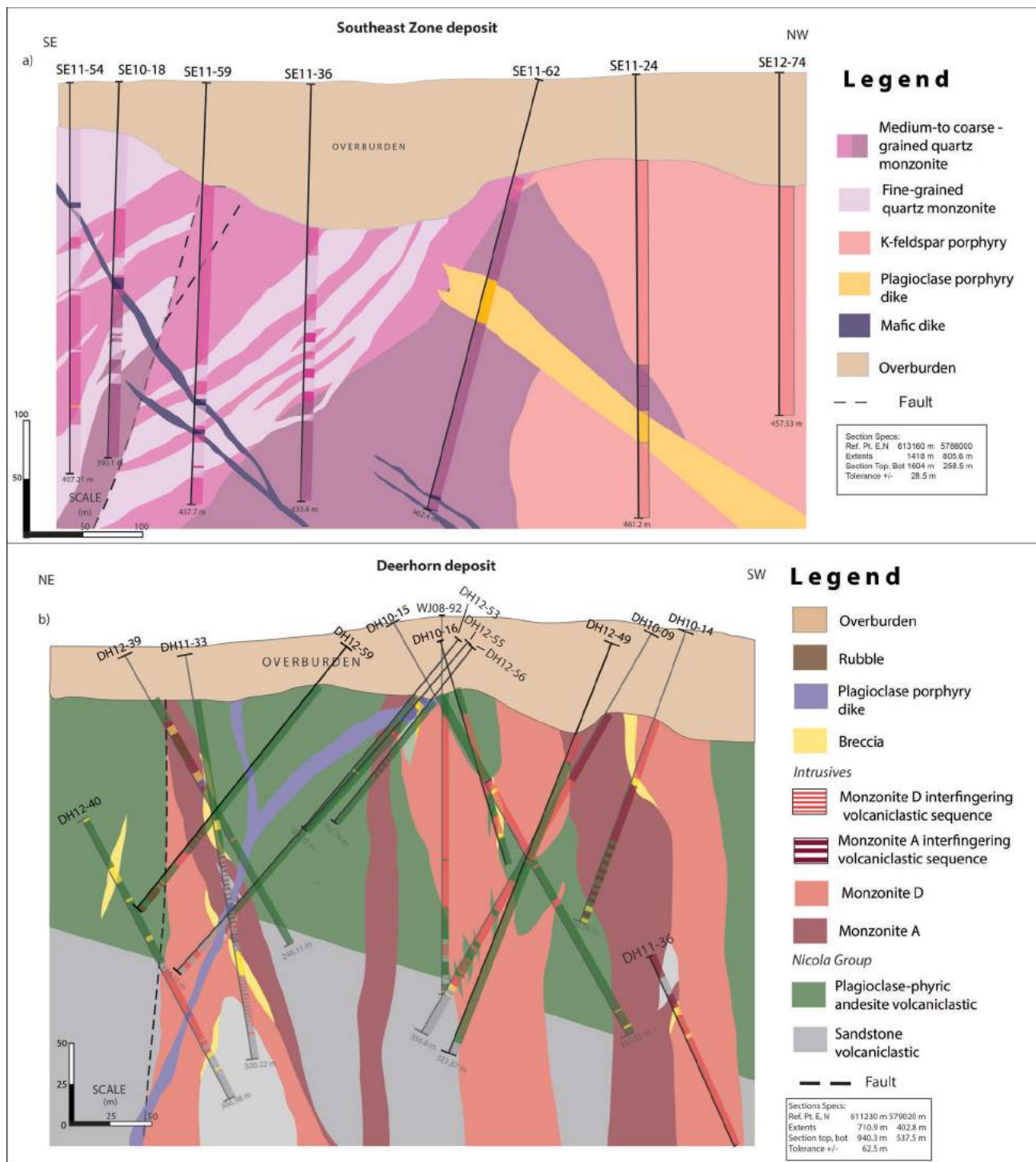


**Figure 3. a)** Southeast cross-section along the line 613160E, 5788000N, NAD 83, UTM Zone 10 (28.5 m thickness) across the Southeast Zone deposit; **b)** northeast cross-section along the line 611230E, 5792020N, NAD 83, UTM Zone 10 (62.5 m thickness) across the Deerhorn deposit.

imentary strata of the Nicola Group and its northern continuation, the Takla Group (McMillan, 1995). The Nicola Group is composed of submarine basaltic to andesitic augite±plagioclase-phyric lava and volcanoclastic and sedimentary units (Mortimer, 1987; Schiarizza et al., 2009; Vaca, 2012). This sequence extends throughout south-central BC.

These rocks were intruded by the Takomkane batholith, a largely calcalkalic intrusion of monzodiorite to granitoid, and locally quartz diorite, composition with a surface expression of approximately 40 by 50 km. The Woodjam Creek unit of the Takomkane batholith occurs on the Woodjam property and is composed of granodiorite, monzogranite and quartz monzonite (Schiarizza et al., 2009). The Nicola and Takomkane units are overlain by the Early Miocene to Early Pleistocene basalt of Chilcotin Group.

## Geology of the Woodjam Property

The Woodjam property is hosted by a succession of Triassic–Jurassic Nicola volcanic and volcano-sedimentary rocks that are intruded by several Jurassic monzonite to syenite stocks. The Takomkane batholith occurs in the eastern and southern parts of the property (Figure 2) and mainly consists of light-grey to pinkish to white hornblende-biotite granodiorite, monzogranite, quartz monzonite and quartz monzodiorite (Schiarizza et al., 2009). Nicola Group rock units comprise a sequence of plagioclase±pyroxene-phyric andesitic rocks, monomictic and polymictic volcanic breccias, and volcanic mudstones and sandstones, all of which dip moderately to the northwest (Rainbow et al., 2013).

Locally, extensive olivine-phyric basalt flows of the Chilcotin Group are characterized by dark grey, aphanitic and vesicular basalt (Schiarizza et al., 2009). These flows range in thickness from less than 20 m to more than 100 m and overlie the Nicola stratigraphy.

Several zones of porphyry-type mineralization occur within and around porphyry stocks that intruded the strata of the Nicola Group. The SEZ deposit is hosted entirely in quartz monzonites of the Takomkane batholith, whereas the Deerhorn deposit is hosted by multiple monzonite intrusions and volcanic rocks of the Nicola Group (Rainbow et al., 2013; Sherlock et al., 2012).

## Hostrock Geology

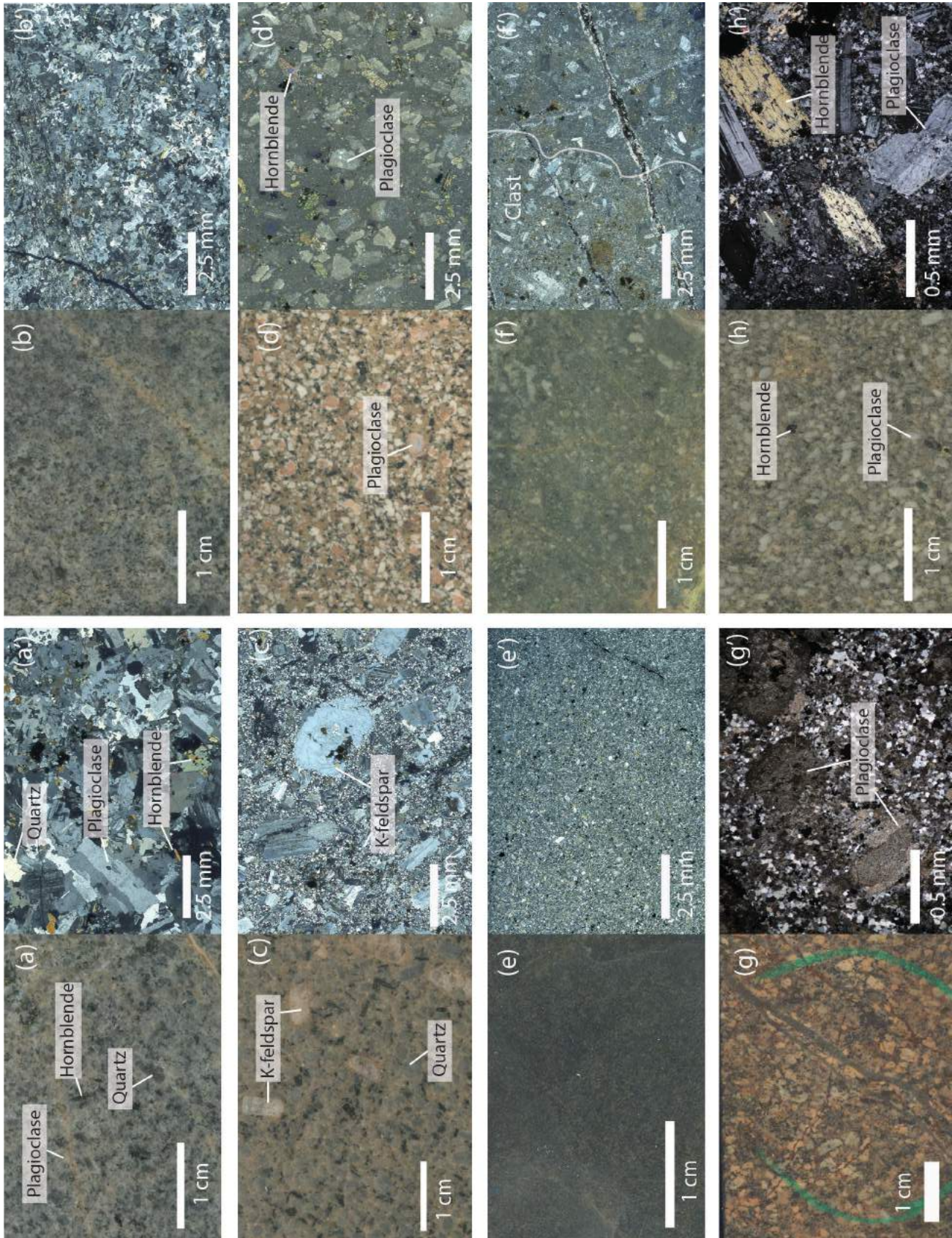
### Southeast Zone Deposit

The Southeast Zone deposit is hosted by a series of texturally variable quartz monzonite intrusive units that strike ~220° and dip ~65–80° to the northwest (Rainbow, 2010). The quartz monzonites are divided texturally into fine-, medium- and coarse-grained units (Figures 3a, 4a, b; Rainbow, 2010). There is no textural or mineralogical difference be-

tween the coarse- and the medium-grained quartz monzonite, only the grain size varies. Fine-grained quartz monzonite cuts both medium- and coarse-grained intrusive rocks. Small aplite dikes cut all quartz monzonite units and the K-feldspar porphyry unit with sharp contacts. All quartz monzonite units are largely equigranular, white-grey to pink and comprise interlocking crystals of plagioclase (~40%), potassium feldspar (~15%) and quartz (~20%; Figure 4a, b). Mafic minerals are typically hornblende (~5%) and less abundant fine-grained biotite (~2%). Quartz monzonites are intruded by K-feldspar porphyry (FP) bodies characterized by a phaneritic medium- to coarse-grained groundmass, and large euhedral and elongated K-feldspar phenocrysts (~15%) that occur sporadically throughout the unit (Figure 4c). The FP forms a wide (>250 m), dike-like intrusion that strikes northeast (Rainbow, 2010; Sherlock et al., 2012). It cuts the quartz monzonite and has a chilled margin. All quartz monzonites were emplaced pre- to synmineralization and are affected by intense alteration, whereas the FP was probably emplaced during final stages of hydrothermal activity and is therefore typically weakly altered. All these units were intruded by postmineralization plagioclase porphyry dikes and late mafic dikes (Figures 3a, 4d; Rainbow, 2010; Sherlock et al., 2012).

### Deerhorn Deposit

The Deerhorn deposit is hosted in both the volcano-sedimentary rocks of the Nicola Group and the monzonitic rocks that intrude the Nicola strata (Figure 3b; Scott, 2012; Rainbow et al., 2013). The host Nicola Group stratigraphy consists of laminated to thickly-bedded volcanoclastic sandstone (Figure 4e), overlain by a plagioclase-hornblende-phyric andesite that alternates between breccia and volcanic facies (Figures 3b, 4f; Rainbow et al., 2013). These units dip ~25° to the north in the deposit area and were intruded by at least two monzonite bodies. Monzonite A occurs as pencil-shaped intrusive bodies with irregular margins that intrude the volcano-sedimentary rocks of the Nicola Group (Figure 3b; Rainbow et al., 2013). Intense alteration obliterated much of the primary texture of monzonite A but remnants of plagioclase and biotite phenocrysts, altered to illite and chlorite, respectively, are locally recognizable (Figure 4g). Monzonite D is characterized by plagioclase (~35%), hornblende (~5%) and biotite (~5%) phenocrysts (Figure 4h) and occurs as dikes with sharp contacts that crosscut monzonite A and Nicola Group stratigraphy (Scott, 2012; Rainbow et al., 2013). The highest Cu and Au values occur in monzonite A and in the surrounding volcanic sandstone, where grades are locally ≤1.5 g/t Au and <0.75% Cu (Blackwell et al., 2012). Mineralization in monzonite D is mainly pyrite and subordinate chalcopyrite with Cu grades between 0.1 and 0.3% (Blackwell et al., 2012). Postmineralization mafic and andesitic dikes crosscut all the Deerhorn hostrocks and phases of mineralization (Rainbow et al., 2013).



## Alteration

Hydrothermal alteration in both the Deerhorn and SEZ deposits affected all hostrocks except for postmineralization mafic and andesitic dikes. Several alteration assemblages are recognized in each deposit (Figures 5, 6, 7, 8). Short-wave infrared (SWIR) spectroscopy was used at both the SEZ and Deerhorn deposits to better characterize clay and white mica minerals and their distribution.

### Southeast Zone

Potassium feldspar-biotite-magnetite is the earliest alteration assemblage in the SEZ deposit and typically occurs as pervasive alteration of K-feldspar replacing feldspar phenocrysts and biotite with magnetite replacing mafic minerals (Figures 5a, 6a, b). Potassium feldspar-biotite-magnetite alteration is very intense (i.e., nearly all original minerals and texture are destroyed) in the centre of the deposit, where secondary K-feldspar can make up to ~25% of the rock volume, biotite ~8% and magnetite ~7%. Weaker alteration at the margin of the deposit consists of secondary biotite (1%) and K-feldspar (5%), and magnetite is largely absent. Albite-(epidote) alteration is recognized at the northern extent of the deposit, where it is juxtaposed against K-feldspar-biotite-magnetite alteration by a large northeast-striking normal fault (Figures 3a, 8a). Albite alteration has a distinct bleached appearance and locally obliterates original rock textures (Figure 5b). In the deepest segment of the marginal area of the deposit, where albite alteration diminishes (~350 m depth), the K-feldspar-biotite-magnetite alteration assemblage appears and becomes more intense with depth, accompanied by higher grades of mineralization. The albite alteration is interpreted as having formed at the margin of the system, locally overprinting the K-feldspar-biotite-magnetite alteration. The albite alteration also occurs at the margin of the Takomkane batholith, near the contact with the Nicola Group strata (Figure 2). Both K-feldspar-biotite-magnetite and albite-(epidote) alterations are overprinted by epidote-chlorite-pyrite, illite and hematite alteration assemblages (Figure 5c).

Chlorite alteration appears throughout the SEZ, replacing secondary biotite and primary hornblende. Chlorite-epidote-pyrite veins are denser at the margins of the deposit. Epidote replaces plagioclase and occurs with hematite haloes at the margins of the deposit.

Illite occurs as three visually and paragenetically distinct types: dark green illite that replaces K-feldspar phenocrysts (Figure 5a); white illite that replaces plagioclase and commonly occurs with smectite; and apple-green illite (Figure 5c) that overprints albite and K-feldspar alterations, and occurs as flooding in the groundmass or as replacement of plagioclase. The white illite occurs mainly in fracture zones, together with hematite, and its distribution appears to be structurally controlled. Together with fracture-controlled white illite, hematite flooding largely occurs at shallow levels within the deposit (Figure 8a) as haloes to the epidote replacing plagioclase in the FP and as a pervasive alteration replacing secondary K-feldspar. Hematite overprints most of the previous alterations described above and also overprints(?) the plagioclase porphyry dike.

### Deerhorn

Alteration assemblages at the Deerhorn deposit are strongly controlled by the distribution of the monzonites (Scott, 2012). Potassium feldspar-biotite-magnetite alteration (i.e., K-silicate) is very intense in monzonite A and in the volcanic rocks immediately surrounding these intrusions (Figures 5d, 8b). The intensity of the K-silicate alteration becomes progressively weaker in the surrounding volcanic rocks the farther it is from monzonite A. Monzonite D is only moderately affected by K-feldspar-biotite-magnetite alteration (Figure 6c, d), indicating that it postdated much of the main-stage alteration. The K-feldspar-biotite-magnetite alteration is overprinted by epidote-chlorite-pyrite, ankerite, calcite, illite and clay alteration assemblages. The epidote-chlorite-pyrite alteration occurs mainly in the surrounding volcanic rocks (Figures 5e, 6e, f, 8b) and, with less intensity, in monzonite D and in the plagioclase por-

**Figure 4.** Examples of hand samples, with corresponding thin-section photomicrographs (sample numbers represent drillhole numbers followed by depth) of hostrocks of the Southeast Zone (a, a', b, b', c, c', d, d') and Deerhorn (e, e', f, f', g, g', h, h') deposits showing: **a)** and **a')** medium-grained quartz monzonite with porphyritic texture; plagioclase phenocrysts are subhedral and up to 5 mm long; hornblende is subhedral and up to 1 mm long; quartz is anhedral and up to 3 mm long; and K-feldspar is anhedral and up to 3 mm in length or diameter (SE11-36; 285.55 m); **b)** and **b')** fine-grained quartz monzonite showing equigranular texture with subhedral plagioclase and hornblende phenocrysts, and anhedral K-feldspar and quartz, with grain size between 0.5 and 1 mm (SE11-36; 276.59 m); **c)** and **c')** K-feldspar porphyry, displaying porphyritic texture and characterized by abundant, large (up to 1 cm) K-feldspar, plagioclase (up to 0.7 cm) and quartz (up to 0.7 cm) phenocrysts; K-feldspar and plagioclase phenocrysts are subhedral, whereas quartz is anhedral (SE11-24; 260.2 m); **d)** and **d')** plagioclase porphyry dike, with plagioclase (up to 4 mm) and rare hornblende (up to 3 mm) phenocrysts in a very fine-grained groundmass (SE11-24; 285.55 m); **e)** and **e')** volcanoclastic sandstone with very fine-grained texture and reworked subhedral plagioclase crystals (DH12-40; 347.5 m); **f)** and **f')** plagioclase-hornblende-phyric andesite with local clast-breccia facies showing porphyritic texture with plagioclase phenocrysts (subhedral and up to 3 mm long); clast boundaries in the breccia facies are difficult to recognize (DH10-14; 105.7 m); **g)** and **g')** monzonite A with very strong alteration making it difficult to recognize the texture and the original mineralogy of the rock, and showing porphyritic texture with plagioclase phenocrysts up to 5 mm long mostly altered to illite; groundmass is altered to secondary K-feldspar (DH10-09; 79.5 m); **h)** and **h')** monzonite D showing porphyritic texture with plagioclase (subhedral and up to 5 mm long), hornblende (subhedral and up to 2 mm long) and biotite (subhedral and up to 2 mm long) phenocrysts; the groundmass is fine-grained plagioclase (DH12-39; 178.9 m).

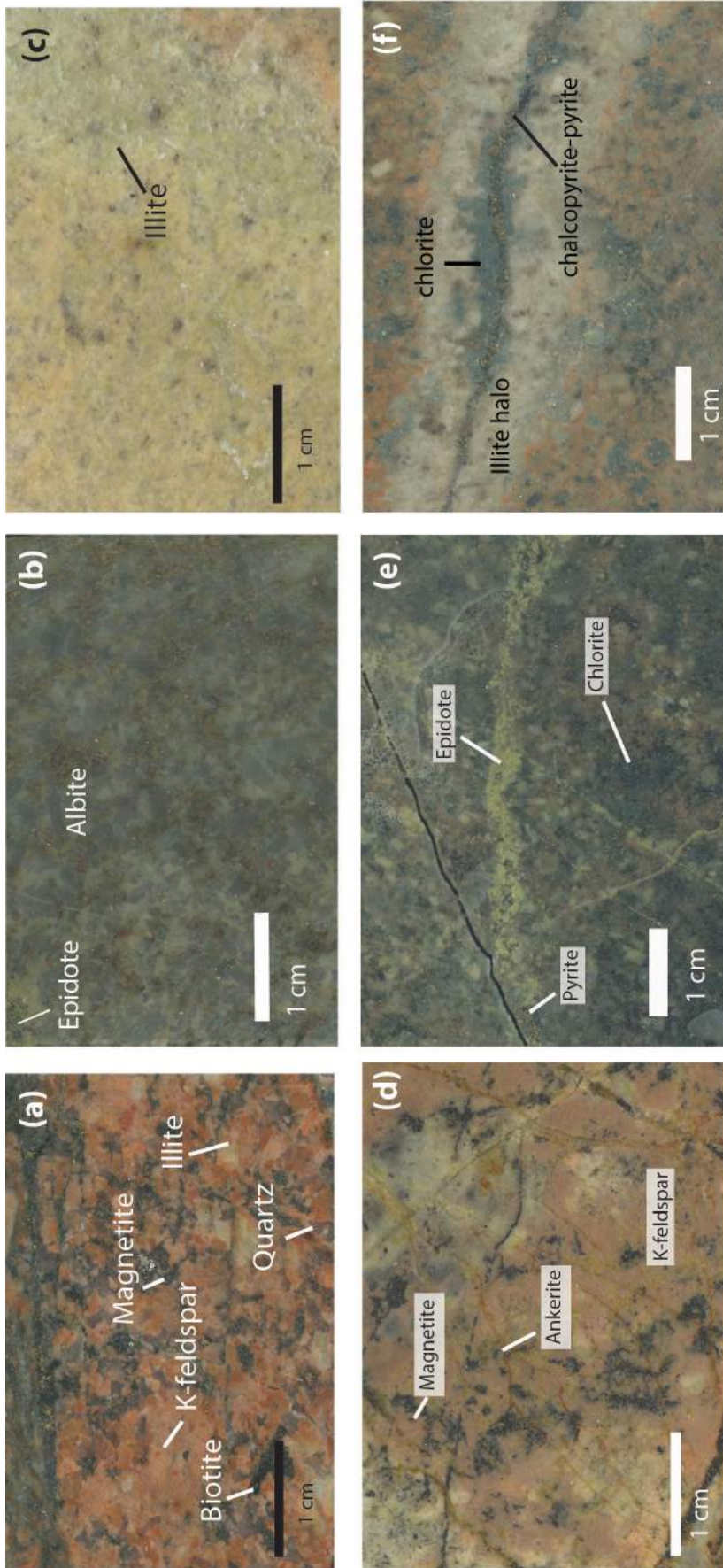


**Figure 5.** Selected drillcore samples showing alteration assemblages at the Southeast Zone (a, b, c) and Deerhorn (d, e, f) deposits: **a)** intense K-feldspar–biotite–magnetite alteration in coarse-grained monzonite locally overprinted by illite; **b)** very intense pervasive albite–(epidote) alteration texture, destructive in medium-grained monzonite; **c)** apple-green pervasive illite alteration overprinting albite and K-feldspar–biotite–magnetite alterations in fine-grained quartz monzonite; **d)** intense K-feldspar–biotite–magnetite alteration in the volcanic hostrock near the contact with monzonite A overprinted by illite and cut by late ankerite veins; **e)** epidote and quartz-pyrite veins in the volcanoclastic andesite hostrock; **f)** illite-vein envelope of chalcopyrite stringer in monzonite D cutting K-silicate alteration.

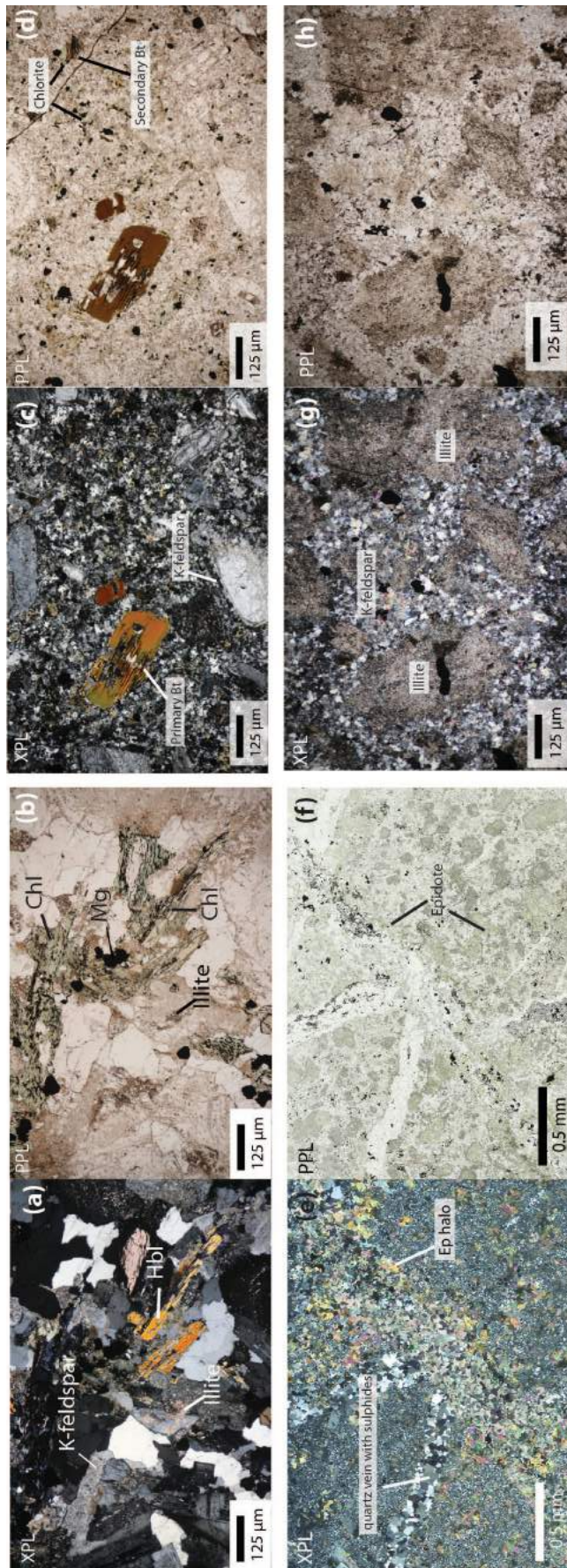


**Figure 6.** Photomicrographs showing alteration assemblages at the Southeast Zone (a, b) and Deerhorn (c, d, e, f, g, h) deposits: **a)** intense K-feldspar–biotite–magnetite alteration in coarse-grained monzonite; illite has partially replaced K-feldspar (XPL); **b)** intense K-feldspar–biotite–magnetite alteration in coarse-grained monzonite; biotite has replaced hornblende and, in turn, has been replaced by chlorite (PPL); **c)** and **d)** monzonite D moderately altered by K-feldspar–biotite–magnetite alteration, showing chlorite alteration replacing secondary biotite; **e)** and **f)** epidote-vein envelope of a late quartz vein that is cutting an early quartz vein with sulphides in the volcanic hostrock; **g)** and **h)** illite selectively replacing plagioclase and overprinting K-feldspar alteration in monzonite A. Abbreviations: bt, biotite; chl, chlorite; ep, epidote; hbl, hornblende; mg, magnetite; PPL, plain polarized light; XPL, crossed polarized light.

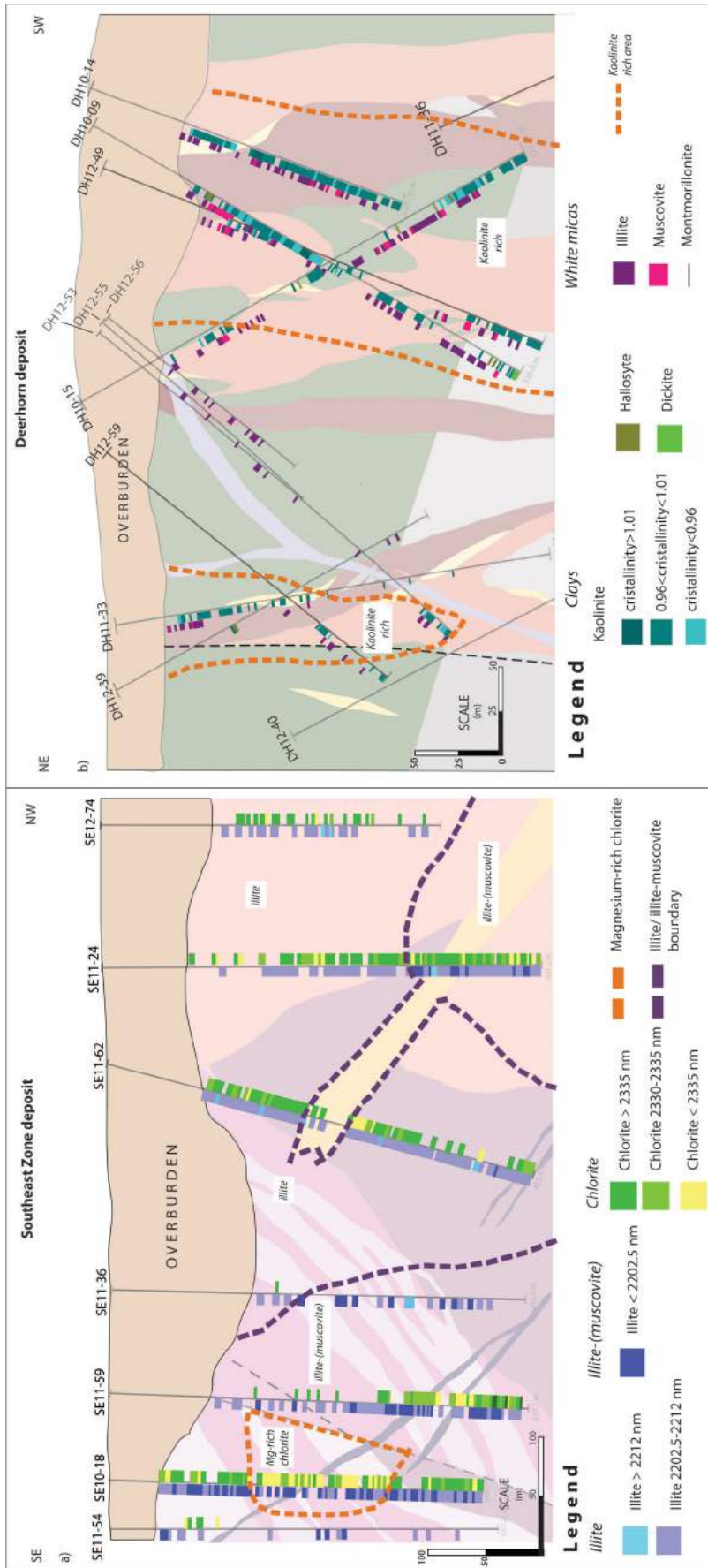


Figure 7. Results of the shortwave infrared spectroscopy (SWIR) analysis of drillhole samples from: a) the Southeast Zone deposit, showing illite and chlorite; b) the Deerhorn deposit, showing various domains of clay and white mica alteration.

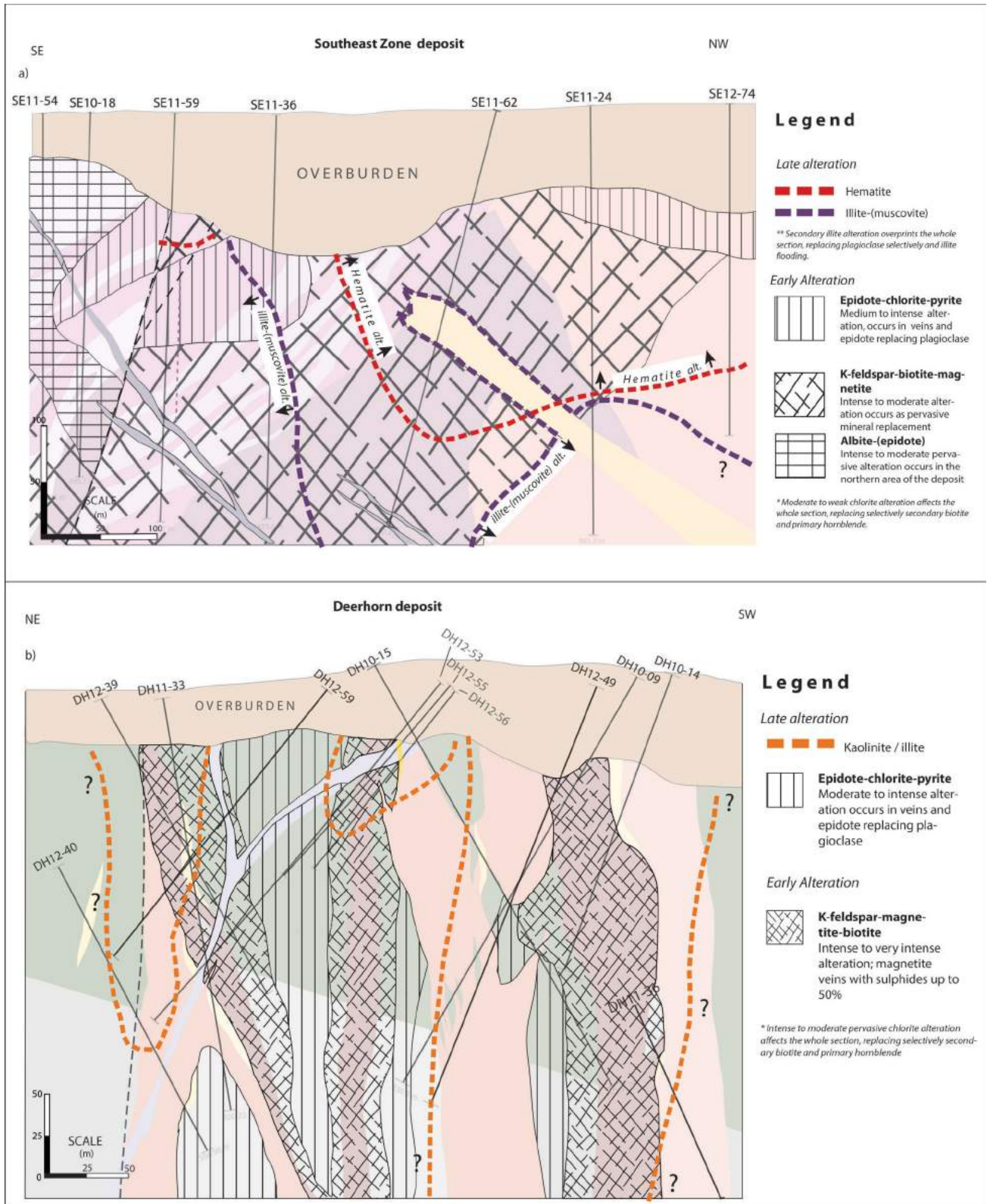


Figure 8. Cross-section of the a) Southeast Zone and b) Deerhorn deposits showing main alteration assemblages.

phyry dike. The alteration assemblage occurs as veins and disseminations (Figure 8b). Chlorite alteration occurs everywhere in the deposit, replacing secondary and primary biotite and primary hornblende.

Light green to white illite occurs as a replacement of plagioclase (Figure 6g, h) and as vein envelopes overprinting K-feldspar haloes (Figure 5f).

Ankerite and calcite veinlets occur throughout all rock types but commonly not together or in the same vein paragenesis. Ankerite occurs in the northeastern part of the area represented by the cross-section, whereas calcite occurs in the centre and southwestern parts. The observed spatial separation between the ankerite and calcite veinlets could be related to the different hostrocks. Ankerite appears related to the northeastern intrusion body of monzonite A, whereas calcite appears to be related to the other intrusive bodies of monzonite A.

## Methods

Shortwave infrared (SWIR) spectroscopy is based upon reflectance and absorption patterns as light with wavelengths between 1300 and 2500 nm interacts with molecular bonds matching the specific wavelengths for molecules, such as OH, H<sub>2</sub>O, AlOH, MgOH and FeOH (Thompson et al., 1999). Two instruments were used in this study: the TerraSpec<sup>®</sup> high-resolution spectrometer made by Analytical Spectral Devices Inc., which uses a 6 nm resolution and enhanced performance in SWIR 1 and 2 regions to characterize alteration assemblages, and the TerraSpec unit from the University of British Columbia (UBC), which is also used for characterizing alterations assemblages, but which is less portable.

### Southeast Zone Deposit

Shortwave infrared spectra of the SEZ deposit were collected in the field using the portable TerraSpec instrument. Measurements were taken every 2 m along the drillcore, except for hole SE11-36 and the first half of holes SE11-59 and SE11-54, where measurements were collected every 7 m, mainly because samples had to be carried to Vancouver for analysis. Samples were measured at UBC also using a TerraSpec instrument. Results were interpreted using spectral features of the minerals, such as wavelength and depth. These analyses show illite and chlorite as the most common alteration(?) phases.

Chlorite spectra at the deposit margin registered a relatively higher 2250 nm absorption feature (corresponding to the FeOH feature) and is therefore more Mg-rich here (Figure 7a). Illite can be divided into two major groups on the basis of the AlOH absorption feature: the first group with a signature of <2201 nm and the second, with a signature of >2201 nm (Figure 7a). The first group corresponds to an

illite-(muscovite) assemblage with a K-rich affinity and occurs at the margins of the deposit surrounding the more intense K-feldspar–biotite–magnetite alteration. The second group corresponds to illite with a slightly phengitic affinity that overprints the entire deposit, but is more widespread in the central parts. These results correlate with petrographic observations: SWIR data suggest that illite with a phengitic affinity corresponds to the dark green illite that replaces plagioclase (Figure 5a) and the apple-green illite (Figure 5c) corresponds to the illite-(muscovite).

### Deerhorn Deposit

At the Deerhorn deposit, SWIR data were collected in the field from cores samples measured in drillholes at 2 m intervals with the portable TerraSpec instrument. Analysis of this data identified chlorite, illite, montmorillonite and kaolinite. The SWIR technique was especially useful for identifying montmorillonite and kaolinite, which were difficult to visually identify during core logging. SWIR results for illite, based on the shifts of the AlOH absorption feature located at about 2200 nm, show the presence of K-rich affinity illite at the Deerhorn deposit, versus the illite at the SEZ. The SWIR analysis results also show a higher presence of muscovite in the Deerhorn deposit relative to that in the SEZ (Figure 7b). Core samples in the Deerhorn deposit are dominated by the presence of montmorillonite and kaolinite. Montmorillonite occurs in all the samples and kaolinite is more common in the northeastern part of the deposit (Figure 7b) along a major structure (Blackwell et al., 2012). Therefore, distribution of the kaolinite appears to be structurally controlled, overprinting illite and muscovite. This alteration seems to be part of a secondary alteration process involving meteoric fluids that used the structures as conduits. This observation stems mainly from the fact that the presence of kaolinite alteration was noted, along with dusty hematite replacing magnetite and secondary chalcocite replacing chalcopyrite that likely formed during supergene alteration.

## Vein Types and Paragenesis

### Southeast Zone Deposit

The earliest veins in the SEZ deposit are rare magnetite stringers and quartz-chalcopyrite-magnetite veins. These veins occur locally in the core of the porphyry (Figure 5a; Figure 9a). In the deep central and marginal areas of the SEZ, fewer (two to eight veins per metre) quartz-chalcopyrite-pyrite±molybdenite±anhydrite (±bornite) veins, locally with K-feldspar haloes, and chalcopyrite-pyrite stringer veins occur (Figure 9b). Pyrite-epidote-chlorite veins (Figure 9c), with epidote±hematite±illite haloes, are the youngest veins that host pyrite with minor chalcopyrite and cut all earlier veins. Quartz-chalcopyrite-pyrite±molybdenite±anhydrite veins, with and without K-feldspar haloes, dominate areas with stronger K-feldspar–biotite–

magnetite alteration but progressively become less abundant toward the margins of the deposit. Pyrite-epidote-chlorite veins occur most commonly at the margins of the deposit, and are associated with the intense epidote±chlorite±pyrite alteration assemblage of the hostrocks. They are rare to absent in the central parts of deposit. Pre- to syn-

mineralization veins such as magnetite, quartz±magnetite±chalcopyrite, and quartz±anhydrite veins with sulphides, and with and without K-feldspar haloes, commonly occur in all quartz monzonite units but are less abundant in the K-feldspar porphyry unit. This unit is largely cut by late pyrite±epidote±chlorite veins, indicating that the K-feldspar

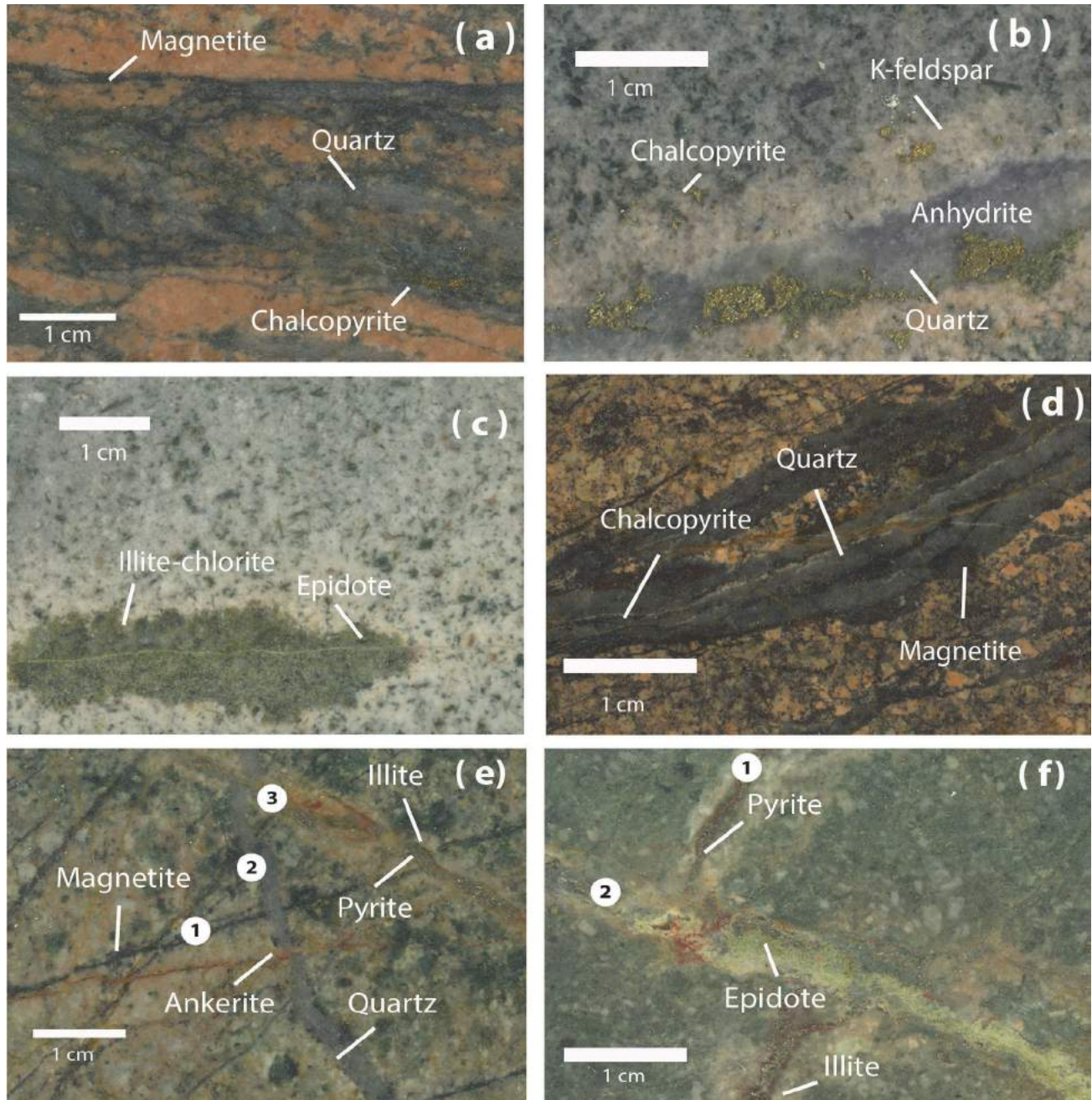


**Figure 9.** Schematic representation of vein assemblages in the Southeast Zone (a, b, c) and Deerhorn (d, e, f) deposits (sample numbers represent drillhole numbers followed by depth): **a)** quartz-magnetite-chalcopyrite veins with very intense K-feldspar–biotite–magnetite alteration in the coarse-grained quartz monzonite (SE11-62; 185.08 m); **b)** quartz-chalcopyrite-molybdenite-pyrite-anhydrite vein with K-feldspar halo in the medium-grained quartz monzonite with disseminated chalcopyrite occurring near mafic minerals (SE11-59; 278.49 m); **c)** epidote-chlorite vein with illite halo (SE11-54; 54 m); **d)** magnetite stockwork and Au-bearing quartz-magnetite-chalcopyrite banded veins in monzonite A (DH10-09; 79.5 m); **e)** magnetite stockwork cut by a quartz-magnetite vein (1), an illite-pyrite-hematite vein (2) and an ankerite vein (3) in monzonite A (DH10-09; 263.2 m); **f)** pyrite-quartz-hematite vein with illite halo (1) cut by a pyrite-chlorite-epidote vein (2) in hostrock (DH12-39; 178.19 m).

porphyry unit is younger than the quartz monzonites and postdates at least part of the main phase of mineralization. All these veins are cut by late carbonate veins.

### Deerhorn Deposit

In the Deerhorn deposit, early magnetite stockwork and banded, Au-bearing quartz-magnetite-chalcopyrite±hematite veins with sulphides (Figure 9d) commonly occur in monzonite A and the adjacent volcanic hostrock. Monzonite D cuts monzonite A and the early Au-bearing quartz-magnetite veins with sulphides. Abundance and mineral proportion of early quartz-magnetite±hematite veins with sulphides vary from high-density and sulphide-rich in monzonite A and the surrounding volcanic rocks to a paucity of sulphides and lower abundance of veins distally. Similar relationships were observed for the early magnetite stockwork. Quartz veins with sulphides, and with and without K-feldspar haloes, occur throughout all units and cut the early quartz-magnetite veins with sulphides (Figure 9e). Locally, quartz veins with sulphides have an illite overprint of a K-feldspar halo, which is interpreted as a later event (Figure 9e). Pyrite-quartz±hematite±epidote veins with white illite haloes, and in less abundance tourmaline, occur throughout all rock units, cutting early veins and being cut in turn by pyrite-chlorite±epidote±calcite±ankerite veins (Figure 9f). Tourmaline was identified locally during this study (in hole DH10-09 at 150 m and DH12-49 at 295 m) occurring in monzonite D or volcanic hostrock near monzonite D. It occurs as a dark grey alteration (Figure 10a) or as black subhedral crystals surrounding a pyrite vein (Figure 10b). Late carbonate and hematite veins occur throughout all hostrocks, including late mafic dikes. These observations indicate that pre- to synmineralization veins such as the Au-bearing quartz-magnetite veins with sulphides occur mainly in monzonite A and in volcanic hostrock adjacent to it, whereas monzonite D is commonly cut by late veins.

A summary of the various vein types and timing relationships observed for each deposit is presented in Figure 11.

### Mineralization

Copper, gold and molybdenum mineralization in the Woodjam property are controlled by the hostrock, alteration, density of veining and location (margins or central area) within the porphyry system. In the SEZ deposit, Cu occurs dominantly in chalcopyrite with subordinate bornite disseminated but more commonly in veins (Figure 9a, b). Molybdenite is observed mainly in veins. Sulphide minerals occur in quartz veins and chalcopyrite-pyrite stringer veins as fine-grained and anhedral grains, whereas sulphide disseminations in the hostrock are intimately related to mafic mineral sites. Areas of high Cu grades (~0.5%; Figure 12a) are characterized by dense stockworks of thin veins and abundant disseminated chalcopyrite in the hostrock. Copper grades decrease with depth (to <0.4% by ~300 m; Figure 12a) as chalcopyrite-pyrite stringer veins become less abundant to absent and Cu mineralization becomes more concentrated in quartz veins (up to 2 cm wide) with K-feldspar haloes. Gold mineralization (less than 1 ppm, rarely up to 4 ppm) may be associated with banded dark quartz-magnetite-chalcopyrite veins that occur in the core of the porphyry deposit.

Sulphide zoning at the SEZ consists of a chalcopyrite±bornite (±pyrite; hole SE11-62) assemblage in the core of the deposit, which changes upward and outward to chalcopyrite±molybdenite±pyrite (holes SE11-59 and SE11-36) and finally, a pyrite-dominated assemblage in the periphery of the deposit (holes SE10-18, SE11-24, SE12-74 and SE11-54). The pyrite:chalcopyrite (py:cpy) ratio defines zones with an approximately southwest orientation similar to the trend of the basalt and andesite porphyry dikes (Figure 12a). In the northwestern part of the deposit, where the FP intrudes, chalcopyrite is less abundant but still shows a

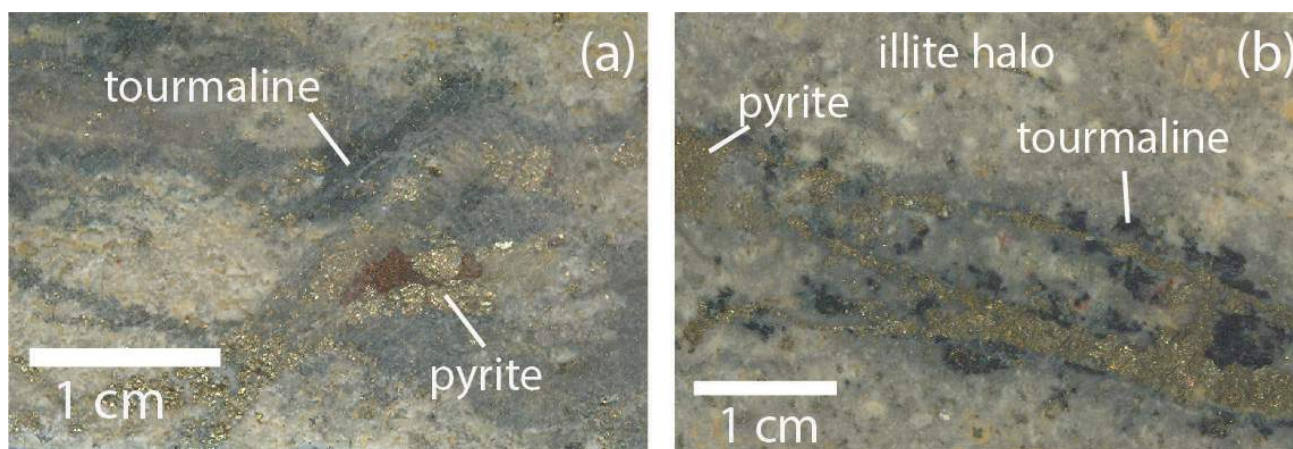


**Figure 10.** Pyrite-quartz±hematite±epidote±illite halo (±tourmaline halo) vein examples with tourmaline halo, showing **a)** dark grey anhydrous tourmaline surrounding a pyrite veinlet (DH10-09; 150 m) in monzonite D; **b)** black subhedral tourmaline surrounding a pyrite vein with an illite halo in volcanic hostrock (DH12-49; 295 m). Sample numbers represent drillhole numbers followed by depth.

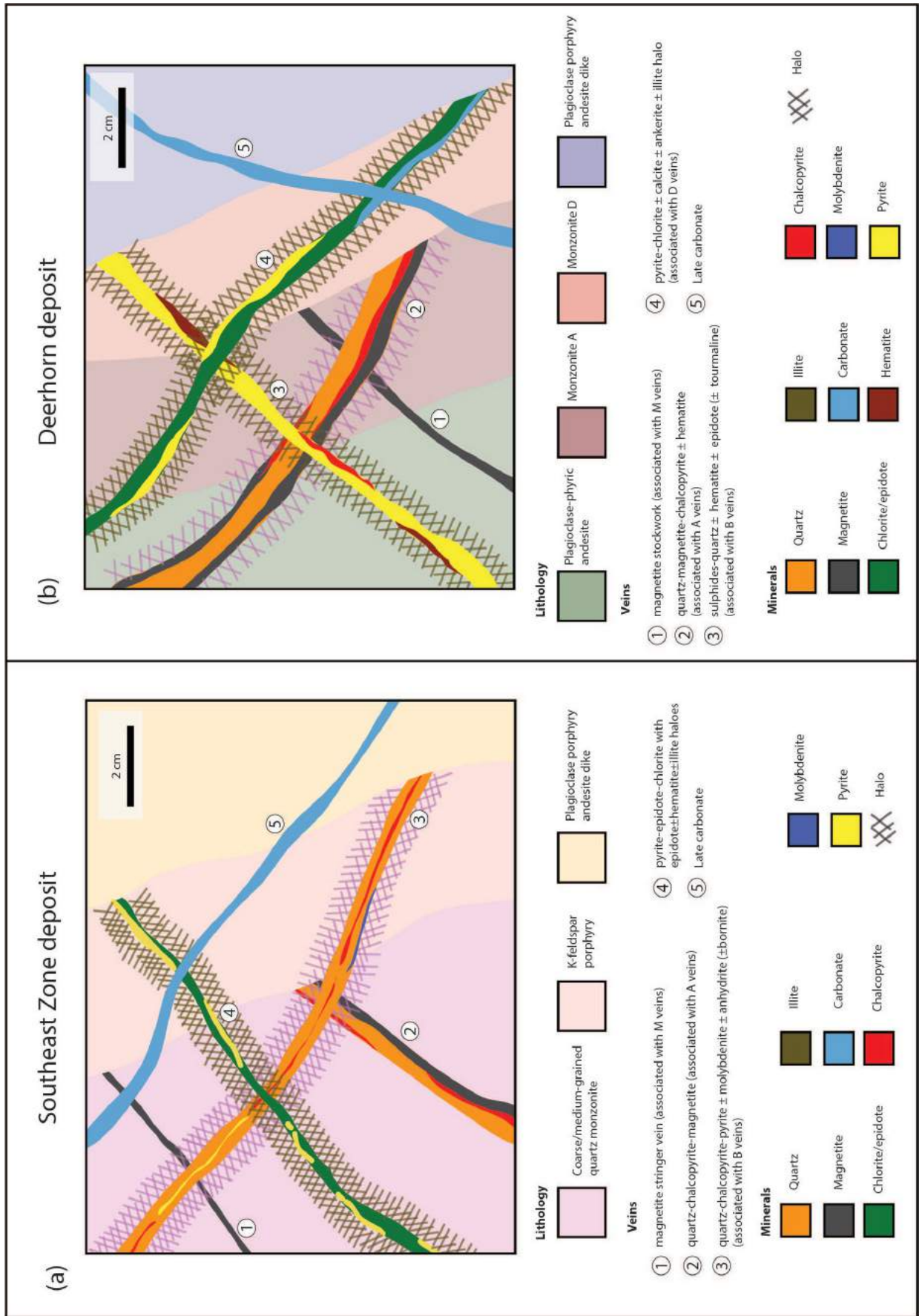


**Figure 11.** Summary of various vein types observed in the **a)** Southeast Zone and **b)** Deerhorn deposits, showing analogies with common vein types (e.g., M, A, B, D veins) in porphyry deposits (Gustafson and Hunt, 1975; Arancibia and Clark, 1996; Sillitoe, 2000, 2010).

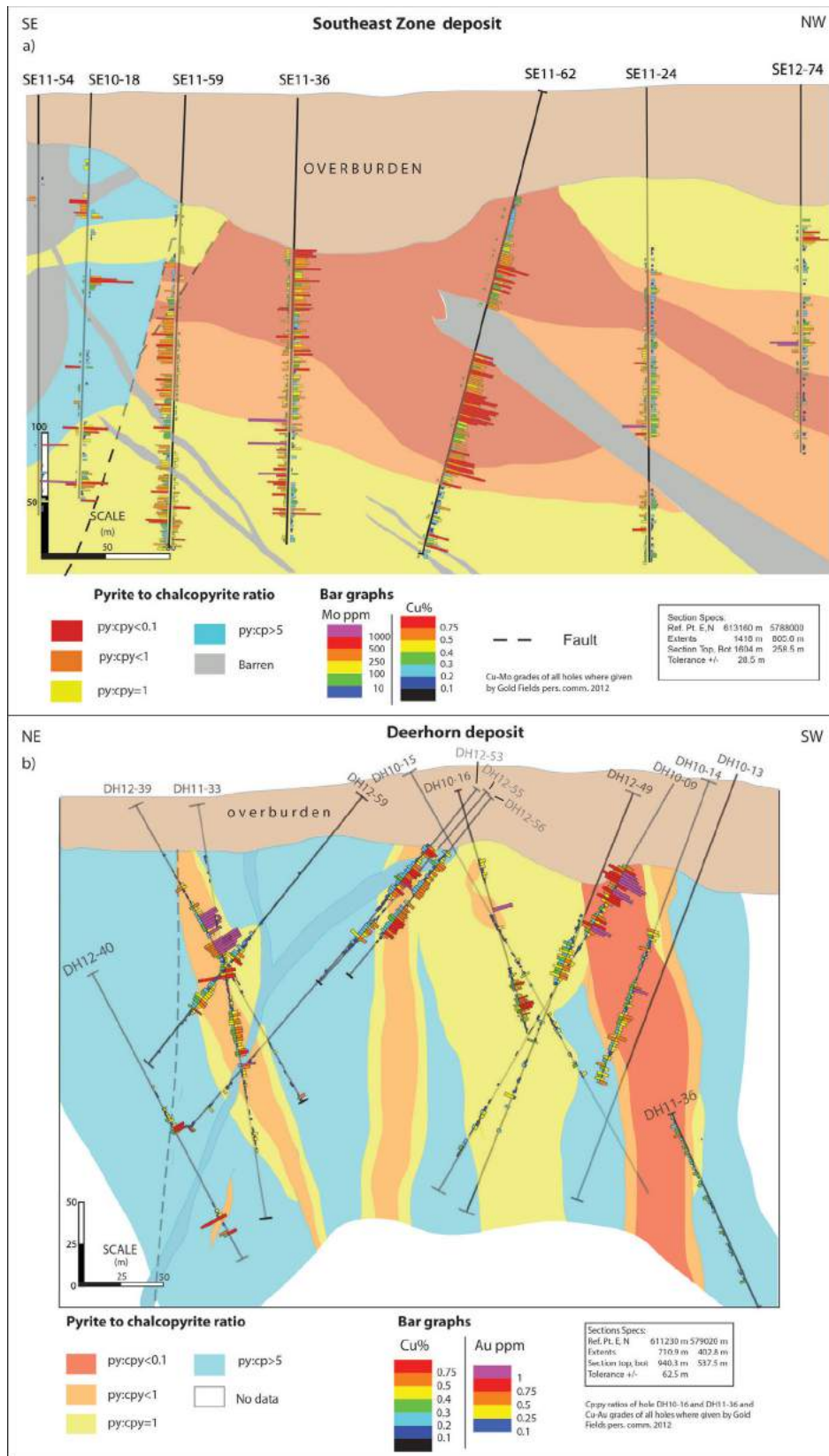


**Figure 12.** Sulphide ratio and Cu, Au, Mo grades for the **a)** Southeast Zone and **b)** Deerhorn deposits. Sulphide ratio calculations are based on core logging done during this study and Gold Fields Canada Exploration assay data. Copper assay values are shown on the right side of the drillhole trace for the Southeast Zone deposit and on the left side for the Deerhorn deposit; Mo on the left side of the drillhole for the Southeast Zone deposit and Au on the right side for the Deerhorn deposit.

py:cpy ratio of  $<0.1$ ; this is attributed to the FP being a late-mineralization intrusion. The southeastern portion of the deposit has a py:cpy ratio of  $>5$  and is locally barren in the shallower and middle portions of the drillcore from this area of the deposit (Figure 12a). This barren portion is related to intense albite alteration. In the deeper part of the deposit (350 m or more), chalcopyrite increases (py:cpy = 1) and albite alteration diminishes. This area of the deposit is interpreted as having been originally shallower in the porphyry system and later displaced by a normal fault.

Mineralization in the Deerhorn deposit differs from mineralization in the SEZ deposit in that it has significantly higher Au grades associated with Cu mineralization (up to  $<1.5$  ppm Au and  $<0.75\%$  Cu; Figure 12b). Mineralization is hosted dominantly in monzonite A (Figure 6d) and the adjacent volcanic hostrocks and occurs either as disseminations or in the early quartz-magnetite-chalcopyrite veins and later quartz veins with sulphides. Monzonite D hosts lower grades of Cu mineralization ( $\sim 0.1$ – $0.3\%$ ; Figure 12b) but does not host significant Au. Trace amounts of molybdenite have been observed in the later-stage quartz veins with sulphides in monzonite D. Sulphide ratios are affected by hostrocks: monzonite A and immediate surrounding volcanic rocks have a py:cpy ratio of  $<0.1$ , whereas the rest of the deposit is dominated by a py:cpy ratio of  $>5$  (Figure 12b). Sulphide ratios, and Cu and Au grades vary in different bodies of monzonite A. For example, the monzonite A body in the southwestern part of the cross-section (Figure 12b) has a py:cpy ratio of  $<0.1$ , whereas the other two monzonite A bodies have py:cpy ratios of  $<1$ . A similar relationship can be seen for Au grades (Figure 12b).

## Discussion

The characteristics of the hostrock, alteration and mineralization of the SEZ and Deerhorn deposits were documented on the basis of field and petrographic observations in order to understand their similarities, differences and possible genetic relationships.

The SEZ deposit is hosted in texturally variable quartz monzonite intrusive rocks that are inferred to be part of the Takomkane batholith. Alteration is zoned from intense K-feldspar–biotite–magnetite in the centre, which becomes weaker toward the margins and is laterally surrounded by albite alteration at the margins of the deposit. Epidote±chlorite±pyrite alteration overprints the K-feldspar–biotite–magnetite alteration and is locally intense at the margins of the deposit, but is weak to absent in the core. Chlorite replaces primary and secondary mafic minerals. Illite alteration occurs as an overprint of K-feldspar and plagioclase. Mineralization is zoned from chalcopyrite-bornite mineralization anomalous in Au ( $\sim 0.2$  ppm) to pyrite-dominated mineralization at the margins. However, the low abundance of quartz veining is not a typical feature of

calcalkalic deposits. Alteration and sulphide-ratio zoning suggest that the deposit has been tilted approximately  $25^\circ$  to the southeast, which coincides with the orientation of the basaltic dikes and the andesitic porphyry dike.

The Deerhorn deposit is hosted in a series of narrow ( $<100$  m) monzonite intrusions that have ‘pencil’ geometries. No modal quartz is observed in the volcanic hostrocks or the monzonite intrusions. The lack of modal quartz is a common characteristic of alkalic porphyry systems in BC (Lang et al., 1995). Alteration is characterized by intense K-feldspar–biotite–magnetite in monzonite A and adjacent volcanoclastic rocks and is moderate to weak in monzonite D. Potassium feldspar–biotite–magnetite alteration is overprinted by epidote+chlorite+hematite+pyrite alteration and a later illite alteration that replaces plagioclase and overprints K-feldspar vein haloes. Calcite+ankerite+pyrite veins overprint earlier alterations. Late kaolinite alteration occurs along a main structure together with dusty hematite replacing magnetite and chalcocite replacing chalcopyrite. These observations suggest that kaolinite is a supergene alteration product(?). Mineralization is hosted in two vein stages: 1) a very dense banded and sheeted network of quartz-magnetite-hematite-chalcopyrite veins that is strongly developed in monzonite A and the adjacent volcanic hostrocks, and 2) later quartz-chalcopyrite-pyrite veins that crosscut all the hostrocks at the Deerhorn deposit, including monzonite D. The K-feldspar–biotite–magnetite alteration assemblage and the vein stages observed at the Deerhorn deposit are consistent with characteristics of Cu–Au calcalkalic porphyry systems (Sillitoe, 2000, 2010). Occurrence of tourmaline alteration (Figure 10) and minor molybdenite in monzonite D are additional features representative of a more calcalkalic system. However, the ‘pencil’-shape intrusive hostrock lacking modal quartz and laminated quartz-magnetite veins with sulphides is consistent with characteristics of Cu–Au quartz-saturated alkalic porphyry systems (Holliday et al., 2002). These observations indicate that the Deerhorn deposit has characteristics of both alkalic and calcalkalic systems; similar to those at the Red Chris deposit in northwestern BC, where the hostrock is a quartz-poor monzonite and mineralization is hosted in banded quartz veins (Norris et al., 2011). Similarly, the Skouries deposit in northern Greece occurs in a syenite that hosts Cu mineralization in banded quartz veins (Frei, 1995).

The SWIR analysis conducted in the SEZ and Deerhorn deposits distinguished different alteration mineralization styles and complemented petrographic observations. Illite was the main mineral observed in the SEZ and was classified into two major types. The first type is an illite-(muscovite) assemblage with a K-feldspar affinity that occurs at the margins of the deposit. This illite alteration is interpreted as having formed above the K-feldspar–biotite–magnetite alteration assemblage and is commonly associ-

ated with a higher concentration of pyrite. In petrographic terms, this alteration occurs as an apple-green illite replacing plagioclase and groundmass flooding. The illite-(muscovite) alteration and the K-feldspar-biotite-magnetite alteration assemblage are overprinted by a second type of illite alteration with more phengitic affinity. The phengitic illite alteration occurs as dark green illite replacing plagioclase and is interpreted as having formed at lower temperatures. Therefore, separating and mapping the various types of illite can vector toward the K-silicate alteration and higher grades. These results are comparable to the alteration observed at the Pebble porphyry deposit, Alaska (Harraden et al., 2013), in which a lower temperature illite alteration (represented as an absorption feature >2200 nm using SWIR) overprints illite-(muscovite) of the quartz-sericite-pyrite alteration assemblage with the K-rich affinity (absorption feature <2200 nm).

The results of SWIR analysis identified kaolinite and montmorillonite alteration at Deerhorn. The kaolinite alteration is structurally controlled and occurs together with dusty hematite replacing magnetite and chalcocite replacing chalcopyrite.

The next stage of this project will focus on determining the geochemistry and magmatic-hydrothermal evolution of these deposits in the Woodjam property and gaining a better understanding of the genetic relationship between the intrusive units of both deposits. Understanding the link between the two deposits will provide insight into the possible existence of a genetic relationship between alkalic and calcalkalic deposits worldwide, and will have important implications for exploration targets in the area and in other areas of BC containing intrusive bodies similar to the Takomkane batholith.

## Acknowledgments

Geoscience BC is acknowledged and thanked for the funding provided for this project. Gold Fields Canada Exploration is thanked for the funding and field support for the project. The entire staff of the Woodjam project, including J. Scott, M. McKenzie, A. Ross, S. Vanderkekhove, K. Rempel and M. Eckfeldt are thanked for their support during the fieldwork. T. Bissig is acknowledged for reviewing this paper.

## References

- Arancibia, O.N. and Clark, A.H. (1996): Early magnetite-amphibole-plagioclase alteration-mineralization in the Island Copper porphyry copper-gold molybdenum deposit, British Columbia; *Economic Geology*, v. 91, p. 402–438.
- Blackwell, J., Black, E. and Skinner, T. (2012): National Instrument 43-101 Technical Report on 2011 Activities on the Woodjam North Property, Cariboo Mining Division, British Columbia, 134 p.
- Casselman, M.J., McMillan, W.J. and Newman, K.M. (1995): Highland Valley porphyry copper deposits near Kamloops, British Columbia: a review and update with emphasis on the Valley deposit; *in* *Porphyry Deposits of the Northwestern Cordillera of North America*, T.G. Schroeter (ed.), Canadian Institute of Mining, Metallurgy and Petroleum, Special Volume 46, p. 161–191.
- Chamberlain, C.M., Jackson, M., Jago, C.P., Pass, H.E., Simpson, K. A., Cooke, D.R. and Tosdal, R.M. (2007): Toward an integrated model for alkalic porphyry copper deposits in British Columbia (NTS 039A, N, 104G); *in* *Geological Fieldwork 2006*, Geoscience BC, Report 2007-1, p. 259–274.
- Del Real, I., Hart, C.J.R., Bouzari, F., Blackwell, J.L., Rainbow A., Sherlock, R. and Skinner, T. (2013): Paragenesis and alteration of the Southeast Zone and Deerhorn porphyry deposits, Woodjam property, central British Columbia (parts of 093A); *in* *Geoscience BC Summary of Activities, 2012*, Geoscience BC, Report 2013-1, p. 79–90.
- Fraser, T.M., Stanley, C.R., Nikic, Z.T., Pesalji, R. and Gorc, D. (1995): The Mount Polley alkalic porphyry copper-gold deposit, south-central British Columbia, *in* *Porphyry Deposits of the Northwestern Cordillera of North America*, T.G. Schroeter (ed.), Canadian Institute of Mining, Metallurgy and Petroleum, Special Volume 46, p. 609–622.
- Frei, R. (1995): Evolution of mineralizing fluid in the porphyry copper system of the Skouries Deposit, Northeast Chalkidiki (Greece): evidence from combined Pb-Sr and stable isotope data; *Economic Geology*, v. 90, no. 4, p. 746–762.
- Gustafson, L.B. and Hunt, J.P. (1975): The porphyry copper deposit at El Salvador, Chile; *Economic Geology*, v. 70, no. 9., p. 857–312.
- Harraden, C.L., McNulty, B. A., Gregory, M.J. and Lang, J.R. (2013): Shortwave infrared spectral analysis of hydrothermal alteration associated with the pebble porphyry copper-gold-molybdenum deposit, Iliamna, Alaska; *Economic Geology*, v. 108, no. 3, p. 483–494.
- Holliday, J.R., Wilson, A.J., Blevin, P.L., Tedder, I.J., Dunham, P.D. and Pfitzner, M. (2002): Porphyry gold-copper mineralization in the Cadia district, eastern Lachlan fold belt, New South Wales and its relationship to shoshonitic magmatism; *Mineralium Deposita*, v. 37, p. 100–116.
- Lang, J.R., Lueck, B., Mortensen, J.K., Russel, J.K., Stanley, C.R. and Thompson, J.M. (1995): Triassic-Jurassic silica undersaturated and silica-saturated alkalic intrusions in the Cordillera of British Columbia: implications for arc magmatism; *Geology*, v. 23, p. 451–454.
- Logan, J.M., Mihalynuk, R.M., Friedman, R.M. and Creaser, R. A. (2011): Age constraints of mineralization at Brenda and Woodjam Cu-Mo±Au porphyry deposits—an early Jurassic calcalkaline event, south-central British Columbia; *in* *Geological Fieldwork 2010*, BC Ministry of Energy and Mines, Paper 2011-1, p. 129–144.
- McMillan, W.J., Thompson, J.F.H., Hart, C.J.R. and Johnston, S.T. (1995): Regional geological and tectonic setting of porphyry deposits in British Columbia and Yukon Territory; *in* *Porphyry Deposits of the Northwestern Cordillera of North America*, T.G. Schroeter (ed.), Canadian Institute of Mining, Metallurgy and Petroleum, Special Volume 46, p. 40–57.
- Mihalynuk, M.G., Nelson, J. and Diakow, L.J. (1994): Cache Creek terrane entrapment: oroclinal paradox within the Canadian Cordillera; *Tectonics*, v. 19, p. 575–595.

- Monger, J. and Price, R. (2002): The Canadian Cordillera: geology and tectonic evolution; Canadian Society of Exploration Geophysicists Recorder, v. 27, no. 2, p. 17–36.
- Mortimer, N. (1987): The Nicola Group: Late Triassic and Early Jurassic subduction-related volcanism in British Columbia; Canadian Journal of Earth Sciences. v. 24, p. 2521–2536.
- Norris, J.R., Hart, C.J.R., Tosdal, R.M. and Rees, C. (2011): Magmatic evolution, mineralization and alteration of the Red Chris copper gold porphyry deposit, northwestern British Columbia (NTS 104H/12W); *in* Geoscience BC Summary of Activities 2010, Geoscience BC, Report 2011-1, p. 33–44.
- Panteleyev, A., Bailey, D.G., Bloodgood, M.A. and Hancock, K.D. (1996): Geology and mineral deposits of the Quesnel River–Horsefly map area, Central Quesnel Trough, British Columbia; BC Ministry of Energy and Mines, Bulletin 97, 156 p.
- Rainbow, A. (2010): Assessment report on 2010 activities on the Woodjam South Property including soil sampling, surface rock sampling and diamond drilling; BC Ministry of Energy and Mines, Assessment Report 32 958, 1260 p.
- Rainbow, A., Blackwell, J., Sherlock, R., Bouzari, F., Skinner, T., Black, E. and Madsen, J. (2013): Geology and age relationships of contrasting styles of Cu-Mo-Au porphyry mineralization at the Woodjam Project, Horsefly, BC; Geoscience for Discovery Conference, Society of Economic Geology, Whistler, BC, September 24–27, 2013.
- Schiarizza, P., Bell, K. and Bayliss, S. (2009): Geology and mineral occurrences of the Murphy Lake area, south-central British Columbia (NTS 93A/03); *in* Geological Fieldwork 2008, BC Ministry of Energy and Mines, Paper 2009-1, p. 169–188.
- Scott, J. (2012): Geochemistry and Cu-Au mineral paragenesis of the Deerhorn prospect: Woodjam porphyry Cu-Au district, British Columbia, Canada; B.Sc. Honours thesis, University of British Columbia Okanagan, 120 p.
- Sherlock, R., Poos, S. and Trueman, A. (2012): National Instrument 43-101 technical report on 2011 activities on the Woodjam South property; Cariboo Mining Division, BC, 194 p., URL <[http://sedar.com/GetFile.do?lang=EN&docClass=24&issuerNo=00032460&fileName=/csfsprod/data132/filings/01934687/00000001/y%3A%5CWeb\\_Documents%5CRADAR%5CE3%5CE3CO0C24%5C23JL12137%5C120723WJSTR\\_jaj.pdf](http://sedar.com/GetFile.do?lang=EN&docClass=24&issuerNo=00032460&fileName=/csfsprod/data132/filings/01934687/00000001/y%3A%5CWeb_Documents%5CRADAR%5CE3%5CE3CO0C24%5C23JL12137%5C120723WJSTR_jaj.pdf)> [November 2013].
- Sillitoe, R.H. (2000): Gold-rich porphyry deposits: descriptive and genetic models and their role in exploration and discovery; Reviews in Economic Geology, v. 13, p. 315–345.
- Sillitoe R.H. (2010): Porphyry copper systems, Economic Geology, v. 105, pp. 3-41
- Thompson, S.S.B., Hauff, P.L. and Robitaille, A.J. (1999): Alteration mapping in exploration: application of shortwave infrared (SWIR) spectroscopy; Society of Economic Geologists, Newsletter 39, p. 16–27.
- Vaca, S. (2012): Variability in the Nicola/Takla Group basalts and implications for alkali Cu/Au porphyry prospectivity in the Quesnel terrane, British Columbia, Canada; M.Sc. thesis, University of British Columbia, 163 p.



# U-Pb Ages, Geochemistry and Pb-Isotopic Compositions of Jurassic Intrusions, and Associated Au(-Cu) Skarn Mineralization, in the Southern Quesnel Terrane, Southern British Columbia (NTS 082E, F, L, 092H, I)

J.K. Mortensen, University of British Columbia, Vancouver, BC, [jmortensen@eos.ubc.ca](mailto:jmortensen@eos.ubc.ca)

---

Mortensen, J.K. (2014): U-Pb ages, geochemistry and Pb-isotopic compositions of Jurassic intrusions, and associated Au(-Cu) skarn mineralization, in the southern Quesnel terrane, southern British Columbia (NTS 082E, F, L, 092H, I); *in* Geoscience BC Summary of Activities 2013, Report 2014-1, p. 83–98.

## Introduction

Mesozoic and Cenozoic intrusive rocks constitute a major component of the Quesnel terrane in southern British Columbia (Figure 1). Early and Middle Jurassic intrusions in this region are of particular interest because of their inferred linkages with a variety of styles of intrusion-related mineralization. World-class Au and Au-Cu skarns that are interpreted as being temporally and genetically related to Jurassic intrusions in the region include the Nickel Plate mine in the Hedley–Apex Mountain area, which produced a total of 71 tonnes of gold from 13.4 million tonnes of ore (Ray et al., 1996), and the Phoenix mine in the Greenwood area, which produced 28.3 tonnes of gold and 235.7 tonnes of copper from 13.1 million tonnes of ore (Figure 1; MINFILE 082ESE020; BC Geological Survey, 2013). In addition, the currently operating Buckhorn Mountain (Crown Jewel) mine, located ~5 km south of the BC-Washington border and approximately 28 km west-southwest of Greenwood (Figure 1), is a Au-bearing skarn deposit, with past production and current resources of 30.1 tonnes of gold, that is also associated with Jurassic intrusive rocks (Scorror, 2012). Despite the clear economic significance of Jurassic intrusions and their associated mineralization in this region, these bodies have been the subject of relatively little detailed study. An investigation of Jurassic intrusive rocks between Hedley and Osoyoos was undertaken as part of a larger study of Paleozoic basement rocks and superimposed Mesozoic magmatism in the southern Quesnel terrane (Mortensen et al., 2011). Locations and brief lithological descriptions of the samples that were included in this study are given in Table 1. Uranium-lead zircon ages are reported here for a total of eight intrusions. The geochemical compositions of these bodies are also compared with Early and Middle Jurassic intrusions in the Greenwood area (Boundary Creek mineral district) and the Buckhorn Mountain area in northern Washington. In addition, Pb-iso-

topic compositions are reported for all of the intrusive rocks and for Au-Cu skarn mineralization from the areas of the Nickel Plate and Phoenix mines. The implications of these results are discussed in terms of constraints on the tectonic evolution of the region and the age(s) of the Au-Cu skarns present.

## Regional Geology

The basement of the southern Quesnel terrane in southern BC comprises a variety of metamorphosed volcanic and sedimentary assemblages of middle and late Paleozoic age (Figure 1). These assemblages are unconformably overlain by mainly Late Triassic volcanic, clastic and carbonate rocks of the Nicola Group, and have been subsequently intruded by several suites of Jurassic, Cretaceous and Paleogene plutons (Figure 1). Middle Jurassic and mid-Cretaceous volcanic rocks are also present, particularly in the region west of Osoyoos. Paleogene volcanic and sedimentary rocks, commonly closely associated with high-level intrusions, occur throughout the region.

## Geology of the Hedley–Apex Mountain Area

The Hedley–Apex Mountain area (Figure 2) is underlain by metasedimentary and mafic metavolcanic rocks of the Apex Mountain Complex of Ray and Dawson (1994; comprising parts of the Independence, Bradshaw, Old Tom and Shoemaker assemblages of Bostock, 1940). The overlying Nicola Group strata in this area are dominantly sedimentary, and have been subdivided into at least six separate rock units (Oregon Claims, French Mine, Hedley, Chuchwayha, Stemwinder and Whistle formations) by Ray and Dawson (1994) and Ray et al. (1996) based on lithofacies and, to some extent, on fossil ages. These authors also identified five distinct intrusive phases of known or inferred Jurassic ages in the area that they interpreted as representing two separate pulses of magmatism. These intrusive units were distinguished based on modal composition and on a limited number of relatively imprecise U-Pb and K-Ar crystallization ages. The Hedley intrusions, which consist of several irregular stocks (Aberdeen, Stemwinder and Toronto) and a very large number of sills and dikes within the Nicola Group units (Figure 2), were interpreted as the old-

---

**Keywords:** *Quesnel terrane, Jurassic intrusions, Au-Cu skarn, U-Pb geochronology, Pb isotopes, litho geochemistry*

*This publication is also available, free of charge, as colour digital files in Adobe Acrobat® PDF format from the Geoscience BC website: <http://www.geosciencebc.com/s/DataReleases.asp>.*

**Table 1.** Locations and brief lithological descriptions of samples used in the study.

Sample no.	Rock unit	Lithology	Location	UTM		Datum
				Easting	Northing	
10-M-04	Bromley batholith	Hornblende granodiorite	Road west from Apex Mountain resort	288431	5476152	NAD27
10-M-05	Lookout Mtn. pluton	Biotite-hornblende quartz monzonite	Logging road west of Nickle Plate Lake	284467	5475953	NAD27
10-M-06	Offshoot of Toronto stock	Fine- to medium-grained diorite	Old access road toward Nickle Plate mine	714559	5471320	NAD27
10-M-07	Offshoot of Toronto stock	Fine- to medium-grained diorite	Old access road toward Nickle Plate mine	714828	5471134	NAD27
10-M-08	Cahill Creek Stock	Biotite quartz monzonite	Main road from Hedley up to Mascot mine	715091	5468977	NAD27
10-M-10	Olalla pluton	Massive syenite	Road up Olalla Creek	292745	5461717	NAD83
10-M-33	Mt Riordan pluton	Massive quartz diorite	Road on west side of Apex Mountain resort	287928	5476012	NAD27
10KL-111	Kruger syenite	Coarse-grained syenite	Roadcut on north side of Highway 3	304934	5432930	NAD27
10KL-115	Bromley batholith?	Hornblende granodiorite	East side of Apex Mountain resort access road	289672	5475444	NAD27

est plutons in the area. The Hedley intrusions are metaluminous and predominantly mafic to intermediate in composition (gabbro to diorite). Four younger intrusive phases, of mainly intermediate composition, are also recognized; these include eastern extensions of the Bromley batholith, as well as the Lookout Ridge pluton, the Mount Riordan stock and the Cahill Creek pluton (Figure 2). Isotopic-age determinations reported by Ray and Dawson (1994) indicated that crystallization ages for these units that ranged

from ca. 194 to 168 Ma. Middle Jurassic subaerial volcanic rocks of the Skwel Peken formation overlie the Nicola Group strata in a small area ~2 km north of the Nickel Plate mine, and a variety of mainly felsic dikes and plugs of uncertain age crosscut most rock units in the area.

Skarn Au(±Cu) mineralization in the Hedley–Apex Mountain area is mainly developed within limestone of the French Mine formation and calcareous siltstone of the Hedley Formation. Skarn development is most prominent where

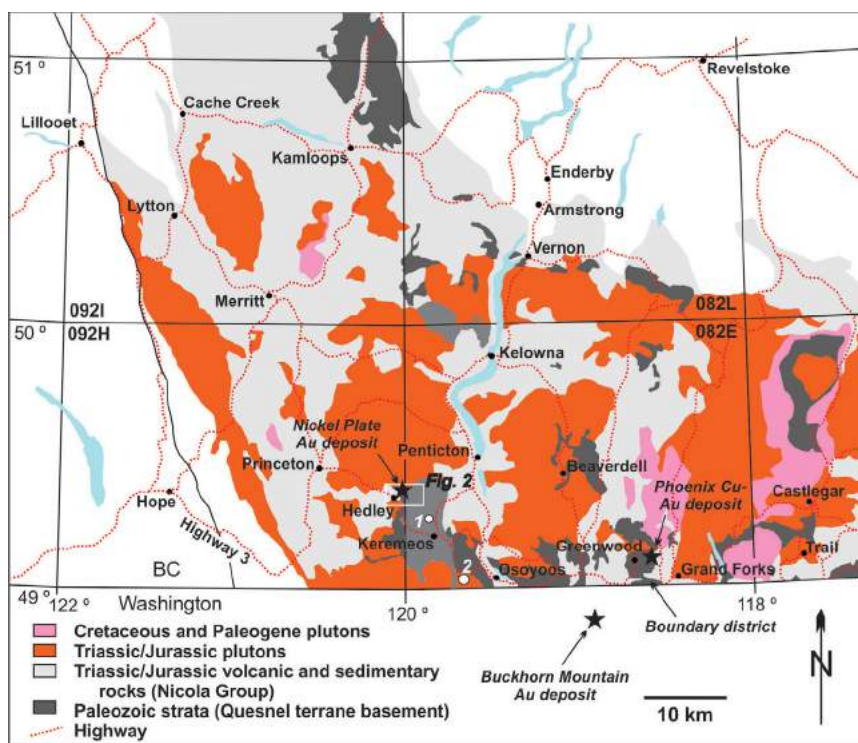


**Figure 1.** Distribution of Paleozoic basement units and Early and Late Mesozoic intrusions in the Quesnel terrane of southern and south-central British Columbia. Star outside the map border shows the location of the Buckhorn Mountain (Crown Jewel) Au-bearing skarn deposit. Location of Figure 2 is shown as the white box. White circles marked 1 and 2 are the locations of the Olalla pluton and Kruger syenite, respectively.

these units are cut by Hedley intrusions, and Ettliger et al. (1992) and Ray et al. (1996) suggested that this close association provides evidence that the Hedley intrusions were likely the main causative intrusions responsible for skarn formation in this area.

### U-Pb Geochronology

Individual samples weighing from 5–10 kg each were collected from surface exposures from eight different plutons. Zircons were separated from the samples through conventional crushing and grinding operations, and using Wilfley table, heavy liquids and Frantz magnetic-separator techniques. Zircons were analyzed by laser-ablation multiple-collector inductively coupled plasma–mass spectrometry (LA-MC-ICP-MS) at the Pacific Centre for Isotopic and Geochemical Research, University of British Columbia, Vancouver, BC. The methodology for zircon selection, mounting and analysis for the U-Pb age determinations by LA-MC-ICP-MS are as described by Tafti et al. (2009) and Beranek and Mortensen (2011). Zircons recovered from the various samples typically comprised stubby to elongated euhedral prisms with no evidence for inherited cores. Twenty zircon grains were analyzed from most of the samples, except for the Olalla pluton sample, which yielded only nine zircon grains of sufficiently high quality for analysis. Analytical results are presented in Table 2 and are

shown graphically in Figures 3 and 4. The individual data sets are interpreted below.

#### Sample 10M-06 (Toronto Stock)

A sample of fine- to medium-grained hornblende diorite was collected from a sill ~3 m thick near the southern edge of the Toronto stock (Figure 2). A total of twenty zircon grains were analyzed (Table 2; Figure 3a, b). All of the analyses were concordant and fifteen grains yielded a calculated weighted-average  $^{206}\text{Pb}/^{238}\text{U}$  age of  $195.5 \pm 1.2$  Ma (mean square of weighted deviates [MSWD] = 0.27; probability of fit = 1.0), which is interpreted as the crystallization age of the sample. Five grains gave a cluster of slightly older ages (average of ca. 202 Ma) that appears to represent a distinct and separate population from the other analyses. These grains are interpreted as xenocrysts that were incorporated into the magma, possibly entrained from Late Triassic Nicola Group units, and the five analyses were excluded from the final calculation of the crystallization age of the sample.

#### Sample 10M-04 (Bromley Batholith)

Twenty zircon grains were analyzed from a sample of very fresh hornblende granodiorite from the Bromley batholith, located north of the Apex Mountain ski resort (Figure 2). All analyses were concordant and eighteen analyses

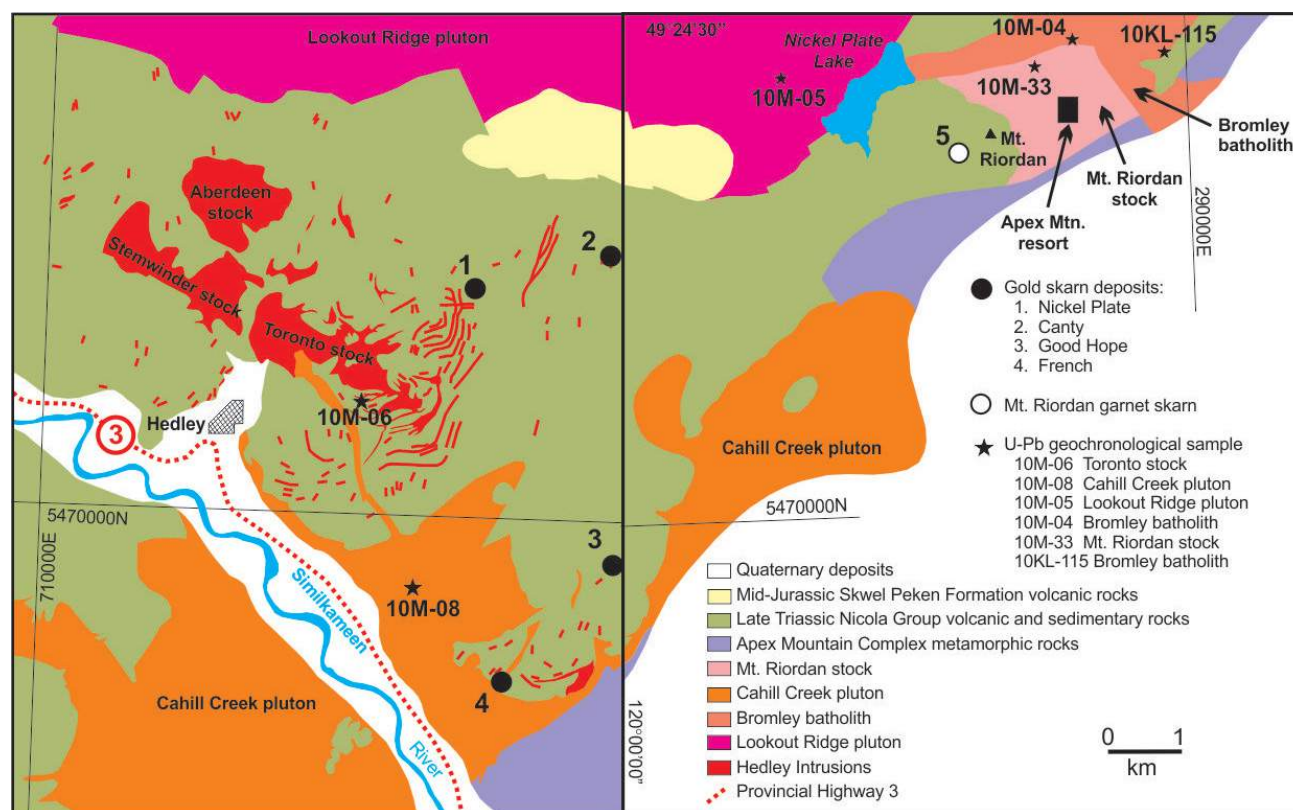


**Figure 2.** Simplified geology of the Hedley–Apex Mountain area (modified from Ray and Dawson, 1994). Locations of samples of the Olalla pluton and Kruger syenite are not shown on the map.

**Table 2.** Results of U-Pb zircon analyses for intrusive rock units from the Hedley–Apex Mountain area. Analyses by Pacific Centre for Isotopic and Geochemical Research, University of British Columbia, Vancouver, BC.

Fraction	Isotopic ratios					Isotopic ages (Ma)					Background corrected mean counts per second at specified mass										
	$^{207}\text{Pb}/^{235}\text{U}$	$1\sigma$ (%)	$^{206}\text{Pb}/^{238}\text{U}$	$1\sigma$ (%)	$\rho$	$^{207}\text{Pb}/^{235}\text{U}$	$1\sigma$ (%)	$^{206}\text{Pb}/^{238}\text{U}$	$1\sigma$	$^{207}\text{Pb}/^{206}\text{Pb}$	$1\sigma$	$^{207}\text{Pb}/^{206}\text{Pb}$	$1\sigma$	202	204	206	207	208	232	235	238
<b>Sample 10M-06 (Toronto stock; 714559E, 5471664N, MAD83)</b>																					
1	0.20796	0.0052	0.03058	0.00027	0.35	0.04889	0.00117	191.8	4.4	194.2	1.7	142.5	55.2	9	2	8605	421	541	22700	1787	269157
2	0.21696	0.00605	0.03095	0.0003	0.35	0.04922	0.00131	199.4	5.1	196.5	1.9	158.5	61.0	31	23	9390	463	617	26929	1886	290553
3	0.22136	0.00638	0.03185	0.00033	0.36	0.05162	0.00142	203.0	5.3	202.1	2.0	268.4	61.7	18	19	7382	382	429	18158	1526	222278
4	0.20916	0.00659	0.03099	0.00034	0.35	0.04887	0.00147	192.8	5.5	196.8	2.1	141.6	69.1	14	0	6049	297	332	13686	1255	187344
5	0.22095	0.00547	0.03181	0.00028	0.36	0.04933	0.00115	202.7	4.6	201.9	1.7	163.4	53.4	32	19	16726	829	1273	53732	3321	505183
6	0.21032	0.00699	0.03093	0.00035	0.34	0.04938	0.00155	193.8	5.9	196.4	2.2	166.1	71.9	19	23	4926	244	493	20696	1031	153324
7	0.2134	0.00594	0.03083	0.0003	0.35	0.04896	0.00127	196.4	5.0	195.7	1.9	146.0	59.8	0	16	8228	405	582	25287	1685	257205
8	0.21289	0.00998	0.03075	0.0005	0.35	0.04872	0.00217	196.0	8.4	195.3	3.1	134.3	101.5	3	21	5427	266	403	16279	1110	170194
9	0.21229	0.00669	0.03091	0.00034	0.35	0.04917	0.00144	195.5	5.6	196.2	2.1	156.0	67.2	0	14	9203	456	573	23208	1907	287345
10	0.21168	0.00724	0.03031	0.00036	0.35	0.05028	0.0016	195.0	6.1	192.5	2.3	208.1	72.2	9	0	9358	474	652	27615	1990	298228
11	0.21202	0.00759	0.03083	0.00038	0.34	0.04937	0.00163	195.3	6.4	195.7	2.4	165.5	75.4	28	8	11798	587	998	41708	2463	370120
12	0.22278	0.01178	0.03202	0.00058	0.34	0.04906	0.00244	204.2	9.8	203.2	3.6	150.8	112.6	6	0	3233	160	414	16679	638	97715
13	0.22375	0.02117	0.03233	0.00106	0.35	0.04931	0.00445	205.0	17.6	205.1	6.6	162.8	198.1	0	23	2253	112	195	8002	445	67480
14	0.22048	0.01007	0.03211	0.00061	0.35	0.04974	0.0021	202.3	8.4	203.7	3.2	182.6	95.6	0	0	7610	381	553	21729	1541	229601
15	0.20669	0.0078	0.0308	0.0004	0.34	0.04853	0.00165	190.8	6.6	195.6	2.5	125.3	78.3	19	1	12797	626	1071	46388	2698	402607
16	0.2136	0.0106	0.03102	0.00053	0.34	0.05041	0.0023	196.6	8.9	196.9	3.3	214.1	102.3	0	3	13872	705	998	44206	2940	433668
17	0.2123	0.01073	0.03063	0.00053	0.34	0.04933	0.00229	195.5	9.0	194.5	3.3	163.7	104.9	8	5	7658	381	452	20234	1597	242474
18	0.21226	0.01236	0.03097	0.00062	0.34	0.04908	0.00264	195.4	10.4	196.6	3.9	151.7	121.5	0	1	7182	355	480	18819	1490	224961
19	0.21209	0.01162	0.03063	0.00058	0.35	0.04996	0.0025	195.3	9.7	194.5	3.6	193.1	112.6	29	15	5430	273	440	17448	1148	172057
20	0.21189	0.01382	0.03093	0.0007	0.35	0.05076	0.00307	195.1	11.6	196.4	4.4	230.1	133.8	0	0	4131	211	381	14412	887	129587
<b>Sample 10M-04 (Bromley batholith; 288431E, 5476152E, NAD83)</b>																					
1	0.20873	0.00814	0.0306	0.00042	0.35	0.04882	0.00183	192.5	6.8	194.3	2.6	139.0	85.9	20	0	3800	189	268	11128	774	119464
2	0.19739	0.00712	0.03027	0.00038	0.35	0.04685	0.00163	182.9	6.0	192.3	2.4	41.3	81.4	10	0	7207	344	780	28976	1491	229041
3	0.2017	0.00537	0.03069	0.00028	0.34	0.04722	0.00121	186.6	4.5	194.9	1.8	59.9	60.6	1	1	6043	290	413	15916	1233	189433
4	0.21345	0.00348	0.03061	0.00019	0.38	0.05121	0.0008	196.4	2.9	194.3	1.2	250.2	35.7	21	24	13310	694	993	41248	2785	418411
5	0.20703	0.00499	0.03059	0.00025	0.34	0.04816	0.00112	191.1	4.2	194.3	1.5	107.2	54.0	10	21	5832	286	481	19796	1183	183417
6	0.21068	0.01258	0.03107	0.00062	0.33	0.04729	0.00272	194.1	10.6	197.2	3.9	63.5	131.9	24	8	3834	184	275	11400	751	118777
7	0.20857	0.00708	0.03014	0.00036	0.35	0.05076	0.00167	192.4	6.0	191.4	2.3	229.9	74.1	21	13	3528	182	426	16320	750	112676
8	0.20743	0.00615	0.03052	0.00032	0.35	0.0483	0.00138	191.4	5.2	193.8	2.0	114.0	66.1	33	0	4318	212	478	19861	878	136173
9	0.21526	0.00545	0.03057	0.00027	0.35	0.05048	0.00123	198.0	4.6	194.1	1.7	216.9	55.5	8	4	4980	255	592	24554	1020	156782
10	0.21547	0.00777	0.03066	0.00038	0.34	0.04931	0.00171	198.1	6.5	194.7	2.4	162.8	79.1	15	3	3603	180	368	15194	721	113114
11	0.21167	0.00913	0.03093	0.00045	0.34	0.04845	0.00201	195.0	7.7	196.4	2.8	121.3	95.0	0	0	3806	187	336	13923	762	118477
12	0.20649	0.00978	0.03025	0.0005	0.35	0.04956	0.00227	190.6	8.2	192.1	3.1	174.4	103.3	0	0	4470	225	276	12006	938	142272
13	0.22367	0.00877	0.03193	0.00044	0.35	0.04884	0.00183	205.0	7.3	202.6	2.7	140.2	85.8	50	36	6586	326	424	17817	1259	198640
14	0.20968	0.00754	0.03069	0.00038	0.34	0.04913	0.00171	193.3	6.3	194.9	2.4	154.0	79.4	21	18	3988	198	255	11361	818	125162
15	0.21355	0.00503	0.03121	0.00025	0.34	0.04941	0.00112	196.5	4.2	198.1	1.6	167.3	52.2	30	13	6045	303	396	16995	1225	186535
16	0.20799	0.01099	0.03025	0.00057	0.36	0.05136	0.00262	191.9	9.2	192.1	3.6	256.9	113.2	0	0	5331	277	387	15087	1153	169795
17	0.20756	0.00557	0.0305	0.00028	0.34	0.04893	0.00127	191.5	4.7	193.7	1.8	144.5	59.6	75	8	5366	266	436	20034	1109	169470
18	0.21177	0.00848	0.03061	0.00042	0.34	0.0482	0.00185	195.0	7.1	194.3	2.7	109.1	88.4	26	12	4166	203	312	11764	831	131128
19	0.21077	0.00722	0.03084	0.00037	0.35	0.05036	0.00167	194.2	6.1	195.8	2.3	211.8	74.9	0	2	4972	253	335	13542	1042	155376
20	0.2057	0.00454	0.02947	0.00023	0.35	0.05034	0.00107	189.9	3.8	187.3	1.5	210.9	48.7	0	3	6549	333	734	29903	1406	214111
<b>Sample 10K-115 (Bromley batholith; 289672E, 5475444N, NAD83)</b>																					
1	0.22543	0.04781	0.03246	0.0018	0.26	0.049	0.01023	206.4	39.6	205.9	11.2	148.0	427.5	0	16	304	14	39	1355	66	10185
2	0.20404	0.04593	0.02953	0.00182	0.27	0.05397	0.01208	188.5	38.7	187.6	11.4	369.7	438.2	14	1	283	15	11	648	75	10406
3	0.20615	0.02549	0.0304	0.00126	0.34	0.05232	0.00632	190.3	21.5	193.1	7.9	299.5	254.5	0	0	990	51	115	4498	252	35361
4	0.18863	0.06364	0.03036	0.00226	0.22	0.05208	0.01748	175.5	54.4	192.8	14.1	288.8	626.4	0	0	192	9	17	668	53	8865
5	0.24766	0.046	0.03074	0.00199	0.35	0.06599	0.0121	224.7	37.4	195.2	12.4	806.1	343.2	18	0	307	20	37	827	82	10855

Table 2 (continued)

Fraction	Isotopic ratios					Isotopic ages (Ma)					Background corrected mean counts per second at specified mass										
	$^{207}\text{Pb}/^{235}\text{U}$	$^{206}\text{Pb}/^{238}\text{U}$	$^{207}\text{Pb}/^{206}\text{Pb}$	$1\sigma$	$\rho$	$^{207}\text{Pb}/^{235}\text{U}$	$1\sigma$	$^{206}\text{Pb}/^{238}\text{U}$	$1\sigma$	$^{207}\text{Pb}/^{206}\text{Pb}$	$1\sigma$	202	204	206	207	208	232	235	238		
6	0.20426	0.0937	0.03085	0.00302	0.21	0.04359	0.01977	188.7	79.0	195.9	18.9	0.1	720.0	0	9	158	6	1	307	33	5576
7	0.288	0.03881	0.03215	0.00147	0.34	0.06822	0.00896	257.0	30.6	204.0	9.2	875.3	250.5	0	21	308	20	23	701	73	10414
8	0.19482	0.02585	0.03072	0.00121	0.28	0.05063	0.007	172.2	22.2	195.0	7.6	224.0	291.3	0	0	452	2	55	1661	124	15987
9	0.20088	0.24106	0.03103	0.00472	0.13	0.03699	0.04423	185.9	203.8	197.0	29.5	0.1	1226.5	0	11	63	2	19	190	11	2227
10	0.21915	0.09059	0.03077	0.00262	0.21	0.06227	0.0258	201.2	75.5	195.4	16.4	683.5	700.6	0	0	92	5	6	291	26	3278
11	0.20521	0.06674	0.02932	0.00181	0.19	0.04419	0.01426	189.5	56.2	186.3	11.3	0.1	546.7	0	3	240	10	25	821	52	8918
12	0.23902	0.04671	0.03392	0.00172	0.26	0.05139	0.00985	217.6	38.3	215.0	10.7	258.5	389.2	0	0	368	18	18	813	79	11794
13	0.21293	0.05366	0.03116	0.00198	0.25	0.05451	0.0112	196.0	44.9	197.8	12.4	0.1	463.5	0	8	299	13	19	1020	63	10452
14	0.19388	0.03959	0.03108	0.00137	0.22	0.0444	0.00896	180.0	33.7	197.3	8.6	0.1	343.8	0	0	372	16	21	145	85	13021
15	0.19438	0.06127	0.03132	0.00299	0.30	0.05067	0.01583	180.4	52.1	198.8	18.7	225.7	596.2	48	0	240	12	31	733	62	8352
16	0.12909	0.01652	0.01623	0.00069	0.33	0.05579	0.00717	123.3	14.9	103.8	4.4	443.9	263.2	0	2	583	32	158	14391	253	39128
17	0.08308	0.01724	0.01722	0.00071	0.20	0.03719	0.00773	81.0	16.2	110.1	4.5	0.1	0.0	50	23	339	12	143	12116	152	21442
18	0.19269	0.02835	0.03061	0.00109	0.24	0.04344	0.00629	178.9	24.1	194.4	6.8	0.1	182.1	0	2	454	19	66	2108	102	16155
19	0.21169	0.03525	0.03102	0.0016	0.31	0.04669	0.00757	195.0	29.5	196.9	10.0	33.1	348.5	0	0	856	40	78	2769	189	30032
<b>Sample 10M-05 (Lookout Ridge pluton; 284467E, 5475953N, NAD83)</b>																					
1	0.21877	0.0049	0.03184	0.00025	0.35	0.04948	0.00107	200.9	4.1	202.0	1.5	170.7	49.5	1	17	7395	370	450	21027	1479	249664
2	0.21915	0.0056	0.03181	0.00029	0.36	0.05029	0.00123	201.2	4.7	201.9	1.8	208.2	56.0	15	16	10295	524	693	28646	2089	347422
3	0.22218	0.00529	0.03195	0.00028	0.37	0.05099	0.00116	203.7	4.4	202.7	1.7	240.5	51.7	24	0	13909	718	1205	53152	2822	466935
4	0.21625	0.0054	0.03116	0.00028	0.36	0.04947	0.00119	198.8	4.5	197.8	1.7	170.2	55.1	43	1	6301	315	705	32522	1274	216672
5	0.21444	0.0042	0.03103	0.00022	0.36	0.05038	0.00095	197.2	3.5	197.0	1.4	212.4	43.0	57	0	8253	420	758	37347	1713	284664
6	0.22368	0.00517	0.0313	0.00026	0.34	0.04895	0.00114	196.0	4.3	198.7	1.7	145.5	53.9	3	0	6832	338	499	23898	1387	233008
7	0.21293	0.00733	0.03082	0.00036	0.34	0.05052	0.00168	196.3	6.1	195.7	2.3	219.2	75.1	10	9	4941	252	350	16327	1033	170996
8	0.21847	0.00739	0.0318	0.00037	0.34	0.05006	0.00163	200.6	6.2	201.8	2.3	197.7	73.9	26	0	6296	318	411	17044	1273	210982
9	0.21129	0.00435	0.03103	0.00023	0.36	0.0493	0.00098	194.6	3.7	197.0	1.4	162.1	45.6	30	21	9163	456	677	31251	1886	314301
11	0.20935	0.00529	0.03105	0.00027	0.34	0.04792	0.00116	193.0	4.4	197.1	1.7	94.4	57.7	31	0	9946	480	828	37083	2008	340329
12	0.21225	0.01042	0.03196	0.00049	0.33	0.04972	0.00226	203.0	8.7	202.8	3.1	181.8	102.5	3	17	2570	128	221	9688	509	85360
13	0.20586	0.0084	0.03017	0.00039	0.32	0.04855	0.00192	190.1	7.1	191.6	2.5	126.4	90.7	19	0	2761	135	270	12131	574	97054
14	0.2212	0.00705	0.03178	0.00036	0.36	0.05199	0.00159	202.9	5.9	201.7	2.3	284.8	68.5	22	17	8757	458	649	33452	1813	291930
15	0.21676	0.00487	0.03089	0.00025	0.36	0.05048	0.00109	199.2	4.1	196.1	1.6	217.0	49.1	0	6	9196	467	720	35982	1887	315066
16	0.21727	0.00696	0.03099	0.00034	0.34	0.05008	0.00154	199.6	5.8	196.7	2.2	198.8	70.1	14	7	5647	284	351	17483	1146	192531
17	0.21517	0.00556	0.03103	0.00028	0.35	0.05008	0.00124	197.9	4.6	197.0	1.8	198.9	56.7	20	0	5916	298	514	22942	1212	201236
18	0.21906	0.00779	0.03075	0.00039	0.36	0.05043	0.00172	201.1	6.5	195.2	2.4	214.7	77.2	0	0	6031	305	425	19581	1222	206818
19	0.20955	0.00797	0.03099	0.0004	0.34	0.04713	0.00172	193.2	6.7	196.7	2.5	55.6	85.4	0	0	6480	307	551	24355	1282	220302
20	0.21243	0.00442	0.03102	0.00023	0.36	0.04848	0.00097	195.6	3.7	196.8	1.4	122.8	46.4	4	0	8006	390	1030	49447	1607	271798
<b>Sample 10M-33 (Mt. Riordan stock; 287928E, 5476012N, NAD83)</b>																					
1	0.22027	0.00804	0.03186	0.00039	0.34	0.0481	0.00169	202.1	6.7	202.2	2.4	104.3	80.8	38	8	3815	183	342	14964	738	115658
2	0.21847	0.00853	0.03157	0.0004	0.32	0.04877	0.00183	200.6	7.1	200.4	2.5	136.6	86.1	10	0	3074	150	330	13713	608	94063
3	0.22329	0.00817	0.03153	0.0004	0.35	0.05094	0.00179	204.6	6.8	200.1	2.5	238.1	79.2	0	0	3375	172	363	13748	683	103416
4	0.21829	0.00691	0.03184	0.00034	0.34	0.04957	0.00151	200.5	5.8	202.1	2.1	175.0	69.7	0	20	3560	176	294	12226	717	108030
5	0.20879	0.00764	0.03059	0.00038	0.34	0.05008	0.00177	192.5	6.4	194.2	2.4	198.6	80.1	22	0	3108	155	258	11110	662	98188
6	0.21824	0.00888	0.03183	0.00049	0.34	0.05023	0.00219	200.4	8.2	202.0	3.1	205.7	98.2	0	0	3589	180	371	14997	734	108972
7	0.22238	0.01199	0.03162	0.00059	0.35	0.04907	0.00254	203.9	10.0	200.7	3.7	151.4	116.8	16	0	4873	239	624	25811	956	148937
8	0.21508	0.01918	0.03102	0.00097	0.35	0.05042	0.00433	197.8	16.0	196.9	6.1	214.4	187.8	0	9	3427	172	389	13864	714	106807
9	0.21034	0.0105	0.03079	0.00053	0.34	0.04878	0.00234	193.8	8.8	195.5	3.3	137.1	109.2	13	6	4027	196	368	15176	830	126411
10	0.22145	0.00854	0.0321	0.00042	0.34	0.04911	0.00182	203.1	7.1	203.7	2.6	152.9	84.5	13	0	3765	184	351	14958	742	113386
11	0.2123	0.01266	0.03071	0.00065	0.35	0.0525	0.00303	195.5	10.6	195.0	4.1	307.3	126.0	5	0	3249	170	353	12767	715	102300
12	0.20859	0.00671	0.03086	0.00034	0.34	0.04894	0.00152	192.4	5.6	195.9	2.1	145.1	71.1	18	0	4325	211	475	21074	904	135528

Table 2 (continued)

Fraction	Isotopic ratios					Isotopic ages (Ma)					Background corrected mean counts per second at specified mass										
	$^{207}\text{Pb}/^{235}\text{U}$	$1\sigma$ (%)	$^{206}\text{Pb}/^{238}\text{U}$	$1\sigma$ (%)	$\rho$	$^{207}\text{Pb}/^{206}\text{Pb}$	$1\sigma$ (%)	$^{207}\text{Pb}/^{235}\text{U}$	$1\sigma$	$^{206}\text{Pb}/^{238}\text{U}$	$1\sigma$	$^{207}\text{Pb}/^{206}\text{Pb}$	$1\sigma$	202	204	206	207	208	232	235	238
13	0.2162	0.00588	0.03072	0.00029	0.35	0.05066	0.00133	198.7	4.9	195.1	1.8	225.2	59.4	27	0	5056	255	692	28289	1055	159131
14	0.20717	0.00651	0.03079	0.00031	0.32	0.04867	0.00148	191.2	5.5	195.5	2.0	132.1	70.0	51	0	4708	228	607	25619	986	147891
15	0.21562	0.0078	0.0306	0.00038	0.34	0.04984	0.00174	196.3	6.5	194.3	2.4	187.5	79.2	27	0	3262	162	338	14143	672	103086
16	0.21176	0.00753	0.03148	0.00037	0.33	0.04814	0.00165	195.0	6.3	199.8	2.3	105.9	79.0	0	30	3281	157	240	9862	665	100826
17	0.21177	0.00824	0.03064	0.0004	0.34	0.04882	0.00183	195.0	6.9	194.5	2.5	139.4	85.9	0	14	3719	180	279	10718	765	117434
18	0.21417	0.01114	0.03183	0.00056	0.34	0.04734	0.00237	197.0	9.3	202.0	3.5	65.7	115.6	0	0	3232	152	298	13975	637	98248
19	0.22087	0.00923	0.03181	0.00045	0.34	0.0495	0.00199	202.6	7.7	201.9	2.8	171.4	91.1	0	9	3939	193	396	15786	788	119797
20	0.21805	0.01728	0.03204	0.00086	0.34	0.0486	0.0037	200.3	14.4	203.3	5.4	128.4	170.1	12	27	3550	171	388	15310	707	107216
<b>Sample 10M-08 (Cahill Creek pluton; 715091E, 5468977N, NAD83)</b>																					
1	0.17324	0.00692	0.02534	0.00035	0.35	0.05	0.00193	162.2	6.0	161.3	2.2	194.8	87.2	12	0	4153	209	400	23311	1075	181123
2	0.17351	0.00487	0.02538	0.00025	0.35	0.04936	0.0013	162.5	4.2	161.5	1.6	164.8	60.6	0	9	8214	408	845	49214	2096	357355
3	0.17293	0.00715	0.02541	0.00036	0.34	0.04781	0.0019	162.0	6.2	161.7	2.3	89.1	92.7	0	15	7863	378	732	41679	1950	341403
4	0.17237	0.00476	0.02547	0.00025	0.36	0.04905	0.00127	161.5	4.1	162.1	1.6	150.2	59.7	41	0	9096	449	1227	74538	2321	393611
5	0.17836	0.00816	0.02535	0.0004	0.34	0.05122	0.00227	166.6	7.0	161.4	2.5	250.9	98.6	0	6	3761	193	330	18201	968	163347
6	0.17293	0.00492	0.02564	0.00025	0.34	0.04843	0.00129	162.0	4.3	163.2	1.6	120.3	61.8	22	0	9569	465	1048	57259	2402	410242
7	0.19032	0.00683	0.02712	0.00034	0.35	0.04952	0.00169	176.9	5.8	172.5	2.1	172.7	77.7	0	7	6521	324	665	38951	1521	264097
8	0.17881	0.00781	0.02611	0.00039	0.34	0.04779	0.002	167.0	6.7	166.2	2.5	88.0	97.4	0	0	5383	258	480	29209	1289	226236
9	0.17466	0.009	0.02536	0.00045	0.34	0.05008	0.0025	163.5	7.8	161.5	2.8	198.6	112.1	0	6	3521	476	435	23849	905	152214
10	0.18461	0.00544	0.02569	0.00026	0.34	0.05141	0.00142	172.0	4.7	163.5	1.7	259.4	62.3	0	0	8488	437	1378	72879	2118	361868
11	0.17476	0.00488	0.02546	0.00025	0.35	0.04927	0.00128	163.5	4.2	162.1	1.6	160.7	59.7	18	0	11267	556	1831	102243	2846	483944
12	0.17985	0.00483	0.02588	0.00024	0.35	0.04959	0.00123	167.9	4.2	164.7	1.5	176.0	57.0	32	15	18549	921	3187	181131	4582	782926
13	0.17957	0.00738	0.02588	0.00037	0.35	0.04902	0.00193	167.7	6.4	164.7	2.3	148.8	89.6	6	19	7282	357	1179	67701	1780	307140
14	0.17637	0.00629	0.0255	0.00031	0.34	0.04877	0.00165	164.9	5.4	162.4	2.0	136.9	77.6	0	0	8536	416	953	56657	2114	139368
15	0.18583	0.00911	0.02566	0.00043	0.34	0.05148	0.00243	173.1	7.8	163.3	2.7	262.6	105.0	18	9	3282	168	536	29087	814	139368
16	0.18768	0.01321	0.02537	0.00062	0.35	0.0551	0.00378	174.6	11.3	161.5	3.9	416.0	146.6	48	0	1748	96	167	8985	459	74975
17	0.17668	0.00811	0.02569	0.00039	0.33	0.04914	0.00217	165.2	7.0	163.5	2.5	154.5	100.3	13	0	2614	128	202	11246	651	110602
18	0.17716	0.00658	0.0255	0.00032	0.34	0.05033	0.00178	165.6	5.7	162.3	2.0	210.5	79.8	2	25	4154	208	454	24469	1056	176890
19	0.18436	0.01092	0.02661	0.00054	0.34	0.04986	0.00285	171.8	9.4	169.3	3.4	188.3	128.0	0	0	2743	136	268	14739	664	111823
20	0.18513	0.00641	0.02559	0.00031	0.35	0.05125	0.00167	172.5	5.5	162.9	1.9	251.9	73.1	22	23	8485	433	817	49202	2102	359408
<b>Sample 10M-10 (Olalia pluton; 292745E, 5461717N, NAD83)</b>																					
1	0.20892	0.02715	0.03052	0.00139	0.35	0.05099	0.00644	192.6	22.8	193.8	8.7	240.3	267.5	0	18	1469	76	498	20992	359	52436
2	0.26407	0.05095	0.03071	0.00204	0.34	0.05773	0.01078	237.9	40.9	195.0	12.7	519.4	364.8	11	0	529	31	85	4368	116	18799
3	0.18801	0.01254	0.03066	0.00071	0.35	0.04493	0.00285	174.9	10.7	194.7	4.4	0.1	87.2	0	15	6065	279	1147	52762	1452	155524
4	0.22635	0.0181	0.03048	0.00083	0.34	0.04954	0.00378	207.2	15.0	193.6	5.2	173.5	169.0	24	11	2221	113	895	43239	487	79420
5	0.19662	0.01017	0.03045	0.00055	0.35	0.04776	0.0023	182.3	8.6	193.4	3.5	86.5	111.4	0	38	16240	799	5658	262414	3953	581328
6	0.20922	0.01141	0.03007	0.00058	0.35	0.04874	0.00248	192.9	9.6	191.0	3.6	135.5	115.5	0	4	8173	411	2755	118889	1908	296338
7	0.20902	0.01412	0.03028	0.00069	0.34	0.04955	0.00319	192.7	11.9	192.3	4.3	174.0	143.4	46	0	2096	107	261	13126	498	75510
8	0.20711	0.01048	0.0303	0.00054	0.35	0.05036	0.00236	191.1	8.8	192.4	3.4	211.4	105.1	38	17	11093	579	3408	161514	2702	399334
9	0.21098	0.01509	0.03033	0.00074	0.34	0.05041	0.00344	194.4	12.7	192.6	4.7	213.8	150.5	0	7	2341	122	353	16980	560	84215
<b>Sample 10KL-11 (Kruger syenite; 304934E, 5432930N, NAD83)</b>																					
1	0.18199	0.00523	0.02677	0.00027	0.35	0.04954	0.00139	169.8	4.5	170.3	1.7	173.4	64.2	5	19	3951	197	580	28755	945	142287
2	0.18258	0.00644	0.02672	0.00031	0.33	0.04796	0.00165	170.3	5.5	170.0	2.0	96.2	80.7	21	5	4075	197	741	37799	941	147045
3	0.18243	0.00378	0.02657	0.0002	0.36	0.04993	0.00101	170.2	3.2	169.1	1.2	191.7	46.3	29	19	8064	406	1289	63384	1941	292547
4	0.18684	0.00807	0.02684	0.0004	0.35	0.05024	0.00212	173.9	6.9	170.8	2.5	206.3	94.9	0	10	3117	158	452	22334	737	111983
5	0.17319	0.00292	0.02662	0.00016	0.36	0.04723	0.00078	162.2	2.5	169.3	1.0	60.6	38.0	11	15	14393	686	2242	115348	345	521423
6	0.17731	0.00351	0.02526	0.00018	0.36	0.05074	0.00098	165.7	3.0	160.8	1.2	228.8	44.1	22	11	9731	498	1773	92346	2452	371493
7	0.18554	0.00353	0.02659	0.00018	0.36	0.04964	0.00092	172.8	3.0	169.2	1.2	178.3	42.5	2	12	9571	479	1205	62601	2256	347130

Table 2 (continued)

Fraction	Isotopic ratios				Isotopic ages (Ma)				Background corrected mean counts per second at specified mass												
	$^{207}\text{Pb}/^{235}\text{U}$	$^{206}\text{Pb}/^{238}\text{U}$	$^{207}\text{Pb}/^{206}\text{Pb}$	$\rho$	$^{207}\text{Pb}/^{235}\text{U}$	$^{206}\text{Pb}/^{238}\text{U}$	$^{207}\text{Pb}/^{206}\text{Pb}$	$1\sigma$	$^{207}\text{Pb}/^{206}\text{Pb}$	$1\sigma$	202	204	206	207	208	232	235	238			
8	0.18389	0.00409	0.02665	0.00021	0.35	0.04937	0.00107	171.4	3.5	169.5	1.3	165.3	49.9	57	8	6609	329	882	43630	1563	239220
9	0.1836	0.00597	0.02673	0.0003	0.35	0.04885	0.00155	171.2	5.1	170.1	1.9	140.5	72.9	0	16	4284	210	845	42806	1004	154579
10	0.18528	0.00551	0.02672	0.00028	0.35	0.0501	0.00145	172.6	4.7	170.0	1.8	199.7	66.0	82	24	5692	287	765	39231	1357	205607
11	0.17705	0.00474	0.02677	0.00025	0.35	0.0467	0.00122	165.5	4.1	170.3	1.6	33.8	60.3	87	0	8208	386	1124	56510	1910	295817
12	0.17831	0.00366	0.02672	0.0002	0.36	0.0492	0.00098	166.6	3.2	170.0	1.2	157.3	46.2	3	6	8219	407	991	50764	2002	296804
13	0.17956	0.01117	0.02629	0.00057	0.35	0.04849	0.00295	167.7	9.6	167.3	3.6	123.4	137.2	0	0	3822	186	541	25043	911	140261
14	0.18878	0.00757	0.02612	0.00038	0.36	0.05059	0.00198	175.6	6.5	166.2	2.4	222.3	87.9	0	22	7215	367	764	39837	1708	266564
15	0.17993	0.00651	0.02665	0.00034	0.35	0.05003	0.00177	168.0	5.6	169.6	2.1	196.2	80.2	29	1	4267	214	804	37934	1048	154531
16	0.18006	0.00471	0.02676	0.00025	0.36	0.04961	0.00126	168.1	4.1	170.2	1.6	177.0	58.4	0	7	9709	484	1889	97073	2365	350230
17	0.17988	0.00803	0.02663	0.00042	0.35	0.05077	0.00222	168.0	6.9	169.4	2.6	230.4	98.0	0	21	2682	136	411	19463	669	97249
18	0.18489	0.00503	0.02668	0.00025	0.34	0.04936	0.00131	172.3	4.3	170.5	1.6	165.0	60.9	0	6	4543	225	751	37458	1073	163684
19	0.18293	0.00342	0.02668	0.00018	0.36	0.0486	0.00088	170.6	2.9	169.7	1.1	128.7	42.1	32	7	9972	486	1734	85349	2345	360873
20	0.17654	0.00367	0.02674	0.0002	0.36	0.04768	0.00096	165.1	3.2	170.1	1.2	82.7	48.2	16	12	9676	463	1303	69308	2314	349392

Analyses by Pacific Centre for Isotopic and Geochemical Research, University of British Columbia, Vancouver, BC.

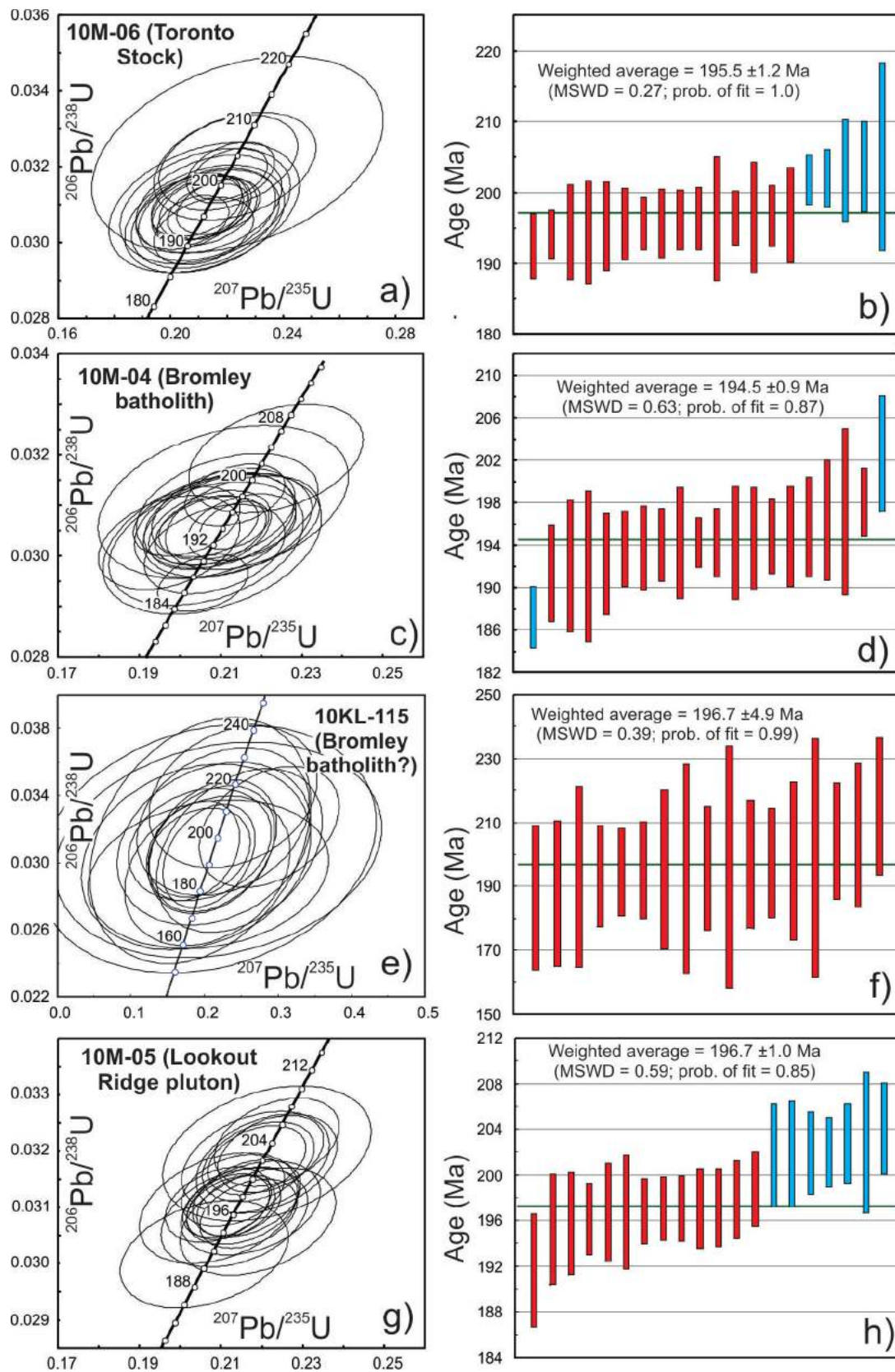


**Figure 3.** Conventional concordia diagrams and plots of weighted-average  $^{206}\text{Pb}/^{238}\text{U}$  ages for zircons from intrusive rock units in the Hedley–Apex Mountain area (part 1). Error ellipses on concordia diagrams and weighted-average  $^{206}\text{Pb}/^{238}\text{U}$  age plots are shown at the  $2\sigma$  uncertainty level. Analyses shown as red bars on weighted-average age plots were used in the age calculations; those shown as blue bars were rejected.

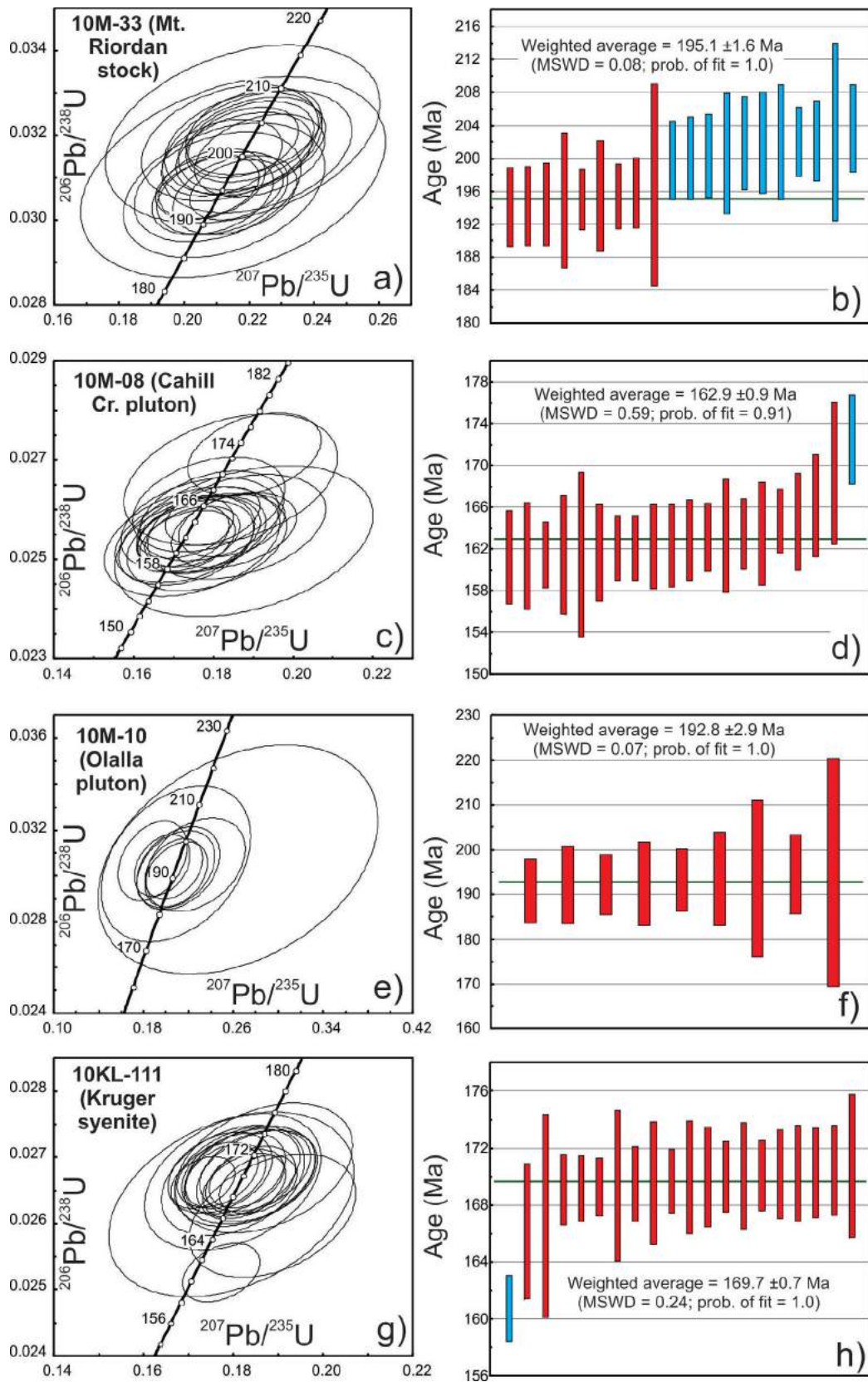


**Figure 4.** Conventional concordia diagrams and plots of weighted-average  $^{206}\text{Pb}/^{238}\text{U}$  ages for zircons from intrusive rock units in the Hedley–Apex Mountain area (part 2). Error ellipses on concordia diagrams and weighted-average  $^{206}\text{Pb}/^{238}\text{U}$  age plots are shown at the  $2\sigma$  uncertainty level. Analyses shown as red bars on weighted-average age plots were used in the age calculations; those shown as blue bars were rejected.

yielded a calculated weighted-average  $^{206}\text{Pb}/^{238}\text{U}$  age of  $194.5 \pm 0.9$  Ma (MSWD = 0.63; probability of fit = 0.87; Table 2, Figure 3c, d), which is interpreted as the crystallization age of the sample. One grain gave a slightly older  $^{206}\text{Pb}/^{238}\text{U}$  age and is interpreted as a xenocryst, and one grain gave a younger age, reflecting the effects of minor post-crystallization Pb loss.

### Sample 10KL-115 (Bromley Batholith)

A second hornblende granodiorite sample was collected from an exposure of what is interpreted as an eastern extension of the Bromley batholith, on the northern side of the Apex Mountain access road, approximately 1.25 km east of the Apex Mountain ski resort (Figure 2). The zircons from this sample were similar in appearance to those from the previous sample; however, the analyses were somewhat less precise, yielding a calculated weighted-average  $^{206}\text{Pb}/^{238}\text{U}$  age of  $196.7 \pm 4.9$  Ma (MSWD = 0.39; probability of fit = 0.99; Table 2, Figure 3e, f). This rather imprecise age determination is in agreement with that obtained from the previous sample (10M-04).

### Sample 10M-05 (Lookout Ridge Pluton)

Twenty zircon grains were analyzed from a sample of massive, very fresh, biotite-hornblende quartz monzonite collected from an area located northwest of Nickel Plate Lake (Figure 2). Seven grains gave a cluster of slightly older ages (average of ca. 202 Ma); however, the remaining 13 grains gave a younger cluster of ages with a calculated weighted-average  $^{206}\text{Pb}/^{238}\text{U}$  age of  $196.7 \pm 1.0$  Ma (MSWD = 0.59; probability of fit = 0.85; Table 2, Figure 3g, h), which is interpreted as the crystallization age of the sample. As with the Toronto stock sample, this older cluster of ages is interpreted as reflecting the presence of a significant older xenocrystic zircon population in the sample, and these analyses were not included in the calculation of the weighted-average age for the sample.

### Sample 10M-33 (Mount Riordan Stock)

A sample of medium-grained quartz diorite of the Mount Riordan stock was collected at a site located approximately 1 km northeast of the summit of Mount Riordan (Figure 2). Twenty zircon grains were analyzed (Table 2; Figure 4a, b) and the results showed two distinct clusters of ages: an older cluster gave ages of ca. 202 Ma, whereas the younger cluster of nine grains gave a calculated weighted-average  $^{206}\text{Pb}/^{238}\text{U}$  age of  $195.1 \pm 1.6$  Ma (MSWD = 0.08; probability of fit = 1.0). The presence of a ca. 202 Ma population of zircons appears to be common within intrusions in this area; hence, the age calculated for the younger cluster of grains is interpreted as the crystallization age of the sample.

### Sample 10M-08 (Cahill Creek Pluton)

Nineteen of twenty zircons recovered from a sample of biotite quartz monzonite of the Cahill Creek pluton, collected on the mine access road east of Hedley (Figure 2), yielded a calculated weighted-average  $^{206}\text{Pb}/^{238}\text{U}$  age of  $162.9 \pm 0.9$  Ma (MSWD = 0.59; probability of fit = 0.91; Table 2, Figure 4c, d). This is interpreted as the crystallization age of the sample, and a single zircon grain that yielded a slightly older age is considered to have been a xenocryst.

### Sample 10M-10 (Olalla Pluton)

Only a small amount of zircon was recovered from this sample of medium-grained trachytic syenite of the composite Olalla pluton collected along the Olalla Creek road. The nine zircons analyzed (Table 2; Figure 4e, f) gave a calculated weighted-average  $^{206}\text{Pb}/^{238}\text{U}$  age of  $192.8 \pm 2.9$  Ma (MSWD = 0.07; probability of fit = 1.0), which is interpreted as the crystallization age of the sample.

### Sample 10KL-111 (Kruger Syenite)

Twenty zircons were analyzed from this sample of massive, coarse-grained, biotite quartz monzonite from a roadcut on the northern side of Highway 3 (Figure 2). Nineteen of these yielded a calculated weighted-average  $^{206}\text{Pb}/^{238}\text{U}$  age of  $169.7 \pm 0.7$  Ma (MSWD = 0.24; probability of fit = 1.0; Table 2, Figure 4g, h), which is interpreted as the crystallization age of the sample. One zircon is slightly discordant and gave a slightly younger age, reflecting the effects of minor postcrystallization Pb loss.

## Discussion

The results of the dating study indicate that most of the intrusive rocks in the vicinity of skarn mineralization in the Hedley–Apex Mountain area, including both the Hedley intrusions and the other intrusive units that were interpreted by Ray et al. (1996) to be somewhat younger, were emplaced during the interval between ca. 197 and 195 Ma. The Cahill Creek pluton, with an emplacement age of 162.9 Ma, is confirmed to be substantially younger than the other intrusions in the area. The composite Olalla pluton, farther to the east, is slightly younger than most of the intrusions in the Hedley–Apex Mountain area, at 192.8 Ma. The Kruger syenite was expected to give an age similar to that of the Olalla pluton; however, it is actually more similar in age to the Cahill Creek pluton.

Uranium-lead zircon ages of  $179.9 \pm 3.8$  Ma and  $171.6 \pm 2.3$  Ma were reported by Massey et al. (2010) for the Greenwood stock near Greenwood and the Gidon Creek porphyry body approximately 8 km south of Greenwood, respectively, both of which are in the Boundary Creek mineral district. Three other intrusive phases in the western part of the Boundary district have also yielded Jurassic U-Pb crystallization ages; these include the Myer's Creek stock (157.0

$\pm 1.2$  Ma), the Mount Baldy granodiorite ( $168.5 \pm 1.4$  Ma) and the Ed James orthogneiss ( $187.7 \pm 1.4$  Ma; Massey et al., 2010). The relationship between various intrusive phases and skarn Au-Cu mineralization in the Boundary district is unknown.

A number of U-Pb zircon ages have been reported by Scorrar (2012) for various intrusive phases from the vicinity of the Buckhorn Mountain (Crown Jewel) Au-bearing skarn deposit immediately south of the BC-Washington border (Figure 1). A diorite body that is interpreted as coeval with at least some of the mafic volcanic rocks near the deposit gave an age of  $193.5 \pm 1.2$  Ma; however, with the exception of much younger bodies that are Paleogene in age, most other intrusions in the area gave crystallization ages in the range of 172–165 Ma (Scorrar, 2012). Dating by the Re-Os method of molybdenite from the Buckhorn skarn deposit

gave ages of  $165.5 \pm 0.7$  Ma and  $162.8 \pm 0.7$  Ma, confirming that skarn mineralization in the Buckhorn Mountain area is related to much younger intrusions than had been interpreted by Ray et al. (1996) for very similar skarn deposits in the Hedley–Apex Mountain area. This is discussed in more detail in a later section.

## Igneous Geochemistry

Major, trace and rare-earth element concentrations were determined for samples of each of the rock units that were dated in this study. Data are given in Table 3 and are shown on a series of geochemical and tectonic discriminant plots in Figure 5. Results of sample analyses from Jurassic intrusive rock units in the Boundary district near Greenwood (from Massey et al., 2010) and from the Buckhorn Mountain area in northern Washington state (from Gaspar, 2005) are also shown for comparison.

**Table 3.** Whole-rock geochemical analyses for Early and Middle Jurassic intrusive rock units from the Hedley–Apex Mountain area.

Sample	Major elements (wt.%)										LOI (wt. %)	Total (wt. %)
	SiO <sub>2</sub>	TiO <sub>2</sub>	Al <sub>2</sub> O <sub>3</sub>	Fe <sub>2</sub> O <sub>3</sub> <sup>t</sup>	MnO	MgO	CaO	Na <sub>2</sub> O	K <sub>2</sub> O	P <sub>2</sub> O <sub>5</sub>		
10M-04 (Bromley batholith)	63.70	0.52	16.20	6.44	0.11	2.36	5.80	3.33	1.70	0.14	1.00	101.48
10M-05 (Lookout Ridge pluton)	72.90	0.24	14.00	2.60	0.09	0.53	1.65	3.97	4.25	0.09	0.79	101.29
10M-06 (Toronto stock)	61.40	0.53	15.35	6.55	0.12	2.81	4.88	3.71	2.25	0.14	1.11	99.07
10M-07 (Toronto stock)	57.30	0.47	18.55	6.59	0.11	3.07	8.00	4.08	0.87	0.14	1.39	100.74
10M-08 (Cahill Creek pluton)	61.20	0.64	17.30	6.40	0.13	2.03	5.41	4.15	2.29	0.23	0.98	100.95
10M-10 (Olalla pluton)	64.00	0.31	16.00	4.00	0.07	1.21	4.07	3.19	4.15	0.14	2.17	99.65
10M-33 (Mt. Riordan stock)	65.20	0.45	15.80	5.09	0.11	2.01	5.28	3.19	2.31	0.11	1.17	100.91
10KL-111 (Kruger syenite)	67.10	0.39	15.40	4.39	0.12	1.20	3.73	3.94	3.51	0.17	1.09	101.22
10KL-115 (Bromley batholith)	60.10	0.56	16.35	6.73	0.12	2.86	5.75	3.15	2.24	0.15	2.02	100.26

Sample	Trace and rare-earth elements (ppm)														
	Ba	Ce	Cr	Cs	Dy	Er	Eu	Ga	Gd	Hf	Ho	La	Lu	Nb	
10M-04 (Bromley batholith)	1270	25.3	30	2.51	3	1.89	0.89	18.4	2.97	2.4	0.62	12.6	0.3	3.6	
10M-05 (Lookout Ridge pluton)	1300	48.8	10	4.92	3.16	2.07	0.7	15.8	3.36	4.9	0.64	32.1	0.38	8.3	
10M-06 (Toronto stock)	1535	27.4	60	4.54	2.73	1.67	0.96	18.4	3	2.9	0.57	13.9	0.25	3.6	
10M-07 (Toronto stock)	892	14.9	30	3.98	1.97	1.19	0.78	18.5	2.14	1.3	0.4	7.2	0.17	1.6	
10M-08 (Cahill Creek pluton)	1320	40	20	1.69	4.93	2.97	1.46	21.2	5.35	4.9	1	18.7	0.44	7.2	
10M-10 (Olalla pluton)	2420	25.7	20	0.96	2.03	1.32	0.7	18.7	2.1	2.3	0.43	14.3	0.23	5.5	
10M-33 (Mt. Riordan stock)	1350	24.8	30	1.88	2.64	1.67	0.79	17.8	2.67	2.8	0.54	13	0.28	3.8	
10KL-111 (Kruger syenite)	932	46.7	10	2.45	2.97	1.71	1.19	18.1	3.53	3.6	0.59	27.5	0.3	9.8	
10KL-115 (Bromley batholith)	1580	22	30	2.48	2.73	1.67	0.94	18.3	3	2.3	0.55	10.8	0.25	3.2	

Sample	Trace and rare-earth elements (ppm)														
	Nd	Pr	Rb	Sm	Sr	Ta	Tb	Th	Tm	U	V	Y	Yb	Zr	
10M-04 (Bromley batholith)	12.1	3.07	64.1	2.86	382	0.3	0.48	3.04	0.3	1.54	148	18.5	1.86	85	
10M-05 (Lookout Ridge pluton)	21.1	6.02	140.5	3.9	189.5	0.9	0.52	16.15	0.33	4.07	25	20.3	2.27	152	
10M-06 (Toronto stock)	12.7	3.29	80.5	2.99	473	0.3	0.45	4.63	0.26	2.44	166	15.9	1.53	96	
10M-07 (Toronto stock)	8	1.9	25.5	1.99	653	0.1	0.33	1.53	0.18	0.78	157	11.1	1.12	45	
10M-08 (Cahill Creek pluton)	22.4	5.24	69.2	5.42	469	0.4	0.83	7.06	0.47	2.62	122	29.6	2.86	182	
10M-10 (Olalla pluton)	10.7	2.87	113.5	2.21	590	0.4	0.32	4.29	0.21	2.7	105	12.5	1.42	82	
10M-33 (Mt. Riordan stock)	11.3	2.89	75.5	2.57	371	0.4	0.43	5.1	0.27	2.18	128	16.3	1.73	91	
10KL-111 (Kruger syenite)	18.3	4.99	131.5	3.74	662	0.9	0.5	11.5	0.28	2.62	86	17	1.82	118	
10KL-115 (Bromley batholith)	11.4	2.77	79.8	2.88	436	0.2	0.45	2.94	0.26	1.55	174	16.4	1.66	80	

Analyses done at ALS Chemex, Vancouver, BC. Major elements determined using ICP-AES methods following lithium-metaborate fusion (ALS analytical package ME-ICP06), and trace and rare-earth elements using ICP-MS methods following lithium-metaborate fusion (ALS analytical package ME-MS81)

On the total alkalis versus silica diagram (Figure 5a) of Le Bas et al. (1986), two samples of the Toronto stock plot as diorite, whereas most of the remaining samples fall in the granodiorite/quartz diorite field. The Lookout Ridge pluton yields a granite composition, and the Olalla plu-

ton falls just into the syenite field. All of the samples are subalkaline in composition according to the alkaline-subalkaline discriminant diagram (Figure 5a) of Irvine and Baragar (1971). There is considerably more scatter in the whole-rock geochemical analyses from the Boundary dis-

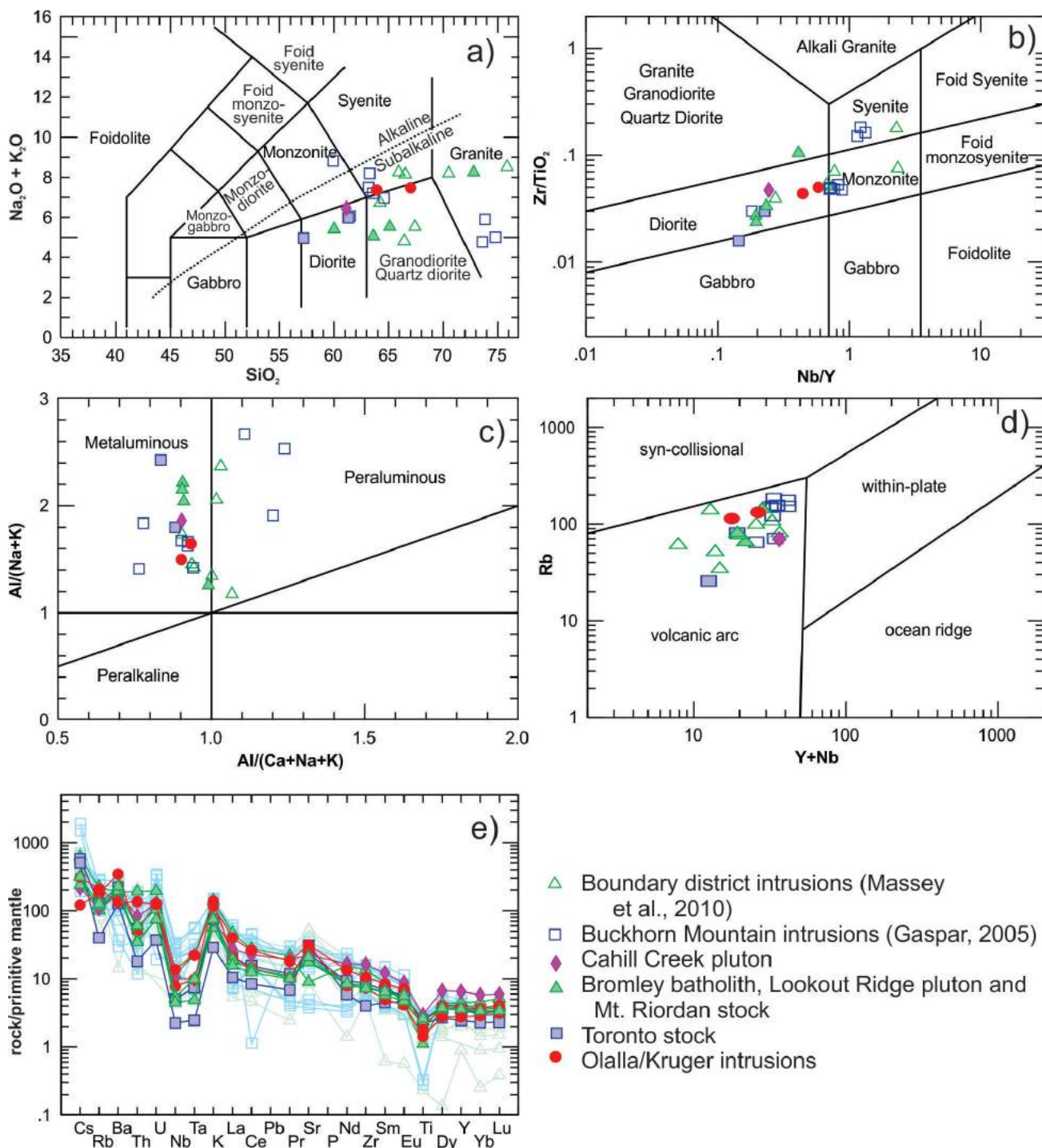


**Figure 5.** Whole-rock geochemistry of Early and Middle Jurassic intrusive rock units from the Hedley–Apex Mountain area, together with data from intrusions in the Greenwood area (from Massey et al., 2010) and intrusions associated with the Buckhorn Au-bearing skarn in northern Washington state (from Gaspar, 2005). Greenwood and Buckhorn Mountain intrusive samples are shown in pale green and blue symbols, respectively, in part (e). References for the various discriminant plots are **a)** Irvine and Baragar (1971) and Le Bas et al. (1986); **b)** Maniar and Piccoli (1989); **c)** Winchester and Floyd (1977); **d)** Pearce et al. (1984); **e)** Sun and McDonough (1989).

trict and the Buckhorn Mountain area, for which samples ranged from diorite to granite, with several samples plotting well into the syenite field (Figure 5a). Only one of the samples, from the Buckhorn Mountain area, yielded an alkaline composition according to the Irvine and Baragar (1971) discriminant plot.

Samples analyzed in this study fall in a relatively tight cluster on a revised Winchester and Floyd (1977) immobile trace-element ratio plot (Nb/Y versus Zr/TiO<sub>2</sub>; Figure 5b). The composition of the Hedley intrusions plots as gabbro to diorite, whereas most of the remaining samples fall in the diorite field, with a single sample plotting slightly into the granite/granodiorite/quartz diorite field. As with the previous plot, much more compositional scatter was displayed by the Jurassic intrusive rocks from the Boundary district (Greenwood area) and Buckhorn Mountain area.

All of the samples from this study fall well within the meta-aluminous field on a Shand-type plot (Maniar and Piccoli, 1989; Figure 5c). There is much more scatter in the Boundary district and Buckhorn Mountain sample suites, with several samples showing peraluminous compositions. It is unclear whether this represents the original geochemistry or may, in part, be an artifact of superimposed hydrothermal alteration on some of the samples.

All samples from this study, as well as those from the Boundary district and Buckhorn Mountain area, fall within the volcanic-arc field on a Rb versus Y+Nb discriminant plot of Pearce et al. (1984; Figure 5d).

On spider diagrams depicting ratios of high-field-strength and rare-earth element concentrations to primitive-mantle-normalized trace-element values (Sun and McDonough, 1989; Figure 5e), samples from this study show a limited amount of scatter, with all samples characterized by Nb and Ti troughs that are typical of subduction-related magmas. Patterns for samples from the Boundary district and Buckhorn Mountain area are generally similar to those in the study area, although they show a somewhat greater degree of scatter.

Despite their considerable age range, geochemical signatures of Jurassic intrusive rocks in the Hedley–Apex Mountain area, and areas to the east that were investigated in this study, show a surprisingly narrow compositional range. Analyses of the syenite phase of the Olalla pluton and the Kruger syenite showed that, in fact, these bodies are, at best, only weakly alkaline. Combined with geochemical analyses of well-dated igneous rocks from the Boundary district and Buckhorn Mountain area, the new analytical results appear to indicate that Jurassic intrusions in the southern Quesnel terrane of southern BC and adjacent parts of northern Washington state reflect sporadic magmatism within a continental magmatic-arc setting over a period of approximately 40 million years.

## Pb-Isotopic Studies of Intrusions and Skarn Mineralization

Lead isotopes can be an effective tool for evaluating the source(s) of metals contained within various styles of mineral deposits. This approach can be particularly useful for intrusion-related mineralization, because one can determine the Pb-isotopic composition of any magmatic fluids that might have been generated during crystallization of the magma by analyzing igneous feldspar (which incorporates significant concentrations of Pb but no U or Th during crystallization, and hence preserves the initial magmatic Pb-isotopic ‘signature’). The Pb-isotopic signature can be established for intrusions of various ages and compositions in the study area, and then compared to the Pb-isotopic compositions of sulphides in the mineralization being investigated (as these sulphides also concentrate Pb but little or no U or Th, and thus preserve the isotopic composition from the time of formation). Ideally, there should be a close match between the Pb-isotopic composition of the mineralization and the causative intrusion(s). In the absence of direct-age information for the mineralization, this can provide indirect information regarding the age of mineralization and also identify the specific intrusion, or intrusive suite, that is preferentially associated with the mineralization. However, there are numerous factors that complicate this simple model. Hydrothermal fluids that precipitate sulphides in vein-style mineralization may not interact significantly with wallrocks during fluid flow and therefore commonly (but not always) yield Pb-isotopic compositions that are close to those of the source reservoir(s). However, intrusion-related mineralization that involves a significant amount of wallrock replacement, such as skarns, mantos or high-sulphidation epithermal veins, commonly shows an array of Pb-isotopic compositions that reflects variable mixtures between the magmatic Pb component and Pb derived from the wallrocks themselves. The nature of these mixing arrays depends on several factors, including the Pb contents and extent of compositional ranges between the mineralizing fluids and the wallrocks that are being replaced.

Lead-isotopic compositions were determined for all but one (Olalla pluton) of the intrusive phases that were dated in this study, as well as for a suite of sulphide samples from the Nickel Plate mine and other skarn deposits in the Hedley–Apex Mountain area, and from the Phoenix mine in the Greenwood area. Analytical data are listed in Table 4 and are plotted on <sup>208</sup>Pb/<sup>206</sup>Pb versus <sup>207</sup>Pb/<sup>206</sup>Pb, and <sup>207</sup>Pb/<sup>204</sup>Pb versus <sup>206</sup>Pb/<sup>204</sup>Pb plots in Figure 6. Two analyses of very scarce galena from the Nickel Plate mine that were reported by Godwin et al. (1988) are also plotted.

Most of the igneous feldspar samples clustered reasonably well on both of the Pb/Pb plots, although several analyses yielded relatively radiogenic compositions, especially in

$^{207}\text{Pb}/^{204}\text{Pb}$  versus  $^{206}\text{Pb}/^{204}\text{Pb}$  space (Figure 6b). This likely reflects a combination of fractionation error and  $^{204}\text{Pb}$  measurement error. This latter source of error is not present in the  $^{208}\text{Pb}/^{206}\text{Pb}$  versus  $^{207}\text{Pb}/^{206}\text{Pb}$  plot (Figure 6a), which shows a tighter clustering of analyses for the igneous feldspar samples. The Toronto stock feldspar analysis is somewhat more radiogenic than most of the other feldspar samples. This may be because this is the only sample for which plagioclase was analyzed rather than K-feldspar (K-feldspar was not present in the sample). Igneous plagioclase typically has substantially lower Pb contents than K-feldspar. Therefore, plagioclase analyses are more susceptible to significant disturbance caused by the addition of even minor amounts of radiogenic Pb resulting from radiogenic ingrowth from minor contained U and/or Th.

Most of the Nickel Plate sulphides (particularly the two galena samples) yielded Pb-isotopic compositions that are close to those from feldspar samples collected in the vicinity of the deposit; however, two of the samples yielded considerably more radiogenic compositions, probably as a result of mixing with radiogenic Pb contained within the hostrocks. All of the sulphides from the Phoenix mine at Greenwood yielded compositions that are substantially

more radiogenic than those of feldspar samples from any of the Jurassic intrusions in the region that have been analyzed thus far. There are no likely causative intrusions in the vicinity of the Phoenix skarn deposit, so fluids responsible for forming the skarn may have travelled somewhat farther from the source and/or interacted more extensively with hostrocks containing a higher concentration of radiogenic Pb than in the Hedley–Apex Mountain area. Alternatively, the mineralizing fluids responsible for formation of the Phoenix skarn may have contained lower concentrations of Pb and therefore would have been more strongly modified by mixing of radiogenic Pb from the wallrocks. However, the measured Pb-isotopic compositions of sulphides in the Nickel Plate and Phoenix skarn deposits are consistent, in general, with the deposits having formed through interaction between metalliferous magmatic fluids that evolved from the Jurassic intrusions and various calcareous hostrocks. Unfortunately, the Pb-isotopic compositions of igneous feldspar samples from the various intrusive units were not sufficiently distinct to provide a ‘fingerprint’ that could be used to determine which intrusion (or intrusive suite) was genetically related to the mineralization.

**Table 4.** Results of Pb-isotopic analyses for intrusive rock units from the Hedley–Apex Mountain area and sulphide minerals from the Nickel Plate mine (Hedley–Apex Mountain area) and Phoenix mine (Greenwood area).

Sample no.	Mineral	Occurrence	Source	$^{208}\text{Pb}/^{204}\text{Pb}$	$1\sigma$ (%)
Hedley-1	Arsenopyrite+pyrite	Disseminated sulphides in massive diopside-garnet skarn, Hedley north pit	1	19.172	0.08
Hedley-2	Pyrrhotite	Disseminated and vein sulphides in massive diopside skarn, Hedley glory hole	1	18.785	0.04
Hedley-Sunny-side-1	Arsenopyrite	Massive arsenopyrite in skarn, Sunnyside deposit	1	18.710	0.03
Hedley-Sunny-side-2	Arsenopyrite	Massive arsenopyrite in skarn, Sunnyside deposit	1	18.782	0.01
Hedley-2-8N stope	Arsenopyrite	Massive arsenopyrite, Hedley 8N stope	1	18.928	0.04
Phoenix-1	Chalcopyrite+pyrite	Lower ore zone	1	19.207	0.06
Phoenix-2	Chalcopyrite	Chalcopyrite in quartz, southeast end of open pit	1	19.251	0.08
Phoenix-3	Chalcopyrite	Chalcopyrite-hematite-quartz ore	1	22.022	0.05
Phoenix-4	Pyrite	High-grade skarn	1	19.207	0.02
Phoenix-5	Chalcopyrite	High-grade skarn	1	19.468	0.01
Phoenix-6	Pyrite	Upper ore zone, east side of Phoenix open pit	1	19.000	0.01
30302-002 *	Galena	Nickel Plate skarn	2	18.724	0.01
30302-003 *	Galena	Nickel Plate skarn	2	18.731	0.03
10-M-07	Feldspar	Offshoot of Toronto stock	3	19.001	0.35
10-M-06	Feldspar	Offshoot of Toronto stock	3	18.970	0.05
10-M-04	Feldspar	Bromley batholith	3	18.807	0.28
10-M-05	Feldspar	Lookout Ridge pluton	3	18.731	0.03
10-M-05	Feldspar	Lookout Ridge pluton	3	18.782	0.01
10-M-33	Feldspar	Mount Riordan pluton	3	18.736	0
10KL-115	Feldspar	Bromley batholith?	3	19.184	0.09
10KL-115 (repl.)	Feldspar	Bromley batholith?	3	18.712	0.12
10-M-08	Feldspar	Cahill Creek stock	3	18.729	0.04
10KL-111	Feldspar	Kruger syenite	3	18.711	0.01
10-M-10	Feldspar	Olalla pluton	3	19.081	0.3

Sample and data sources: 1, University of British Columbia mineral deposit sample collection (exact locations uncertain); 2, Godwin et al. (1988); 3, this study.

## Implications for Timing of Magmatism and Skarn Formation in the Southern Quesnel Terrane

Results of this study, together with those of previous work done in the Boundary Creek mineral district by Massey et al. (2010) and the Buckhorn Mountain area by Gaspar (2005) and Scorrar (2012), demonstrate that magmatism in this part of the southern Quesnel terrane occurred sporadically over an extended period of at least 40 m.y. (from ca. 197 to 157 Ma). Geochemical compositions of these intrusions are consistent with all of this magmatism having occurred within a continental or continental-margin volcanic-arc setting. The Jurassic intrusions were emplaced into an older arc assemblage (the Nicola Group), which itself was built on middle and late Paleozoic metasedimentary and metavolcanic basement rocks. The age of the formation of Au and Au-Cu skarn mineralization in the Hedley–Apex Mountain area and the Boundary district remains unresolved by direct dating methods. Scorrar (2012) has shown that the Buckhorn Au skarn in the Buckhorn Mountain area formed between 168 and 162 Ma. Although there are close similarities between the Buckhorn skarn and deposits in the Hedley area, Ray et al. (1996) provided compelling evidence, based on field observations in the Hedley area, that

skarn deposits there are considerably older than the Buckhorn deposit and are likely related to the 196 Ma Toronto stock. It is unclear whether the Mount Riordan garnet skarn (Figure 2) formed at the same time as the better-studied Au skarns in the area. Developing a more robust exploration model for new Au-Cu skarn deposits in this area will require further work in both the Hedley and Boundary Creek mineral district areas to better constrain the age of the skarns and identify the specific intrusive events with which the skarn deposits are associated.

### Acknowledgments

This project was funded by Geoscience BC. The author thanks J. Monger and K. Lucas for their assistance with sample collection, and M. Allan, who provided a review of an earlier version of the manuscript.

### References

- BC Geological Survey 2013: MINFILE BC mineral deposits database; BC Ministry of Energy and Mines, BC Geological Survey, URL <<http://minfile.ca/>> [November 2013].
- Beranek, L.P. and Mortensen, J.K. (2011): The timing and provenance record of the Late Permian Klondike orogeny in

Table 4 (continued)

Sample no.	$^{207}\text{Pb}/^{204}\text{Pb}$	$1\sigma$ (%)	$^{206}\text{Pb}/^{204}\text{Pb}$	$1\sigma$ (%)	$^{208}\text{Pb}/^{206}\text{Pb}$	$1\sigma$ (%)	$^{207}\text{Pb}/^{206}\text{Pb}$	$1\sigma$ (%)
Hedley-1	15.656	0.08	38.446	0.08	0.8166	0.007	2.0053	0.002
Hedley-2	15.613	0.04	38.395	0.04	0.8311	0.009	2.0440	0.005
Hedley-Sunny-side-1	15.606	0.02	38.404	0.03	0.8341	0.005	2.0526	0.004
Hedley-Sunny-side-2	15.615	0.01	38.391	0.01	0.8313	0.006	2.0440	0.005
Hedley-2-8N stope	15.613	0.04	38.391	0.04	0.8248	0.006	2.0282	0.007
Phoenix-1	15.655	0.06	38.652	0.06	0.8151	0.007	2.0124	0.006
Phoenix-2	15.576	0.08	38.415	0.08	0.8091	0.019	1.9955	0.010
Phoenix-3	15.791	0.05	38.675	0.05	0.7170	0.012	1.7562	0.013
Phoenix-4	15.682	0.02	38.918	0.02	0.8165	0.010	2.0262	0.008
Phoenix-5	15.625	0.01	38.407	0.01	0.8026	0.005	1.9729	0.008
Phoenix-6	15.647	0.01	38.523	0.01	0.8235	0.001	2.0275	0.002
30302-002 *	15.605	0.02	38.354	0.02	0.8334	0.01	2.0485	0.01
30302-003 *	15.607	0.03	38.368	0.04	0.8332	0.01	2.0483	0.01
10-M-07	15.553	0.21	38.858	0.47	0.8186	0.28	2.0451	0.311
10-M-06	15.692	0.05	38.667	0.05	0.8272	0.019	2.0383	0.02
10-M-04	15.652	0.28	38.507	0.28	0.8323	0.04	2.0475	0.03
10-M-05	15.578	0.03	38.356	0.03	0.8317	0.007	2.0478	0.003
10-M-05	15.632	0	38.511	0.01	0.8323	0.003	2.0505	0.002
10-M-33	15.601	0	38.383	0	0.8326	0.001	2.0486	0.002
10KL-115	15.631	0.09	38.678	0.09	0.8148	0.013	2.0162	0.012
10KL-115 (repl.)	15.694	0.12	38.484	0.12	0.8387	0.015	2.0566	0.019
10-M-08	15.609	0.04	38.406	0.04	0.8334	0.01	2.0506	0.011
10KL-111	15.585	0	38.339	0.01	0.8329	0.002	2.049	0.001
10-M-10	15.531	0.29	38.435	0.31	0.8139	0.061	2.0143	0.068

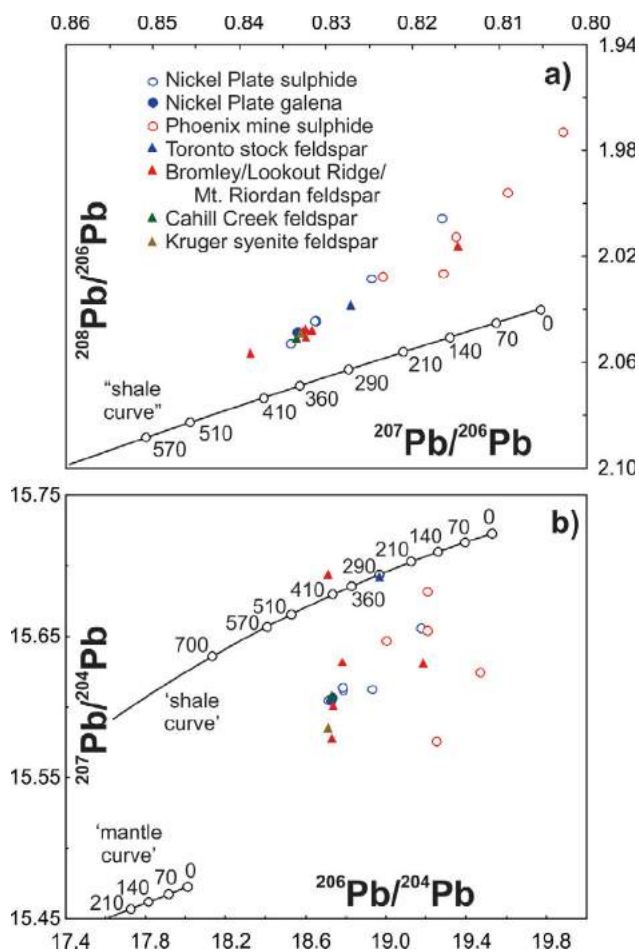


**Figure 6.** Lead-isotopic compositions for sulphide minerals from the Nickel Plate mine in the Hedley–Apex Mountain area and the Phoenix mine in the Greenwood area, as well as for igneous feldspar samples from dated Early and Middle Jurassic intrusive rocks in the Hedley–Apex Mountain area and the Kruger syenite. Analyses of galena from the Nickel Plate mine are from Godwin et al. (1988). The ‘shale curve’ is a model growth curve for the evolution of Pb-isotopic compositions in the miogeocline of the North American Cordillera (from Godwin and Sinclair, 1982). The ‘mantle curve’ is a model growth curve for Pb-isotopic evolution in the mantle (from Doe and Zartman, 1979).

northwestern Canada and arc-continent collision along western North America; *Tectonics*, v. 30, p. TC5017.

Bostock, H.S. (1940): *Geology, Olalla*; Geological Survey of Canada, Map 628A, scale 1:63 360.

Doe, B.R. and Zartman, R.E. (1979): *Plumbotectonics, the Phanerozoic*; in *Geochemistry of Hydrothermal Ore Deposits* (Second Edition), H.L. Barnes (ed.), John Wiley and Sons, p. 22–70.

Ettlinger, A.D., Meinert, L.D. and Ray, G.E. (1992): *Skarn evolution and hydrothermal fluid characteristics in the Nickel Plate deposit, Hedley district, British Columbia*; *Economic Geology*, v. 87, p. 1541–1565.

Gaspar, L.M.G. (2005): *The Crown Jewel gold skarn deposit*; unpublished Ph.D. thesis, Washington State University, 325 p.

Godwin, C.I. and Sinclair, A.J. (1982): *Average lead isotope growth curves for shale-hosted zinc-lead deposits, Canadian Cordillera*; *Economic Geology*, v. 77, p. 675–690.

Godwin, C.I., Gabites, J.E. and Andrew, A. (1988): *Leadtable—a galena lead isotope database for the Canadian Cordillera, with a guide to its use by explorationists*; BC Ministry of Energy and Mines, Geological Survey Branch, Paper 1988-4, 188 p.

Irvine, T.N. and Baragar, W.R.A. (1971): *A guide to the chemical classification of the common volcanic rocks*; *Canadian Journal of Earth Sciences*, v. 8, p. 523–548.

Le Bas, M.J., Le Maitre, R.W., Streckeisen, A. and Zanettin, B. (1986): *A chemical classification of volcanic rocks based on the total alkali-silica diagram*; *Journal of Petrology*, v. 27, p. 745–750.

Maniar, P.D. and Piccoli, P.M. (1989): *Tectonic discrimination of granitoids*; *Geological Society of America, Bulletin*, v. 101, p. 635–643.

Massey, N.W.D., Gabites, J.E., Mortensen, J.K. and Ullrich, T.D. (2010): *Boundary Project: geochronology and geochemistry of Jurassic and Eocene intrusions, southern British Columbia (NTS 082E)*; in *Geological Fieldwork 2009*, BC Ministry of Energy and Mines, BC Geological Survey, Paper 2010-1, p. 1–16.

Mortensen, J.K., Lucas, K., Monger, J.W.H. and Cordey, F. (2011): *Geological investigations of the basement of the Quesnel terrane in southern British Columbia (NTS 082E, F, L, 092H, I): progress Report*; in *Geoscience BC Summary of Activities 2010, Report 2011-1*, p. 133–142.

Pearce, J.A., Harris, N.B.W. and Tindle, A.G. (1984): *Trace element discrimination diagrams for the tectonic interpretation of granitic rocks*; *Journal of Petrology*, v. 25, p. 956–983.

Ray, G.E. and Dawson, G.L. (1994): *The geology and mineral deposits of the Hedley gold skarn district, southern British Columbia*; BC Ministry of Energy and Mines, BC Geological Survey, Bulletin 87, 156 p.

Ray, G.E., Dawson, G.L. and Webster, I.C.L. (1996): *The stratigraphy of the Nicola Group in the Hedley district, British Columbia, and the chemistry of its intrusions and Au skarns*; *Canadian Journal of Earth Sciences*, v. 33, p. 1105–1126.

Scorror, B.A. (2012): *The age and character of alteration and mineralization at the Buckhorn gold skarn, Okanogan County, Washington, USA*; M.Sc. thesis, University of British Columbia, 204 p.

Sun, S.S. and McDonough, W.F. (1989): *Chemical and isotopic systematics of oceanic basalts: implications for mantle composition and processes*; in *Magmatism in the Ocean Basins*, A.D. Saunders and M.J. Norry (ed.), Geological Society, Special Publication 42, p. 313–345.

Tafti, R., Mortensen, J.K., Lang, J.R., Rebagliati, M., and Oliver, J.L. (2009): *Jurassic U-Pb and Re-Os ages for the newly discovered Xietongmen Cu-Au porphyry district, Tibet, PRC: implications for metallogenic epochs in the southern Gangdese belt*; *Economic Geology*, v. 104, p. 127–136.

Winchester, J.A. and Floyd, P.A. (1977): *Geochemical discrimination of different magma series and their differentiation products using immobile elements*; *Chemical Geology*, v. 20, p. 325–343.

# U-Pb Dates for the Nelson and Bayonne Magmatic Suites in the Salmo-Creston Area, Southeastern British Columbia: Tectonic Implications for the Southern Kootenay Arc (Parts of NTS 082F/02, /03, /06, /07)

E.R. Webster, Department of Geoscience, University of Calgary, Calgary, AB, [erwebste@ucalgary.ca](mailto:erwebste@ucalgary.ca)

D.R.M. Pattison, Department of Geoscience, University of Calgary, Calgary, AB

---

Webster, E.R. and Pattison, D.R.M. (2014): U-Pb dates for the Nelson and Bayonne magmatic suites in the Salmo-Creston area, southeastern British Columbia: tectonic implications for the southern Kootenay Arc (parts of NTS 082F/02, /03, /06, /07); in Geoscience BC Summary of Activities 2013, Geoscience BC, Report 2014-1, p. 99–114.

## Introduction

This paper presents new U-Pb zircon dates for igneous intrusions belonging to the Nelson and Bayonne magmatic suites between Creston and Salmo in southeastern British Columbia. This area experienced magmatism, metamorphism and deformation from the Early Jurassic through to the Eocene (Archibald et al., 1983, 1984; Brown et al., 1995; Moynihan and Pattison, 2013; Webster and Pattison, 2013). Determining the age of these intrusions provides constraints on the tectonometamorphic evolution of the area and associated mineralization events.

## Regional Geology

The region between Nelson, Salmo and Creston in southeastern BC straddles the tectonic interface between the ancestral North American margin and pericratonic rocks (including Quesnellia) that formed outboard of the margin to the west (Monger et al., 1982; Unterschutz et al., 2002; Figure 1). The accretion and juxtaposition of these rocks occurred during Cordilleran orogenesis from the Early Jurassic through to the Eocene. Three structural domains meet within this area: the Purcell Anticlinorium, the Priest River Complex and the Kootenay Arc (Figure 1). The Purcell Anticlinorium is a large, northerly plunging, Mesozoic fold structure comprising rift-related sedimentary rocks from the Mesoproterozoic Belt-Purcell and Neoproterozoic Windermere supergroups (Price, 2000). The Kootenay Arc occurs on the western flank of the Purcell Anticlinorium and is a narrow arcuate structural feature that is characterized by an increase in metamorphic grade and structural complexity, and a decrease in stratigraphic age compared to the Purcell Anticlinorium (Warren, 1997). The Priest River Complex (PRC) is an Eocene metamorphic core complex that exposes midcrustal rocks and Archean basement. It oc-

curs mainly in Idaho and Washington, but its northerly termination occurs in the study area. The PRC is bounded by two normal fault systems: the west-dipping eastern Newport fault and east-dipping Purcell Trench fault (Rhodes and Hyndman, 1984; Doughty and Price, 1999, 2000; Figure 1).

The bedrock geology of the study area consists primarily of deformed and metamorphosed sedimentary strata. Mesoproterozoic Belt-Purcell Supergroup strata outcrop in the eastern portion of the study area. To the west they are unconformably overlain by the Neoproterozoic Windermere Supergroup (Devlin and Bond, 1988; Warren, 1997; Figure 1). The two supergroups are dominantly composed of clastic, rift-related sedimentary rocks in addition to minor mafic volcanic rocks and sills. Unconformably overlying the Windermere Supergroup, and exposed in the western part of the study area, are early Paleozoic coarse clastic and carbonate rocks.

Numerous granitoid intrusions intrude all of these sedimentary rocks (Figures 2, 3). They range in age from Middle Jurassic to Eocene and are part of larger intrusive suites that extend across southeastern BC (Ghosh, 1995a). Intrusive rocks of the Nelson suite (Nelson batholith, Kuskanax batholith, Bonnington pluton, Trail pluton, Mackie pluton, Mine and Wall stocks) were emplaced between ca. 179 and 159 Ma (Ghosh, 1995a; Evenchick et al., 2007). The rocks of the Nelson intrusive suite are I-type granitoids that range in composition from tonalite to granite (Figure 1; Little, 1960; Ghosh and Lambert, 1995). The Middle Jurassic intrusions typically have staurolite-bearing contact aureoles and were emplaced at depths ranging from 12 to 18 km (Ghent et al., 1991; Pattison and Vogl, 2005). These intrusive suites formed in a magmatic arc, above an east-dipping subduction zone (Ghosh, 1995b).

Quesnel Lake (Figure 1; Quesnel Lake is situated 300 km northwest of Salmon Arm, BC; Logan, 2001). The Bayonne suite is primarily peraluminous, containing two-mica granites with less significant subalkalic granodiorites, aplites and pegmatites (Logan, 2001). Cordierite-bearing

---

**Keywords:** U-Pb LA-MC-ICP-MS, Nelson plutonic suite, Bayonne magmatic suite, Kootenay Arc, Purcell Anticlinorium

This publication is also available, free of charge, as colour digital files in Adobe Acrobat® PDF format from the Geoscience BC website: <http://www.geosciencebc.com/s/DataReleases.asp>.

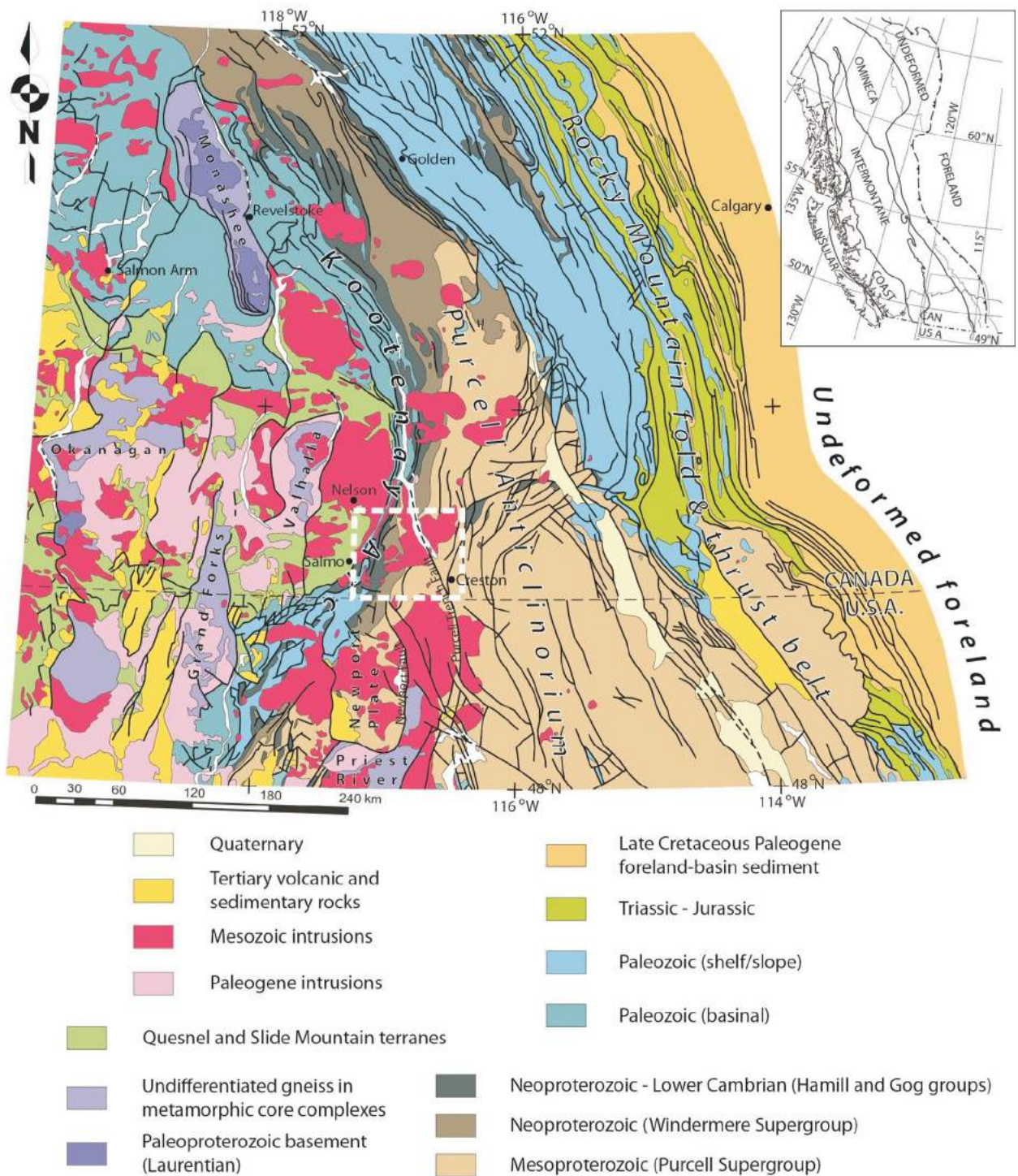


**Figure 1.** Regional geology of the southeastern Canadian Cordillera. Eocene core complexes are labelled on the map as Priest River, Okanagan, Grand Forks, Monashee and Valhalla. The study area is highlighted by the white dashed square. Map modified from Moynihan and Pattison (2013), originally after Wheeler and McFeely (1991).

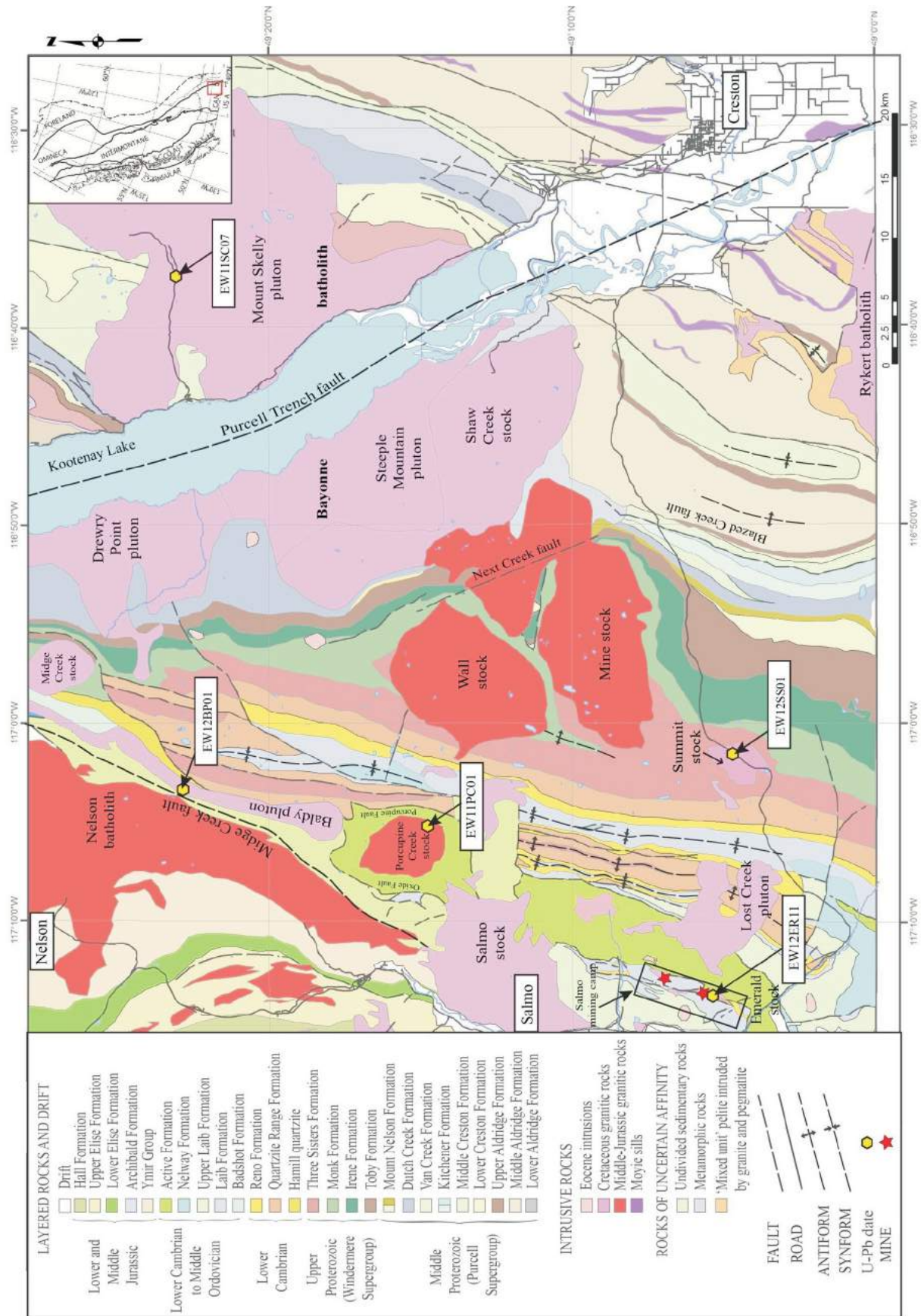


**Figure 2.** Map showing igneous intrusive bodies within the study area, modified after Webster and Pattison (2013) and compiled from Reesor (1996), Höy and Dunne (1998), Paradis et al. (2009) and Glombick et al. (2010). The Kuskanax batholith, Bonnington pluton, Trail pluton, Mackie pluton are not included on this map. The yellow hexagons represent sample sites used for U-Pb analysis. The two minesites represent the Emerald (south) and Dodger (north) mines of the Salmos mining camp.

contact metamorphic mineral assemblages found adjacent to plutons of the Bayonne suite suggest emplacement depths of less than 12 km (Archibald et al., 1983; Webster and Pattison, 2013). What is referred to as the ‘Bayonne batholith’ (Figure 2) comprises multiple phases: the Mount Skelly pluton, the Shaw Creek stock, Heather Creek pluton, Drewry Point pluton and Steeple Mountain plutons (Leclair, 1988). Existing geochronology by Davis (1995) and Brown et al. (1999) have shown that individual phases range in age from 99 (Steeple Mountain) to 76 Ma (Shaw Creek).

## Description of Granitoid Intrusive Rocks and their Tectonic Setting

### Porcupine Creek Stock

The Porcupine Creek stock (PCS) is situated between the tail of the Nelson batholith and the Jurassic Mine and Wall stocks and occupies approximately 15 km<sup>2</sup> (Figures 2, 3). It was emplaced into the Ordovician Active Formation and is bounded on the east and west sides by the Porcupine Creek and Oxide faults, respectively (McAllister, 1951; Einarsen, 1994). The Porcupine Creek fault is a westward-verging thrust fault that dips steeply to the east and strikes north-northeast, and is likely a continuation of the Black Bluff fault. The Oxide fault is an overturned, eastward-verging thrust fault that dips steeply to the east and strikes north-northeast, and is an extension of the Argillite fault to the southwest (Einarsen, 1994).

The PCS has no discernible tectonic fabric and crosscuts regional Jurassic fold structures (Figure 2). The intrusion and its contact aureole also appear to have been unaffected by Cretaceous deformation and Barrovian metamorphism in the footwall of the Midge Creek fault (Webster and Pattison, 2013). The PCS has developed a low pressure (~3.0–3.5 kbar) cordierite-andalusite-biotite contact aureole, similar to the southern part of the Nelson batholith aureole (Pattison and Vogl, 2005).

The sample is composed of a K-feldspar–phyric, biotite-hornblende quartz monzodiorite (Figure 4a). Plagioclase laths and K-feldspar crystals are typically 3–7 mm and form subhedral to anhedral grains. The feldspars are typically intergrown with quartz and the mafic phases, with individual quartz crystals typically <1 mm in size. Abundant biotite and hornblende form ragged crystals up to 2 mm in size. Clinopyroxene crystals are sparse and typically less than 1 mm in diameter. Accessory magnetite and apatite are common, with abundant ~1 mm size titanite crystals. Sericitization of feldspar, and minor alteration of biotite and hornblende to chlorite, is common in this monzodiorite and other intrusive rocks in this study.

### Baldy Pluton

The Baldy pluton is an elongate intrusive body that is parallel to the regional structural trend and is situated in the footwall of the Midge Creek fault, adjacent to the tail of the Nelson batholith (Figure 2). It occupies approximately 35 km<sup>2</sup> and was emplaced into regionally metamorphosed Cambrian to Ordovician strata. It formed prior to, or during, penetrative deformation (Leclair et al., 1993). The intrusion is foliated and has a strong mineral lineation that is parallel to those in the adjacent metamorphosed sedimentary rocks. The pluton consists of a coarse-grained, K-feldspar–phyric, biotite-clinopyroxene granodiorite with fine-grained recrystallized quartz, plagioclase and secondary epidote defining a strong lineation. The K-feldspar phenocrysts are locally megacrystic, anhedral and typically have a crystal size between 2 and 5 mm (Figure 4b). Biotite and secondary muscovite crystals are typically 1 mm in size. Accessory magnetite and titanite are common.

### Mount Skelly Pluton

The Mount Skelly pluton is the eastern most phase of the Bayonne batholith and occurs on the eastern side of Kootenay Lake, occupying approximately 300 km<sup>2</sup>. It is situated in the hangingwall of the Purcell Trench fault (PTF) and has intruded the middle and upper Belt-Purcell Supergroup. The pluton has imparted a low pressure cordierite-andalusite-biotite contact aureole on the surrounding metasedimentary rocks (Webster and Pattison, 2013). The intrusion has no discernible tectonic fabric. The rock sampled is an equigranular, biotite-muscovite granite. The K-feldspar and plagioclase crystals are anhedral to euhedral and are typically 2–5 mm (Figure 4c). Abundant primary biotite and muscovite grains are 1–2 mm and comprise approximately 25% of the rock. Quartz grains are normally <1 mm but some larger grains exist (2–3 mm).

### Summit Stock

The Summit Stock is exposed over approximately 5 km<sup>2</sup> at the top of Kootenay Pass (Figure 2) and has intruded into coarse clastic rocks of the Neoproterozoic Three Sisters Formation. This intrusion and the Lost Creek pluton to the west have imparted a low pressure contact aureole on the surrounding low-grade country rocks. The mineral assemblage zonal sequence is cordierite, andalusite±cordierite and sillimanite±K-feldspar (Bjornson, 2012). The contact aureole envelopes both intrusions, with the highest grade mineral assemblages found between them, implying that the two intrusions may be connected at depth. The Summit stock has no tectonic fabric and is a biotite-muscovite granite (Figure 4d). Euhedral to subhedral plagioclase laths are up to 3 mm in size and occasionally show oscillatory zoning. The K-feldspar crystals are subhedral to anhedral and are typically 3–5 mm. Biotite and primary muscovite crystals are euhedral and are typically about 1 mm. Quartz

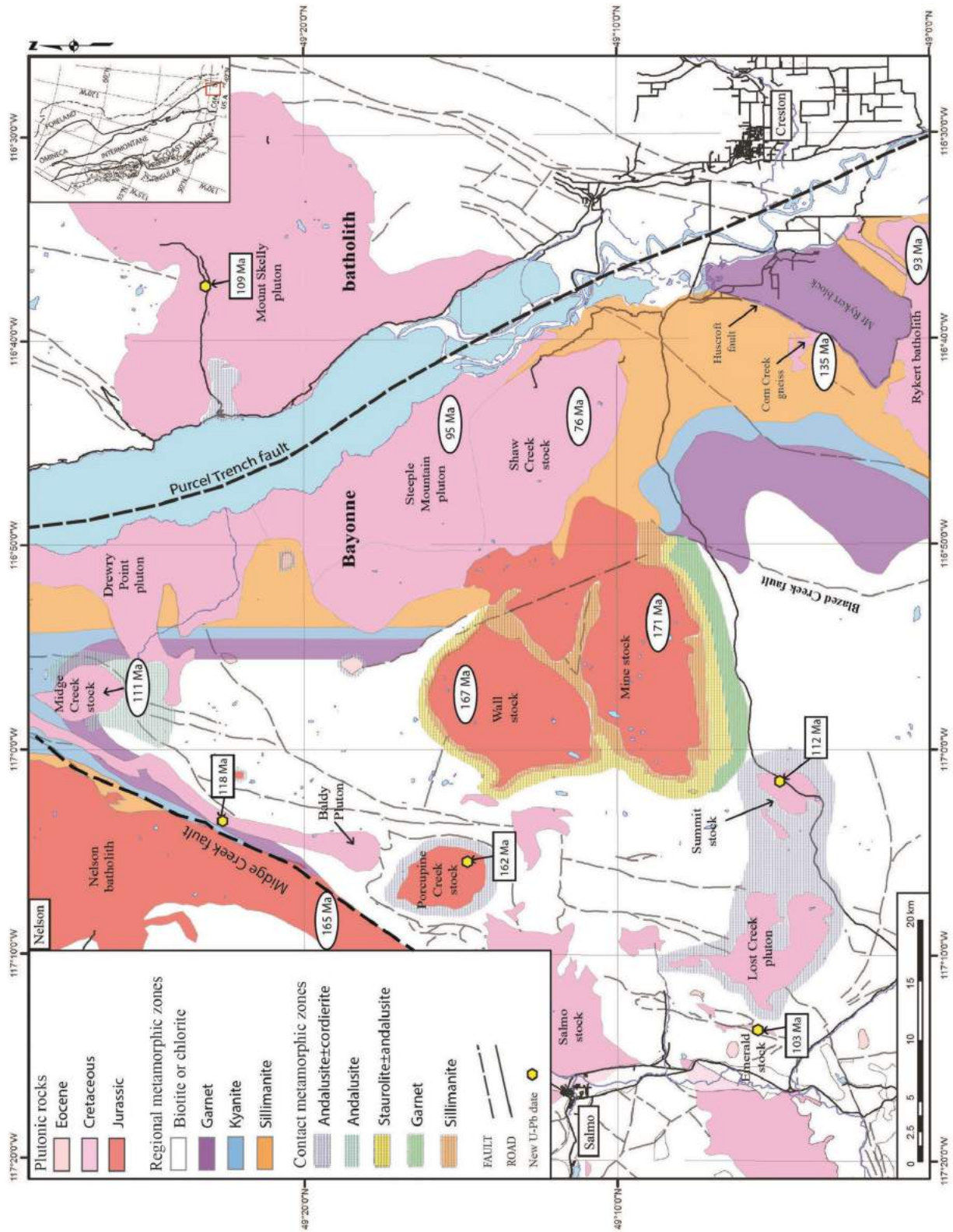


**Figure 3.** Metamorphic zones and plutonic rocks of the study area, compiled from Glover (1978), Archibald et al. (1983), Leclair (1988), Doughty et al. (1997) and new data. Areas with no shading are of low metamorphic grade. Rectangular boxes are new U-Pb dates from this study and those in oval-shaped boxes are existing ages from previous studies.

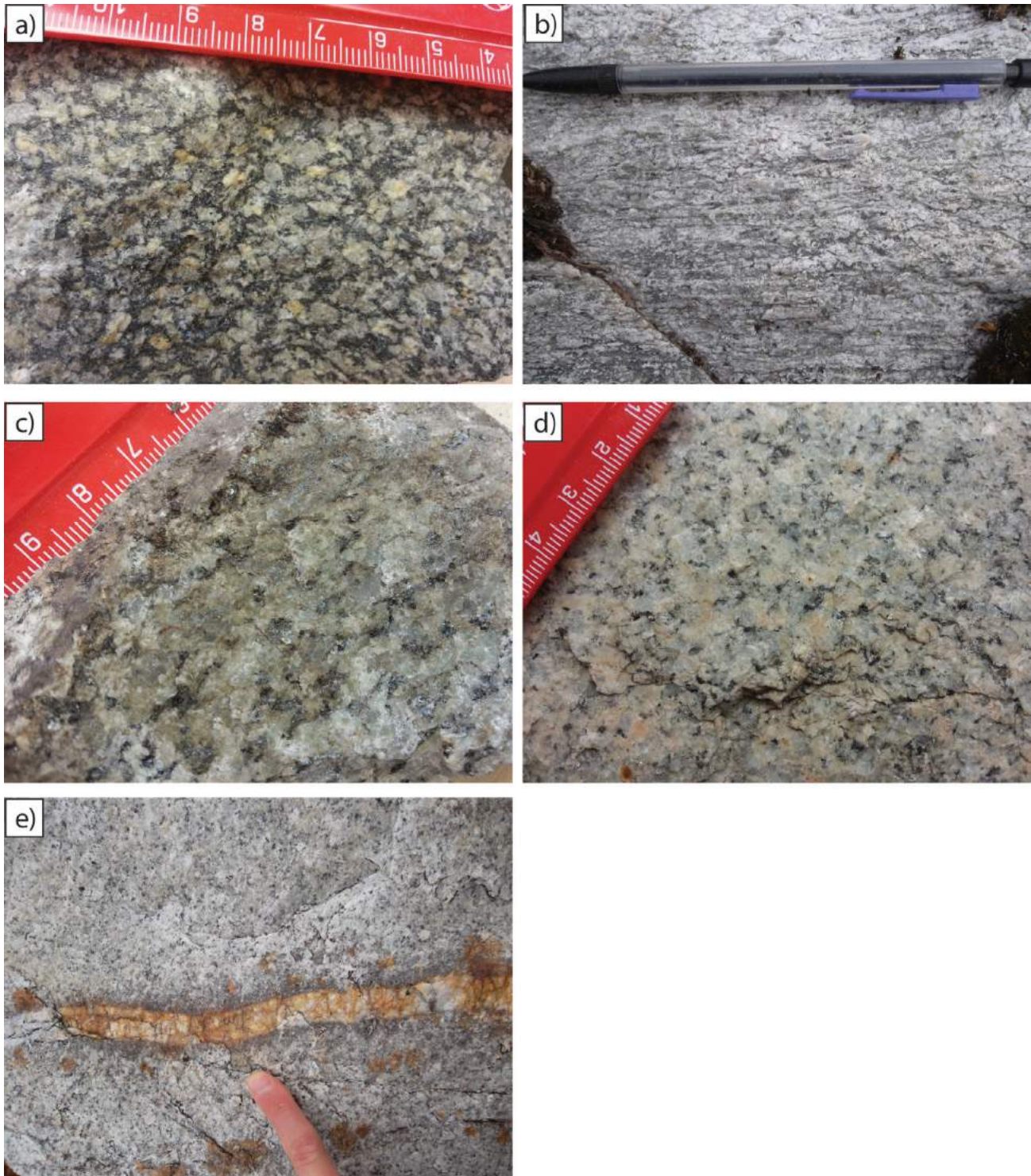


**Figure 4.** Field pictures of the various igneous intrusive rocks found throughout the study area: **a)** monzodiorite of the Porcupine Creek stock (PCS); **b)** lineated, granodiorite from the Baldy pluton; **c)** two-mica granite of the Mount Skelly pluton; **d)** biotite-muscovite granite of the Summit stock; **e)** biotite granite of the Emerald stock with mineralized quartz vein.

grains are typically 1–2 mm in size. There is accessory magnetite throughout the intrusion.

### Emerald Stock

The Emerald Stock crops out over approximately 0.4 km<sup>2</sup> and has intruded into the sedimentary rocks of the Cambrian Laib and Reno formations and also the Ordovician Active Formation, within the historic Salmo mining camp. The carbonate sedimentary rocks (Laib Formation), in contact with the Emerald stock, are typically altered, with rock types ranging from coarse marble to garnet-pyroxene skarn. The skarns are host to Mo-W mineralization, which was mined from the past-producing Emerald and Dodger mines (1.6 million tons grading 0.76% W, Giroux and Grunenberg, 2009; Figure 2). The intrusion is an undeformed, equigranular biotite-granite. Plagioclase and K-feldspar crystals are subhedral to anhedral and are typically about 1 mm (Figure 4e). Biotite phenocrysts are ragged and typically 2–3 mm in diameter, although they have been almost completely replaced by chlorite, with secondary rutile. Accessory magnetite occurs throughout the intrusion.

### Analytical Techniques

One sample from each intrusion was collected for U-Pb zircon isotopic age dating at the Radiogenic Isotope Facility (RIF) in the Department of Earth and Atmospheric Sciences, at the University of Alberta. Zircon grains were separated from samples using standard magnetic and heavy liquid separation techniques at the Apatite to Zircon Inc. laboratories (Viola, Idaho). The zircon separates were mounted in 1 cm<sup>2</sup> epoxy pucks that were subsequently ground down to expose the internal structure of the zircon, before being polished for analysis. The pucks were washed in 5.5M HNO<sub>3</sub> at 21°C for 20 seconds to minimize surface Pb contamination.

Prior to U-Pb dating, cathodoluminescence (CL) images were obtained using a Gatan MonoCL4 Elite detector attached to a FEI Quanta 250 FEG field emission scanning electron microscope at the Department of Geoscience, University of Calgary. Laser-ablation inductively coupled plasma–mass spectrometry (LA-ICP-MS) analyses were acquired with a New Wave UP-213 Nd:YAG laser ablation system in conjunction with a Nu Plasma multiple-collector, inductively coupled plasma–mass spectrometry (MC-ICP-MS) instrument. The latter is equipped with a collector block including 12 Faraday collectors and 3 ion counters (Simonetti et al., 2005) allowing static collection of both U and Pb isotopes. The laser diameter was 30 µm with a laser frequency of 4 Hz and ~3 J/cm<sup>2</sup> energy density. Data were collected over a 30 second cycle in 1 second increments. An in-house monazite standard from Madagascar with a <sup>206</sup>Pb/<sup>238</sup>U age of 517.9 Ma was used as a primary calibration ref-

erence. This has been dated by isotope dilution–thermal ionization mass spectrometry (ID-TIMS; Heaman, unpublished data) and is the same as that used by Simonetti et al. (2006).

### Results

The U-Pb isotopic data are shown in Table 1 for five plutonic rocks from the study area. Isotopic ratios are uncorrected for common Pb, and errors are reported at the 2σ level. Inherited cores were observed in all five samples and they consistently yielded older dates that hindered the determination of the crystallization age (Figure 5). As a result of this common feature, multiple analyses were excluded from each sample. Analyses containing high common Pb values, highly discordant ages and obvious outliers were discarded. After data reduction, weighted mean <sup>206</sup>Pb/<sup>238</sup>U ages and Tera-Wasserburg U-Pb concordia plots (Tera and Wasserburg, 1972) were calculated using Isoplot v. 3.0 (Ludwig, 2003).

### Porcupine Creek Stock

Sample EW11PC01 from the Porcupine Creek stock contains zircon grains that are typically euhedral, prismatic and 50–100 µm long (Figure 5a). The grains display well-developed oscillatory zoning, with some grains displaying a complex internal structure that is possibly inherited or detrital in origin. The cores yielded significantly older ages and were disregarded from future consideration. Twenty-six analyses from 25 zircon grains yielded an average <sup>206</sup>Pb/<sup>238</sup>U age of 162.6 ± 1.3 Ma (Mean Square Weighted Deviation, MSWD = 1.15), interpreted to be the age of crystallization (Figure 5c).

### Baldy Pluton

Sample EW12BP01 from the Baldy Pluton contains zircon grains that are euhedral, prismatic and typically 75–100 µm in length (Figure 5b). The crystals have well-developed oscillatory zoning and resorbed, anhedral cores with complex internal structures (Figure 5b). Four spots ablated through the well-zoned rim and likely partly analyzed the complex internal core, yielding significantly older ages. These analyses were excluded from the calculations. Twenty-five analyses from 23 zircon grains yielded an average <sup>206</sup>Pb/<sup>238</sup>U age of 117.5 ± 1.3 Ma (MSWD = 1.13; Figure 5d).

### Mount Skelly Pluton

Sample EW11SC07 from the Mount Skelly pluton of the Bayonne batholith contains zircon grains that are typically euhedral to subhedral, with the latter showing evidence of partial resorption (25–75 µm long; Figure 6a). Most of the grains display oscillatory zoning and have complex, resorbed, internal cores. As a result of the smaller size

**Table 1.** U-Pb zircon isotopic data for five granitic rocks from the study area. Data was acquired using laser-ablation, multiple-collector, inductively coupled plasma-mass spectrometry.

Sample number	<sup>206</sup> Pb		<sup>207</sup> Pb/ <sup>206</sup> Pb		Isotopic ratios				<sup>207</sup> Pb/ <sup>206</sup> Pb <sup>i</sup>		<sup>207</sup> Pb/ <sup>235</sup> U		<sup>206</sup> Pb/ <sup>238</sup> U		$\rho$		<sup>206</sup> Pb/ <sup>238</sup> U		<sup>207</sup> Pb/ <sup>235</sup> U		$2\sigma$		
	(cps)	<sup>204</sup> Pb (cps)	2 $\sigma$	2 $\sigma$	2 $\sigma$	2 $\sigma$	2 $\sigma$	2 $\sigma$	2 $\sigma$	2 $\sigma$	2 $\sigma$	2 $\sigma$	2 $\sigma$	2 $\sigma$	2 $\sigma$	2 $\sigma$	2 $\sigma$	2 $\sigma$	2 $\sigma$	2 $\sigma$	2 $\sigma$	2 $\sigma$	2 $\sigma$
EW11PC01-1A	154132	598	0.0501	0.0014	0.1746	0.0095	0.0253	0.0012	0.866	199	62	163	8	161	7								
EW11PC01-1B	136407	519	0.0500	0.0014	0.1784	0.0086	0.0259	0.0010	0.802	195	66	167	7	165	6								
EW11PC01-2	173623	892	0.0510	0.0016	0.1871	0.0135	0.0266	0.0017	0.898	241	72	174	7	169	11								
EW11PC01-3	427013	454	0.0494	0.0013	0.1706	0.0080	0.0250	0.0010	0.816	167	62	160	7	159	6								
EW11PC01-4	161852	360	0.0494	0.0014	0.1780	0.0095	0.0261	0.0012	0.853	168	64	166	8	166	7								
EW11PC01-5	98764	369	0.0505	0.0017	0.1754	0.0091	0.0252	0.0010	0.787	220	75	164	8	160	6								
EW11PC01-8	143546	267	0.0487	0.0015	0.1646	0.0084	0.0245	0.0010	0.811	136	69	155	7	156	6								
EW11PC01-9	196342	388	0.0507	0.0015	0.1741	0.0088	0.0249	0.0010	0.808	226	68	163	8	159	6								
EW11PC01-10	156744	338	0.0485	0.0013	0.1664	0.0085	0.0249	0.0011	0.843	126	64	156	7	158	7								
EW11PC01-11	159662	284	0.0492	0.0014	0.1687	0.0082	0.0248	0.0010	0.813	159	65	158	7	158	6								
EW11PC01-12	699219	209	0.0867	0.0025	0.9601	0.0874	0.0803	0.0069	0.948	1354	55	683	44	498	41								
EW11PC01-13	147836	682	0.0519	0.0015	0.1775	0.0090	0.0248	0.0010	0.828	281	64	166	8	158	7								
EW11PC01-14	155172	738	0.0529	0.0016	0.1916	0.0098	0.0262	0.0011	0.810	327	67	178	8	167	7								
EW11PC01-15	146591	811	0.0515	0.0014	0.1871	0.0092	0.0264	0.0011	0.826	263	62	174	8	168	7								
EW11PC01-16	219504	668	0.0510	0.0014	0.1829	0.0090	0.0260	0.0010	0.822	243	63	171	8	165	7								
EW11PC01-17	148349	637	0.0508	0.0014	0.1826	0.0096	0.0261	0.0012	0.853	233	62	170	8	166	7								
EW11PC01-18	137889	870	0.0622	0.0035	0.2264	0.0155	0.0264	0.0010	0.559	680	117	207	13	188	6								
EW11PC01-19	186897	508	0.0500	0.0014	0.1753	0.0089	0.0254	0.0011	0.845	196	62	164	8	162	7								
EW11PC01-20	143891	517	0.0516	0.0014	0.1826	0.0084	0.0257	0.0009	0.799	266	62	170	7	163	6								
EW11PC01-21	174064	432	0.0500	0.0013	0.1761	0.0097	0.0256	0.0010	0.870	193	62	165	8	163	8								
EW11PC01-22	107698	495	0.0507	0.0014	0.1776	0.0082	0.0254	0.0010	0.806	228	62	166	8	162	6								
EW11PC01-23	143644	526	0.0534	0.0017	0.1929	0.0108	0.0262	0.0012	0.823	345	71	179	9	167	8								
EW11PC01-24	173808	304	0.0507	0.0014	0.1771	0.0080	0.0253	0.0009	0.781	227	64	166	7	161	6								
EW11PC01-25	171321	313	0.0492	0.0013	0.1699	0.0073	0.0251	0.0008	0.778	156	62	159	6	160	5								
EW11PC01-26	153332	391	0.0505	0.0014	0.1808	0.0079	0.0259	0.0008	0.773	219	63	169	7	165	5								
EW11PC01-27	158112	456	0.0505	0.0014	0.1808	0.0084	0.0260	0.0010	0.795	218	64	169	7	165	6								
EW11PC01-28	254688	400	0.0548	0.0027	0.2157	0.0194	0.0286	0.0022	0.839	403	106	198	16	182	13								
EW11PC01-29	197674	379	0.0490	0.0013	0.1706	0.0074	0.0253	0.0009	0.777	146	63	160	6	161	5								
EW11PC01-30	196760	393	0.0499	0.0014	0.1769	0.0067	0.0257	0.0006	0.662	188	64	165	6	164	4								
EW12BP01-1	342874	850	0.0489	0.0008	0.1276	0.0067	0.0189	0.0010	0.955	143	36	122	6	121	6								
EW12BP01-2	147126	695	0.0498	0.0009	0.1206	0.0063	0.0175	0.0009	0.944	188	39	116	6	112	5								
EW12BP01-3B	190442	680	0.0488	0.0008	0.1274	0.0073	0.0189	0.0010	0.960	139	38	122	7	121	7								
EW12BP01-3	127623	754	0.0494	0.0009	0.1295	0.0091	0.0190	0.0013	0.967	165	41	124	8	122	8								
EW12BP01-4	239506	680	0.0486	0.0008	0.1203	0.0062	0.0179	0.0009	0.952	130	37	115	6	115	6								
EW12BP01-6	252352	683	0.0554	0.0015	0.1994	0.0158	0.0261	0.0020	0.944	427	57	185	13	166	12								
EW12BP01-7	1451648	684	0.0940	0.0043	1.8414	0.4778	0.1420	0.0363	0.984	1509	85	1060	158	856	202								
EW12BP01-8	597700	718	0.0798	0.0055	0.8428	0.1855	0.0766	0.0160	0.950	1191	130	476	97	476	95								
EW12BP01-9	581938	1032	0.0556	0.0015	0.1384	0.0084	0.0180	0.0010	0.898	438	58	132	7	115	6								
EW12BP01-10	257809	699	0.0484	0.0008	0.1228	0.0060	0.0184	0.0008	0.943	119	38	118	5	118	5								
EW12BP01-11	338820	671	0.0484	0.0007	0.1183	0.0064	0.0177	0.0009	0.959	118	36	114	6	113	6								
EW12BP01-12	317908	622	0.0509	0.0013	0.1277	0.0064	0.0192	0.0013	0.939	238	57	122	8	116	8								
EW12BP01-13	325196	722	0.0494	0.0008	0.1263	0.0065	0.0186	0.0009	0.950	165	37	121	8	119	6								
EW12BP01-14	323267	687	0.0487	0.0008	0.1256	0.0085	0.0187	0.0012	0.970	133	38	120	8	119	8								
EW12BP01-15	362643	609	0.0480	0.0008	0.1260	0.0062	0.0190	0.0009	0.947	99	37	120	6	122	6								
EW12BP01-16	229035	600	0.0483	0.0008	0.1168	0.0105	0.0175	0.0016	0.982	113	40	112	10	112	10								
EW12BP01-17	290212	651	0.0485	0.0008	0.1248	0.0060	0.0187	0.0008	0.941	124	38	119	5	119	5								
EW12BP01-17B	354986	632	0.0483	0.0008	0.1208	0.0060	0.0182	0.0009	0.946	113	38	116	5	116	5								
EW12BP01-18	246695	609	0.0481	0.0008	0.1257	0.0065	0.0189	0.0009	0.951	105	37	120	6	121	6								

Table 1 (continued)

Sample number	$^{206}\text{Pb}$		$^{207}\text{Pb}/^{235}\text{U}$		$^{206}\text{Pb}/^{238}\text{U}$		$^{207}\text{Pb}/^{206}\text{Pb}^1$		$^{207}\text{Pb}/^{235}\text{U}$		$^{206}\text{Pb}/^{238}\text{U}$				
	(cps)	(cps)	$2\sigma$	$\rho$	$2\sigma$	$2\sigma$	age (Ma)	$2\sigma$ error (Ma)	age (Ma)	$2\sigma$ error (Ma)	age (Ma)	$2\sigma$ error (Ma)			
EW12BP01-19	39778	544	0.0506	0.0017	0.1261	0.0071	0.0181	0.0008	0.799	76	121	6	116	5	
EW12BP01-20	129426	536	0.0495	0.0010	0.1225	0.0059	0.0179	0.0008	0.909	46	117	5	115	5	
EW12BP01-21	298525	575	0.0487	0.0008	0.1246	0.0066	0.0185	0.0009	0.948	39	119	6	118	6	
EW12BP01-22	169034	482	0.0492	0.0012	0.1189	0.0069	0.0175	0.0009	0.907	56	114	6	112	6	
EW12BP01-23	293664	479	0.0486	0.0008	0.1225	0.0062	0.0183	0.0009	0.949	37	117	6	117	6	
EW12BP01-24	269535	528	0.0499	0.0009	0.1307	0.0066	0.0190	0.0009	0.933	42	125	6	121	6	
EW12BP01-26	223998	515	0.0488	0.0008	0.1270	0.0065	0.0189	0.0009	0.946	39	121	6	121	6	
EW12BP01-27	3226855	662	0.0988	0.0015	2.5223	0.1313	0.1852	0.0092	0.955	28	1278	37	1095	50	
EW12BP01-28	381725	592	0.0480	0.0008	0.1259	0.0071	0.0190	0.0010	0.955	39	120	6	122	6	
EW12BP01-30	435674	554	0.0486	0.0008	0.1252	0.0064	0.0187	0.0009	0.947	38	120	6	119	6	
EW11SC07-1	553055	318	0.0553	0.0017	0.1543	0.0113	0.0202	0.0013	0.905	68	146	10	129	8	
EW11SC07-2	1222072	52	0.0987	0.0039	1.7887	0.4079	0.1314	0.0295	0.985	1600	1041	139	796	166	
EW11SC07-3	439729	42	0.0476	0.0013	0.1137	0.0054	0.0173	0.0007	0.831	62	109	5	111	4	
EW11SC07-5	345152	542	0.0573	0.0017	0.1735	0.0090	0.0220	0.0009	0.808	66	162	8	140	6	
EW11SC07-6	197464	570	0.0557	0.0019	0.1482	0.0087	0.0193	0.0009	0.817	73	140	8	123	6	
EW11SC07-8	613081	436	0.0719	0.0035	0.3600	0.0481	0.0363	0.0045	0.931	984	312	35	230	28	
EW11SC07-9	530693	494	0.0484	0.0013	0.1105	0.0047	0.0166	0.0005	0.777	117	106	4	106	3	
EW11SC07-10	519694	386	0.0789	0.0062	1.0720	0.3031	0.0985	0.0267	0.960	1171	740	139	606	155	
EW11SC07-11	491507	332	0.0594	0.0038	0.1933	0.0293	0.0236	0.0032	0.907	133	179	25	150	20	
EW11SC07-13	545551	376	0.0488	0.0013	0.1127	0.0052	0.0168	0.0006	0.811	62	108	5	107	4	
EW11SC07-15	581477	602	0.0513	0.0016	0.1218	0.0051	0.0172	0.0005	0.668	255	117	5	110	3	
EW11SC07-18	435449	383	0.0554	0.0028	0.1415	0.0115	0.0185	0.0012	0.779	110	134	10	118	7	
EW11SC07-19	594387	271	0.0609	0.0036	0.1970	0.0281	0.0235	0.0030	0.912	121	183	24	149	19	
EW11SC07-26	309287	225	0.0488	0.0013	0.1183	0.0055	0.0176	0.0007	0.813	62	113	5	112	4	
EW11SC07-27	611177	253	0.0485	0.0013	0.1105	0.0048	0.0165	0.0006	0.789	124	106	4	105	3	
EW11SC07-27B	772281	200	0.0478	0.0013	0.1085	0.0043	0.0164	0.0005	0.743	91	105	4	105	3	
EW11SC07-34	574207	446	0.0479	0.0013	0.1138	0.0047	0.0172	0.0006	0.772	94	109	4	110	4	
EW11SC07-35	929693	506	0.0761	0.0022	0.8093	0.0561	0.0771	0.0049	0.910	1097	602	31	479	29	
EW11SC07-36	159564	166	0.0486	0.0013	0.1178	0.0052	0.0176	0.0006	0.788	127	113	5	112	4	
EW11SC07-37B	572510	216	0.0516	0.0016	0.1231	0.0112	0.0173	0.0015	0.936	266	71	118	10	111	9
EW11SC07-39	621565	218	0.0630	0.0019	0.2133	0.0084	0.0246	0.0006	0.658	708	196	7	156	4	
EW11SC07-40	457085	211	0.0478	0.0013	0.1111	0.0049	0.0169	0.0006	0.801	87	107	4	108	4	
EW11SC07-41	812426	321	0.0478	0.0013	0.1117	0.0047	0.0169	0.0005	0.773	90	108	4	108	3	
EW11SC07-42	183276	238	0.0475	0.0013	0.1119	0.0048	0.0171	0.0006	0.782	72	108	4	109	4	
EW11SC07-43	594015	276	0.0491	0.0014	0.1182	0.0052	0.0175	0.0006	0.764	154	113	5	112	4	
EW11SC07-44	738853	257	0.0479	0.0013	0.1146	0.0053	0.0173	0.0007	0.822	96	110	5	111	4	
EW11SC07-45	449615	150	0.0477	0.0013	0.1124	0.0052	0.0171	0.0006	0.817	86	108	5	109	4	
EW11SC07-46	630513	159	0.0478	0.0013	0.1116	0.0051	0.0169	0.0006	0.814	88	107	5	108	4	
EW12SS01-1	110074	461	0.0487	0.0006	0.1154	0.0048	0.0172	0.0007	0.951	30	111	4	110	4	
EW12SS01-2	156073	418	0.0491	0.0006	0.1214	0.0059	0.0179	0.0008	0.968	151	116	5	115	5	
EW12SS01-3	127935	418	0.0490	0.0006	0.1171	0.0043	0.0173	0.0006	0.940	29	112	4	111	4	
EW12SS01-4	360149	369	0.0481	0.0005	0.1183	0.0044	0.0179	0.0006	0.959	103	114	4	114	4	
EW12SS01-5	252120	409	0.0483	0.0005	0.1129	0.0052	0.0170	0.0008	0.972	25	109	5	108	5	
EW12SS01-6	355400	331	0.0488	0.0007	0.1139	0.0047	0.0169	0.0007	0.938	33	110	4	108	4	
EW12SS01-7	313877	320	0.0479	0.0005	0.1156	0.0050	0.0175	0.0007	0.967	94	111	5	112	5	
EW12SS01-8	66232	277	0.0471	0.0008	0.1129	0.0051	0.0174	0.0007	0.925	55	109	5	111	5	
EW12SS01-9	172338	255	0.0481	0.0007	0.1168	0.0050	0.0176	0.0007	0.948	105	112	5	113	5	
EW12SS01-10	343860	311	0.0482	0.0005	0.1163	0.0052	0.0175	0.0008	0.971	25	112	5	112	5	

Table 1 (continued)

Sample number	<sup>206</sup> Pb (cps)		<sup>204</sup> Pb (cps)		Isotopic ratios						<sup>207</sup> Pb/ <sup>206</sup> Pb <sup>1</sup>		<sup>207</sup> Pb/ <sup>235</sup> U		<sup>206</sup> Pb/ <sup>238</sup> U		<sup>206</sup> Pb/ <sup>232</sup> U				
					<sup>207</sup> Pb/ <sup>235</sup> U	2σ	<sup>206</sup> Pb/ <sup>238</sup> U	2σ	ρ	2σ	age (Ma)	error (Ma)	2σ	age (Ma)	error (Ma)	2σ	age (Ma)	error (Ma)	2σ	age (Ma)	error (Ma)
EW12SS01-11	420076	283	0.0482	0.0005	0.1161	0.0056	0.0175	0.0008	0.974	0.0008	107	25	112	5	112	5	112	5	112	5	5
EW12SS01-12	130685	248	0.0482	0.0006	0.1157	0.0067	0.0174	0.0010	0.978	0.0010	110	29	111	6	111	6	111	6	111	6	6
EW12SS01-13	600286	316	0.0479	0.0005	0.1178	0.0048	0.0178	0.0007	0.965	0.0007	97	25	113	4	114	4	114	4	114	4	4
EW12SS01-14	56963	287	0.0494	0.0013	0.1169	0.0059	0.0172	0.0007	0.864	0.0007	167	58	110	5	110	5	110	5	110	5	5
EW12SS01-15	163014	255	0.0481	0.0007	0.1186	0.0047	0.0179	0.0007	0.938	0.0007	104	32	114	4	114	4	114	4	114	4	4
EW12SS01-16	148142	318	0.0497	0.0008	0.1202	0.0053	0.0175	0.0007	0.930	0.0007	181	37	115	5	112	5	112	5	112	5	5
EW12SS01-17	100994	399	0.0499	0.0008	0.1193	0.0052	0.0173	0.0007	0.935	0.0007	192	36	114	5	111	4	111	4	111	4	4
EW12SS01-18	235442	366	0.0535	0.0032	0.1286	0.0115	0.0174	0.0011	0.735	0.0011	348	131	123	10	131	10	131	10	131	10	7
EW12SS01-19	34807	385	0.0549	0.0022	0.1311	0.0077	0.0173	0.0007	0.728	0.0007	410	88	125	7	111	5	111	5	111	5	5
EW12SS01-20	161616	419	0.0489	0.0006	0.1172	0.0049	0.0174	0.0007	0.961	0.0007	142	27	113	4	111	4	111	4	111	4	4
EW12SS01-21	1043904	453	0.0483	0.0005	0.1170	0.0055	0.0176	0.0008	0.971	0.0008	114	26	112	5	112	5	112	5	112	5	5
EW12SS01-22	867949	421	0.1077	0.0011	4.9656	0.2274	0.3345	0.0149	0.975	0.0149	1760	18	1813	38	1860	38	1860	38	1860	38	72
EW12SS01-22B	525409	427	0.1064	0.0032	4.8173	0.3798	0.3285	0.0239	0.923	0.0239	1738	55	1788	64	1831	64	1831	64	1831	64	115
EW12SS01-23	66602	423	0.0514	0.0013	0.1229	0.0060	0.0174	0.0007	0.844	0.0007	257	59	118	5	111	5	111	5	111	5	5
EW12SS01-24	258631	447	0.0487	0.0005	0.1185	0.0053	0.0177	0.0008	0.969	0.0008	133	26	114	5	113	5	113	5	113	5	5
EW12SS01-25	91785	347	0.0488	0.0007	0.1179	0.0059	0.0175	0.0008	0.953	0.0008	137	35	113	5	112	5	112	5	112	5	5
EW12SS01-26	880697	375	0.0481	0.0005	0.1172	0.0045	0.0177	0.0007	0.961	0.0007	103	25	113	4	113	4	113	4	113	4	4
EW12SS01-27	883260	323	0.0478	0.0005	0.1185	0.0043	0.0180	0.0006	0.959	0.0006	90	24	114	4	115	4	115	4	115	4	4
EW12SS01-28	234529	272	0.0480	0.0006	0.1159	0.0086	0.0175	0.0013	0.985	0.0013	99	30	111	8	112	8	112	8	112	8	8
EW12SS01-29	453932	245	0.0480	0.0005	0.1163	0.0047	0.0176	0.0007	0.964	0.0007	98	25	112	4	112	4	112	4	112	4	4
EW13ER11-1	256432	565	0.0506	0.0009	0.1119	0.0057	0.0160	0.0008	0.944	0.0008	224	39	108	5	103	5	103	5	103	5	5
EW13ER11-2	176365	511	0.0525	0.0010	0.1823	0.0167	0.0252	0.0022	0.976	0.0022	309	45	170	14	160	14	160	14	160	14	14
EW13ER11-4	31488	342	0.0465	0.0010	0.1019	0.0055	0.0159	0.0008	0.911	0.0008	26	52	99	5	102	5	102	5	102	5	5
EW13ER11-4B	43936	260	0.0461	0.0008	0.1017	0.0054	0.0160	0.0008	0.938	0.0008	4	44	98	5	102	5	102	5	102	5	5
EW13ER11-6	84705	373	0.0520	0.0016	0.1155	0.0067	0.0161	0.0008	0.850	0.0008	283	69	111	6	103	6	103	6	103	6	6
EW13ER11-7	137683	328	0.0472	0.0008	0.1121	0.0061	0.0172	0.0009	0.947	0.0009	59	41	108	6	110	6	110	6	110	6	6
EW13ER11-8	29751	306	0.0470	0.0019	0.1066	0.0070	0.0164	0.0008	0.781	0.0008	50	95	103	6	105	6	105	6	105	6	5
EW13ER11-9	164354	519	0.0506	0.0014	0.1147	0.0062	0.0164	0.0008	0.860	0.0008	224	63	110	6	105	6	105	6	105	6	5
EW13ER11-10	315584	559	0.0553	0.0013	0.1032	0.0056	0.0135	0.0007	0.907	0.0007	424	51	100	5	87	5	87	5	87	5	4
EW12ER11-11	598715	1180	0.0550	0.0025	0.0827	0.0059	0.0109	0.0006	0.776	0.0006	413	98	81	6	70	6	70	6	70	6	4
EW12ER11-12	179680	919	0.0612	0.0028	0.1333	0.0086	0.0158	0.0007	0.700	0.0007	647	96	127	8	101	8	101	8	101	8	5
EW12ER11-13	260021	861	0.0488	0.0008	0.1100	0.0057	0.0163	0.0008	0.950	0.0008	140	38	106	5	104	5	104	5	104	5	5
EW12ER11-14	143686	763	0.0487	0.0008	0.1096	0.0057	0.0163	0.0008	0.950	0.0008	132	38	106	5	104	5	104	5	104	5	5
EW12ER11-15	272119	792	0.1064	0.0033	2.6289	0.4975	0.1793	0.0335	0.986	0.0335	1738	56	1309	130	1063	130	1063	130	1063	130	180
EW12ER11-16	139390	748	0.0486	0.0008	0.1065	0.0051	0.0159	0.0007	0.931	0.0007	131	40	103	5	102	5	102	5	102	5	4
EW12ER11-18	338499	714	0.0495	0.0008	0.0986	0.0057	0.0145	0.0008	0.959	0.0008	170	38	95	5	93	5	93	5	93	5	5
EW12ER11-19	163182	693	0.0495	0.0014	0.1005	0.0057	0.0147	0.0007	0.866	0.0007	172	65	97	5	94	5	94	5	94	5	5
EW12ER11-19B	99005	734	0.0493	0.0009	0.1020	0.0050	0.0150	0.0007	0.935	0.0007	163	40	99	5	96	5	96	5	96	5	4
EW12ER11-21	66183	687	0.0496	0.0010	0.1126	0.0059	0.0165	0.0008	0.930	0.0008	178	44	109	5	106	5	106	5	106	5	5
EW12ER11-22	96857	600	0.0491	0.0009	0.1100	0.0057	0.0166	0.0008	0.933	0.0008	152	42	108	5	106	5	106	5	106	5	5
EW12ER11-25	325856	837	0.0599	0.0021	0.1086	0.0074	0.0132	0.0008	0.852	0.0008	599	75	105	7	84	7	84	7	84	7	5
EW12ER11-26	162347	520	0.0481	0.0009	0.1108	0.0053	0.0167	0.0007	0.918	0.0007	103	45	107	5	107	5	107	5	107	5	5
EW12ER11-31	520703	726	0.0482	0.0007	0.1039	0.0051	0.0156	0.0007	0.948	0.0007	109	36	100	5	100	5	100	5	100	5	5
EW12ER11-32	604139	683	0.0484	0.0008	0.1037	0.0050	0.0151	0.0007	0.939	0.0007	118	39	97	5	97	5	97	5	97	5	4
EW12ER11-33	132001	678	0.0492	0.0012	0.1063	0.0060	0.0157	0.0008	0.899	0.0008	155	57	103	6	100	6	100	6	100	6	5

<sup>1</sup>Radiogenic Pb

Abbreviations: cps, counts per second

range and large internal detrital cores, 13 spots were excluded from the calculations. Fifteen spot analyses from 14 zircon grains produced an average  $^{206}\text{Pb}/^{238}\text{U}$  age of  $108.8 \pm 1.2$  Ma (MSWD = 1.5; Figure 6c).

### Summit Stock

Zircon crystals from sample EW12SS01, taken from the Summit stock, are typically anhedral, display well-developed oscillatory zoning and fall in the size range 50–100  $\mu\text{m}$  long (Figure 6b). The majority of the zircon crystals have complex, resorbed cores that appear bright in the CL images. Six spots yielded significantly older ages and were excluded from the calculations. Twenty-three analyses from 23 zircon grains produced an average  $^{206}\text{Pb}/^{238}\text{U}$  age of  $111.83 \pm 0.86$  Ma (MSWD = 0.58; Figure 6d).

### Emerald Stock

Sample EW12ER11 from the Emerald stock yielded anhedral zircon grains that display well-developed oscillatory zoning and are typically 50–100  $\mu\text{m}$  in length (Figure 6e). Seven spots yielded significantly older cores and were removed from the calculations. Seventeen analyses from 16 zircon grains yielded an average  $^{206}\text{Pb}/^{238}\text{U}$  age of  $101.7 \pm 2.2$  Ma (MSWD = 3.5; Figure 6f). The large MSWD of 3.5 indicates there are likely two populations of zircons. This may be the result of a prolonged crystallization period or multiple pulses of magmatism.

### Discussion

The five new zircon U-Pb dates, from granitic intrusive rocks in the Creston-Salmo area, provide improved age

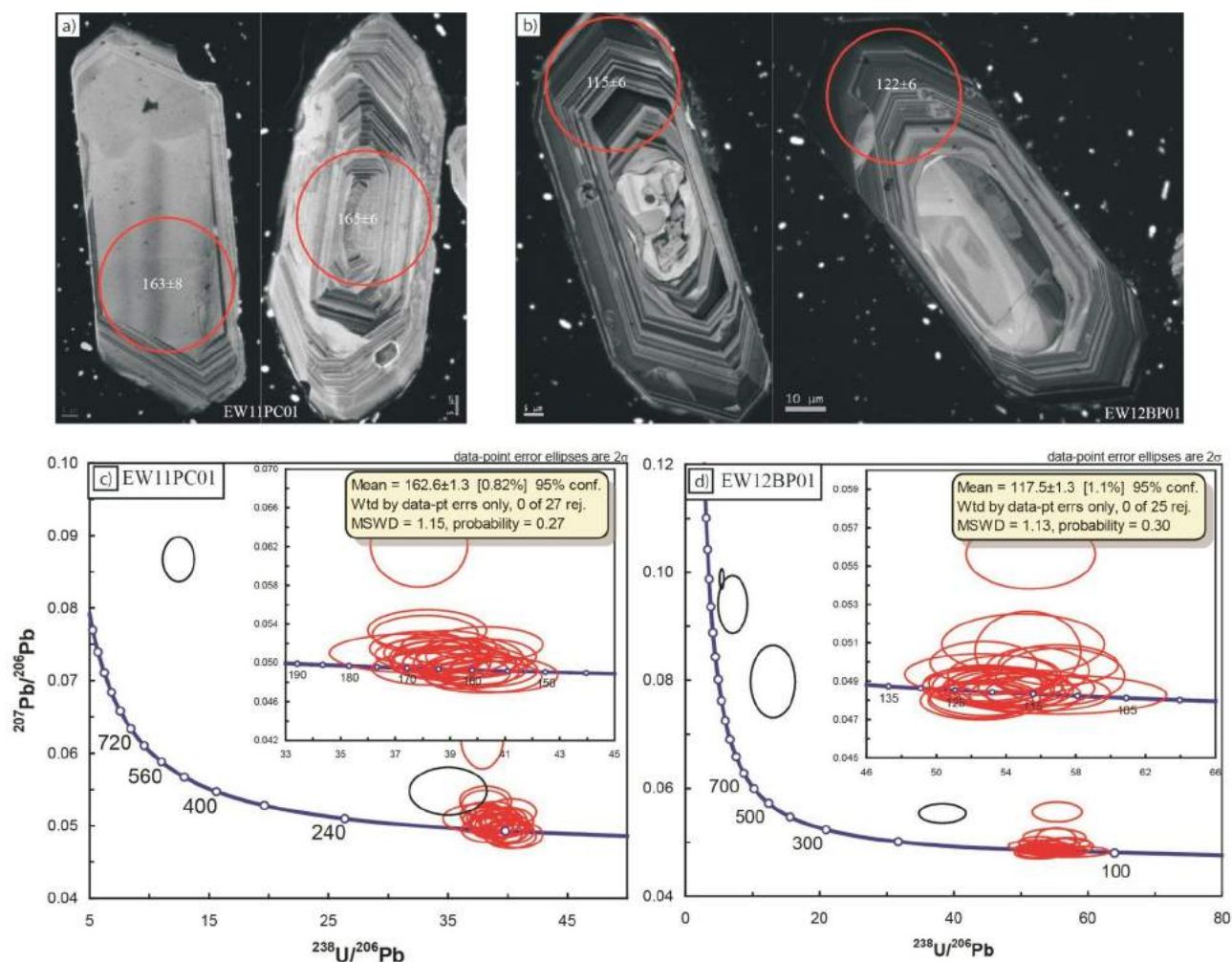


**Figure 5.** a) Cathodoluminescence images of select zircon grains from the Porcupine Creek stock. The red circles represent the location of the laser spot when acquiring analysis. The associated values are the  $^{206}\text{Pb}/^{238}\text{U}$  ages and corresponding  $2\sigma$  errors. b) Cathodoluminescence images of select zircon grains from the Baldy pluton. c) Tera-Wasserburg U-Pb concordia plot for sample EW11PC01. The analyses corresponding to the red error ellipses were used in determining a date for the intrusion, the black error ellipses were discarded. This is the same for all of the Tera-Wasserburg U-Pb concordia plots. d) Tera-Wasserburg U-Pb concordia plot for sample EW12BP01.

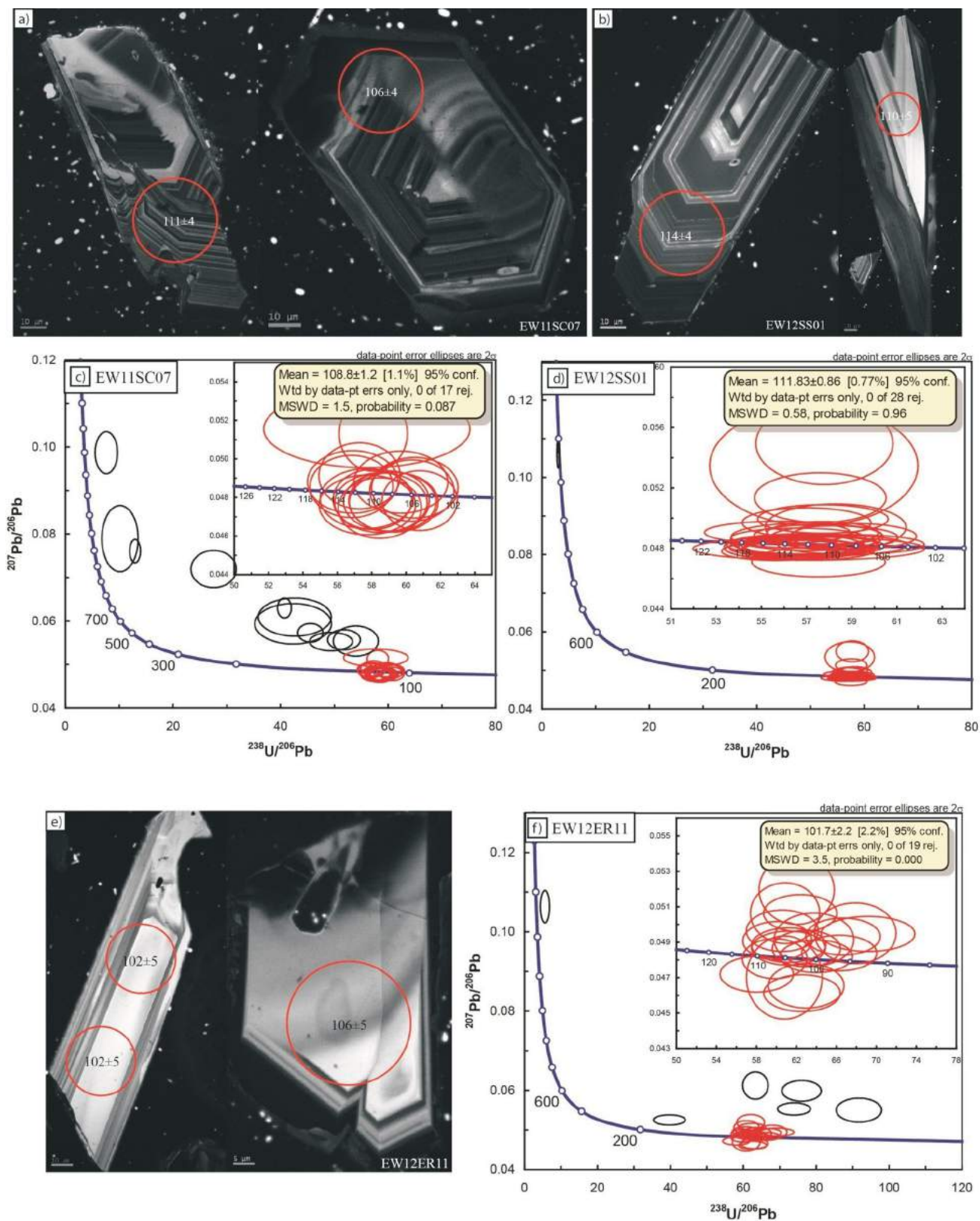


**Figure 6. a)** Cathodoluminescence images of select zircon grains from the Mount Skelly pluton. The red circles represent the location of the laser spot when acquiring analysis. The associated values are the  $^{206}\text{Pb}/^{238}\text{U}$  ages and corresponding  $2\sigma$  errors. **b)** Cathodoluminescence images of select zircon grains from the Summit stock. **c)** Tera-Wasserburg U-Pb concordia plot for sample EW11SC07. **d)** Tera-Wasserburg U-Pb concordia plot for sample EW12SS01. **e)** Cathodoluminescence images of select zircon grains from the Emerald stock. **f)** Tera-Wasserburg U-Pb concordia plot for sample EW12ER11.

constraints for magmatism and deformation in this region of southeastern BC. The U-Pb zircon date of  $162.6 \pm 1.3$  Ma for the Porcupine Creek stock is interpreted as the crystallization age. Ages obtained by Ghosh (1995a) for the nearby Nelson plutonic suite (172–161 Ma) overlap with this age, suggesting the Porcupine Creek stock is part of the Nelson suite.

The low pressure cordierite and andalusite contact aureole, adjacent to the Porcupine Creek stock (163 Ma), formed at a lower pressure than the staurolite-bearing contact aureole around the older (171 and 167 Ma) Mine and Wall stocks (Figure 3; Webster and Pattison, 2013). This implies that the crust in this area was being eroded or tectonically unroofed during the Middle Jurassic. The granitoid and its surrounding contact aureole were unaffected by subsequent deformation and regional metamorphism (Webster and Pattison, 2013).

The deformed Baldy pluton yielded a U-Pb zircon date of  $117.5 \pm 1.3$  Ma, interpreted as the crystallization age. This age is consistent with, and overlaps within, the uncertainty of the  $117 \pm 4/-1$  Ma U-Pb (combined titanite and allanite) age of Leclair et al. (1993). Because the Baldy pluton contains the same deformation fabrics as those in the enveloping metamorphic rocks, the new date constrains the upper limit of penetrative deformation in the footwall of the Midge Creek fault to approximately 118 Ma ( $D_2/M_2$  of Leclair et al., 1993 and Moynihan, 2012; Figure 3). The Baldy pluton crosscuts the band of deformed Barrovian metamorphism, implying that it postdates peak metamorphism (Figure 3).

The Midge Creek stock (MCS) is situated between the Nelson and Bayonne batholiths (Figure 2) and cuts the penetrative structures and regional metamorphic isograds at the northern end of the Baldy pluton. It is undeformed, except at its northern tip, where the dominant foliation parallels the regional trend (Leclair, 1988). Leclair et al. (1993) interpreted the crystallization age of the MCS to be  $111 \pm 4$  Ma (mid-Cretaceous) from U-Pb (allanite) analyses. If this interpretation is correct it indicates that the MCS was emplaced during the latest stages of regional metamorphism and deformation in the area, with peak conditions occurring prior to 111 Ma. Combined with the work of Moynihan and Pattison (2013) to the north, and the new 118 Ma age of the deformed Baldy pluton, the age of deformation and regional metamorphism is constrained to the interval 143–111 Ma (Figure 3).

The postkinematic Summit stock yielded a U-Pb zircon date of  $111.8 \pm 0.8$  Ma, which is interpreted to be the age of crystallization. The similar mineralogy and age of both the Midge Creek stock and Summit stock confirm they are part of the Bayonne magmatic suite. Low pressure (staurolite free) andalusite-bearing contact aureoles, adjacent to both

the Summit stock and the MCS, imply that they were emplaced at 7–11 km (Webster and Pattison, 2013; Figure 3). Biotite and hornblende K-Ar cooling ages for these stocks (102 and 109 Ma, respectively) are only several million years younger than the crystallization ages, implying that they crystallized, cooled and remained at a temperature below  $\sim 300^\circ\text{C}$ , (i.e., at shallow depth), following their emplacement (Archibald et al., 1984).

The new U-Pb zircon age of  $101.7 \pm 2.2$  Ma for the crystallization age of the Emerald stock is also the timing of mineralization. Drillhole results and underground mine workings show that the Dodger and Emerald stocks are connected at depth, and are therefore of the same age (Lawrence, 1997). The new U-Pb age is in agreement with a K-Ar biotite age of  $100 \pm 3$  Ma from the Dodger stock (Dandy, 1997). These two results are within error of each other, implying that the mineralizing system and intrusion quickly cooled to below  $\sim 300^\circ\text{C}$  following crystallization.

The new age of  $108.8 \pm 1.2$  Ma for the Mount Skelly pluton, combined with existing ages, requires a reinterpretation of the Bayonne batholith. The intrusive rocks that comprise the Bayonne batholith crystallized over an extended period of time, ca. 30 m.y. The plutons have different compositions, structural histories and varying depths of emplacement, confirming the Bayonne batholith is a composite body.

The cordierite-andalusite contact aureole around the Mount Skelly pluton is hosted in regionally metamorphosed lower-greenschist-facies Belt-Purcell Supergroup rocks in the hangingwall of the Purcell Trench fault (Webster and Pattison, 2013). The intrusion and surrounding strata in the hangingwall of the Purcell Trench fault are characterized by older K-Ar and Ar-Ar cooling ages (99–70 Ma) than the rocks in the footwall of the fault (60–46 Ma; Archibald et al., 1984). Based on the new U-Pb date, thermochronology and pressure and temperature estimates of contact metamorphism of the Mount Skelly contact aureole, the intrusion remained below  $300^\circ\text{C}$  after crystallization (i.e., at 7–11 km or higher in the crust). This contrasts with the geological history in the footwall of the Purcell Trench fault, south of the Bayonne batholith. Following the crystallization of the Mount Skelly pluton at 7–11 km in the crust, the rocks in the footwall of the PTF were later buried (ca. 80 Ma) to approximately 20 km, undergoing deformation and middle-amphibolite-facies metamorphism (Webster and Pattison, 2013).

## Acknowledgments

This work was funded by a 2011 Geoscience BC grant to D.R.M. Pattison and E.R. Webster (1022684) and by Natu-

ral Sciences and Engineering Research Council (NSERC) Discovery Grant 037233 to D.R.M. Pattison. Insightful reviews provided by D.A. Archibald, D.P. Moynihan, A.L. Clifford, B. Hamilton and P. Starr improved this paper. Thanks to A. Dufrane for his assistance with LA-MC-ICP-MS analyses and C. Debuhr for his help on the SEM. Thanks also to J. Bjornson and C. Richardson for their excellent field assistance, and to W. Matthews for additional help.

## References

- Archibald, D.A., Glover, J.K., Price, R.A., Farrar, E. and Carmichael, D.M. (1983): Geochronology and tectonic implications of magmatism and metamorphism, southern Kootenay Arc and neighbouring regions, southeastern British Columbia, part 1: Jurassic to mid-Cretaceous; *Canadian Journal of Earth Sciences*, v. 20, no. 12, p. 1891–1913.
- Archibald, D.A., Krogh, T.E., Armstrong, R.L. and Farrar, E. (1984): Geochronology and tectonic implications of magmatism and metamorphism, southern Kootenay Arc and neighbouring regions, southeastern British Columbia, part 2: mid-Cretaceous to Eocene; *Canadian Journal of Earth Sciences*, v. 21, no. 5, p. 567–583.
- Bjornson, J. (2012): Contact metamorphism around the Lost Creek pluton and Summit Creek stock in the Summit Creek map area, southeastern British Columbia; B.Sc. thesis, University of Calgary, 66 p.
- Brown, D.A., Doughty, T.P., Glover, J.K., Archibald, D.A., David, D.W. and Pattison, D.R.M. (1999): Field trip guide and road log: Purcell Anticlinorium to the Kootenay Arc, southeastern British Columbia, Highway 3—Creston to Summit Pass and northern Priest River Complex, west of Creston; BC Ministry of Energy and Mines, BC Geological Survey, Information Circular 1999-2.
- Brown, D.A., Doughty, T.P. and Stinson, P. (1995): Geology and mineral occurrences of the Creston map area (82F/2); BC Ministry of Energy and Mines, BC Geological Survey, Open File 1995-15, 2 p., 1 map at 1:50 000 scale, URL <<http://www.empr.gov.bc.ca/Mining/Geoscience/PublicationsCatalogue/OpenFiles/1995/Documents/OF1995-15.pdf>> [November 25, 2013].
- Dandy, L. (1997): Geological, geochemical and diamond drill report on the Jersey-Emerald property; BC Ministry of Energy and Mines, Assessment Report 24 910, 57 p.
- Davis, D. (1995): Report on the U-Pb geochronology of rocks from the Priest River Complex, southeastern British Columbia; Royal Ontario Museum, Geology Department, unpublished report.
- Devlin, W.J. and Bond, C.G. (1988): The initiation of the early Paleozoic Cordilleran miogeocline: evidence from the uppermost Proterozoic–Lower Cambrian Hamill Group of southeastern British Columbia; *Canadian Journal of Earth Sciences*, v. 25, p. 1–19.
- Doughty, P.T. and Price, R.A. (1999): Tectonic evolution of the Priest River Complex, northern Idaho and Washington: a reappraisal of the Newport fault with new insights on metamorphic core complex formation; *Tectonics*, v. 18, p. 375–393.
- Doughty, P.T. and Price, R.A. (2000): Geology of the Purcell Trench rift valley and Sandpoint conglomerate: Eocene en échelon normal faulting and synrift sedimentation along the eastern flank of the Priest River metamorphic complex, northern Idaho; *Geological Society of America Bulletin*, v. 112, no. 9, p. 1356–1374.
- Doughty, P.T., Brown, D.A. and Archibald, D.A. (1997): Metamorphism of the Creston map area, southeastern British Columbia (82F/2); BC Ministry of Energy and Mines, BC Geological Survey, Open File 1997-5, 14 p. and 1 map at 1:50 000 scale, URL <<http://www.empr.gov.bc.ca/Mining/Geoscience/PublicationsCatalogue/OpenFiles/1997/Documents/OF1997-05.pdf>> [November 25, 2013].
- Einarsen, J.M. (1994): Structural geology of the Pend d’Oreille area and tectonic evolution of the southern Kootenay Arc; Ph.D. thesis, University of Calgary.
- Evenchick, C.A., McMechan, M.E., McNicoll, V.L. and Carr, S.D. (2007): A synthesis of the Jurassic-Cretaceous tectonic evolution of the central and southeastern Canadian Cordillera: exploring links across the orogen; *Geological Society of America Special Paper 433*, p. 117–145.
- Ghent, E.D., Nicholls, J., Simony, P.S., Sevigny, J. and Stout, M. (1991): Hornblende geobarometry of the Nelson Batholith, southeastern British Columbia: tectonic implications; *Canadian Journal of Earth Sciences*, v. 28, p. 1982–1991.
- Ghosh, D.K. (1995a): U-Pb geochronology of Jurassic to early Tertiary granitic intrusives from the Nelson-Castlegar area, southeastern British Columbia, Canada; *Canadian Journal of Earth Sciences*, v. 32, no. 10, p. 1668–1680.
- Ghosh, D.K. (1995b): Nd- Sr isotopic constraints on the interactions of the Intermontane Superterrane with the western edge of North America in the southern Canadian Cordillera; *Canadian Journal of Earth Sciences*, v. 32, no. 10, p. 1740–1758.
- Ghosh, D.K. and Lambert, R.S.J. (1995): Nd-Sr isotope geochemistry and petrogenesis of Jurassic granitoid intrusives, southeast British Columbia, Canada; *in* *Jurassic Magmatism and Tectonics of the North American Cordillera*, D.M. Miller and C. Busby (ed.), *Geological Society of America Special Paper 299*, p. 141–157.
- Giroux, G. and Grunenberg, P. (2009): Summary report and preliminary resource calculations for the east Emerald and Emerald mine tungsten zones Jersey-Emerald property, BC; Sultan Minerals Inc., 80 p., URL <[http://www.sultanminerals.com/i/pdf/NI43-101\\_EmeraldMineTungsten.pdf](http://www.sultanminerals.com/i/pdf/NI43-101_EmeraldMineTungsten.pdf)> [November 25, 2013].
- Glombick, P., Brown, D.A. and MacLeod, R.F., compilers (2010): Geology, Creston, British Columbia; Geological Survey of Canada, Open File 6152, scale 1:50 000, URL <[ftp2.cits.rncan.gc.ca/pub/geott/ess\\_pubs/261/261631/gscof\\_6152\\_e\\_2010\\_mn01.pdf](ftp2.cits.rncan.gc.ca/pub/geott/ess_pubs/261/261631/gscof_6152_e_2010_mn01.pdf)> [November 25, 2013], doi:10.4095/288925
- Glover, J.K. (1978): Geology of the Summit Creek area, southern Kootenay Arc, British Columbia; Ph.D. thesis, Queen’s University, 144 p.
- Höy, T. and Dunne, P.E.K. (1998): Geological compilation of the Trail map area, southeastern British Columbia (082F/3, 4, 5, 6); BC Ministry of Energy and Mines, BC Geological Survey, Geoscience Map 1998-1, scale 1:100 000, URL <[http://www.empr.gov.bc.ca/Mining/Geoscience/PublicationsCatalogue/Maps/GeoscienceMaps/Documents/GM1998-01\\_Trail.pdf](http://www.empr.gov.bc.ca/Mining/Geoscience/PublicationsCatalogue/Maps/GeoscienceMaps/Documents/GM1998-01_Trail.pdf)> [November 25, 2013].
- Lawrence, E.A. (1997): Diamond drilling report on the Jersey property, Nelson Mining Division, Salmo, BC; BC Ministry of Energy and Mines, Assessment Report 25 349, 39 p.

- Leclair, A.D. (1988): Polyphase structural and metamorphic histories of the Midge Creek area, southeast British Columbia: implications for tectonic processes in the central Kootenay Arc; Ph.D. thesis, Queen's University, 264 p.
- Leclair, A.D., Parrish, R.R. and Archibald, D.A. (1993): Evidence for Cretaceous deformation in the Kootenay Arc on U-Pb and  $^{40}\text{Ar}/^{39}\text{Ar}$  dating, southeastern British Columbia; *in* Current Research, Part A, Geological Survey of Canada, Paper 93-1A, p. 207–220.
- Little, H. W. (1960): Nelson map area, British Columbia; Geological Survey of Canada, Memoir 308.
- Logan, J.M. (2001): Prospective areas for intrusion-related gold-quartz veins in southern British Columbia; in Geological Fieldwork 2000, BC Ministry of Energy and Mines, BC Geological Survey, Paper 2000-1, p. 231–252, URL <[http://www.empr.gov.bc.ca/Mining/Geoscience/Publications/Catalogue/Fieldwork/Documents/2000/Logan\\_p231-252.pdf](http://www.empr.gov.bc.ca/Mining/Geoscience/Publications/Catalogue/Fieldwork/Documents/2000/Logan_p231-252.pdf)> [December 2013].
- Ludwig, K.R. (2003): User's manual for Isoplot 3.0: a geochronology toolkit for Microsoft<sup>®</sup> Excel<sup>®</sup>; Berkeley Geochronology Center, Berkeley, CA, Special Publication 4, 74 p.
- McAllister, A.L. (1951): Ymir map-area, British Columbia; Geological Survey of Canada, Paper 51-4, 58 p.
- Monger, J.W.H., Price, R.A. and Templeman-Kluit, D.J. (1982): Tectonic accretion and the origin of the two major metamorphic and plutonic belts in the Canadian Cordillera; *Geology*, v. 10, p. 70–75.
- Moynihan, D.P. (2012): Metamorphism and deformation in the central Kootenay Arc, southeastern British Columbia; Ph.D. thesis, University of Calgary.
- Moynihan, D.P. and Pattison, D.R.M. (2013): Barrovian metamorphism in the central Kootenay Arc, British Columbia: petrology and isograd geometry; *Canadian Journal of Earth Sciences*, v. 50, p. 769–794, doi:10.1139/cjes-2012-0083
- Paradis, S., MacLeod, R.F. and Emperingham, R., compilers (2009): Bedrock geology, Salmo, British Columbia; Geological Survey of Canada, Open File 6048, scale 1:50 000, URL <[ftp://ftp2.cits.mcan.gc.ca/pub/geott/ess\\_pubs/247/247443/of\\_6048.pdf](ftp://ftp2.cits.mcan.gc.ca/pub/geott/ess_pubs/247/247443/of_6048.pdf)> [November 25, 2013], doi:10.4095/247443
- Pattison, D.R.M. and Vogl, J.J. (2005): Contrasting sequences of metapelitic mineral-assemblages in the aureole of the tilted Nelson Batholith, British Columbia: implications for phase equilibria and pressure determination in andalusite-sillimanite type settings; *Canadian Mineralogist*, v. 43, p. 51–88.
- Price, R.A. (2000): The southern Canadian Rockies: evolution of a foreland fold and thrust belt; Geological Association of Canada–Mineralogical Association of Canada, Joint Annual Meeting (GeoCanada 2000), Field Trip Guidebook 13, 246 p.
- Reesor, J.E. (1996): Geology, Kootenay Lake, British Columbia; Geological Survey of Canada, Map 1864A, scale 1:100 000, URL <[ftp://ftp2.cits.mcan.gc.ca/pub/geott/ess\\_pubs/207/207805/gscmap-a\\_1864a\\_e\\_1996\\_mg01.pdf](ftp://ftp2.cits.mcan.gc.ca/pub/geott/ess_pubs/207/207805/gscmap-a_1864a_e_1996_mg01.pdf)> [November 25, 2013], doi:10.4095/207805
- Rhodes, B.P. and Hyndman, D.W. (1984): Kinematics of mylonites in the Priest River “metamorphic core complex”, northern Idaho and northeastern Washington; *Canadian Journal of Earth Sciences*, v. 21, p. 1161–1170.
- Simonetti, A., Heaman, L.M., Chacko, T. and Banerjee, N.R. (2006): In situ petrographic thin section U-Pb dating of zircon, monazite, and titanite using laser ablation-MC ICP-MS; *International Journal of Mass Spectrometry*, v. 253, p. 87–97.
- Simonetti, A., Heaman, L.M., Hartlaub, R.P., Creaser, R.A., McHattie, T.G. and Böhm, C.O. (2005): U-Pb zircon dating by laser ablation-MC-ICP-MS using a new multiple ion counting faraday collector array; *Journal of Analytical Atomic Spectrometry*, v. 20, no. 8, p. 677–686.
- Tera, F. and Wasserburg, G.J. (1972): U-Th-Pb systematics in three Apollo 14 basalts and the problem of initial Pb in lunar rocks; *Earth and Planetary Science Letters*, v. 14, no. 3, p. 281–304.
- Unterschutz, J.L.E., Creaser, R.A., Erdmer, P., Thompson, R.I. and Daughtry, K.L. (2002): North American margin origin of Quesnel terrane strata in the southern Canadian Cordillera: inferences from geochemical and Nd isotopic characteristics of Triassic metasedimentary rocks; *Geological Society of America Bulletin*, v. 114, no. 4, p. 462–475.
- Warren, M.J. (1997): Crustal extension and subsequent crustal thickening along the Cordilleran margin of ancestral North America, western Purcell Mountains, southeastern British Columbia; Ph.D. thesis, Queen's University, 361 p.
- Webster, E.R. and Pattison, D.R.M. (2013): Metamorphism and structure of the southern Kootenay Arc and Purcell Anticlinorium, southeastern British Columbia (parts of NTS 082F/02, /03, /06, /07); *in* Geoscience BC Summary of Activities 2012, Geoscience BC, Report 2013-1, p. 103–118.
- Wheeler, J.O. and McFeely, P. (1991): Tectonic assemblage map of the Canadian Cordillera and adjacent parts of the United States of America; Geological Survey of Canada, Map1712A, scale 1:2 000 000.



# SEEK Project Update: Stimulating Exploration in the East Kootenays, Southeastern British Columbia (parts of NTS 082F, G, J, K)

A.L. Clifford, Geoscience BC, Vancouver, BC, clifford@geosciencebc.com

Clifford, A.L. (2014): SEEK Project update: stimulating exploration in the East Kootenays, southeastern British Columbia (parts of NTS 082F, G, J, K); in Geoscience BC Summary of Activities 2013, Geoscience BC, Report 2014-1, p. 115–118.

## Introduction

The East Kootenay region has a long successful history of mineral exploration and mining. One of the world's largest Pb-Zn deposits, the former Sullivan mine, sustained the economy of Kimberley and the East Kootenay region for almost 100 years. In November 2011, Geoscience BC, in partnership with the East Kootenay Chamber of Mines, announced the SEEK Project (Stimulating Exploration in the East Kootenays; Geoscience BC, 2011). The SEEK Project was initiated to capitalize on the region's rich exploration history through the compilation of existing mineral prospect and exploration information, primarily by capturing knowledge from local prospectors and exploration geologists. This local knowledge represents invaluable information that the SEEK Project aims to compile and release into the public domain. Hartlaub (2013) presented a review of the geology, metallogeny and mineral potential of the SEEK Project area within the Belt-Purcell Basin (Figure 1).

The SEEK Project recently extended funding to help create the new East Kootenay Chamber of Mines Core Library. This core library collects, restores and catalogues a selection of historically important core from the region, including core from the Sullivan sedimentary exhalative (SEDEX) deposit and surrounding areas. Individuals or companies engaging in mineral exploration in the area are able to examine type sections of both mineralized and nonmineralized strata of the Belt-Purcell Basin. The contents of this library are available to individuals, companies and research institutions.

A second SEEK project, completed in 2012, was a compilation of ground-station gravity data from the region (Sanders, 2012). The majority of gravity data in the database were obtained from data listings in assessment reports on the Assessment Report Indexing System (ARIS) website (BC Ministry of Energy and Mines, 2013).

**Keywords:** *SEEK Project, gravity survey, East Kootenay Gravity Database, paleomagnetic study, Hughes Range*

*This publication is also available, free of charge, as colour digital files in Adobe Acrobat® PDF format from the Geoscience BC website: <http://www.geosciencebc.com/s/DataReleases.asp>.*

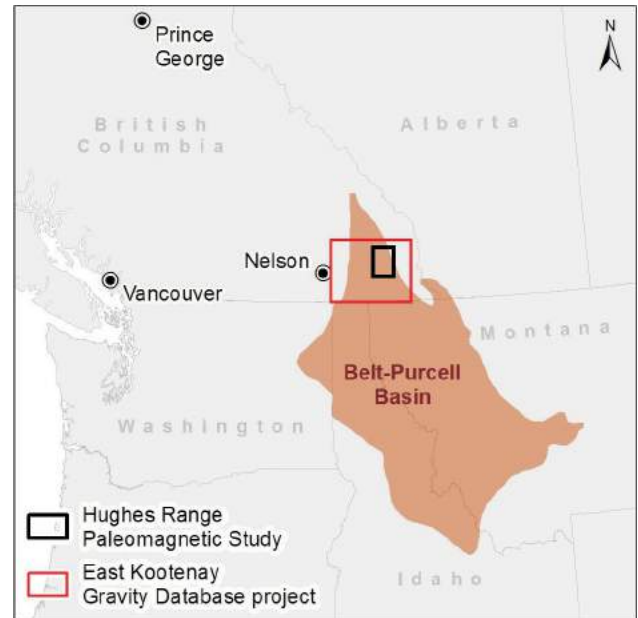


**Figure 1.** Outline of Geoscience BC's SEEK Project area in relation to the Belt-Purcell Basin. Data from United States Department of the Interior (2005).

## 2013–2014 SEEK Project Activities

Two separate SEEK projects were granted funding in 2013 and field activities for each project are complete. One project focused on acquiring new ground-station gravity data in the East Kootenay region and updating the East Kootenay Gravity Database (EKGDB) with additional ARIS data that recently became public. The second project will use new paleomagnetic data to help unravel the movement history of faults in the Hughes Range. Understanding fault movement in this mountain range is critical, as the area hosts several Pb-Zn deposits, including the past-producing Kootenay King and Estella mines.

### Updated East Kootenay Gravity Database and St. Mary Gravity Survey

The EKGDB was first compiled by SEEK project proponent T. Sanders and released through Geoscience BC's website in December 2012 (Sanders, 2012; Figure 2). The data release consists of the EKGDB in Excel format and a report that describes the collection of the ground-station gravity data, the majority of which were obtained from data listings

in assessment reports on the Assessment Report Indexing System (ARIS) website (BC Ministry of Energy and Mines, 2013). Other sources included 1) contributed data from gravity surveys not available on the ARIS website, 2) a subset of the Geological Survey of Canada (GSC) database, and 3) a digitized Bouguer gravity anomaly map (obtained from an ARIS file that did not contain raw data). The EKGDB contains 27 fields of levelled and reprocessed gravity data, and includes raw and reduced Bouguer gravity anomaly values for all stations using three rock densities.

In 2013, T. Sanders undertook additional work to add to the 2012 version of the EKGDB. A new gravity survey was conducted, called the St. Mary Gravity Survey, and additional gravity data were added from ARIS files that had recently become nonconfidential. The St. Mary Gravity Survey acquired 217 new ground gravity stations during July and September, which were laid out to complement gravity data already compiled within the EKGDB (Sanders, 2013; Figure 2). The entire updated EKGDB now contains re-

cords for more than 5300 individual ground gravity stations from the following sources:

- 217 newly acquired ground gravity stations (2013 St. Mary Gravity Survey)
- 202 gravity stations contributed by B. Kostiuk (collected in October 2011 and recently became nonconfidential)
- 485 stations acquired between 1954 and 1979 that were extracted from the GSC Gravity Database
- 3686 stations from 18 individual ARIS files
- 735 stations from a digitized map of tied Bouguer gravity anomaly values

According to Sanders (2013), the acquisition of new gravity data in the St. Mary River area, in combination with the previously compiled EKGDB, could help revitalize exploration interest in the area. The St. Mary Gravity Survey was conducted primarily over areas underlain by Aldridge Formation that previously had no gravity data. The station spacing was tight enough to highlight information from

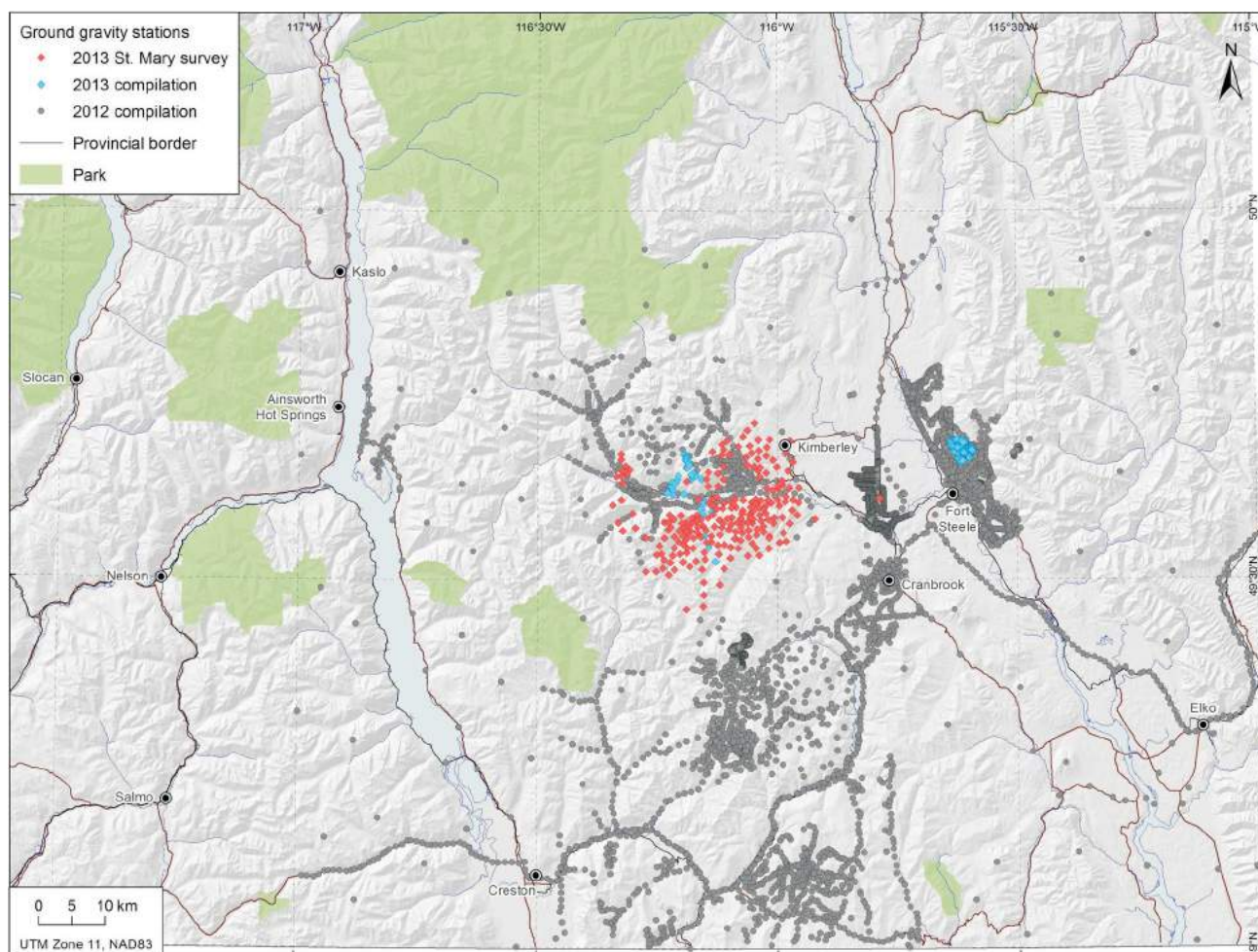


**Figure 2.** Ground gravity stations that constitute the East Kootenay Gravity Database (EKGDB). Data from GeoBase® (2004), Natural Resources Canada (2007), DataBC (2008) and Massey et al. (2005).

shallower sources (i.e., potential shallow-sourced density contrasts related to mineralized areas) but not tight enough to provide specific detail. The survey data allowed for interpretation of closure to a gravity anomaly (low) in the same location as the Matthew Creek metamorphic zone (MCMZ) and pegmatite stock. The anomaly infers that a granitic intrusion with a negative density contrast to the surrounding metasedimentary rocks exists beneath the MCMZ and could be the source of the Matthew Creek pegmatite stock and the domed structure. Results from the gravity survey suggest that the Hellroaring Creek pegmatite stock (12 km southwest of the Matthew Creek stock) is larger than previously considered, yet they revealed no deep-sourced gravity anomaly associated with the Hellroaring Creek stock as there is with the Matthew Creek stock. This information will change a few concepts of, yet add to the tectonic story presented by, McFarlane (1997) and McFarlane and Pattison (2000). It will also further the regional geological understanding and thereby potentially promote exploration investment in the search for new SEDEX deposits in the area.

### Hughes Range Paleomagnetic Study

The northern Hughes Range, a subrange of the Rocky Mountains, is directly east of the Rocky Mountain Trench (RMT), approximately 30–40 km east of Kimberley, BC (Figure 3). The Sullivan mine at Kimberley is in the Purcell Mountains and west of the RMT. The Estella and Kootenay King mines, also past Pb-Zn producers, are in the northern Hughes Range. A series of low-angle faults has been mapped and inferred in the northern Hughes Range by Höy (1978), Ransom (1991) and Thompson (2010). Normal faults at the Sullivan mine dip steeply west and are called ‘Sullivan-type’ faults. Similar faults are found in regional mapping extending from east of the Sullivan mine to the limit of outcrop on the west side of the Rocky Mountain Trench. There are no steep Sullivan-type faults known in the Hughes Range.

SEEK project proponent P. Ransom proposes that the low-angle faults and steeper bedding dips on the east side of the Hughes Range resulted from significant rotation caused by east-side-down normal faulting on a listric fault. Determination of the paleomagnetic signature of postfolding, 100 Ma intrusions (dikes and stocks) may indicate how much rotation there has been.

Eight sets of 7–12 oriented core samples were collected from different locations in and adjacent to the northern Hughes Range during the 2013 field season (Figure 3). The study will compare paleomagnetic measurements from several of the Cretaceous granitic and monzonitic intrusions, including related dikes, to determine the relative amount of rotation during postmagmatic cooling.

A hand-held gasoline-powered drill, designed for paleomagnetic studies, was used to collect core samples approximately 10 cm long. Orientation of each sample was measured with a hand-held Brunton compass and, on sunny days, solar azimuth was measured and compared to the ‘MrSun’ app (Amber Digital, 2010). A new state-of-the-art paleomagnetic laboratory is presently being established at Okanagan College by T. Day. This lab will be used to analyze the samples collected as part of this study. Project deliverables will include a spreadsheet of raw data, a final report that will contain an expanded account of the geological setting in relation to paleomagnetic results, and graphical representation of the paleomagnetic information that compares the different signatures obtained.

### Summary

Since announcement of the SEEK Project two years ago, Geoscience BC has provided funding for the East Kootenay Chamber of Mines core-storage facility; creation of the

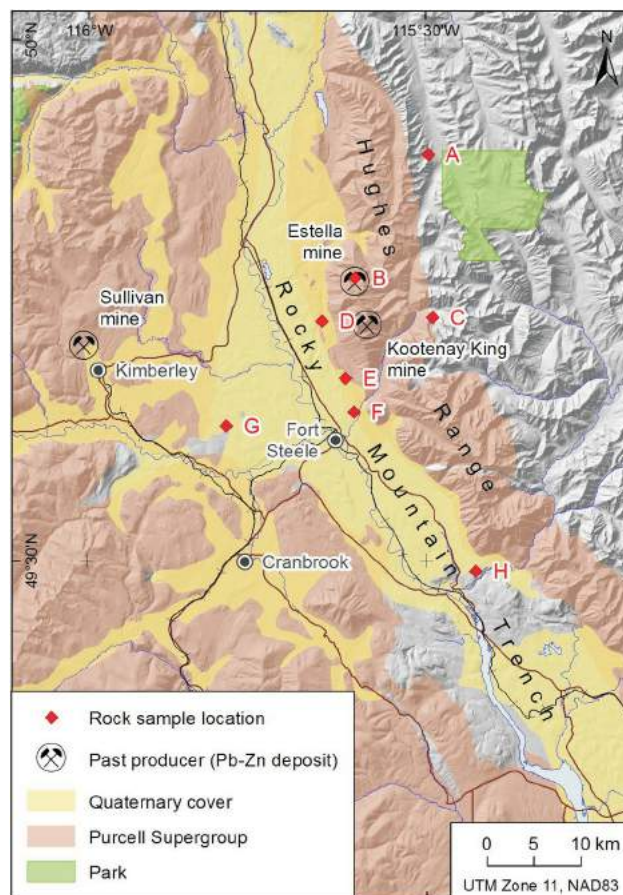


**Figure 3.** Paleomagnetic sample locations in relation to the past-producing Sullivan, Estella and Kootenay King mines: A, Nivlac (originally called Lussier north); B, Estella stock; C, East Wild Horse stock; D, Saugum Canyon dike; E, Sully dike; F, Innis Springs dike; G, Reade Lake stock; H, Bull River stock. Data from MINFILE 082FNE052, 082GNW008, 082GNW009 (BC Geological Survey, 2013); Massey et al., 2005; GeoBase®, 2004; DataBC, 2008.

East Kootenay Gravity Database (EKGDB), plus subsequent updating and data acquisition for the EKGDB by proponent T. Sanders; and a recently commenced paleomagnetic study by proponent P. Ransom. The 2013 paleomagnetic samples will be analyzed in the newly established lab at Okanagan College. Geoscience BC will consider for funding under the SEEK Project umbrella future project proposals that aim to add geoscience information to the East Kootenays and promote economic activity and investment related to mineral exploration in and around the Belt-Purcell Basin by acquiring, compiling and adding value to public- and private-sector mineral exploration information.

## Acknowledgments

The manuscript benefited from guidance from SEEK project proponents P. Ransom and T. Sanders, and review by SEEK Project Co-ordinator, R. Hartlaub. F. Ma created the figures and K. Shimamura of the Geological Survey of Canada prepared the elevation model in Figure 1.

## References

- Amber Digital (2010): MrSun, version 1.1; Apple iPhone application, URL <<https://itunes.apple.com/ca/app/mrsun/id354008995#>> [November 2013].
- BC Geological Survey (2013): MINFILE BC mineral deposits database; BC Ministry of Energy and Mines, BC Geological Survey, URL <<http://minfile.ca>> [November 2013].
- BC Ministry of Energy and Mines (2013): Assessment Report Indexing System (ARIS); BC Ministry of Energy and Mines, BC Geological Survey, URL <<http://aris.empr.gov.bc.ca>> [November 2013].
- DataBC (2008): TANTALIS—parks, ecological reserves, and protected areas; BC Ministry of Forests, Lands and Natural Resource Operations, URL <<https://apps.gov.bc.ca/pub/geometadata/metadataDetail.do?recordUID=54259&recordSet=ISO19115>> [November 2013].
- GeoBase® (2004): Canadian digital elevation data; Canadian Council on Geomatics, URL <<http://www.geobase.ca/geobase/en/data/cded/description.html>> [November 2013].
- Geoscience BC (2011): Geoscience BC Launches a new project in the East Kootenays; Geoscience BC, press release, November 16, 2011, URL <[http://www.geosciencebc.com/s/NewsReleases.asp?ReportID=490708&\\_Type=News&\\_Title=Geoscience-BC-Launches-a-New-Project-in-the-East-Kootenays](http://www.geosciencebc.com/s/NewsReleases.asp?ReportID=490708&_Type=News&_Title=Geoscience-BC-Launches-a-New-Project-in-the-East-Kootenays)> [November 2013].
- Hartlaub, R.P. (2013): The SEEK Project: stimulating exploration in the East Kootenays, southeastern British Columbia (parts of NTS 082F, G, J, K); *in* Geoscience BC Summary of Activities 2012, Geoscience BC, Report 2013-1, p. 119–124, URL <[http://www.geosciencebc.com/i/pdf/SummaryofActivities2012/SoA2012\\_Hartlaub.pdf](http://www.geosciencebc.com/i/pdf/SummaryofActivities2012/SoA2012_Hartlaub.pdf)> [November 2013].
- Höy, T. (1978): Geology of the Estella–Kootenay King area, Hughes Range (NTS 082G/11, 12, 13, 14); BC Ministry of Energy and Mines, BC Geological Survey, Preliminary Map 36, scale 1:50 000, URL <<http://www.empr.gov.bc.ca/Mining/Geoscience/PublicationsCatalogue/Maps/PreliminaryMaps/Pages/36.aspx>> [November 2013].
- Massey, N.W.D., MacIntyre, D.G., Desjardins, P.J. and Cooney, R.T. (2005): Digital geology map of British Columbia: whole province; BC Ministry of Energy and Mines, GeoFile 2005-1, URL <<http://www.empr.gov.bc.ca/Mining/Geoscience/PublicationsCatalogue/GeoFiles/Pages/2005-1.aspx>> [November 2013].
- McFarlane, C.R.M. (1997): Metamorphism, structure and tectonic evolution of the Matthew Creek metamorphic zone, Kimberley, British Columbia; M.Sc. thesis, University of Calgary, 400 p.
- McFarlane, C.R.M. and Pattison, D.R.M. (2000): Geology of the Matthew Creek metamorphic zone, southeast British Columbia: a window into Middle Proterozoic metamorphism in the Purcell Basin; Canadian Journal of Earth Sciences, v. 37 no. 7, p. 1073–1092.
- Natural Resources Canada (2007): Atlas of Canada base maps; Natural Resources Canada, Earth Science Sector, URL <<http://geogratis.gc.ca/geogratis/search?lang=en>> [November 2013].
- Ransom, P. (1991): 1991 Exploration report, Estella property, Fort Steele Mining Division, BC, NTS 082G/13E; BC Ministry of Energy and Mines, Assessment Report 21935, 123 p., URL <[http://aris.empr.gov.bc.ca/search.asp?mode=repsum&rep\\_no=21935](http://aris.empr.gov.bc.ca/search.asp?mode=repsum&rep_no=21935)> [November 2013].
- Sanders, T. (2012): Stimulating exploration in the East Kootenays (SEEK project): East Kootenay gravity database; Geoscience BC, Report 2012-12, 27 p., URL <<http://www.geosciencebc.com/s/Report2012-12.asp>> [November 2013].
- Sanders, T. (2013): Stimulating exploration in the East Kootenays (SEEK project): the updated East Kootenay gravity database and the 2013 St. Mary Gravity Survey; Geoscience BC, Report 2013-23, 47 p., URL <<http://www.geosciencebc.com/s/Report2013-23.asp>> [November 2013].
- Thompson, R.I. (2010): Technical report, geology of the Rocky Mountains claim block with recommendations for further exploration, Fort Steele Mining Division, BC, NTS 082G/12; BC Ministry of Energy and Mines, Assessment Report 31437, 54 p., URL <[http://aris.empr.gov.bc.ca/search.asp?mode=repsum&rep\\_no=31437](http://aris.empr.gov.bc.ca/search.asp?mode=repsum&rep_no=31437)> [November 2013].
- United States Department of the Interior (2005): State boundaries of the United States; *in* National Atlas of the United States, United States Department of the Interior, Reston, VA, URL <<http://nationalatlas.gov/atlasftp.html?openChapters=chpbound#chpbound>> [July 2009].

# Update on Regional Seismograph Network in Northeastern British Columbia (NTS 094C, G, I, O, P)

C.J. Salas, Geoscience BC, Vancouver, BC, [salas@geosciencebc.com](mailto:salas@geosciencebc.com)

D. Walker, BC Oil and Gas Commission, Victoria, BC

---

Salas, C.J. and Walker, D. (2014): Update on regional seismograph network in northeastern British Columbia (NTS 094C, G, I, O, P); in Geoscience BC Summary of Activities 2013, Geoscience BC, Report 2014-1, p. 123–126.

## Introduction

Recently, BC Oil and Gas Commission (BCOGC) released a report titled *Investigation of Observed Seismicity in the Horn River Basin* (BC Oil and Gas Commission, 2012). The report noted that during the study period from April 2009 to December 2011, along with the routine microseismicity created by hydraulic fracturing (fracking), 250 low magnitude seismic events were triggered by fluid injection while fracking. It was additionally noted that over 8000 high-volume hydraulic fracturing completions were conducted since 2007 with no associated seismicity. None of these events caused any injury, property damage or was found to pose any risk to public safety or the environment.

As a result of the study, BCOGC recommended augmenting the existing Canadian National Seismograph Network's (CNSN) coverage in northeastern British Columbia to better track the effects of completions/fluid injection and induced seismicity. Enhancements to the seismograph network would increase the understanding of induced seismicity and its relationship to oil and gas operations, such as fracking and injection of disposal fluids. Natural gas policy makers and regulators, the natural gas industry, communities and First Nations have a common interest in learning more about this issue to support the responsible development of BC's natural gas resources. The improvement to this seismograph array network would increase the understanding of the relationship between multistage fracking and induced seismicity.

In mid-2012, a consortium headed by Geoscience BC, along with the Canadian Association of Petroleum Producers (CAPP), BCOGC and Natural Resources Canada (NRCAN), initiated a project to add six seismograph stations to complement the two pre-existing CNSN stations in northeastern BC. The state-of-the-art stations were installed by late March 2013 and fully integrated into the CNSN by August 2013.

---

**Keywords:** *seismicity, unconventional gas, seismograph, fracking*

*This publication is also available, free of charge, as colour digital files in Adobe Acrobat® PDF format from the Geoscience BC website: <http://www.geosciencebc.com/s/DataReleases.asp>.*

## Background

The BCOGC report was commissioned in response to public and regulatory concerns with respect to induced seismicity associated with hydrofracturing operations in the Horn River Basin. The study looked at seismic events occurring in the Horn River Basin between April 2009 and December 2011, during which time 38 low-level seismic events were recorded by the CNSN's two stations near Hudson's Hope and Fort Nelson (Figure 1). These events ranged in magnitude between 2.2 and 3.8 on the Richter scale. The largest event was recorded on May 19, 2011, and was felt on the surface, although no damage or injuries were reported. The last seven events occurred during the period between December 8 and December 13, 2011. Prior to April 2009, the seismograph network had not detected any seismicity in the Horn River Basin. The seismograph stations can only detect events as low as approximately 2.4 Richter; hence it was not possible to demonstrate whether smaller level events occurred during this time period. Seismic events in the range of 0.5–2.0 Richter are very common and are termed micro-earthquakes whereas those between 2.0–3.9 Richter are called minor earthquakes. Those events within the lower end of the range (i.e., 2.0 Richter) are rarely felt whereas those within the upper range (i.e., 3.9 Richter) are often felt, but rarely cause damage.

The CNSN had several technical limitations when used for the study of induced seismicity (BC Oil and Gas Commission, 2012). The first shortcoming was due to the limited station coverage, which resulted in a 5–10 km uncertainty of the epicentre's location while carrying an even larger uncertainty of the focal depth. Secondly, although the instrument's minimum magnitude detection is approximately 2.4 Richter, calibration with an oil and gas industry-operated seismic array found that it had failed to detect 15 events of >2.4 Richter during a two-month period. Therefore, it is likely that events in the 2.0–3.0 Richter range have been historically under-reported.

Using CNSN's data, along with help from industry, NRCAN, the University of BC and the Alberta Geological Survey (AGS), BCOGC noted the low-level seismic events

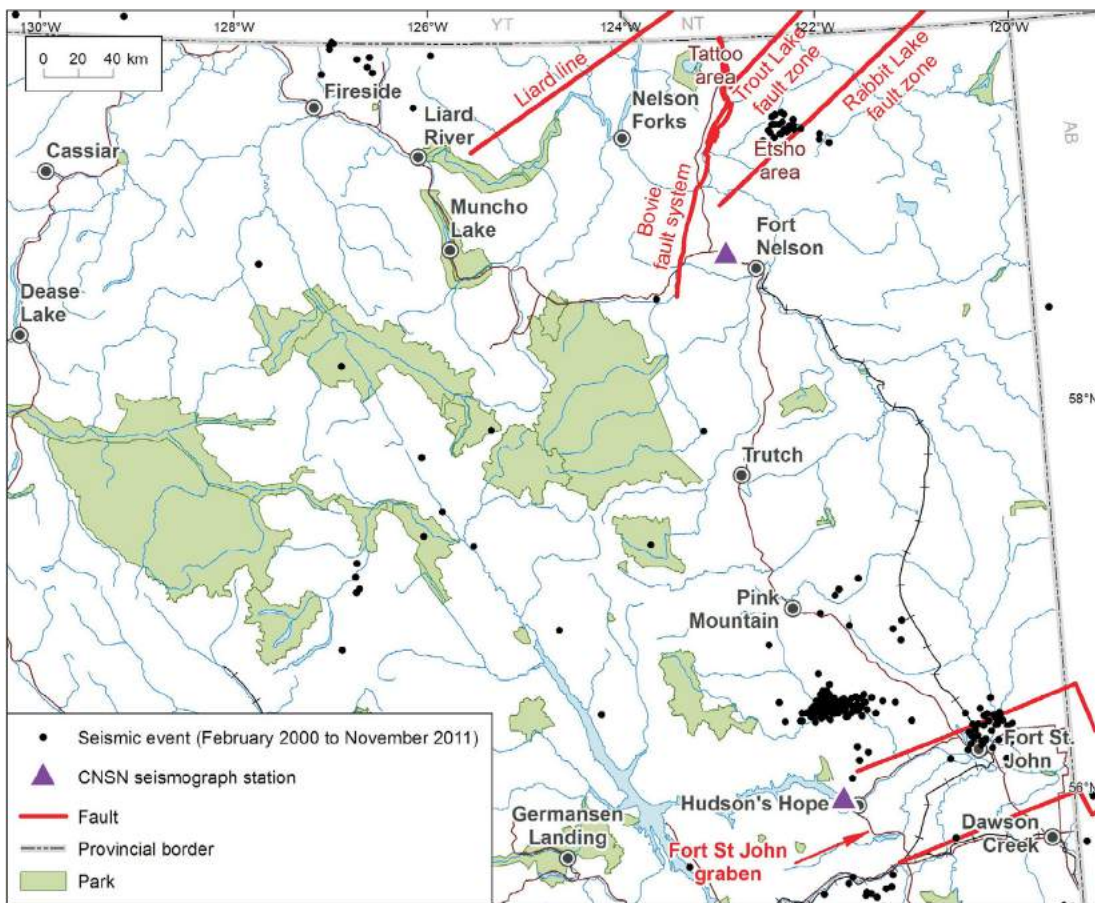


**Figure 1.** Location of Canadian National Seismic Network (CNSN) seismograph stations and anomalous induced seismic events recorded between February 2000 and November 2011, northeastern British Columbia.

were centred on the Etsho and Tattoo areas of northeastern BC (Figure 1). Additional dense array data provided by operators conducting completion operations captured an additional 212 anomalous seismic events (>2.0 Richter) in the greater Etsho area. The BCOGC’s study concluded that these events were synchronous with fracturing operations and occurred at approximately the same depths as the frac stages. Furthermore, it was surmised that the anomalous induced seismicity recorded over the period between April 2009 and December 2011 was the result of fault movement due to fluid injection during hydraulic fracturing.

In addition, BCOGC stated that during the study period, the low level seismic events did not incur any property damage or injuries, nor did these events pose any risk to public safety or the environment.

Based on the study, BCOGC made seven recommendations in their report, namely

- improve accuracy of CNSN with respect to induced seismicity in northeastern BC;
- perform geotechnical assessments to identify pre-existing faulting;
- establish procedures and requirements for identification of induced seismicity;

- place ground motion sensors in selected northeastern BC communities;
- BCOGC to study use of mobile dense arrays;
- require submission of microseismic reports; and
- study the relationship between fracturing and seismicity.

In response to BCOGC’s first recommendation, a research consortium was created between Geoscience BC, CAPP, BCOGC and NRCan to help improve the accuracy of the CNSN. A memorandum of understanding (MOU) was signed between the partners in July 2012 with a mandate to collect, interpret and make public, the data collected from the installation of six new seismograph stations to complement the pre-existing CNSN network. The project has \$1 million in funding from 50/50 equity partners Geoscience BC and CAPP (through Science Community Environmental Knowledge Funding) with in-kind support from BCOGC and NRCan. The project has a mandate to monitor induced seismic activity for a total of five years (until June 2017) with an interim review scheduled for June 2014 to assess the project’s performance.

The project is managed by joint steering and technical committees largely comprising representatives from each of the partners. There are four members from each of the partners

in the steering committee, and its role is to oversee general project direction and execution with respect to the MOU and to provide financial guidance to the technical committee. A communication plan has been drafted by the steering committee to aid in regular stakeholder communication along with missives that may be necessary in response to an anomalous induced seismic event. At present, all events registered by the network are published on the Earthquakes Canada (NRCan) website (<http://www.earthquakescanada.nrcan.gc.ca/index-eng.php>).

The technical committee's mandate is to oversee operation and maintenance of the seismographs and review and advise on all technical aspects relating to the project. The technical committee comprises seven individuals: three from industry, one academia and three from government agencies (NRCan, BCOGC and AGS). During the initial installation and testing stages, both committees are meeting on a quarterly basis.

## Summary of Activities

In early January 2013, the final locations of the stations were approved by the technical committee. Their placement allows for strategic coverage of the Liard, Horn River and Cordova basins along with the Montney gas play.

The lead technical partner, NRCan, recommended the use of the Nanometrics-made Trillium 120PH broadband seismometer, as it is a state-of-the-art unit. The recommendation was based on technical criteria such as

- continuous data transmittal with minimal power consumption (6 W or less, a necessary requisite given they are solar powered);
- ability for placement in any kind of terrain, such as in soil and/or gravel or directly on bedrock;
- high tilt tolerance (i.e., tolerant of the angle the hole is drilled at);
- tolerance of very cold temperatures;
- excellent reliability, with a solid worldwide reputation; and
- compatibility with CNSN.

Given the outlined points, a decision was made by the partners to sole source the instruments and their installation to Nanometrics Inc.

Installation of the seismometers began in February 2013 and was completed by mid-March 2013. At four of the six locations, the seismographs were mounted on screw-piled, 5 by 5 m pads, set to a depth of approximately 10 m. These sites typically used pre-existing well pads. The other two seismographs were mounted directly on bedrock. All stations went 'live' by the end of March (Figure 2) and were fully incorporated into the CNSN by mid-August 2013.



**Figure 2.** Installed seismograph near Fort Nelson, northeastern British Columbia.

Data collected by the stations are sent via satellite (a central site VSAT System) to NRCan's Pacific Geoscience Centre in Sidney, BC, where the data are processed by an Apollo server (a seismic-specific software package), which converts it to CNSN-compatible format. The data stream is then redirected to both the AGS and the Geological Survey of Canada where it is processed with data from the CNSN. Routine analysis of seismic events is not done in real time, unless the seismic event is >4.0 Richter. In this case, analyses would be reported in real time. There is typically a one-to two-day delay between when the data arrives and when the interpretation of the seismic event is posted. The interpreted seismic events are posted on the Earthquakes Canada webpage.

Since the stations came online in late March, events have been recorded in three general areas: Altares and Graham, Fort St. John and Septimus, and Beg (Figure 3).

Between March 31 and November 8, 2013, the area around Altares and Graham experienced 23 low magnitude events (<2.5 Richter) whereas the area around Fort St. John and Septimus recorded six events; one event measured on May 27 was interpreted as a 4.2 Richter event, and was felt on surface in Fort St. John (11 km north of the epicentre). No damage or injuries were reported. There were two subsequent aftershocks of 2.8 and 2.5 Richter on May 28 and June 2, respectively. Subsequent work by NRCan has put the focal depth of the original event at approximately 3 km below surface. The Beg area has noted 10 events, all within a 5 km radius suggesting good epicentre resolution.

## Additional Work

The network is continuously being reviewed by the technical partners to ensure that the best accuracy and precision is achieved. The initial five months of operation have demonstrated epicentre accuracy that appears to be in the 2–15 km range. Epicentre resolution, although inconsistent, has

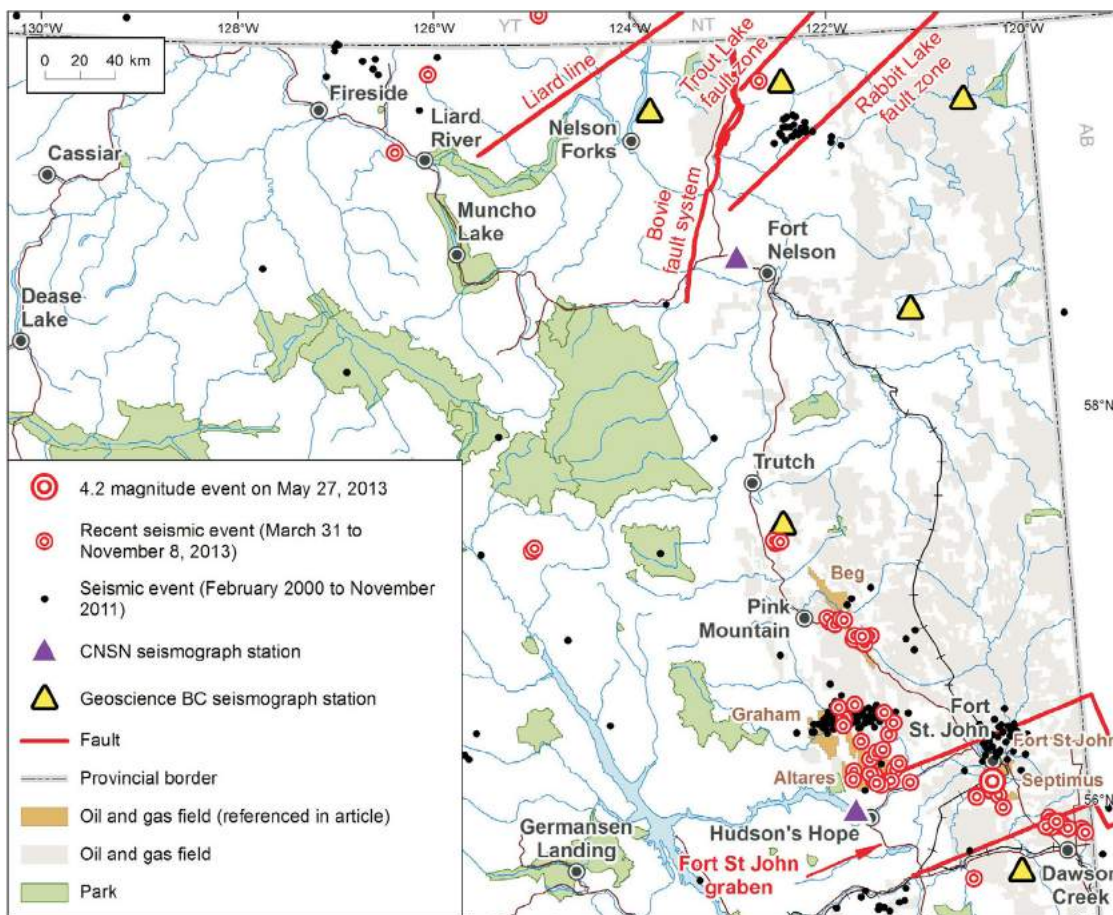


**Figure 3.** Location of anomalous seismic events captured by the CNSN network from February 2000 to November 2011 and by the enhanced network from March 31 to November 8, 2013, northeastern British Columbia.

been steadily improving with additional calibration to industry, high density, microseismic arrays, and is now generally estimated to be within 5 km. Epicentre resolution also seems to vary spatially across the region. Minimum magnitude resolution has been estimated to be 1.5–2.0  $M_L$  (local magnitude). Further technical work is necessary to optimize and calibrate the system for it to reach its expected potential. A technical plan is currently being devised to further improve magnitude and epicentre resolution.

The data collected by the network is currently being used by BCOGC, not only for monitoring induced seismicity, but also for the development of protocols necessary for responsible hydrofracturing operations.

It is expected that NRCan and BCOGC in conjunction with the University of BC, among others, will publish studies based on data collected from the consortium’s seismic network.

At the end of the five-year project, several outcomes could ensue:

- termination of the project,
- additional funding for more monitoring,
- transfer of the stations to the CNSN or

- decommissioning of the network.

## Conclusion

The consortium’s regional seismograph network was installed mid-March and has been fully integrated into the CNSN as of August 2013. Epicentre and magnitude resolution have been improved greatly since installation of the network. The technical committee will continue to look for ways to optimize the network.

The network has noted low magnitude events concentrated in the Beg, Altares and Graham, and Fort St. John and Septimus areas. The data collected by the network is being used by BCOGC to develop the needed protocols for responsible fracturing and fluid disposal operations. It is expected the collected data will initiate future academic studies into fracturing and fluid disposal induced seismicity.

## Reference

BC Oil and Gas Commission (2012): Investigation of observed seismicity in the Horn River Basin; BC Oil and Gas Commission, Technical Report, 29 p, URL <<http://www.bco.gc.ca/document.aspx?documentID=1270>> [August 2012].

# Subsurface Aquifer Study to Support Unconventional Oil and Gas Development, Liard Basin, Northeastern British Columbia (NTS 094J, K, N, O)

B.J.R. Hayes, Petrel Robertson Consulting Ltd., Calgary, AB, bhayes@petrelrob.com

S. Costanzo, Petrel Robertson Consulting Ltd., Calgary, AB

Hayes, B.J.R. and Costanzo, S. (2014): Subsurface aquifer study to support unconventional oil and gas development, Liard Basin, north-eastern British Columbia (NTS 094J, K, N, O); in Geoscience BC Summary of Activities 2013, Geoscience BC, Report 2014-1, p. 127–134.

## Introduction

The Liard Basin in northeastern British Columbia is highly prospective for unconventional gas and oil development (Figure 1). Stacked, regionally extensive, unconventional reservoirs have great potential for long-term development, which will eventually encompass large continuous areas. Validation of this potential in northeastern BC occurred in 2012, when both Apache Corporation (Apache) and Paramount Resources Ltd. announced major shale gas discoveries in the Liard Basin (Macedo, 2012; Adams, 2013).

Industry has had great success in developing unconventional reservoirs elsewhere in northeastern BC using horizontal wells stimulated by multiple hydraulic fractures, or frac jobs. Each frac requires large amounts of water, depending upon the particular frac design. Stimulated reservoirs eventually flow back much of the frac fluid, contaminated by various chemicals used in the frac process and by naturally occurring materials from the reservoir. Companies developing unconventional hydrocarbon resources thus require water sources capable of delivering large water volumes at high rates, and water disposal zones capable of accepting comparable volumes and rates.

Although surface water or shallow aquifers may be suitable locally for source water, deeper aquifers with brackish or saline waters offer options to avoid conflicts with other water consumers and possible negative environmental impacts. In addition, only deep subsurface aquifers are suitable for water disposal, to avoid contamination of potable water supplies at surface or in shallow aquifers.

Petrel Robertson Consulting Ltd. (PRCL) has recently completed a comprehensive six-month study of deep subsurface aquifers in the Liard Basin for Geoscience BC, in support of systematic sourcing and disposal of frac waters for unconventional hydrocarbon development.

**Keywords:** Liard Basin, shale gas, aquifer, Bovie fault zone, Mattson Formation, Fantasque Formation, Rundle Group, Dunvegan Formation, Chinkeh Formation

This publication is also available, free of charge, as colour digital files in Adobe Acrobat® PDF format from the Geoscience BC website: <http://www.geosciencebc.com/s/DataReleases.asp>.

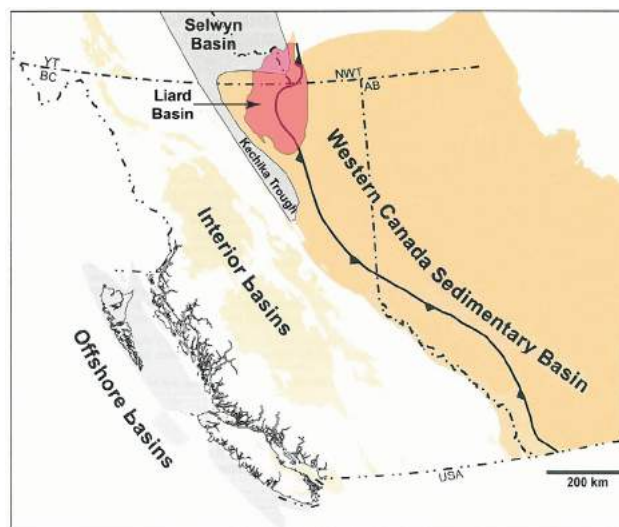


Figure 1. Liard Basin, northeastern British Columbia (from Ferri et al., 2011).

## Regional Setting

The Liard Basin is a structurally bounded segment of the Western Canada Sedimentary Basin in northeastern BC, and extends into the Northwest Territories and Yukon (Figure 1). It hosts a relatively undeformed sedimentary section measuring several thousand metres thick (Figure 2). Morrow and Shinduke (2003) described the Liard Basin as a late Paleozoic and Cretaceous depocentre bounded on the east by the Bovie fault zone, along which several stages of movement have occurred. Extensional faulting during the Carboniferous and Early Cretaceous provided accommodation space for abrupt westward thickening of the Upper Carboniferous (Mattson Formation) and Cretaceous sections (Figure 2). Morrow and Shinduke (2003) also noted at least two episodes of contraction during the late Paleozoic and the latest Cretaceous Laramide orogeny, both of which contributed to structural complexity and conventional hydrocarbon trapping opportunities in the Bovie fault zone. Structural elevations drop 1000 m or more from east to west across the highly complex Bovie fault zone, which cannot be adequately characterized without detailed seismic control (McLean and Morrow, 2004).

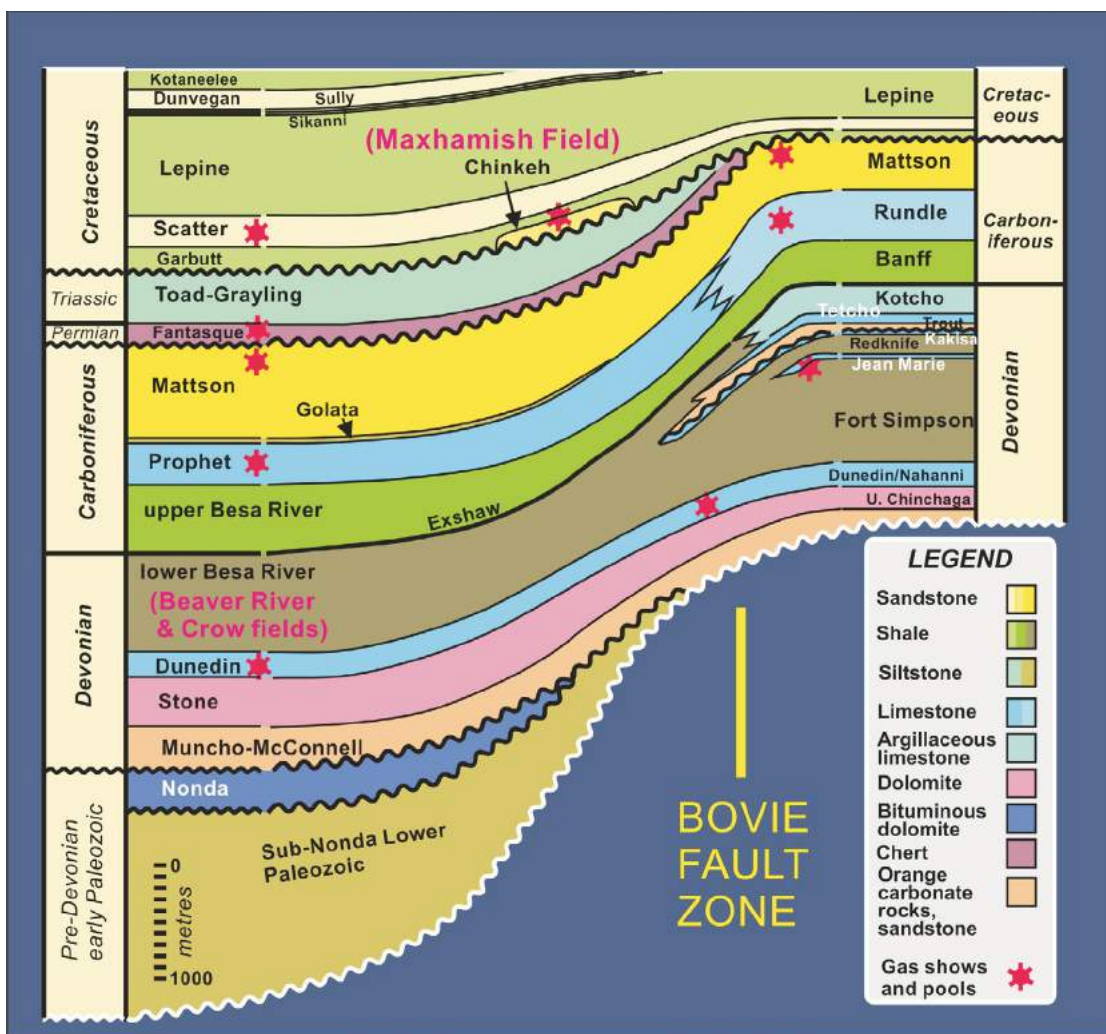


Figure 2. Schematic west-east cross-section, Liard Basin, northeastern British Columbia (from Morrow and Shinduke, 2003; published with permission of the Canadian Society of Petroleum Geologists).

### Study Methodology

Relevant well data were collected across aquifer intervals from public and proprietary sources and supplemented with regional geological mapping and information from outcrop. Consistent regional correlations were created by constructing a grid of regional stratigraphic cross-sections tied to core and sample cuttings data; these formed the foundation for picking a stratigraphic database focused on potential aquifer intervals.

Regional gross isopach maps of each potential major aquifer unit were produced, and net porous reservoir isopach maps were prepared where sufficient supporting data could be assembled. Hydrogeological characterization was undertaken, drawing on a well test database comprising 256 tests from 157 well entities. Formation permeabilities and reservoir pressures were interpreted from drillstem tests screened for adequate data quality. Pressure-elevation graphs were used to characterize regional aquifer systems. Formation water samples from drillstem test recoveries

were geochemically analyzed and the data summarized for each regional aquifer unit.

### Mattson Formation

Four aquifer intervals were investigated in detail: Mississippian platform carbonate rocks (comprising the Rundle Group, including the Debolt Formation; the younger Fantasque Formation is included in this aquifer interval as well), Mattson Formation sandstone, Lower Cretaceous sandstone (Chinkeh and Scatter formations) and Upper Cretaceous Dunvegan Formation sandstone and conglomerate (Figure 2).

Geological mapping in the Liard Basin is constrained by scarce and irregularly distributed well control (see Figure 3). Regional stratigraphic cross-sections demonstrate that major stratigraphic units can be carried across the basin, but that finer scale subdivisions are difficult to correlate between widely spaced wells. Abrupt thinning of the entire section at the eastern margin of the basin near the Bovie

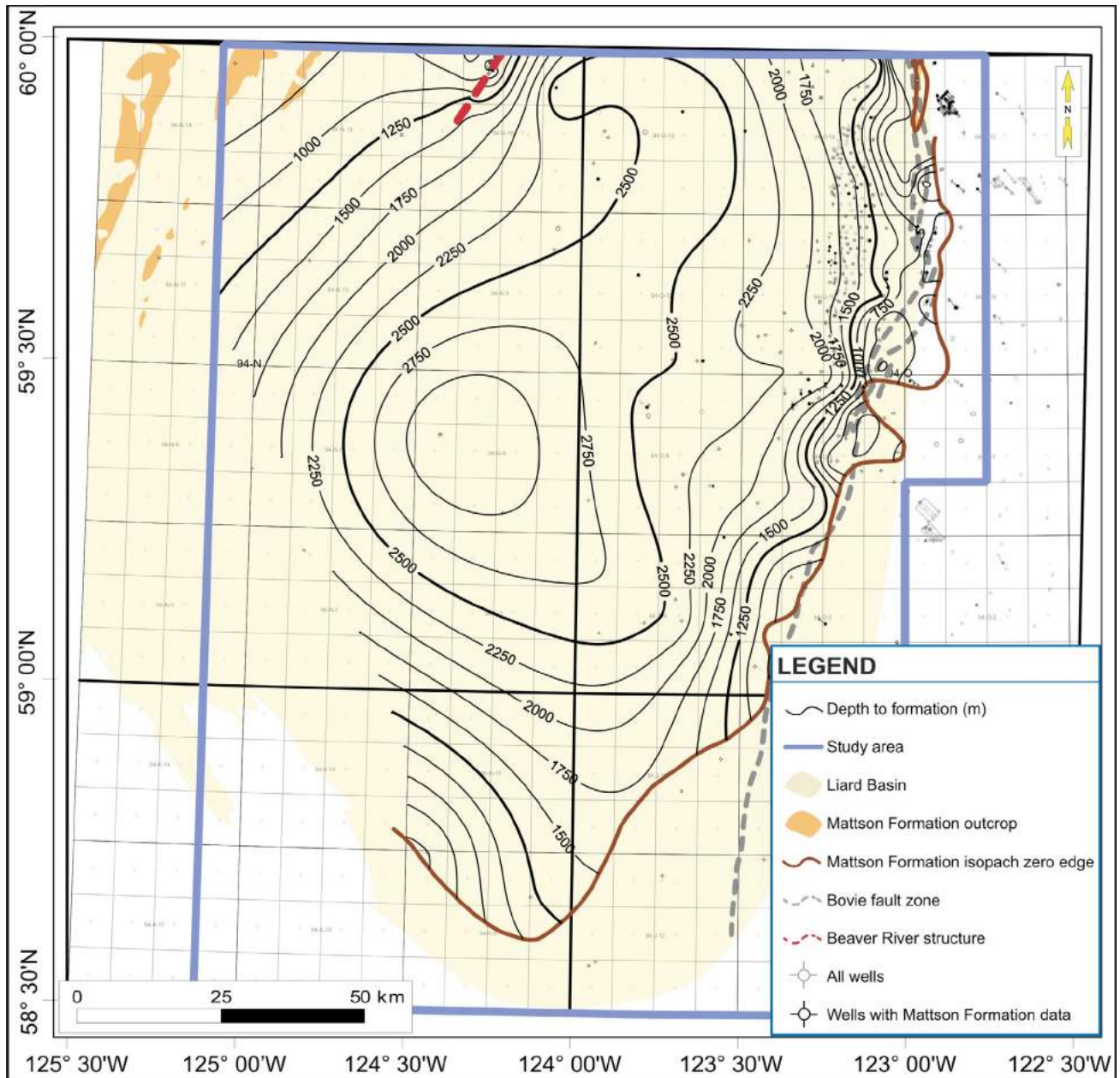


Figure 3. Depth to formation map, Mattson Formation, northeastern British Columbia.

fault zone makes correlations challenging in that area, even though well control is generally denser here.

Analysis of the Mattson Formation, the most prospective aquifer interval, is summarized in this paper as a representative example of the work completed. Conclusions for all four investigated intervals are presented at the end of this paper.

### Regional Geology

In the Liard Basin, the top of the Mattson Formation lies at depths varying from <500 m along the Bovie fault zone to >3000 m near the basin centre (Figure 3). Subsurface distri-

bution in the west is complicated by structural elements, and very scant well control in central and western areas makes burial depth uncertain over most of the basin.

The Mattson Formation grades upward from marine shale of the Golata Formation below, and is overlain unconformably by the Fantasque Formation or Kindle Formation succession of younger rocks.

At its type section in Yukon, the Mattson Formation consists of coarsening- and sandier-upward prodeltaic fine clastic rocks, overlain by deltaic to fluvial and floodplain strata. Richards et al. (1993) interpreted the Mattson Formation to have been deposited as fluvially dominated,

wave- and tide-influenced deltas of lobate form. In the east and north, thick braided-stream sandstone occurs interbedded with finer grained and coaly delta plain deposits. Southward, the Mattson Formation grades to a fully deltaic section and in northeastern BC, passes into prodelta clastic rocks and equivalent basinal shale.

Figure 4, a gross isopach map of the Mattson Formation, shows it to thicken abruptly westward from the eastern isopach zero edge and into the Bovie fault zone. Northwestward, toward the deltaic depocentre in Yukon and NWT, it thickens to >800 m. Southward and away from the source area, it thins to an apparent isopach zero edge in the southern Liard Basin. Presence of the Mattson Formation

in two wells in NTS 094K/09 is rather problematic; these sections are difficult to correlate, and may relate more to time-equivalent Stoddart Group deposition to the south. If this is the case, there may be little Mattson Formation rock south of NTS 094O/04 and N/01.

Well control is not sufficient to break out clear subunits or depositional trends within the Mattson Formation, but clean, thick, reservoir-quality sandstone is common in many wells. Mattson Formation sandstone is typically a quartzarenite; minor framework components include chert, phosphate and detrital carbonate grains. Silica is the primary cement, mostly in the form of quartz overgrowths.

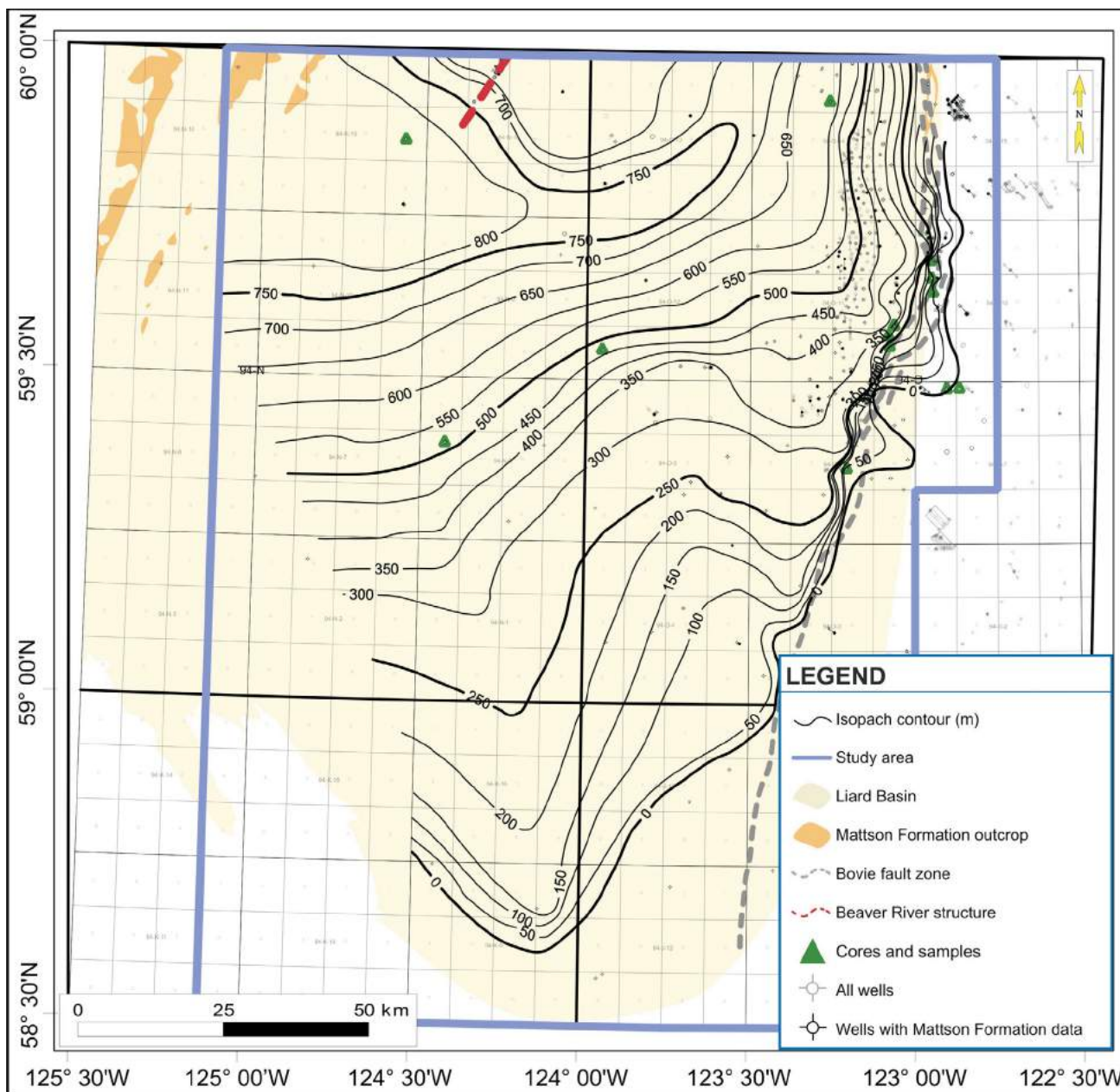


Figure 4. Gross isopach map, Mattson Formation, northeastern British Columbia.

## Reservoir Quality

Reservoir quality ranges from very poor in very fine grained rocks and tightly cemented sandstone to excellent in well-sorted quartz sandstone. Porosities locally exceed 20%, and permeabilities range into the hundreds of millidarcies (mD). Porosity is primarily intergranular, augmented by secondary solution of chert and carbonate grains.

Sample cuttings from the eastern Liard Basin wells document thicker, sand-dominated, variably cemented Mattson Formation sections. To the west, samples indicate a much poorer quality Mattson Formation reservoir. Natural fracturing was observed, particularly in more tightly cemented intervals, and is likely related to tectonic activity along the Bovie fault zone.

Reviewing drillstem test data and the porosity-permeability crossplot from available core analysis data (Figure 5), a porosity of 10% (equivalent to about 3 mD permeability) was selected as the net porous sandstone cutoff value. Net porous sandstone values were calculated from all wells with adequate logs, using a clean gamma-ray cutoff of 60 API units and the 10% porosity value on sandstone density logs. A net porous sandstone isopach map (Figure 6) shows total thicknesses ranging up to 18 m. The most consistent porosity development is in the relatively shallow

sections along the Bovie fault zone, although several wells on the Beaver River structure and southward exhibit substantial porous sections as well. Wells in the central and southern parts of the basin exhibit limited or no net porous sandstone.

## Hydrogeology

Seventy-nine drillstem tests have been conducted in the Mattson Formation in 41 wells, four of these straddling other formations. Tests are focused along the Bovie fault zone, where many Mattson Formation tests have been drilled pursuing structural trap objectives. Twenty-one valid water tests in 16 wells were identified, and relatively high permeabilities are common.

The Mattson Formation produces gas from a number of areally small, conventionally trapped, structural closures associated with the Bovie fault zone. It is in hydraulic communication with the Fantasque Formation and Rundle Group. True formation water is found within a relatively consistent range, from 12 497 to 34 095 mg/L.

## Water Wells in the Liard Basin

Examination of existing water source and disposal/injection wells can assist in assessing the characteristics of deep saline aquifers. No water source wells in deep saline aquifers were identified in the Liard Basin.

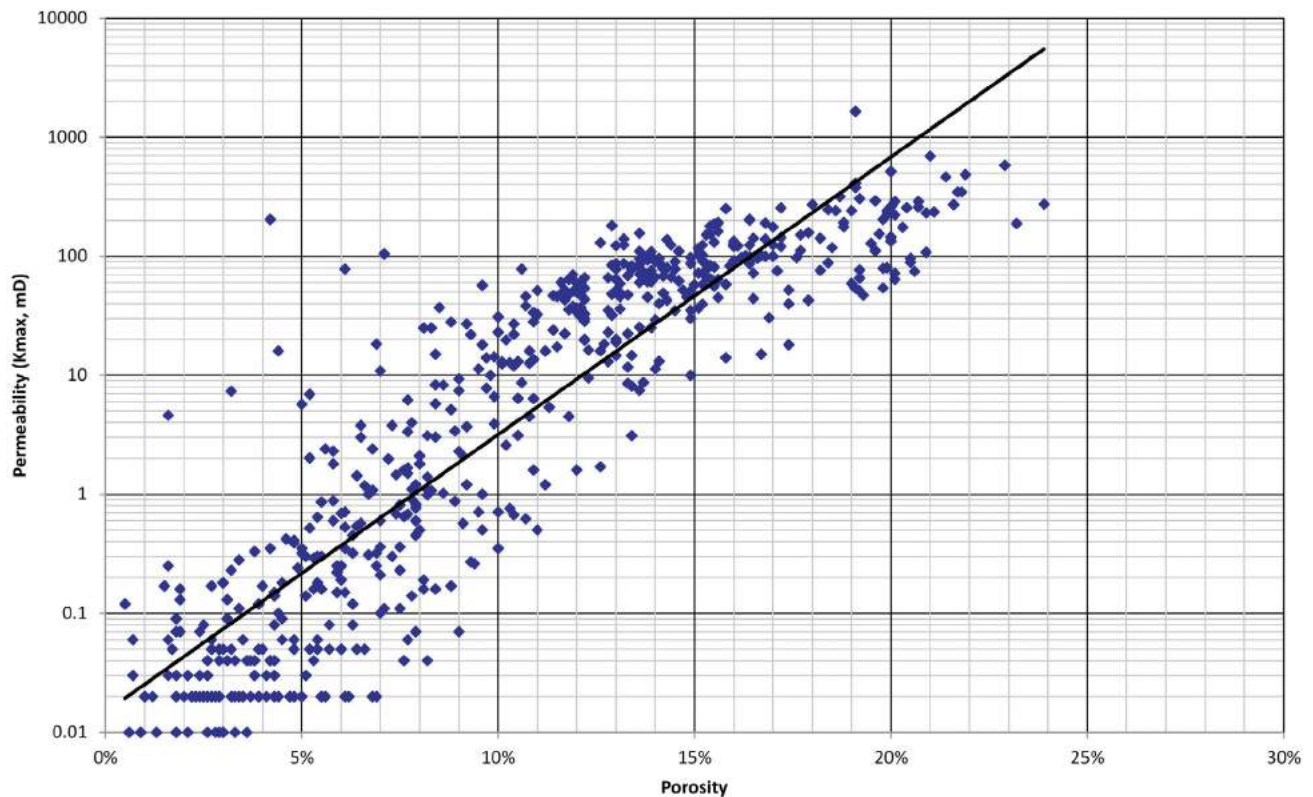


**Figure 5.** Porosity-permeability crossplot from core analysis data, Mattson Formation, northeastern British Columbia. Abbreviation: mD, millidarcies.

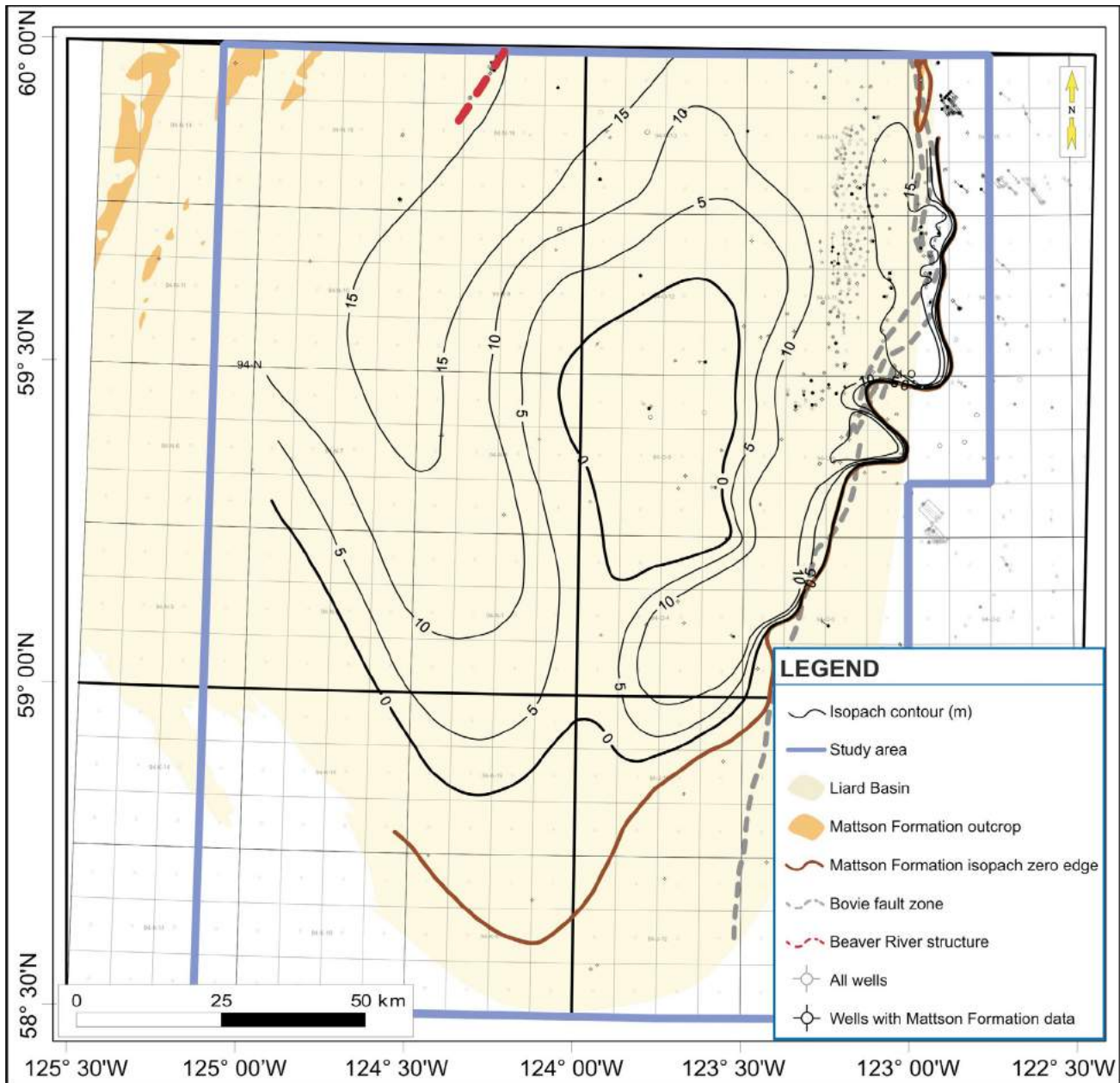


Figure 6. Net porous sandstone isopach map, Mattson Formation, northeastern British Columbia.

Eight water disposal zones in six wells were identified. Injection zones are Rundle Group (two zones), Mattson Formation (three zones), Fantasque and/or Mattson Formation (two zones) and Sikanni Formation (one zone).

Analyzing water well performance using only injection statistics entails some uncertainty, as injection rates and volumes are likely controlled by volumes available and not by the capacity of the zone being injected. However, the following observations can be made:

- Thick sand-rich Mattson Formation sections at Beaver River Field are capable of accepting high water volumes

and rates; these waters were probably produced from gas wells with high water to gas ratios in the Beaver River Field.

- The Rundle Group can accept more modest water volumes in the Bovie fault zone area with appropriate stimulation. At least some of the water capacity appears related to matrix porosity development in dolomite.
- The Sikanni Formation, although not addressed in this study, has been used for water disposal by Apache in the east-central part of the basin. It is speculated that Apache needed this capacity to handle produced waters from its new shale play wells in the area.

## Summary and Conclusions

Conclusions regarding subsurface aquifer potential in the Liard Basin are tempered by the limited distribution of wellbore data, particularly as many of the wells in more remote parts of the basin were drilled as exploratory tests several decades ago.

- Mattson Formation sandstone offers very good to excellent water source and disposal zone potential in the northern and northeastern portions of the Liard Basin. Depth of burial is quite shallow in the Bovie fault zone, but increases rapidly southward and westward. Waters are modestly saline. Crossformational connectivity of Mattson Formation tests with Rundle Group and Fantasque Formation tests indicates potential for very large aquifer volumes.
- Dunvegan Formation sandstone and conglomerate offer very good to excellent water source potential in the north-central part of the basin. Depth of burial is very shallow, making water sourcing attractive but likely precluding any water disposal potential.
- Rundle Group and Fantasque Formation rocks exhibit moderate reservoir potential in some wellbores, but reservoir quality appears to be substantially poorer than in the Mattson Formation. Tighter, more brittle rocks dominate both sections—carbonate rocks in the Rundle Group and siliceous sedimentary rocks in the Fantasque Formation, with relatively isolated better reservoir in dolomitized intervals, sandstone and fractured intervals.
- Chinkeh Formation sandstone exhibits moderate to poor aquifer potential. To the northeast, just east of the Bovie fault zone, a thick basal Cretaceous sandstone package on logs appears to have very good reservoir

quality and water saturations. Combined with the substantial Mattson Formation potential, this area may have the best subsurface water source and disposal potential in the region.

- Scatter Formation sandstone exhibits poor aquifer potential in Liard Basin.

## References

- Adams, C. (2013): Summary of shale gas activity in northeast British Columbia 2012; *in* Oil & Gas Reports 2013, BC Ministry of Natural Gas Development, p. 1–27.
- Ferri, F., Hickin, A.S. and Huntley, D.H. (2011): Besa River Formation, western Liard Basin, British Columbia (NTS 094N): geochemistry and regional correlations; *in* Geoscience Reports 2011, BC Ministry of Energy and Mines, p. 1–18.
- Macedo, R. (2012): Apache validates new shale play in B.C.'s Liard Basin; Daily Oil Bulletin, June 14, 2012, URL <<http://www.dailyoilbulletin.com/issues/article.asp?article=dob%5C120614%5Cdob2012%5Fue0032%2Ehtml>> [November 2013].
- MacLean, B.C. and Morrow, D.W. (2004): Bovie structure: its evolution and regional context; *Bulletin of Canadian Petroleum Geology*, v. 52, p. 302–324.
- Morrow, D.W. and Shinduke, R. (2003): Liard Basin, northeast British Columbia: an exploration frontier; *Canadian Society of Petroleum Geologists/Canadian Society of Exploration Geophysicists Joint Convention (Partners in a New Environment)*, abstract, 4 p., URL <<http://www.cspg.org/documents/Conventions/Archives/Annual/2003/283S0131.pdf>> [November 2013].
- Richards, B.C., Bamber, E.W., Higgins, A.C. and Utting, J. (1993): Carboniferous; Subchapter 4E *in* *Sedimentary Cover of the Craton in Canada*, D.F. Stott and J.D. Aitken (ed.), Geological Survey of Canada, *Geology of Canada Series* no. 5, p. 202–271.



## Horn River Basin Water Project Update, Northeastern British Columbia (Parts of NTS 094I, J, O, P)

C.J. Salas, Geoscience BC, Vancouver, BC, [salas@geosciencebc.com](mailto:salas@geosciencebc.com)

D. Murray, Kerr Wood Leidal Associates Ltd., Victoria, BC

C. Davey, Kerr Wood Leidal Associates Ltd., Victoria, BC

---

Salas, C.J., Murray, D. and Davey, C. (2014): Horn River Basin Water Project update, northeastern British Columbia (parts of NTS 094I, J, O, P); in Geoscience BC Summary of Activities 2013, Geoscience BC, Report 2014-1, p. 135–138.

### Introduction

Water availability plays a pivotal role in the development of the Horn River Basin; however, the available hydrological and climate information in the basin is very limited. Geoscience BC and the Horn River Basin Producers Group (HRBPG), the Fort Nelson First Nation and the Fort Liard First Nation (Acho Dene Koe) all have a strong commitment to effective water management in the area. In order to meet this commitment, the Horn River Basin Water Project was initiated in 2008 to study the deep, shallow and surface water components. The deep and shallow water components of the study are complete, and work on the surface water aspect of the study is ongoing. The objectives of the study are to 1) understand water quantity in the region, 2) determine water quality, 3) use alternate biomonitoring methodology (benthic sampling) to evaluate environmental health, and 4) build First Nation capacity in water management.

As part of Phase II of the project, a three-year program was started in the late spring of 2011 to study the regional surface water system. This program included the installation of seven hydrometric stations and three climate stations to help provide the baseline water quantity information needed (Figure 1).

This year provided the first full season of environmental information. Information collected from this project is now available from the Geoscience BC website (<http://www.geosciencebc.com/s/HornRiverBasin.asp>). Water quality sampling was initiated this year with the benthic sampling.

A new important component to the study was initiated this year by the Cold Regions Research Centre (CRRC;

---

**Keywords:** *hydrometric station, climate station, Horn River Basin, slickwater, fracking, stage-discharge curve, SDR, biomonitoring, benthic sampling, snow pillow*

*This publication is also available, free of charge, as colour digital files in Adobe Acrobat® PDF format from the Geoscience BC website: <http://www.geosciencebc.com/s/DataReleases.asp>.*

B. Quinton and J. Baltzer, Wilfred Laurier University; E. Johnson, BC Ministry of Natural Gas Development; M. Hayashi, University of Calgary). They will examine the water balance in areas of muskeg and discontinuous permafrost along with temporal variations in discontinuous permafrost.

### Background

The Horn River Basin covers an area of 11 000 km<sup>2</sup>, much of it covered in muskeg, and spans 42 major watersheds in northeastern BC. It also has an estimated mean case of 448 tcf of gas-in-place ultimate potential reserves (BC Ministry of Natural Gas Development and National Energy Board, 2010), making it one of the richest gas basins in North America. Unconventional gas development in the basin is water intensive with an average well using upward of 80 000 m<sup>3</sup> of water (Johnson, 2012) in slickwater completions (i.e., high volume of water with a low concentration of sand and friction reducers). In 2011, 133 wells used 7 million m<sup>3</sup> of water from the basin for oil and gas activities.

The HRBPG recognized the need for a water management plan that would enable sustainable and responsible development of unconventional gas in the Horn River Basin. In late 2008, the HRBPG, along with Geoscience BC, and the BC Ministry of Natural Gas Development, initiated the Horn River Basin Water Project, which would aid in responsible development of the gas resource. Phase II of this project is the Horn River Basin Water Study, part of which is the study of the deep, shallow and surface water components. The deep and shallow groundwater components of the study have been finished, and currently, the research consortium is on the second year of a three-year regional surface water study, managed by Kerr Wood Leidal Associates Ltd. (KWL), which is focusing on collecting data with respect to water quality and quantity. The Fort Nelson and Acho Dene Koe First Nations partners are providing people who are being trained as water monitors.

Additionally, in order to better understand surface-shallow groundwater interaction in areas of muskeg and discontinu-

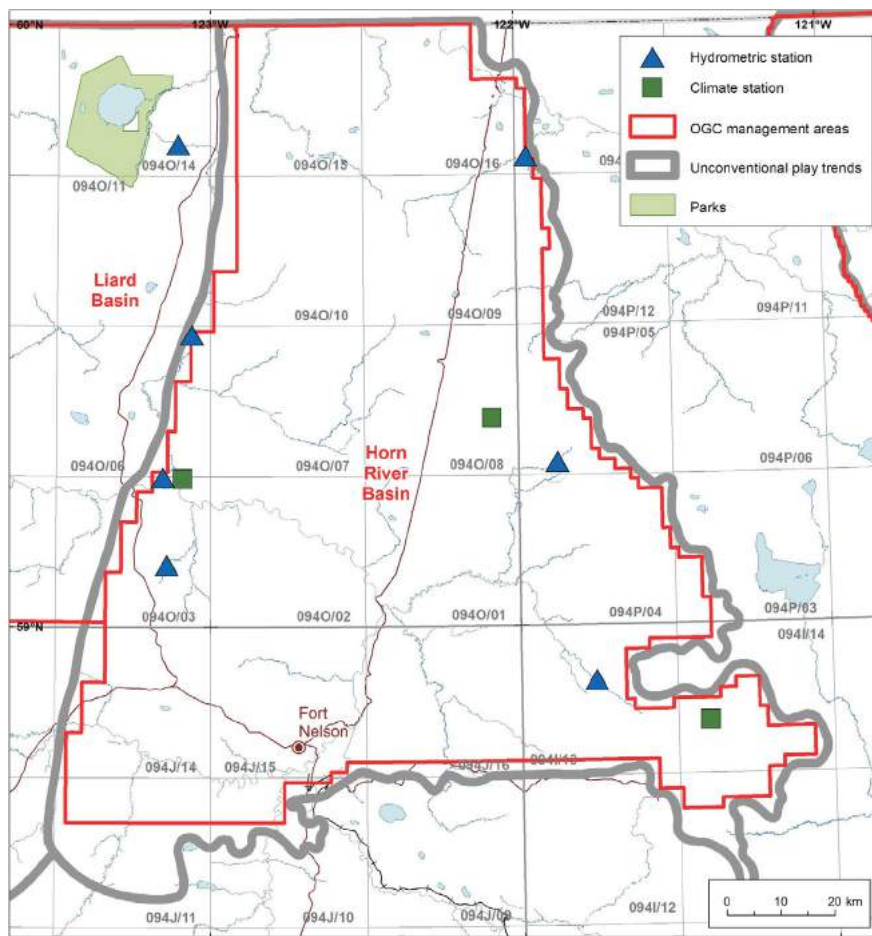


**Figure 1.** Location of hydrometric and climate stations, Horn River Basin, northeastern British Columbia. Abbreviations: OGC, BC Oil and Gas Commission.

ous permafrost, and to properly understand the water balance in these complex areas, an additional study has been undertaken by CRRC. Research into this subject will not only give a better understanding as to water availability in these regions but also provide important information with respect to temporal variations in the discontinuous permafrost—critical information that is necessary when building infrastructure in these areas.

### Objectives of Surface Water Component

The primary objectives of the surface water component of the Horn River Basin Water Study are

- 1) to collect accurate water flow, water quality and climate data, which will allow the characterization of baseline conditions and provide better accuracy and reliability for water use;
- 2) to train First Nations representatives in all aspects of water monitoring;
- 3) to aid and support the sustainable planning and use of water in unconventional gas development; and
- 4) to provide the necessary data needed for informed decisions by the HRBPG and the BC Oil and Gas Commission.

The objectives of the surface water component of the study are being attained through the installation and monitoring of an environmental monitoring network. The environmental monitoring network comprises 1) hydrometric and climate monitoring, 2) water quality and biological monitoring, and 3) data management and reporting. Although not part of the environmental monitoring network per se, the acquisition of the scientific data necessary for the understanding of the muskeg groundwater-surface water interaction and its impact on the water balance in areas of discontinuous permafrost will be very important in resolving the water balance question.

### Hydrometric and Climate Monitoring Program

Seven hydrometric monitoring sites were installed by a field team (supported by First Nation water monitoring trainees; Table 1) and were placed in time to capture the spring freshet of 2012—four of these stations capture real-time data. The data is uploaded (via satellite) every six hours and transmitted to a proprietary website housing a hydrometric program (FlowWorks), which is owned and operated by KWL. This data can be accessed and downloaded through the Geoscience BC website (<http://www.geosciencebc.com/s/HornRiverBasin.asp>).

The real-time stations consist of a data logger fixed inside an enclosure and placed a few metres from the stream bank above flood level (stage). Stage (depth) data from the streams are collected using pressure transducers encapsulated within metal sleeves inserted into the stream bed/bank. Discharge is not measured directly, thus stage-discharge relationships (SDR) are created by measuring instantaneous discharge at different water levels and relating them to a fixed staff gauge. The pressure transducer measures stage (water level) every 15 minutes. Discharge (flow) is then related to the stage measurements through the SDR developed over time. This SDR is used to convert the stage measurements recorded by the pressure transducer into discharge values for the creation of a hydrograph. The discharge measurements collected under this baseline program generally meet ‘Class A’ hydrometric data standards and are typically given an uncertainty value of  $\pm 7\%$ .

Three climate stations were installed shortly after the hydrometric stations in June 2012 (Table 1). All of the climate stations capture real-time data. Each climate station consists of a data logger and transmitter with various sensors, a 5 m tower for the wind sensors, a telemetry antenna and a 3 m diameter snow pillow, which lies adjacent to the station collecting snowpack information (Figure 2). Each climate station collects information on barometric pressure, dew point temperature, precipitation, relative humidity, solar radiation, snow-water equivalent, temperature (minimum and maximum), wind speed and direction.

## Water Quality Program

Five watersheds were chosen for the surface water program: Dilly Creek, Kiwigana River, Sahtaneh River, D'Easum Creek and Stanolind Creek. The locations of the water sampling sites correspond to the seven hydrometric station sites. Each standard sampling trip consists of water sample collection for laboratory analyses and recording of field parameters such as temperature, dissolved oxygen, pH, conductivity, salinity, total dissolved solids and turbidity. Analytical parameters for laboratory analyses include general water chemistry, major ions, nitrogen speciation, metals (total and dissolved), volatile organic compounds (benzene, toluene, ethylbenzene, xylene), and extractable petroleum hydrocarbons (EPH). A standard quality assurance–quality control program used trip blanks and field blanks to ensure data quality. All sampling was conducted using nitrile gloves to avoid contamination and samples were shipped to the lab within 72 hours of collection.

## Benthic Program

The intent of the benthic biomonitoring program is to use an alternate biomonitoring methodology (benthic sampling) to evaluate environmental health.

A large set of reference site data comprising 30 or more samples from the Horn River region is being developed by Environment Canada. Five benthic biomonitoring sites

were selected and sampled in 2011 for the dataset. These were all candidate reference sites. A kick net method was employed to collect the benthic invertebrates at each site. The kick net was placed on the bottom of a creek, and a person kicked up rocks (for three minutes) in front of it so the net captured a large sample of benthic invertebrates floating within the water. The invertebrates were collected in sample bottles, preserved and sent to the lab for analyses. Benthic invertebrates in the samples are being categorized in the lab and reported into the database. In 2012, six sites were selected and sampled, all of which were test sites. Once the set of reference site data is finalized, then individual test sites can be compared against the reference data to determine if the water quality at the test site is impaired.

## Initial Program Results

To date, seven open water measurements of discharge have been collected from each hydrometric monitoring site—excluding Dilly Creek, which has six open water measurements of discharge. Generally, BC hydrometric standards recommends a minimum of ten discharge measurements well distributed through the range of flows to develop a rating curve. Therefore, the SDRs developed to date are considered preliminary. However, the manual measurements of discharge collected to date are very well distributed and thus there is a high degree of confidence in the SDRs. A representative SDR and accompanying hydrograph from the Kiwigana River station is shown in Figure 3. It is anticipated that by the end of 2013, ten or more manual readings of discharge will have been collected, enabling the finalization of the SDRs. It should also be noted that the recommended upper limit of applicability for each SDR is a measure of how far the curve can be confidently extrapolated beyond the highest discharge measurement.

**Table 1.** Name and UTM location for hydrometric and climate stations, Horn River Basin, northeastern British Columbia.

Site	Station type	Easting*	Northing *
D'Easum Creek (real time)	Hydrometric	494095	6629320
Delkpay Creek	Hydrometric	496640	6594093
Dilly Creek (real time)	Hydrometric	558226	6627266
Kiwigana River (real time)	Hydrometric	491233	6567759
Komie Creek	Hydrometric	564187	6570824
Sahtaneh Creek (real time)	Hydrometric	571554	6530452
Stanolind Creek	Hydrometric	491929	6551504
Two Island Lake (real time)	Climate	551981	6578887
Kiwigana River (real time)	Climate	494843	6567568
Sierra (real time)	Climate	592552	6523137

\*UTM Zone 10



**Figure 2.** Photograph of Kiwigana River climate station, northeastern British Columbia. The white object on the ground, to the right of the climate station, is a snow pillow. Photo courtesy of B. Ortman, Peace Country Technical Services Ltd.

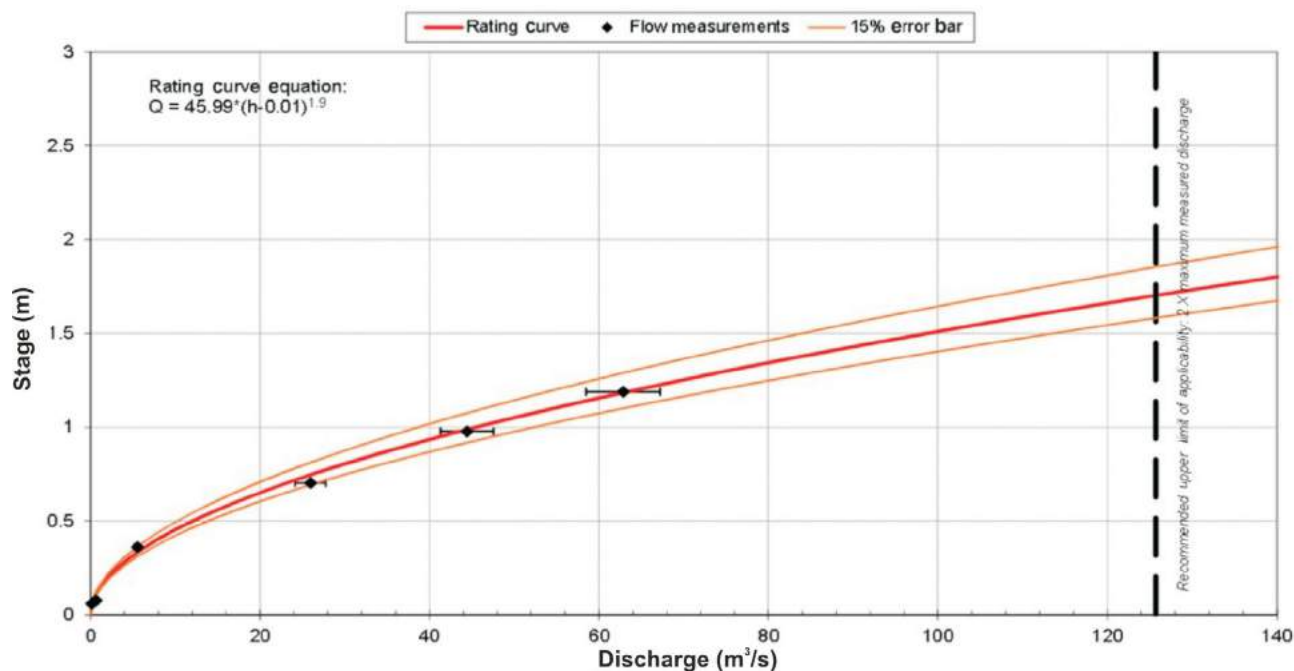


**Figure 3.** Preliminary stage-discharge curve for hydrometric station on Kiwigana River (northeastern British Columbia) with corresponding hydrograph (produced by Kerr Wood Leidal Associates Ltd.). The stage-discharge curve has been estimated by the method of maximum likelihood. In the rating curve equation, Q is the discharge and h is the gauge height.

Data collected from all the stations show very low base flows after the 2012 freshet. Based on the limited hydrometric data record presented here, the ability to withdraw water from the Horn River Basin streams is greatest, and most predictable, during the spring freshet. The use of real-time stations to monitor stream-flow conditions and the climate variables (precipitation and temperature, in particular) allow better prediction of possible limitations to near-term water withdrawals.

Three official water quality sampling events have been completed, and benthic sampling has also been initiated; however, until a larger dataset is collected comparisons between sites cannot be made.

Data from the climate stations indicate that warmest and coldest recorded temperatures occurred at the Kiwigana station (+33.1 and -37.9°C). Precipitation data collected by the climate stations also corroborates the drought conditions (50–70 mm over the summer months) seen from the hydrometric stations during the summer of 2012. The use of real-time climate stations, which allow monitoring of precipitation events, in conjunction with an enhanced understanding of surface-groundwater interflow may allow for better water-use practices in the future.

### Conclusion

As part of the Horn River Basin Water Project, the second year of the three-year study of surface water is being com-

pleted. Core to the study has been the installation of seven hydrometric and three climate stations to help determine baseline water quantity. Additionally, water quality is being studied through traditional water chemistry techniques and less traditional biomonitoring programs. A separate study has been initiated this year to increase the understanding of surface-shallow groundwater interaction in areas of muskeg and discontinuous permafrost.

### References

- BC Ministry of Natural Gas Development and National Energy Board (2010): Ultimate potential for unconventional natural gas in northeastern British Columbia's Horn River Basin; BC Ministry of Natural Gas Development, Oil and Gas Reports 2011-1, 39 p., URL <[http://www.empr.gov.bc.ca/OG/Documents/HornRiverEMA\\_2.pdf](http://www.empr.gov.bc.ca/OG/Documents/HornRiverEMA_2.pdf)> [November 2013].
- BC Ministry of Environment (2009): Manual of British Columbia hydrometric standards; prepared for Resources Information Standards Committee, 204 p., URL <[http://www.ilmb.gov.bc.ca/risc/pubs/aquatic/hydrometric/man\\_BC\\_hydrometric\\_stand\\_V1.0.pdf](http://www.ilmb.gov.bc.ca/risc/pubs/aquatic/hydrometric/man_BC_hydrometric_stand_V1.0.pdf)> [November 2013].
- Johnson, E. (2012): Water issues associated with hydraulic fracturing in northeast British Columbia; Unconventional Gas Technical Forum, Victoria, April 2–3, 2012, 25 p. (presentation), URL <<http://www.empr.gov.bc.ca/OG/oilandgas/petroleumgeology/UnconventionalGas/Documents/E%20Johnson.pdf>> [November 2013].